Section 3

Better Understanding of Treatments

Plasma-Reduction: Its Potential for Use in the Conservation of Metals

K. Schmidt-Ott[a]

Swiss National Museum, Centre for Conservation, Hardturmstr. 185, CH- 8005 Zurich

Abstract

The use of optical emission spectroscopy has lead to an optimization of the plasma parameters for the handling of iron artefacts. The effects of plasma reduction have also been investigated through metallographic sampling of iron nails.
It is shown that a pure hydrogen plasma is more effective in reducing corrosion layers than a mixture of hydrogen and argon. As a consequence the temperature of iron artefacts during plasma reduction can be reduced to around 80 °C. Plasma is further applied in the reduction of silver sulphide layers from art historical silver artefacts without altering the surface structures or interfering with the information contained within the historical metalwork.

Keywords: plasma reduction, iron artefacts, silver objects, optical emission spectroscopy, metallographic sampling, scanning electron microscope

1. Introduction

Gas plasmas have been the subject of various investigations since their initial application to metals conservation in 1979 (Daniels, Holland, and Pascoe 1979, Patscheider and Vepřek 1986). Since 1994, plasma reduction has become an integral part of treatment procedures for archaeological iron conservation at the Swiss National Museum. It has also been successfully applied to the conservation of historical silver artifacts.

There are two major advantages to using plasma treatment for iron artefacts. These are firstly the reduction of oxides in the conglomerate layer and the subsequent facilitating of mechanical removal of disfiguring corrosion layers. And secondly, there is the advantage of speeding up the desalination process with alkaline sulphite (Schmidt-Ott 1997).

As applies to silver corrosion, hydrogen plasma can remove the sulphide or chloride layers without removing any metallic silver.

Modern optical emission spectroscopy (OES) was used to monitor the plasma process (Keppner, Kroll, Torres, Goetz and Meier 1997). By measuring gas excitation the plasma operation was optimized. A better understanding of the process has given way to changes in the plasma parameters applied. The effects observed have been cross-checked by the investigation of metallographic samples of archaeological iron artefacts prior to and after plasma reduction.

2. Materials and Methods

2.1 Plasma reduction

Atomic hydrogen is considered to be the key radical produced in hydrogen plasma that leads to a chemical reduction of corrosion products.

The applied plasma is produced by a powerful 27 MHz generator in a 0,7 m^3 quartz vessel at a gas pressure of about 15 to 50 Pa (0.1-0.4 Torr). This reactor is equipped with gas inlets and mass flow meters for hydrogen and argon and a pumping system. Power supplies, matching network, thermocouples for direct temperature measurement and a digital recording of all treatment parameters are parts of this system (Voûte 1997, Schmidt-Ott and Boissonnas 2002).

For conservation purposes, a low ionization plasma is used formed by a mixture of ions, electrons and neutral gas. Placed in the plasma the object becomes negatively charged. This effect is related to higher electron mobility, than ion mobility in the gas. As a consequence, positive ions bombard the object`s surface and as they

Tel: ++41- (0)1-2186830
Fax: ++41-(0)1-2186823
email: katharina.schmidt-ott@slm.admin.ch

become neutralised act as a strong reducing agent in the case of nascent atomic hydrogen. Thereby iron corrosion products can be chemically reduced to a lower oxidation state and silver corrosion products to metallic silver.

Gas mixtures using methane and/or nitrogen in addition to hydrogen and argon which were proposed at an earlier stage to be useful for surface protection (Vepřek, Eckmann and Elmer 1988), are regarded today as being less than ideal. This is because they can introduce carbon and nitrogen to the artefact and therefore change the contained metallurgical information.

Until recently mixtures of hydrogen and argon were applied to iron artefacts, the argon being used to stabilize the plasma and to enhance the effect of surface interaction. Argon ions receive larger momentum than hydrogen ions, and if argon is added the object will become warmer during reduction treatment.

It is of importance to avoid changes in metallographic information due to the effect of increased temperature and local heat production. For example, iron artefacts originally subjected to quenching will have a metallurgical structure that is susceptible to higher temperatures (Tylecote and Black 1980, Archer and Barker 1987). Silver artefacts may also be affected if the temperature during treatment reaches the recrystallization temperature (Scott 1991) or age hardening occurs (Thompson and Chatterjee 1954, Schweizer and Meyers 1978). Temperature is therefore the foremost measure that is continuously determined on the objects themselves during plasma reduction. The use of thermocouples enables an online temperature measurement of the artefacts with respect to the plasma parameters applied as well as the surface condition and composition of each artefact.

2.2 Optical emission spectroscopy

Within the plasma reactor measurements were initially performed without specimens. An optical emission spectrometer (OES, Avantes AVS SD2000) sensitive to the radiation of atomic and molecular species was used to monitor the process. It was focused in the middle of the reactor from outside through a quartz glass window in the door.

The formation of atomic hydrogen was measurable by the Balmer H□ line at 656.30 nm (nanometre). The presence of argon in the gas was indicated by a strong line at 706.22 nm. For line identification the software Plasus SpecLine was applied to the measured spectra giving, in many cases, precise and facilitated interpretation. It is assumed that by optimization of gas excitation the plasma operation is also optimized.

During incipient experiments with pure hydrogen and hydrogen-argon mixtures, parameters of gas mixture, gas flow, pressure and power of the generator were varied. Optimal settings were then assumed to also be valid for the treatment of metal artefacts. A group of archaeological iron artefacts was processed with these “ideal” parameters. Another group of artefacts was treated using the “standard” parameters current for the time and compared with the “ideal” group.

2.3 Metallographic sampling of iron artefacts

A group of twenty roman nails (site of Wetzikon-Kempten Hinwilerstr. 1, No. 99) was chosen with typical, visible corrosion damage. These objects underwent radiography before further handling. The artefacts were then cleaned by air abrasion to remove only superficial soil. Metallurgical sampling prior to and after the reduction was performed to help estimate the effect of treatment.

Sample profiles before and after plasma application were then observed under a scanning electron microscope and polarized light microscope. Polished micro sections from the nails were prepared for this purpose (Scott 1991).

The radiographs were used to define similar situations of corrosion states where sampling before and after plasma treatment was planned. The metallographic samples were taken by a precision diamond wire saw (Well 3242), with dimensions of 1 mm thickness and 1-2 mm in depth of the nail. Attention was paid to the fact that the nails were not cut into too deeply so as not to change significantly the electric conductivity of the artefact for the following plasma reduction.

All nails were stored in controlled silicagel for ten months prior to treatment.

The nails were then divided into 3 groups. A reference group of nails was submitted to drying in a vacuum oven at a temperature of ca. 80 °C for 6 hours, as is usual for archaeological iron objects before plasma reduction.

A second group was simply pre-dried in silicagel before undergoing plasma reduction at the parameters currently applied to iron artefacts. Values applied were of hydrogen-argon plasma with 6 litre normal per hour (ln/h) hydrogen and 0.6 ln/h argon, 1100 Watt, at an average pressure of 34 Pa.

A third group was also pre-dried in silicagel only and then treated in a pure hydrogen plasma with 2 ln/h and 1100 Watt. Due to the lower gas inlet, the pressure was lower (about 15 Pa).

From each of the nails in the three groups at least two samples were taken, one before and one after drying and/or plasma treatment. All samples were mounted in a liquid photo curing resin based on mono and difunctional methacrylates (Technovit 2000LC by Kulzer) and then ground, and subsequently polished using a Struers Dap-V polishing device.

Observations of sample surfaces before and after plasma application were made under a polarized light microscope and under a scanning electron microscope (SEM, Amray 3200 ECO-SEM).

2.4 Treatment of silver artefacts

As could be shown previously hydrogen plasma can remove sulphide and chloride from silver samples with artificially produced silver sulphide and silver chloride layers, without any damage to the sample surface (Schmidt-Ott 2004).

In the meantime a number of art historical silver artefacts have been treated in a pure hydrogen plasma. The examinations of a silver spoon (LM 17672) with an apostle figurine on the handle, engraving and mercury gilding are of special interest since the object shows the combination of silver with gold. The spoon dates from 1650-1700, and is 16 cm long and 4.7 cm wide.

Prior to plasma reduction the spoon was examined under the SEM at a magnification of 500x and analysis of the surface composition was performed by means of energy dispersive X-ray fluorescence analysis (EDS). The object was treated for 90 minutes in a pure hydrogen plasma (hydrogen 4 ln/h, 20 Pa, 770 Watt and maximum temperature of artefact being 82 °C) and then was investigated again with SEM and EDS.

Another example shows a dark and uneven tarnished chalice from 1938 (LM 79223) which was also treated in hydrogen plasma for 2.5 hours. The treatment parameters being: hydrogen 6 ln/h, about 29 Pa, 1030 Watt and temperature of object maximum 85° C. This artefact was chosen due to its three dimensional shape to see if plasma reduction, as applied to smaller silver artefacts, could remove the disfiguring sulphide layer from all sides of such an object at one time or if it would be necessary to turn it between treatments.

3. Results

3.1 Measurements with optical emission spectroscopy (OES)

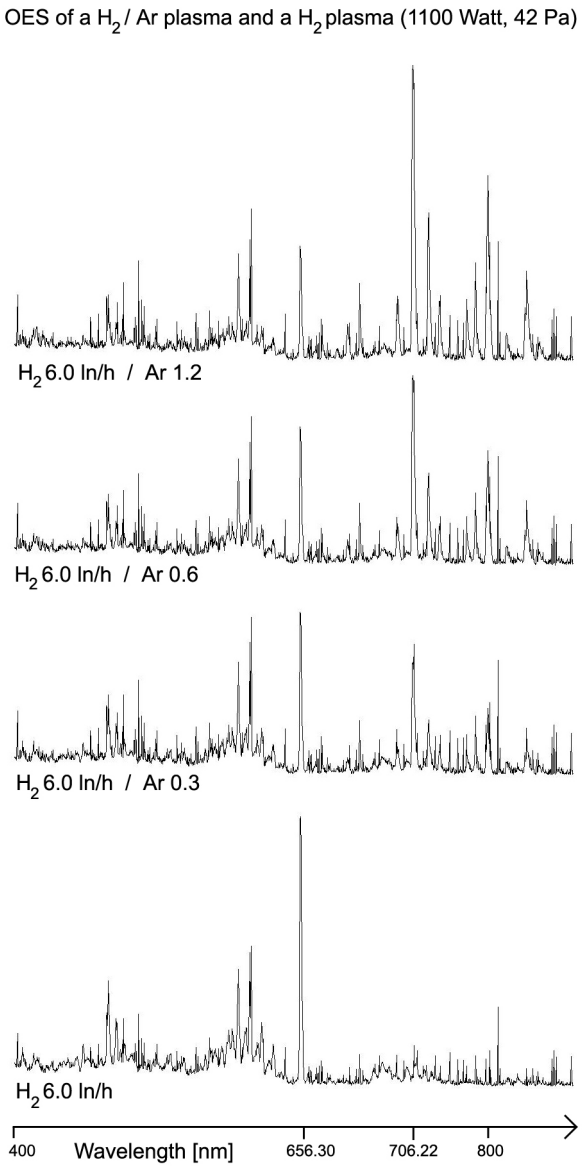

Figure 1. Typical OES from a hydrogen-argon and pure hydrogen plasma at a pressure of 42 Pa and at 1100 Watt. As a parameter the gas-flow ratio was varied. The line at 656.30 nm refers to the hydrogen emission; the line at 706.22 nm refers to argon.

Figure 1 shows OES spectra from hydrogen argon as well as from a pure hydrogen plasma. Only the most significant lines of the emission spectrum are labelled. Since atomic hydrogen plays the key role in the reduction of corrosion products its measurement is of special interest.

Atomic hydrogen has a strong red emission line at 656.30 nm. It is assumed that the intensity of this line is proportional to the steady-state concentration of atomic hydrogen produced from molecular hydrogen gas. Argon has a strong emission at 706.22 nm. If argon is added the intensity of the hydrogen line is reduced. Qualitatively the higher the argon concentration the smaller the hydrogen line becomes. In comparison a pure hydrogen plasma clearly shows a hydrogen line of higher intensity. All measurements were performed at the same level of generator power, and at the same pressure, which was adjusted by regulating the valve of the pump. It can be concluded that in the former standard reduction with 6-8 ln/h hydrogen and 0.6-0.8 ln/h argon, less atomic hydrogen is available in the vessel than in a pure hydrogen plasma.

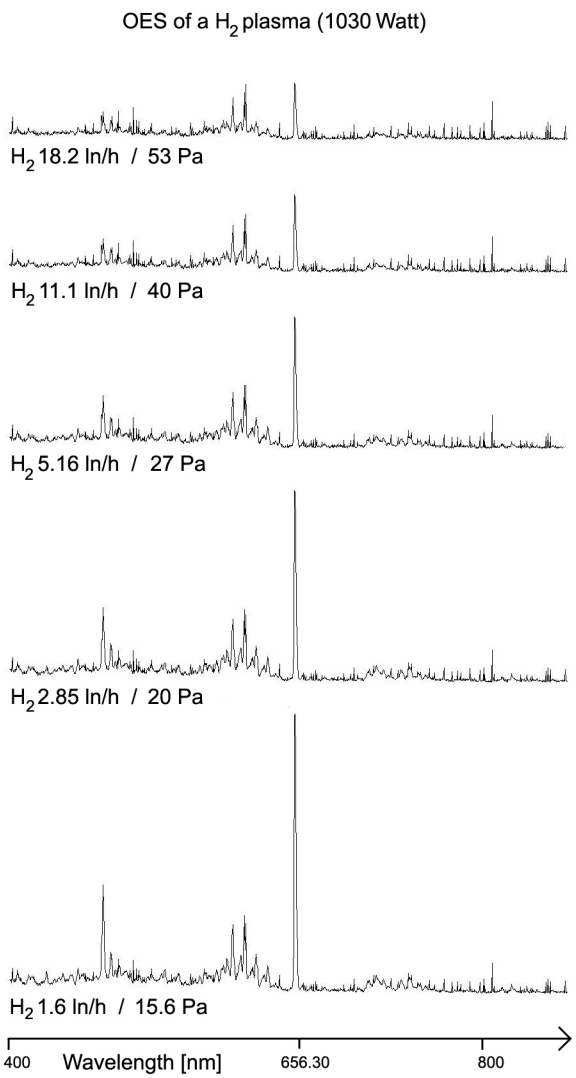

Figure 2. OES spectra observed in pure hydrogen plasma at different pressures in the vessel at 1030 Watt, fully open pump valve and increasing increments of hydrogen. The intensity of the line at 656.30 nm is assumed to be proportional to the steady-state concentration of atomic hydrogen produced.

Thus there might be an optimal amount of hydrogen for a most effective plasma reduction treatment. Figure 2 shows typical OES spectra observed in a pure hydrogen plasma at different pressures in the vessel. This was arranged with a fully open pump valve and by increasing increments of hydrogen. The capacity of the generator was kept to 1030 Watt in this series. It can be seen that there is a clear relationship between pressure and the intensity of the hydrogen line. At 15.6 Pa and 1.6 ln/h hydrogen flow the highest intensity of the hydrogen line is measured. Then the main free path for excitation and ionization corresponds approximately to the sheath layer. Below a flow of 1.4 ln/h hydrogen the plasma becomes unstable and the discharge may even collapse. It can be concluded that it is useful to reduce the amount of hydrogen to about 2 ln/h for the treatment of artefacts.

Similar characteristics can be expected during the treatment of pre-dried iron artefacts. In addition, when placed in the plasma the chemical elements emitted from the artefacts can be traced by their characteristic lines when the released elements and/or formed compounds are present in high-enough concentrations.

The pure hydrogen plasma which because of its gentle treatment nature, was applied only to sensitive materials such as silver, is now also applied to archaeological iron artefacts. The same reduction effect can now be achieved at lower temperatures. For pre-dried iron artefacts the surface temperatures lie around 80 °C as compared to ~120 °C in a typical hydrogen-argon plasma.

3.2 Metallographic sampling of iron nails

All samples showed a clear stratigraphy between outer disfiguring corrosion layers, original surface, and metal cores if still existent.

The SEM images were of special interest since back scattered electron imaging (BSI) shows different states of corrosion. When a sample is being scanned with the electron beam, backscattered electrons are also formed. Their intensity is dependent on the atomic number of the excited element. Light areas in the backscattered electron images correspond to high average atomic numbers. Areas with a metal core are therefore light, heavily corroded areas appear darker (the atomic number of iron is 26, of oxygen 8, of hydrogen 1).

Results between the two groups that had undergone hydrogen and hydrogen-argon plasma reduction showed no significant differences. In many cases, after plasma reduction for the pure hydrogen as well as for the hydrogen-argon, a clear separation of the outer corrosion layer from the original surface was observed. It can be assumed that this separation contributes to the facilitation of the mechanical cleaning.

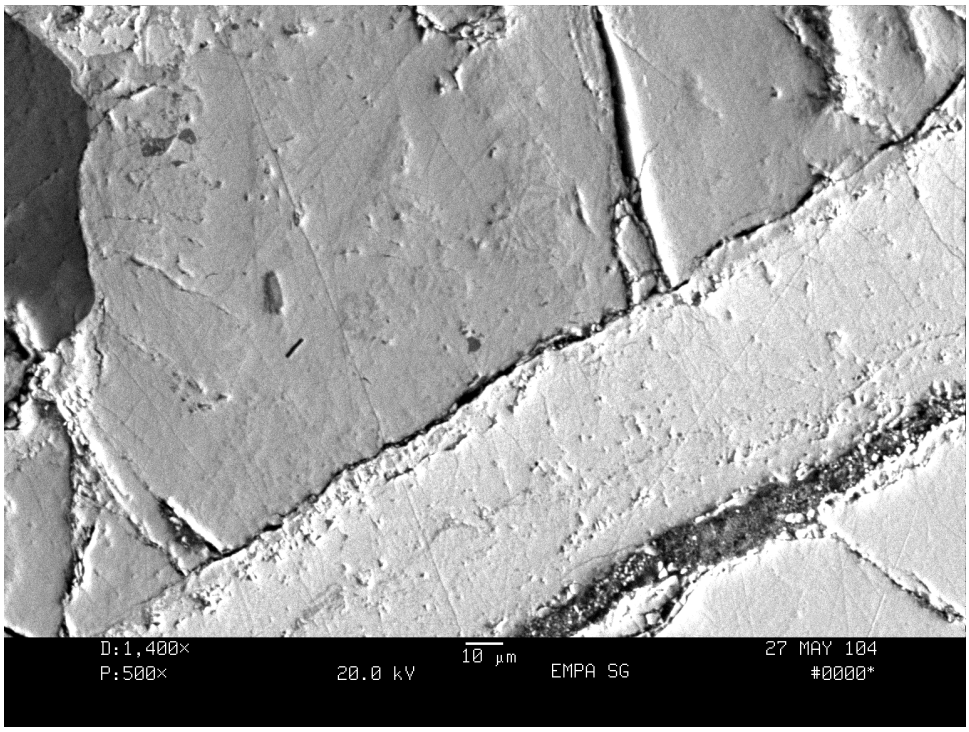

Figure 3. SEM of a polished sample of a nail (No 99.15) after hydrogen-argon plasma reduction, at a magnification of 500x the artefacts temperature being maximum 116 °C.

Figure 3 shows a nail of the group selected for the hydrogen-argon plasma after plasma reduction. The artefact`s temperature measured with thermocouples had reached maximum 116°C.

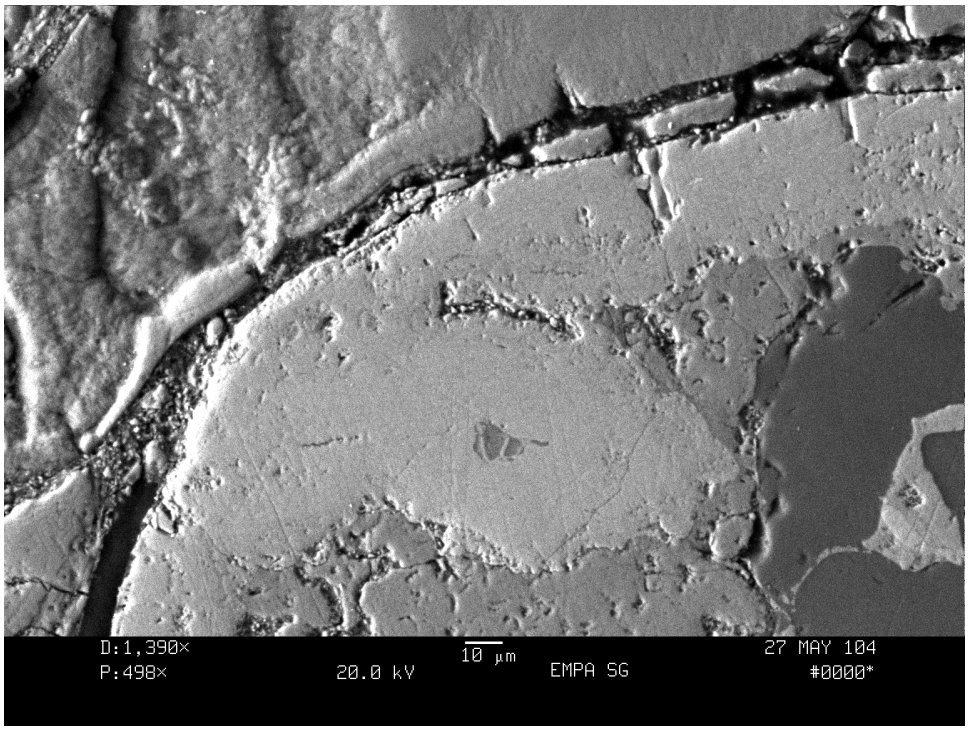

Figure 4. SEM of sample of a nail (No 99.2) selected for the pure hydrogen reduction after treatment, at a magnification of 498x, the artefacts` temperature during reduction was around 70 °C.

Figure 4 shows a representative of the group treated in a hydrogen plasma and at lower pressure after reduction. On account of a connection between pressure and sample temperature, the temperatures measured during plasma were ca. 70 °C.

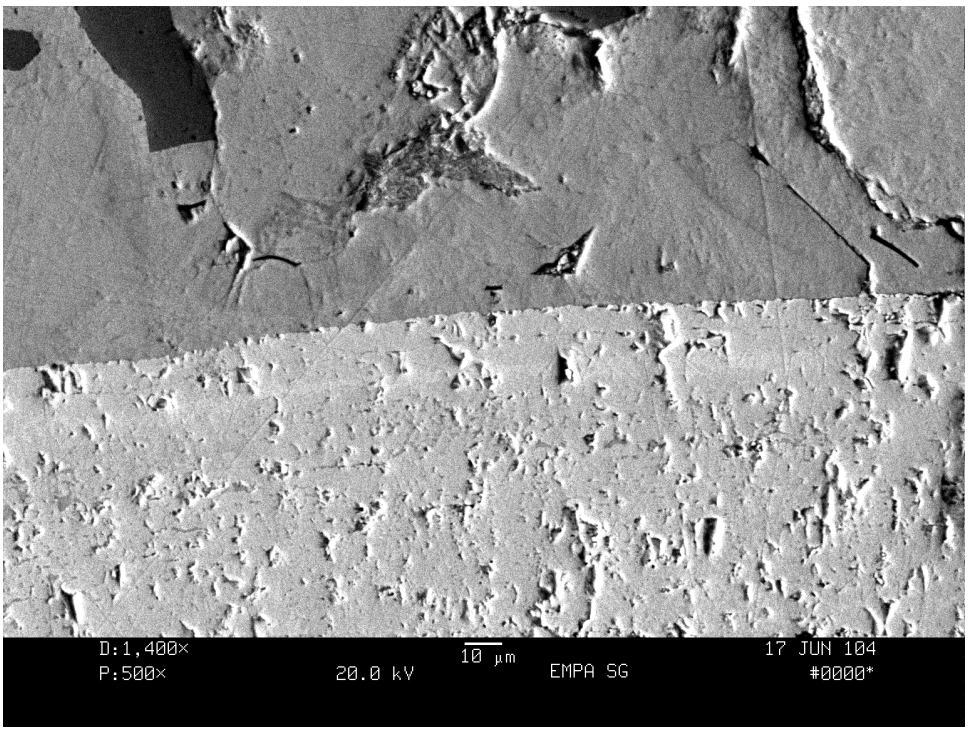

Figure 5. SEM image of metallographic sample of a nail (No 99.16) after pre-drying in a vacuum oven at 85 °C. At a magnification of 500x no separation between disfiguring corrosion layers and original surface can be seen.

The metallographic samples of the nails that had only undergone pre-drying showed no relatable changes in their structure or stratigraphy. Figure 5 shows the sample of a nail after the treatment in the vacuum oven at ca. 85 °C.

From this it can be concluded that the pre-drying at ca. 80 °C as is usually applied to archaeological iron artefacts prior to plasma reduction, will not lead to an improved facilitation of the removal of corrosion layers.

3.3 Silver artefacts

The spoon (LM 17672) was examined prior to and after the plasma reduction. It was of special interest whether the plasma treatment would change any details important to the manufacturing of the artefact.

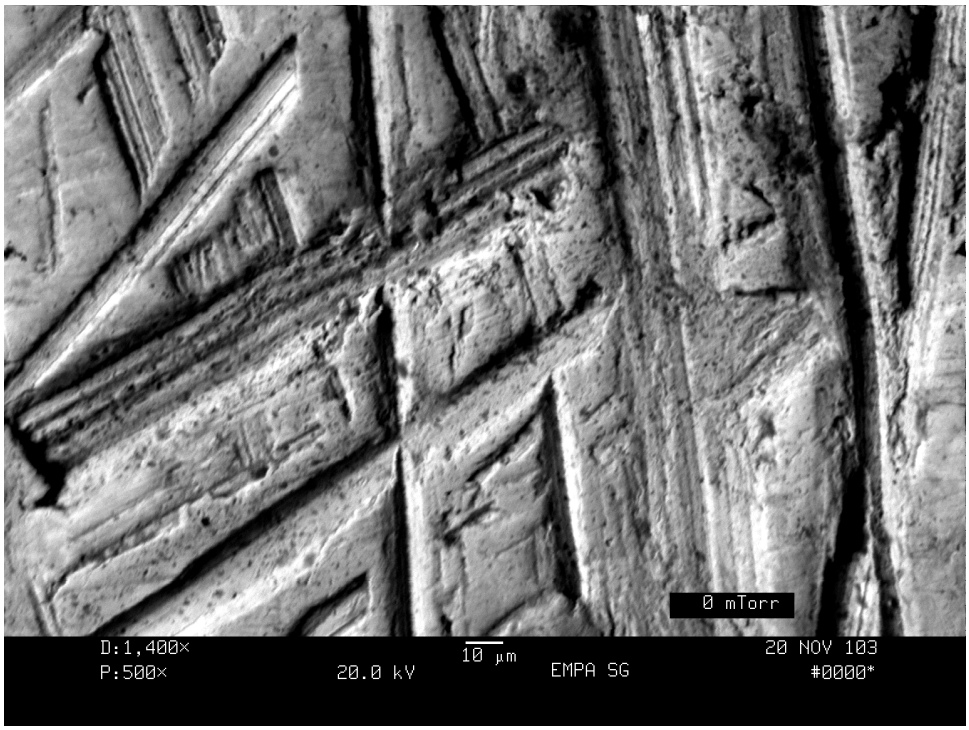

Figure 6. Detail of silver spoon prior to plasma reduction at 500x magnification under the SEM, scratches being visible.

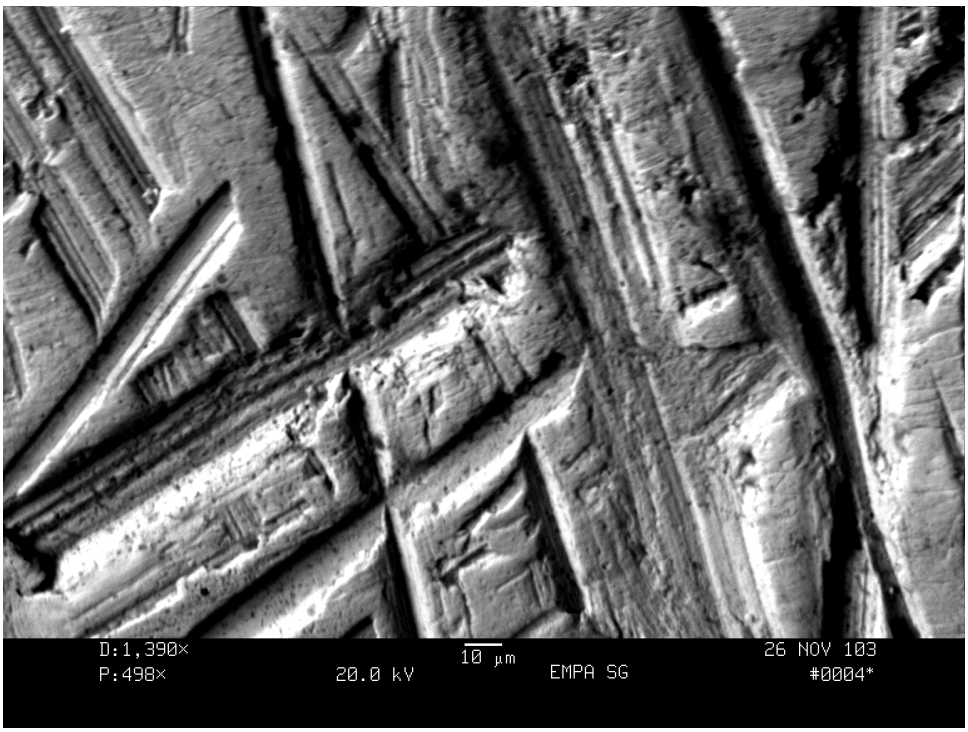

Figure 7. Detail of spoon after hydrogen reduction at 500x magnification, no change of surface structure or additional damage to the surface is visible.

Prior to the reduction treatment, the surface of the artefact showed heavy scratches due to prior handling and possibly also cleaning as can be seen in Figure 6. Figure 7 shows the same detail after plasma reduction. At a magnification of 500x no change of surface structure or additional damage to the surface is visible. As expected the EDS spectrum prior to the plasma reduction showed lines of silver and gold but also of sulphur, mercury and copper, see Figure 8.

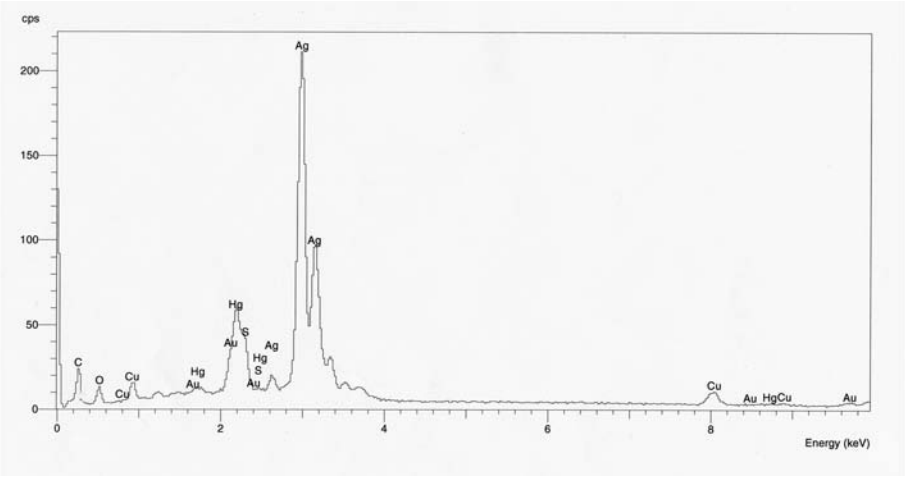

Figure 8. EDS spectra of silver spoon prior to plasma reduction showing lines of silver and gold but also of sulphur, mercury and copper.

After the plasma treatment the EDS spectrum (Figure 9) shows that sulphur has been removed whereas silver, gold, mercury and copper are still present. Here the presence of mercury indicates the gilding method used. It is important that this finding can still be detected after plasma reduction.

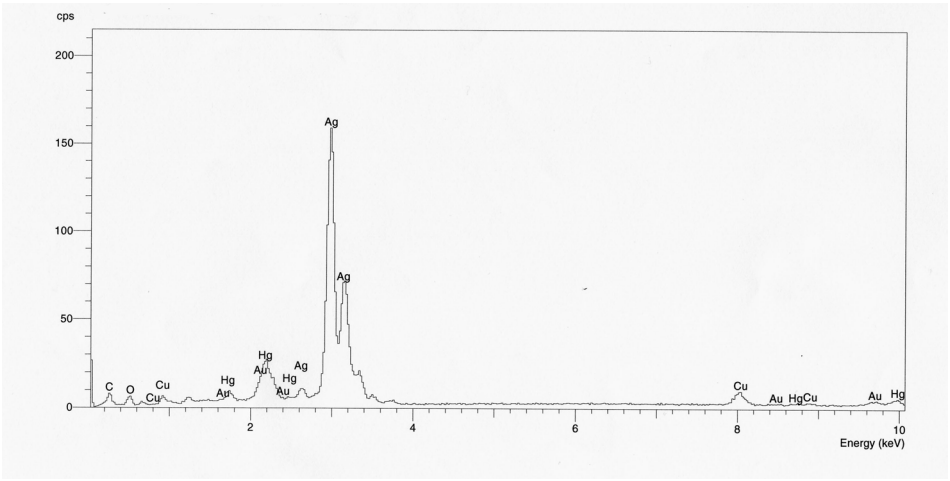

Figure 9. EDS spectra of silver spoon after plasma reduction, showing that sulphur has been removed whereas silver, gold, mercury and copper are still present.

The example also shows that it is possible to remove the tarnish layers with hydrogen plasma reduction without noticeably effecting other chemical elements.
The object looks nicely cleaned after the plasma treatment and is still showing darker areas in the depths and therefore a lively appearance. This is considered to be a major advantage of the method in opposite to electro-chemical and chemical silver cleaning methods. In this case no other surface treatment has been applied.

For the tarnished silver chalice (LM 79223), the tarnish layer was gradually removed within half an hour of the hydrogen plasma reduction, with a few dark areas remaining. After another hour of treatment the dark areas were almost completely lightened.
The object was placed in the reactor lying on glass grids and had not been turned during treatment.

Figure 10. Silver chalice (LM 79223) prior to hydrogen plasma reduction with disfiguring tarnish layer.

Figure 11. Silver chalice after 2.5 hours of hydrogen plasma reduction, no other surface treatment has been applied.

Figure 10 and 11 show the object before and after the plasma treatment and no other surface treatment has been applied in this case.

If very thick tarnish layers were present the surface could appear slightly matt after the plasma treatment. A combination of plasma reduction and gentle polishing with pure cotton wool has been shown to slow down the rate of retarnishing without leading to new scratches (Schmidt-Ott 2004).

4. Discussion

Until recently treatment with pure hydrogen plasma and the application of low pressure during reduction had been applied to silver artefacts only. It has been considered a "softer" process in which the object temperatures remain fairly low (av. 50-80 °C).

The optical spectroscopy of hydrogen plasmas at smaller operation pressure showed that not only lower treatment temperatures can be reached, but also an increase of radical density is present as compared to the hydrogen-argon treatment. It can therefore be assumed that pure hydrogen plasmas with less hydrogen and at lower pressure also supply a high amount of ionized hydrogen and are therefore more effective for reduction of corrosion products than are mixtures of hydrogen and argon which have been applied as a standard treatment for iron artefacts so far.

To cross-check this optical result, the effects of the different plasma applications on iron artefacts were investigated. Pure hydrogen plasma and the hydrogen argon plasma show similar effects on metallographic samples examined so far. In both cases a clear line of separation between outer corrosion layers and original surfaces can be seen and the facilitation of the mechanical cleaning after plasma reduction is ascribed to this fact. Since such a separation also seems to work after application of a pure hydrogen plasma at even lower temperatures it is intended to use such a plasma not only for silver but also for iron artefacts.

5. Conclusions

The introduction of optical spectrometry into the conservation process has delivered a means by which to monitor the plasma reduction. This allows one to visualize the effectiveness of operation parameters applied; the aim being to provide the highest rate possible of ionized hydrogen considered necessary for an effective reduction process.

After such systematic investigation of the plasma it seems that the pure hydrogen plasma originally considered to be less effective than a mixture of hydrogen and argon proved to be at least as efficient. This is of special interest since a pure hydrogen plasma at low pressure causes a reduction of the iron artefact's temperature to about 80 °C during plasma treatment. A change of the metallographic information contained in the artefact during treatment is, therefore, improbable. The positive effect of the facilitation of mechanical cleaning and the speeding-up of the subsequent desalination in alkaline sulphite for archaeological iron artefacts, continues to be a major advantage of plasma reduction for pure hydrogen plasmas as well.

The potential of hydrogen plasma for the reduction of silver sulphide layers remains extraordinary. Sulphides and also chlorides are removed without any damage to the artefact's surface. Compared to other established silver cleaning methods, plasma reduction exhibits many advantages: there is no change to surface structures, no residues from the treatment remain in or on the artefact, and no loss of silver occurs.

Plasma reduction is, therefore, a suitable method for silver artefacts, which are too fragile to be cleaned mechanically or chemically.

Acknowledgements

This work was performed at the Swiss National Museum Zurich in collaboration with the PhD programme in object conservation at the State Academy of Art and Design Stuttgart. The Swiss National Museum is thanked for the conducive working conditions that contribute towards the realisation of the measurements and Prof. Dr. G. Eggert, State Academy of Art and Design Stuttgart, for his ongoing interest in this new project.
The author would also like to thank Prof. Dr. H. Keppner, Ecole d'Ingenieurs du Canton de Neuchâtel for stimulating exchange of results of OES in the plasma.
Further the author would like to thank the archaeological service of the Kanton of Zurich for supply of iron artefacts for metallurgical sampling and study purposes. Special thanks is also due to the Swiss Federal Laboratories for Materials` Testing and Research (EMPA) in St. Gallen, for making possible the use of the SEM and EDS equipment.

References

Archer P.J. and Barker B.D. (1987). Phase changes associated with the hydrogen reduction conservation process for ferrous artefacts, Journal of the Historical Metallurgy Society, 21, 86-91.

Daniels V., Holland L. and Pascoe C. (1979). Gas plasma reactions for the conservation of antiquities, Studies in Conservation, 24, 85-92

Keppner H., Kroll U., Torres P., Goetz M and Meier J. (1997). Process-enhancement of hydrogen-plasma treatment by argon?, Zeitschrift für Schweizerische Archäologie und Kunstgeschichte (ZAK), 54, 25-28

Patscheider J. and Vepřek S. (1986). Application of low-pressure hydrogen plasma to the conservation of ancient iron artefacts, Studies in Conservation, 31, 29-37

Schmidt-Ott K. (1997). Application of low pressure plasma treatment at the Swiss National Museum and assessment of the results, Zeitschrift für Schweizerische Archäologie und Kunstgeschichte (ZAK), 54, 45-50

Schmidt-Ott K. and Boissonnas V. (2002). Low-pressure hydrogen plasma: an assessment of its application on archaeological iron, Studies in Conservation, 47, 81-87

Schmidt-Ott K. (2004). Plasmareduktion von Silberoberflächen, In Ogden, J. (ed.) Postprints Exposure 2001, accepted for publishing

Scott D.A. (1991). Metallography and microstructure of ancient and historic metals, Getty Conservation Institute, (Singapore: Tien Wah Press. Ltd.)

Schweizer F. and Meyers P. (1978). Structural changes in ancient silver alloys: the discontinuous precipitation of copper. ICOM 5th Trienal Meeting, Zagreb Rapport 78, 23, 5

Thompson F.C. and Chatterjee A.K. (1954). The age-embrittlement of silver coins. Studies in Conservation, 1, 115-125

Tylecote R.F. and Black J.W.B. (1980). The effect of hydrogen reduction on the properties of ferrous materials, Studies in Conservation, 25, 87-96

Vepřek S., Eckmann C. and Elmer J. (1988). Recent progress in the restoration of archaeological metallic artifacts by means of low-pressure plasma treatment, Plasma Chemistry and Plasma Processing, 8, 4, 225-241

Voûte A. (1997). The plasma equipement at the Swiss National Museum- observations and improvements, Zeitschrift für Schweizerische Archäologie und Kunstgeschichte (ZAK), 54, 41-44

A study of the analysis and removal of chloride in iron samples from the “*Hunley*”
M. Drews, P. de Vivies, N. Gonzalez, P. Mardikian
pp. 247-260

An approach to the conservation of deeply corroded archaeological silver: the *polos* from Crucinia

A. Archi Olsoufieff [a], O. Colacicchi Alessandri [b], M. Ferretti [c*]

[a] Conservator restorer, Roma, Italy
[b] Laboratorio di Restauro, Museo Nazionale Romano, Soprintendenza Archeologica di Roma, Italy
[c] CNR – Istituto per le Tecnologie Applicate ai Beni Culturali, Monterotondo St. (Roma), Italy

Abstract

This work presents a case study on the conservation of highly deteriorated archaeological silver objects; the subject is a *polos* that is, a rich and sophisticated headgear, made of silver laminae, embossed and gilded, belonging to a priestess' burial from Southern Italy, dated around the 6th century B.C. The conservation treatment was particularly complex due to a unique concomitance of different problems such as the extreme fragility and distortion of the pieces, the lack of comparisons, and the poor context information.
Scientific investigations concerned both the conservation-related aspects and the fabrication technique: radiographies allowed location of cracks and areas of deep corrosion, whereas scanning electron microscopy provided information on the corrosion patterns and the gilding technique.

Resumen

Este trabajo presenta el estudio de un caso de conservación de objetos de plata arqueológica fuertemente corroídos; se trata de un *polos*, esto es un rico y sofisticado casco hecho de láminas de plata, repujado y dorado, perteneciente al enterramiento de una princesa del sudeste de Italia, y datado en el siglo VI a.C. aproximadamente. El tratamiento de conservación fue particularmente complejo debido a la concomitancia única de distintos problemas como la extrema fragilidad y distorsión de las piezas, la falta de elementos de comparación y la poca información del contexto.
Las investigaciones científicas trataron tanto los aspectos relacionados con la conservación como las técnicas de fabricación: las radiografías permitieron localizar las fracturas y zonas de corrosión intensa antes de la limpieza, mientras que la microscopía electrónica proporcionó información acerca de las capas de corrosión y de la técnica de dorado.

Keywords: polos, archaeological silver, conservation, gilding, corrosion, Crucinia Metaponto

1. Introduction

In 1991 a rich burial site reputedly of a priestess (Guzzo, 1996, De Siena, 2000, Lippolis, 2002) dated around the 6th century BC, was excavated at Crucinia (Metaponto, Southern Italy). Among the objects, was one of outstanding archaeological and artistic importance: a headgear of the *polos* type, which is known to have a religious meaning. The shape of the *polos* was probably cylindrical (Figure 1, left); it was made of silver bands, some of which were gilded, decorated with appliques and a succession of *kouroi* (naked standing virile figures) and horses, embossed in silver lamina and gilded. The *kouroi* and horses are embossed in the form of closed shells, the two valves being obtained from a single folded lamina (Giumlia-Mair, 2001, Giumlia-Mair et al., 2001) Further *korai* (dressed standing feminine figures), constructively similar to the previous ones, are supposed to function as pendants at the head's sides. The metallic structure was fixed to a support made of organic material, possibly cloth or leather, which is now lost; the existence of this support proved by numerous silver staples inserted in the bands.

* Corresponding author: tel +39 06 9067 2690; fax +39 06 9067 2373; email: marco.ferretti@itabc.cnr.it

A preliminary analysis of the object's conservation conditions found serious deterioration, due to the burial conditions (Figure 1, centre) but also caused by the urgency with which it was rescued (Figure 1, right) and to the incompleteness of previous cleaning treatments. The observed alterations include:

- the almost complete mineralization and the consequent fragility of the laminae;
- the presence of complex corrosion patterns involving thick layers of silver chloride hiding the gilding, sometimes alternated to calcium carbonate, also thick and adherent to the gilding;
- the distortion of some fragments and the incompleteness of the left-hand side, due to the pressure of the deceased preistess's head;
- the extreme and diffused fragmentation;
- the loss of the organic support material and of some joining elements.

Further problems related to the urgency of the rescue, to the consequent poor documentation of the excavation and to the loss of connections and pertinences experienced by the *polos* after the find.

These considerations provide a realistic idea of the complexity of the restoration – that the CO.RE.AR. group and A. Archi Olsoufieff were to carry out – not only as regards cleaning and consolidation of the laminae, but also – and mainly – as regards the assembly and recomposition of the artifact, given the exiguity of typological comparisons (CO.RE.AR. et al., 2002).

Figure 1. Graphical interpretation of the *polos* (left); detail of the conservation conditions of bands A and B after the rescue (centre); the *polos* during the urgent rescue (right); photographs: courtesy of the Soprintendenza Archeologica della Basilicata.

2. Conservation treatment

Before the conservation treatment, a number of preliminary activities took place; these included:

- photographic documentation of the material as received;
- sorting, visual identification and typological grouping of all the pieces, carried out with the aid of the poor pre-existing documentation. During these operations many connections among the fragments were found;
- establishment of an identification system related to the bands; these were identified with the letters A to G starting from the top (Figure 2).

Following these preliminary operations, the pieces were radiographed.

Figure 2. First recomposition of the polos resulting from the preliminary identification of the fragments (photograph by P. Rizzi).

2.1 General principles

Different cleaning strategies were considered, with special regard for mechanical and chemical methods; these had to be suitable to remove the thick layers of silver chloride that hid most of the gilded surfaces, thus preventing their readability (Figure 3). In this phase considerable support was provided by radiographies and scanning electron microscope investigations.


Figure 3. Details of the corrosion products and deposits covering the fragments (left and centre) and of the gilding conditions (right).

Mechanical cleaning was mostly used, due to the possibility of better controlling the cleaning level. Optical aids for the magnification of the concerned areas were extensively used. A mechanical and chemical combined cleaning was used for those areas with alternate stratification of silver chloride and calcium carbonate and on the appliques, that were particularly delicate due to the small dimensions and thin lamina (Plenderleith et al., 1971; Angelini et al., 1987; Marabelli, 1995).

Due to the almost complete mineralization and the consequent fragility of the pieces, it was decided to limit the cleaning treatment of the laminae to the front surface only. For the non-gilded bands and where the gilding

was missing, the deep corrosion made the identification of the original surface particularly complex. It was therefore decided that the optimum cleaning level was the one that left a thin layer of chloride allowing a view of the underlying details of the original surface.

2.2 Operational aspects

The general sequence of the operations is as follows:

- removal of the materials resulting from the previous conservation treatments by means of suitable solvents and mechanical cleaning;
- mechanical removal of soil and incoherent corrosion products from the rear surface of the laminae;
- in case of chemical cleaning, the rear of the laminae was consolidated and protected from the chemicals by applying a layer of high concentration acrylic resin;
- before mechanical cleaning, the fragments were temporarily consolidated by back-veiling with cotton gauze stuck with acrylic resin (Figure 4, left); silicone rubber moulds were made to support the pieces and avoid concentrated stresses during mechanical cleaning (Figure 4, centre);
- removal of the thick layers of silver chloride and calcium carbonate by means of mechanical cleaning of the surfaces, carried out with surgical blades, abrasive micro-spheres mounted on a prosthetic drill, soft brushes (Figure 4, right). It was preferred to leave part of the silver chloride on the most fragile edges of the laminae;
- in the presence of extended alternate stratifications of silver chloride and calcium carbonate – particularly on the appliques – mechanical cleaning was alternated with immersions in 10% sodium thiosulphate and 10 to 20% trisodic EDTA solutions (Marabelli, 1995). Localized concretions of calcium carbonate on the gilded surfaces were treated with ion-exchange strong cationic resins;
- surface finish with damp pads and bicarbonate of soda and/or ethanol pads and silversmith pastes of different fineness;
- removal of the temporary veilings with acetone;
- removal of the products residues by rinsing in distilled water and/or ethanol;
- drying with infra-red lamps;
- consolidation of the fragments by means of low concentration (1.5%) acrylic resin;
- completion of the search of connections among the fragments;
- gluing of the fragments and integration of little lacunae with epoxy resin, suitably coloured by inorganic pigments;
- consolidation of the recomposed laminae by back-veiling with polyester fabric and 10% acrylic resin (Marabelli, 1995);
- final protection of non-gilded surfaces with acrylic resin;
- gluing of the detached decorations – rosettes, ram heads, doric *kimation* – to the bands A, C and D by nitrocellulosic resin; the latter was used because it is easily reversible and commercially available at the right concentration (Marabelli, 1995).

Figure 4. Temporary back-veiling of the fragments (left); piece supported by a silicone rubber mould during mechanical cleaning (centre); result of the mechanical cleaning with respect to uncleaned areas (right).

Before the final back-veiling of the laminae, all the recomposed elements were graphically documented (by C. Damiani, Roma) as placed in their final position. Special consideration was made for the position of the staples and the holes used to connect the *kouroi* and the horses to the laminae and the laminae to the organic support.

3. Reconstruction hypotheses and final lay-out

The conservation treatment and recomposition of the fragments allowed a more accurate interpretation of the surfaces, as well as the collection of more information concerning the original positions of the *polos*' elements. The identification of the connections among the bands allowed to accurately estimate the headgear height to 25 cm. The circumference is more uncertain: given the deceased priestess' skull dimensions, it is probably about 54 cm.

Four hypotheses were proposed for the object reconstruction, differing from one another mainly as regards the positions of the *kouroi* and horses on band B. The uncertainties are related to problems of symmetry and to the fact that, among the 22 *kouroi* and horses, only 12 had an identified position.

The lay-out resulting from the final hypothesis is shown in Figure 5. Given the deformations in the central part of the *polos*, it was impossible to arrange the fragments on a support structure that would suggest a headgear. It was therefore decided to set the pieces on four separate plexiglass bands, provided with suitable templates to support the distorted parts; all the elements were attached to the plexiglass by nylon threads; an inclined plexiglass plane supported the whole.

Figure 5. Polos recomposed on the support system: full view (left) and detail (right); photographs by P. Rizzi.

4. Scientific investigations

The polos was investigated in two steps: the first one was commissioned from AB2 Art, the results will be referred to as "(AB2 Art 2001)"; the remaining investigations were directly carried out by the authors within collaborations acknowledged in the due section. Radiography and scanning electron microscopy were employed to study both conservation-related aspects and the fabrication technique. In particular, given the unreadability of the surfaces, X-rays showed – before cleaning – cracks and areas of deep corrosion. It was also possible to identify some of the systems used to mechanically join the appliques to the bands. Further information on the gilding technique, the corrosion patterns, alternation of different layers of silver chloride and calcium carbonate and mineralization of the laminae was provided by scanning electron microscopy.

4.1 Radiographies

X-rays were carried out on all the pieces immediately after their preliminary classification. The working conditions are: high voltage 80kV, current 4mA, exposure time 5-8min (AB2 Art, 2001). Figure 6, left. shows

the radiographic detail of one of the horses and part of the adjacent lamina: cracks and areas of deep corrosion are clearly visible. The radiographs also show (right) the details of the shape of a *kore*. Figure 7 shows different fragments of band D: the top-most fragment is relatively uncorroded and shows numerous staples – used to join the lamina to the organic support – in their seats. A flower and some empty loops are also visible; the band at the bottom of the image is more corroded and cracked; it only has empty loops. Besides the usual cracks, areas of deep corrosion and staples, Figure 8 shows an interesting – digitally processed – detail of a loose decoration element hidden behind a flower on band C.

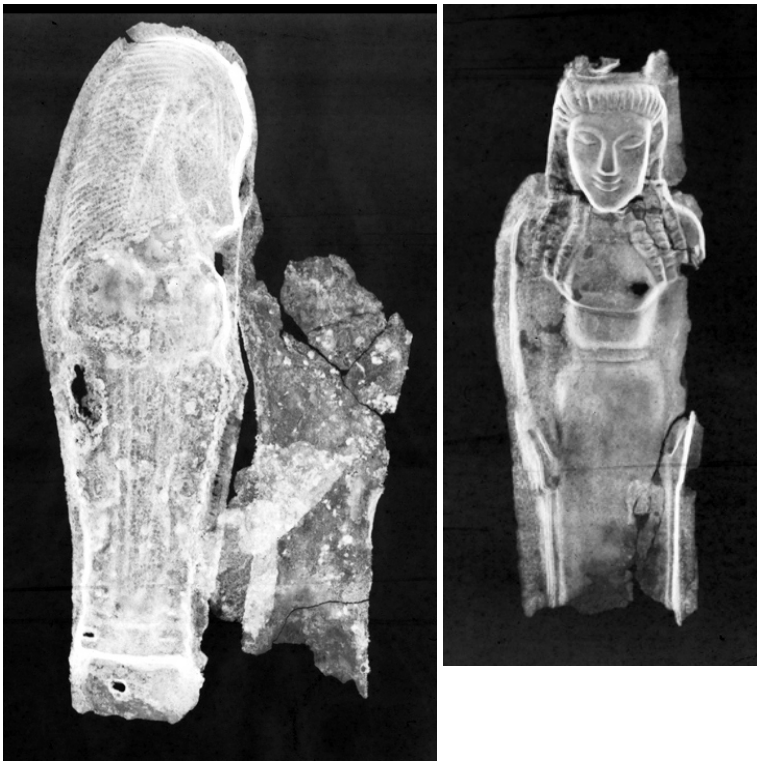

Figure 6. X-ray images of one of the horses with part of the adjacent lamina (left) and a *kore* (right).

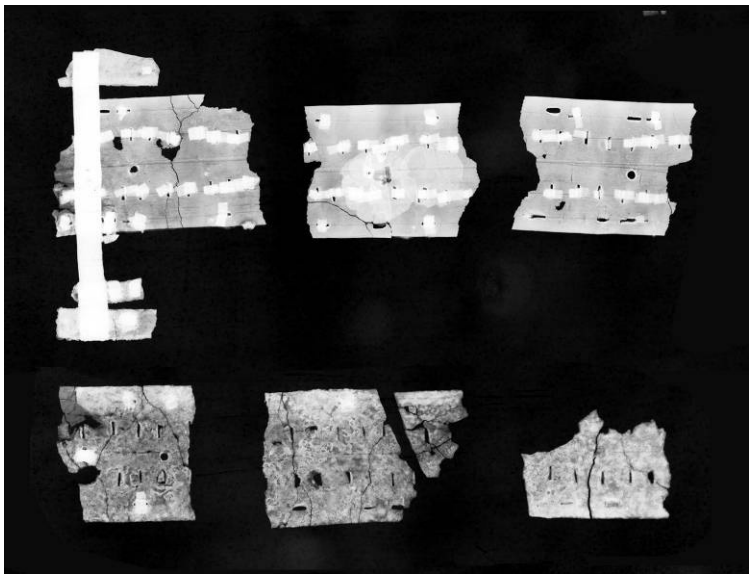

Figure 7. X-ray image of different fragments of band D.

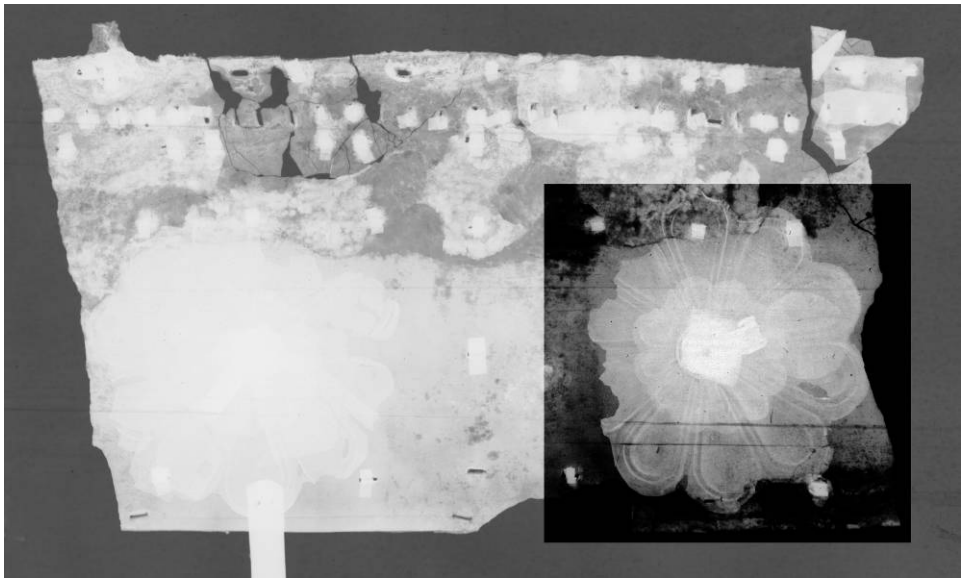

Figure 8. X-ray image of band C; digital processing of a detail showing a flower that hides a loose rosette behind the corolla.

4.2 Scanning electron microscopy

Band C, half-rosette, sample C1: Figure 9 left shows the corrosion pattern typical of this object: below the gilding, the lamina is entirely mineralized; further alternately stratified corrosion products (silver chloride) and deposits (calcium carbonate) grow on the non-gilded side of the lamina; the stratification is possibly related to the periodical floodings and droughts experienced in the tomb. A detail of the mineralized lamina is shown on the right: from the surface (right) inwards (leftwards), it is possible to observe:

- a deposit of calcium carbonate;
- a solid layer of silver chloride, just above the gold leaf;
- the gold leaf;
- just below the gold leaf, a spongy structure of silver chloride and calcium carbonate, corresponding to the original silver lamina; the calcium carbonate may precipitate due to the cathodic reduction of oxygen to hydroxyl in the presence of calcium ions and carbonic acid (Marabelli, 1995).Measured in different parts of the spongy structure, the relative concentration ratios of Ag, Cl and Ca appear reasonably constant;
- calcium carbonate alone and a solid layer of silver chloride.

The described corrosion structure and the concerned elemental maps are shown in Figure 10 at higher magnification: the leaf thickness is about 3 microns, no Hg is detected in any part of the cross-section.

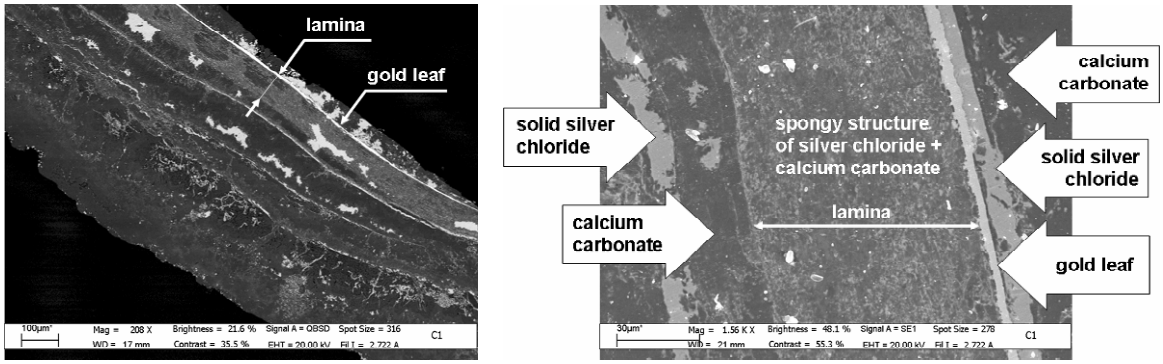

Figure 9. Band C, half-rosette, sample C1, cross-section: backscattered electron images of the corrosion pattern (left) and a detail of the lamina (right).

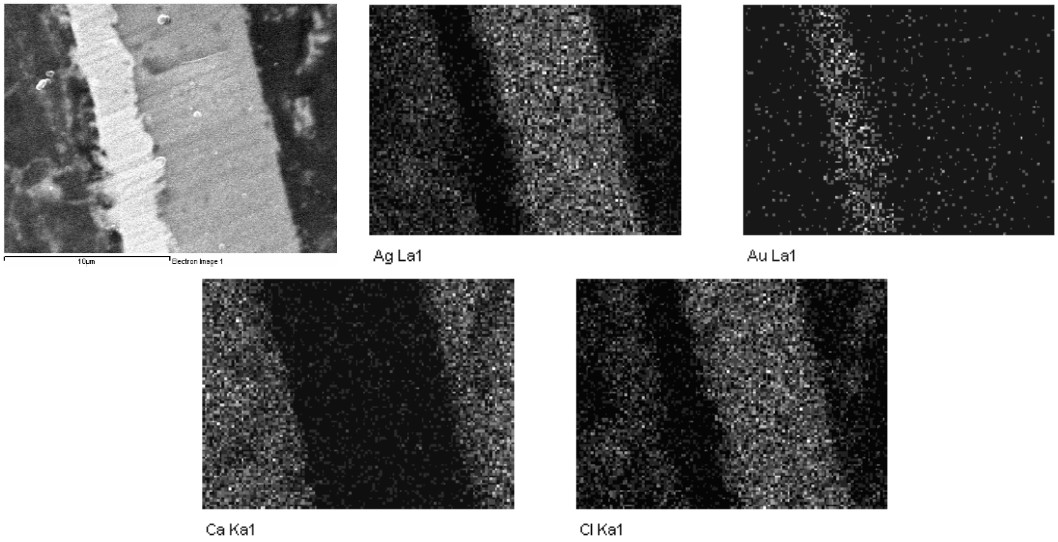

Figure 10. Band C, half-rosette, sample C1, cross-section: backscattered electron image and elemental maps of the leaf and its immediate surrounds

Further information about the gilding technique (provided by Figure 11) that shows the partial detachment between two gold leaves in an overlapping zone; this indicates the exclusion, with reasonable certainty, that the so-called diffusion bonding (Oddy, 1993) ever took place. It is likely that the gold leaf was applied after the embossing and no heating was carried out.

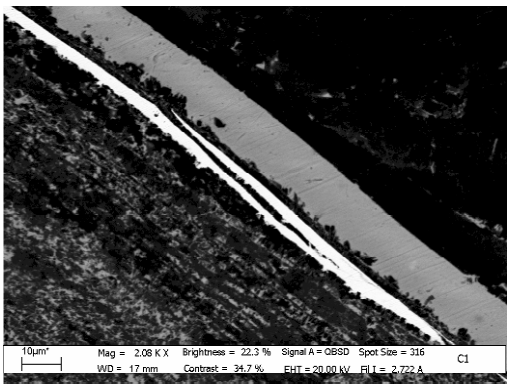

Figure 11. Band C, half-rosette, sample C1, cross-section: backscattered electron image showing the detachment between two gold leaves in an overlapping zone.

Band G, staple, sample C2: Figure12 shows the cross-section of a staple and the surrounding lamina, the concerned elemental maps are shown as well. Similarly to sample C1, it is possible to observe the complex corrosion pattern made of solid silver chloride and the spongy structure of silver chloride and calcium carbonate.

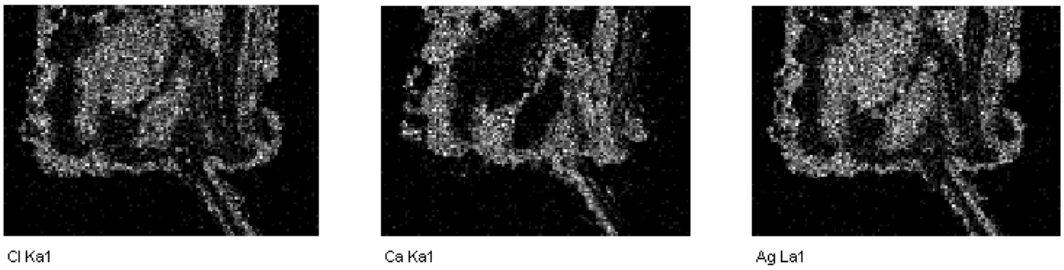

Figure 12. Band G, staple, sample C2, cross-section: backscattered electron image and elemental maps of a staple and the surrounding lamina.

Microanalysis shows the presence of Pb and Sn on the head of the staple (Figure 13, left). The method of joining some decorative components to the bands still remains unclear, as no joining elements were found; therefore it is possible that these are the remains of soft solder used for joining. Several areas of the sample (Figure 13, left and right) show a peculiar structure – whose nature is not understood at the moment – made by the alternate overlapping of numerous gold layers and silver chloride layers, the former being thinner than the gilding.

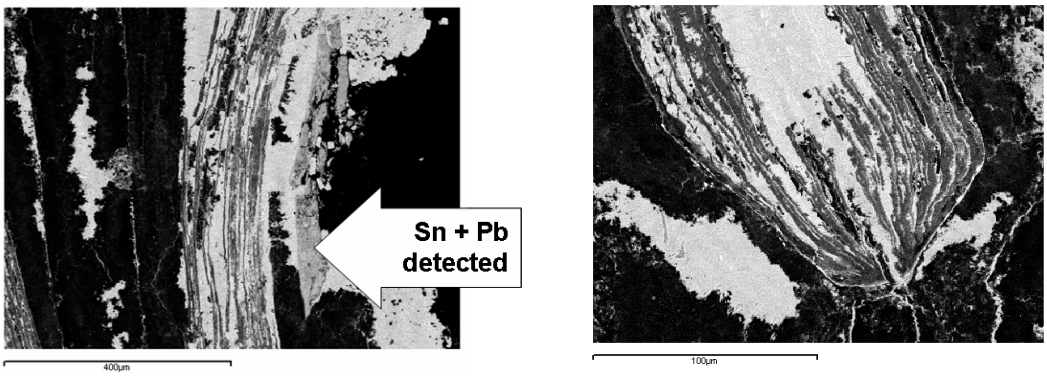

Figure 13. Band G, staple, sample C2, cross-section: backscattered electron image of the staple's head (left) and the tip of the wing (right).

Band D2, sample C3: the sample is almost uncorroded, the microanalysis shows almost pure silver, in particular there is no alloying copper. In the optical microscope view the etched cross-section shows the slipping planes due to cold-working (Figure 14, AB2 Art, 2001).

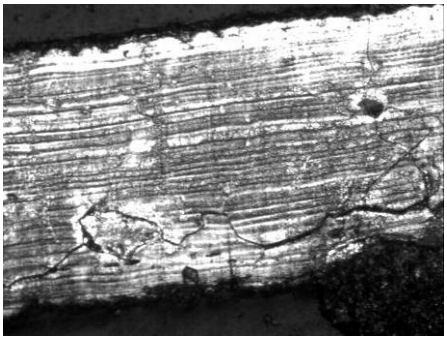

Figure 14. Band D2, sample C: optical microscope image of the etched cross-section showing the slipping planes due to cold-working.

Band C, fragment of flower: the images (Figure 15) are indications of the bad conservation conditions, frequently found on the gold leaf. They show the leaf edge detached and folded with the underlying silver chloride (left); and the working marks, left in the metal to assist the adhesion of the leaf to the substrate (right).

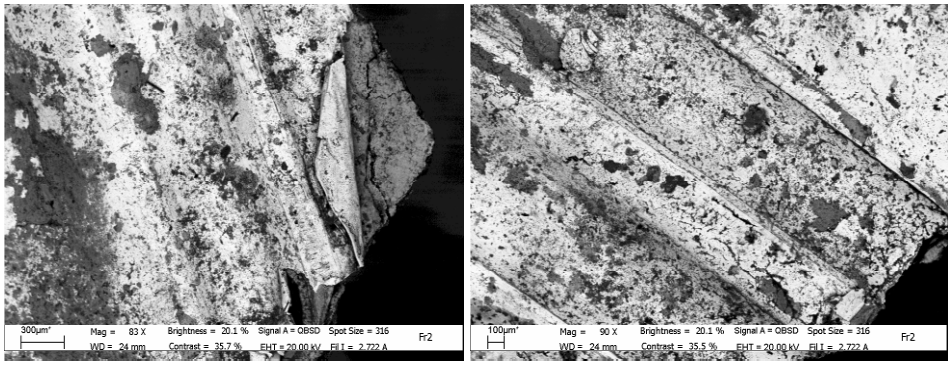

Figure 15. Band C, fragment of flower: backscattered electron images of the gold leaf showing a detachment (left) and the working marks (right).

Band C, petal of flower, sample C5: Figure 16 shows an example of lamina gilded on both sides (AB2 Art, 2001).

For the samples investigated, the thickness of the laminae ranges between 200 microns for band D – which has a structural function – and 50-80 microns for the decorations. Other parts such as band C and the vertical supporting sticks (E) were not investigated, but visually appear even thicker.

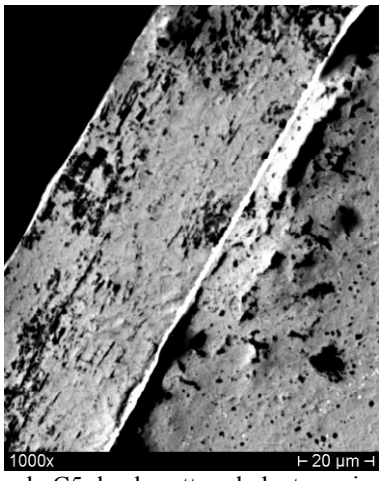

Figure 16. Band C, petal of flower, sample C5: backscattered electrons image of a lamina gilded on both sides.

5. Conclusions

The paper has discussed the case of the *polos* from Crucinia as a significant example of the problems concerned with the conservation of archaeological silver objects. The conservation treatment, the reconstruction and the study of the *polos* were particularly complex and delicate: the very bad conservation conditions and the fragmentation of the pieces were only two of the reasons. Further problems came from the poor documentation concerning both the excavation – carried out in conditions of extreme urgency – and the previous cleaning. The conservation treatment recovered the interpretation of the morphology by removing the thick layers of deposits and corrosion products and by consolidating the constituent materials. It also recovered the readability of the artefact as a whole by recomposing the pieces on a support system. The system – actually the availability of a plausible reconstruction hypothesis – was possible thanks to the extensive knowledge of the construction technique acquired during the restoration of the object.

An important contribution was provided by scientific investigations, mainly radiography and scanning electron microscopy; as the surfaces were almost completely visually unreadable. X-rays focused on the location of cracks and areas of deep corrosion; in a few lucky cases they also located loose fragments hidden below other pieces and allowed the identification of some of the systems used to mechanically join the appliques to the bands. Besides the assessment of the mineralization of the laminae, replaced by a spongy structure of silver chloride and calcium carbonate, scanning electron microscopy provided information on the corrosion patterns, mainly consisting in alternated layers of silver chloride and calcium carbonate. With regard to the gilding technique it was also possible to assess that the artefact was leaf-gilded after embossing: the detachment of two overlapped gold leaves shows that the so-called diffusion bonding was not used on this artifact.

Acknowledgements

We are grateful to those who contributed to the conservation project; in particular to:

- Prof. Luigi Campanella and Dr. Giuseppe Caruso, *Dipartimento di Chimica, Università di Roma "La Sapienza"*, for having allowed and carried out, respectively, the second SEM survey;
- Prof. Ferdinando Felli and Mr. Carmine Panzironi, *Dipartimento di Ingegneria Chimica e dei Materiali, Università di Roma "La Sapienza"*, for having allowed and carried out, respectively, the first SEM survey;
- Dr. Cecilia Bartuli and Mr. Mauro Spinosi, *Dipartimento di Ingegneria Chimica e dei Materiali, Università di Roma "La Sapienza"*, for the support in samples preparation;
- Mrs. Alessandra Libotte and Mrs. Barbara Gregni, CO.RE.AR., Roma, for the technical collaboration and general support.

References

AB2 Art (2001) *Indagine radiografica, analitica e microstrutturale del polos della tomba 238 di Crucinia (Metaponto)*, technical report.

Angelini, M., Muleo, A. (1987) *Problemi conservativi dell'argento di scavo: i reperti argentei da Lavello*, Istituto Centrale del Restauro degree dissertation, Roma.

CO.RE.AR., Olsoufieff-Archi, A. (2002) *Intervento di restauro ed osservazioni sui frammenti in argento ed argento dorato costituenti il Polos ed altri elementi del corredo della tomba 238 da Crucinia*, conservation report.

De Siena, A. (2000) *Oreficerie nelle colonie greche di Metaponto e Siris-Herakleia*, in Ornamenti e lusso, la donna nella Basilicata antica, Roma, 21-25.

Giumlia-Mair, A. (2001) *Argento il metallo della luna*, in Giumlia-Mair, A., Rubinich, M. (eds.) Le arti di Efesto – Capolavori in metallo dalla Magna Grecia. Silvana Editoriale, Milano, 123-131.

Giumlia-Mair, A., Meriani, S., Lucchini, E. (2001) *Indagini archeometallurgiche su dorature antiche: analisi, tecniche e varianti*, in Proc. I Bronzi Antichi: produzione e tecnologia, XV Convegno Internazionale sui Bronzi Antichi. Monografies Intrumentum 21, Ed. Monique Mergoil, Montagnac, 338-343.

Guzzo, P.G. (1996) *Oreficerie dei Greci d'Occidente*, in G. Pugliese Caratelli (ed.) I Greci in Occidente, exibition catalogue, Milano, 471-480.

Lippolis, E. (2002) *Produzione e circolazione degli oggetti in argento*, in Giumlia-Mair, A.,Rubinich, M. (eds.) Le arti di Efesto – Capolavori in metallo dalla Magna Grecia. Silvana Editoriale, Milano, 115-121.

Marabelli, M. (1995) *Conservazione e restauro dei metalli d'arte*. Accademia Nazionale dei Lincei, Roma, 59-73, 121-130, 167-171.

Oddy, A. (1993) *Gilding of metals in the Old World*, in Metal Plating & Patination, La Niece, S., Craddock, P. (eds.), Butterworth-Heinemann Ltd, Oxford, 171-181.

Plenderleith, H.J., Werner, A.E.A. (1971) *The Conservation of Antiquities and Works of Art*, Oxford University Press, Oxford, 228.

Proceedings of Metal 2004 National Museum of Australia Canberra ACT 4–8 October 2004

ABN 70 592 297 967

Atmospheric corrosion of historical organ pipes: influence of acetic and formic acid vapour and water leaching on lead

A. Niklasson [a], L-G. Johansson [b], J-E. Svensson [c]

[a, c] Department of Environmental Inorganic Chemistry, Chalmers University of Technology, SE-412 96 Göteborg, Sweden
[b] Department of Chemistry, Göteborg University, SE-412 96 Göteborg, Sweden,

Abstract

A field campaign and laboratory exposures have been performed. Comparably high concentrations of acetic and formic acid vapour are present in the wind system of heavily corroded baroque organs in Europe. The corrosivity of these gases is investigated in lab exposures of polished samples. Corrosion rate was measured gravimetrically and the corrosion products were analysed qualitatively and quantitatively. The atmospheric corrosion of lead is strongly accelerated by traces of acetic acid (ethanoic acid). The results imply that acetic acid vapour is a very important corrosive agent for lead pipes in historical organs. Formic acid (methanoic acid) is slightly less corrosive than acetic acid. Water leaching has no apparent effect on the corrosion rate of lead in the presence of acetic acid vapour.

Keywords: Atmospheric corrosion, lead, acetic acid, formic acid, water leaching, organ pipe

1. Introduction

The atmospheric corrosion of ancient lead organ pipes in European churches has recently attracted attention. The organ heritage found in all countries of Europe includes more than 10,000 historically valuable organs and they are all important parts of the cultural heritage. A unique organ, originally built 1467, rebuilt 1636-37 to its present state by the famous organ builder Friedrich Stellwagen, gives a relevant illustration of the problem, see Figure 1. After more than 500 years, the irreplaceable lead-tin pipes from 1467 are suffering from very aggressive corrosion. When a pipe is corroding it gradually develops cracks and holes, and finally collapses and there is no other way to solve the problem than replacing the historic pipes with modern ones – and a part of the sounding cultural heritage is forever lost. The corrosion of lead-tin alloy organ pipes appears to be accelerating all over Europe.

We are partners in the EC project "Collapse" - Corrosion of Lead and Lead-Tin Alloys of Organ Pipes in Europe. The aim of the project is to identify which factors cause the atmospheric corrosion of organ pipes by combining field work with laboratory investigations. In addition, laboratory experiments within COLLAPSE also aim at identifying and testing a set of surface treatments for the protection of lead-rich pipes from corrosion (Chiavari et al., 2004).

Corresponding author: TEL: +46(0)317722859; FAX: +46(0)317722853; email: annikan@chem.chalmers.se

Figure 1. Heavily corroded organ pipe from the Stellwagen organ in Lübeck. (Photo: Ibo Ortgies, GOArt)

ABN 70 592 297 967

Compared to an ordinary indoor atmosphere, the church environment to which these organs are exposed is characterized by relatively low temperature and high relative humidity. Another characteristic is the presence of wood structures. Wood is known to emit a variety of organic vapours, including acetic acid (Arni et al., 1965).

Studies of the degradation of lead were initiated in 1923 (Vernon, 1927). High concentrations of organic acid vapours are known to be corrosive to lead (Graedel, 1994, Tétreault et al., 1998, 2003, Black et al., 1999, 2000). We have previously shown in laboratory studies that low concentrations of acetic acid vapours (0.1-1ppm) accelerate the atmospheric corrosion of lead, the mass gain being a linear function of time and concentration (Niklasson et al., 2004:1).

In the present work we present results from field investigations regarding mapping of the environment inside of the organ wind system. In addition metal coupons were exposed inside the organs. Laboratory studies were performed in order to investigate the influence of low concentrations of acetic or formic acid vapour on the atmospheric corrosion of lead. In addition, we investigated if the corrosion rate can be reduced by water leaching (cleaning) of exposed samples. The combined input from field investigations and laboratory experiments is essential in order to identify the corrosive factors. This in turn gives us the possibility to prohibit the corrosion by changing the corrosive environment and by applying surface protection treatments.

2. Experimental

2.1 Field studies

Field campaigns have been performed in four geographical areas and countries in Europe. Heavily corroded and slightly corroded organs were selected and the environmental conditions inside of the organ wind system were compared. Temperature and relative humidity were logged during one year. The concentration of different air pollutants were measured at four different positions in each church: In the pallet box, outside the wind chest, in the bellows room and in the church room. Samples of carboxylic acids and aldehydes were collected by pumping known volumes of air on alkaline traps. These measurements were performed in collaboration with the SP (Swedish National Testing and Research Institute). Polished samples that mimic the material used in the historical organ pipes have been exposed in several organs up to one year. The samples were brought in for corrosion product analysis and corrosion rate determination. Water-soluble anions were determined by ion chromatography.

2.2 Laboratory studies

2.2.1 Influence of organic acid vapours

Lead of electrolytic grade (99.95% purity) was used in all experiments. The concentration of acetic acid was 170 ppb and the concentration of formic acid was 195 ppb. The concentration of pollutant gases is given in ppb (parts per billion, v/v). The samples had a geometrical area of 20 cm^2 (30×30×2 mm). A hole was drilled in each sample for suspension. The samples were polished mechanically on 220 mesh SiC paper in water and then on 1000 mesh in ethanol. Then they were ultrasonically cleaned in ethanol two times, each cleaning lasting two minutes, dried and stored in a desiccator over silica gel. Within 24 hours the samples were weighed and put into the exposure chambers. In each experiment eight samples were exposed. The exposure time was four weeks. The laboratory exposures are performed to provide detailed information regarding the interplay of different environmental factors in the corrosion process such as pollutant concentration, humidity, and temperature.

The experimental set-up is presented in Figure 2. The apparatus is entirely made of glass and teflon. There are eight parallel chambers through which the gas is sequentially distributed, the whole gas flow passing through each chamber in turn for 15 seconds. The gas flow was 1000 ml/min in all experiments, corresponding to a gas velocity of 7 mm/s. Each sample was suspended on a nylon string in the middle of the chamber. Only one sample was exposed in each chamber. The chambers have an inner diameter of 55 mm and a volume of 0.4 l. The corrosion chambers are immersed in a water tank held at 22.00 °C. The temperature in the room was kept at 25 °C to avoid condensation in the parts of the system outside the water tank. Relative humidity (RH) was regulated by mixing dry air and air saturated with water vapour. RH was 95% in all exposures and was controlled with an accuracy of ± 0.3 %. Pure carbon dioxide was added from a gas bottle and a CO_2-analyser (BINOS 1000) was used to monitor the concentration (350 ppm v/v) in the exposure gas. To monitor the corrosion process, the samples were weighed during exposure. The wet mass gain was recorded rather thas the dry mass gain in order to minimise the disturbance of the corrosion process. The dry mass gain signifies the weight gain of samples stored over a desiccant at ambient pressure and room temperature for one week after exposure.

ABN 70 592 297 967

The amount of water-soluble anions in the corrosion product layer was determined by ion chromatography, IC. The chromatograph used was an IONPAC AD9-SC Analytic Column. To determine the amounts of carbonate in the corrosion products, some of the samples were transferred to an acid desorption cell consisting of a three-necked flask made of Pyrex glass containing 1M $HClO_4$ (aq). Immersing the samples in the acid quantitatively converted carbonate to carbon dioxide. A stream of nitrogen was used to expel the carbon dioxide from the solution and carry it to the CO_2 analyzer (Binos 100). The sensitivity of this analysis corresponded to 10×10^{-9} mol CO_2/sample. By introducing weighed amounts of $BaCO_3$(s) into the system, the precision of the analysis was found to be ± 2 %. Crystalline corrosion products were analysed by X-ray diffraction (XRD). A Siemens D5000 power diffractometer (CuK_α radiation) was used. The diffractometer was equipped with a grazing incidence beam attachment combined with a Göbel mirror. With this technique it is possible to analyse very thin oxide films.

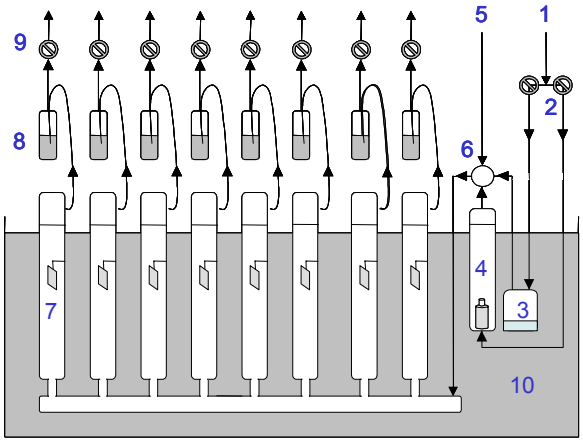

Figure. 2 Experimental set-up for corrosion exposures. (1) dried purified air; (2) flow control; (3) humidifier; (4) vessels for permeation tubes; (5) CO_2 inlet; (6) mixer; (7) eight exposure chambers; (8) wash bottles, (9) eight-channel solenoid valve; (10) water tank at constant temperature.

2.2.2 Effect of water leaching

The development of methods to clean the corroded pipe metal surface is a necessary part of the conservation procedure. Cleaning the corroded pipe is done primarily to decrease the rate of corrosion by removing corrosion compounds (salts) from the surface. The insoluble corrosion products (e.g. lead white) are not to be removed. Cleaning should not affect the metal itself. This is very important for the surfaces in the pipe mouth area. The sound is generated in the mouth area (lower and upper lip and the languid) and the tone quality is extremely sensitive to changes in the mouth area geometries, edges and surface structure. In order to investigate if water leaching is beneficial or not several different exposures were performed, see Table 1. In all the experiments samples of pure lead was exposed to gaseous acetic acid, HAc, (170 ppb) for two weeks. After two weeks of exposure the samples were removed from the exposure chambers. Some samples were leached in pure milli-Q water three times, each cleaning lasting for one minute. The exposures were then continued for two more weeks in either pure air or in air containing acetic acid.

Table 1. Exposures performed. Acetic acid (HAc) concentration was 170 ppb and relative humidity 95%.

No.	Exposure (2 weeks)	Water leaching	Exposure (2 weeks)
1.	HAc	No	HAc
2.	HAc	No	Pure air
3.	HAc	Yes	HAc
4.	HAc	Yes	Pure air

ABN 70 592 297 967

3. Results and Discussion

3.1 Corrosive factors found at the reference organs in the field study

The field measurements performed throughout Europe as a part of this study show that comparably high concentrations of organic acid vapours (e.g. acetic and formic acid) are present in the wind system of heavily corroded organs. Acetaldehyde (ethanal) and formaldehyde (methanal) were also found in smaller amounts. A comprehensive presentation of the field results is given elsewhere (Niklasson et al., 2004:2). As an example of the field measurements, results from the organ wind system in the Stellwagen organ in Lübeck are presented in Fig 3. High concentrations of acetic acid were found inside of the palletbox (700 ppb). In addition to acetic acid, formic acid, acetaldehyde, and formaldehyde were detected (50-250 ppb). It may be noted that the concentration of organic acid vapours is significantly lower (less than half) in organs less affected by corrosion. The concentration of organic acid vapours in indoor environments is typically in the range 0.05-40 ppb (Tétreault et al., 2003). Analysis of the metal coupons exposed in the Stellwagen organ for 3-12 months show that acetates, formiates and small amounts of chlorides and sulphates had accumulated on the sample surface. The presence of acetate and formiate indicates that the organic acid vapours react with the lead surface.

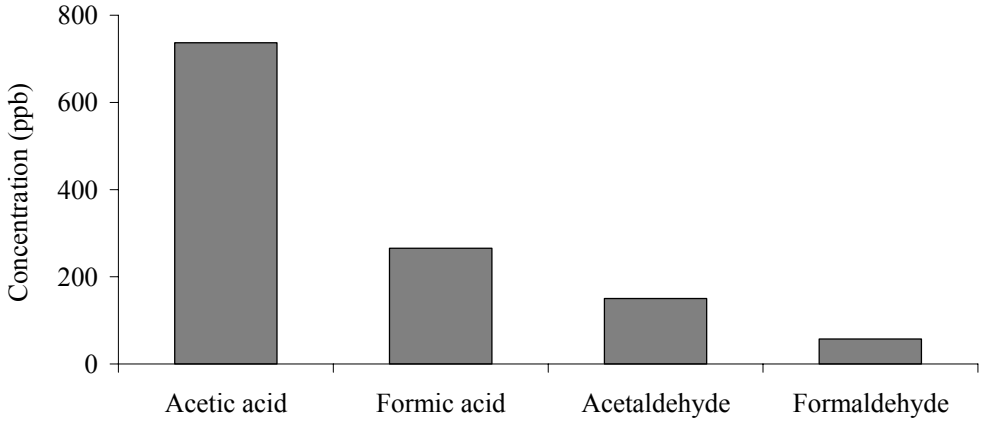

Figure. 3 Concentration of different organic gases in the pallet box in the Stellwagen organ in Lübeck.

3.2 Laboratory studies

3.2.1 Influence of organic acid vapours

The relatively high concentration of organic acid vapours in the organ environment and the accumulation of acetates and formiates on the lead coupons indicate that organic acids play a role in the corrosion of the organ pipes. To address this point, the effect of acetic and formic acid vapour on the atmospheric corrosion of lead was investigated in the laboratory. Figure 4 presents mass gain as a function of exposure time for lead samples exposed to 170 ppb acetic acid or 195 ppb formic acid vapour at 22.00 °C, RH 95 % and 350 ppm CO_2 for four weeks. The atmospheric corrosion of lead is strongly accelerated by traces of acetic acid, the mass gain being linear with time. While formic acid also accelerates lead corrosion, it appears to be slightly less corrosive than acetic acid.

By X-ray diffraction, plumbonacrite ($Pb_{10}O(OH)_6(CO_3)_6$), lead acetate oxide hydrate ($Pb(CH_3COO)_2{\cdot}2PbO{\cdot}H_2O$) and traces of massicot (β- PbO) were detected after exposure to acetic acid vapour, see Table 2. Lead formate hydroxide (Pb(HCOO)(OH)) and plumbonacrite were identified in the presence of formic acid vapour. Table 3 shows that the deposition of formic acid vapour is considerably faster compared to the corresponding figures for acetic acid. In contrast, corrosion is slower in the presence of formic acid. Consequently, the samples exposed to acetic acid form more carbonate and oxide than the samples exposed to formic acid. In the presence of acetic acid the corrosion product is made up from 50 % lead acetate oxide hydrate, 40 % plumbonacrite and 10 % massicot. In the case of formic acid about 90 % of the corrosion product mass consisted of lead formate hydroxide.

ABN 70 592 297 967

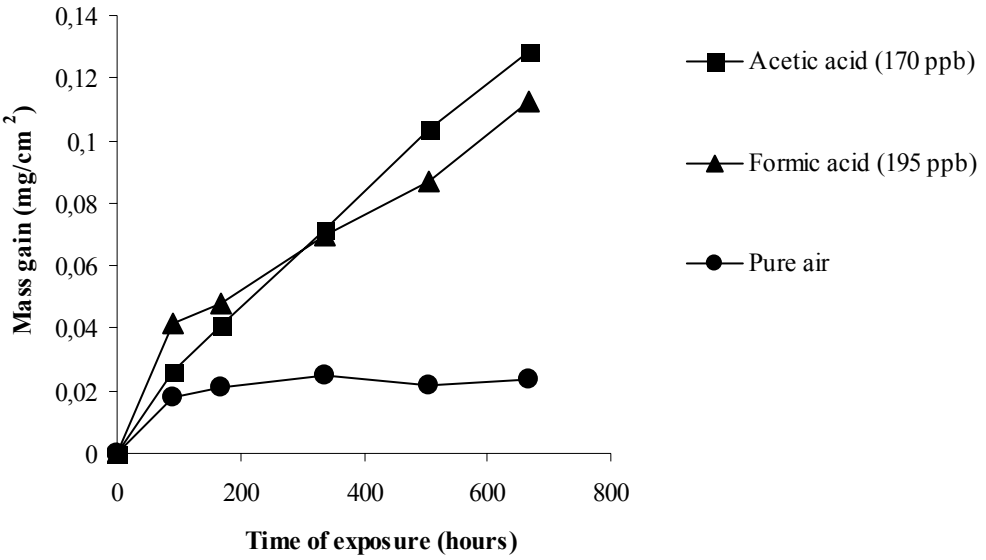

Figure 4. Mass gain vs. exposure time of lead samples exposed to 170 ppb acetic acid or 195 ppb formic acid vapour at 22.00°C, RH 95% and 350 ppm CO_2.

Table 2. Summary presentation of corrosion products identified by XRD.

Exposure environment	Corrosion product
Acetic acid vapour (170 ppb)	Plumbonacrite ($Pb_{10}O(OH)_6(CO_3)_6$) Lead acetate oxide hydrate ($Pb(CH_3COO)_2{\cdot}2PbO{\cdot}H_2O$) Massicot (β-PbO)
Formic acid vapour (195 ppb)	Plumbonacrite Lead formate hydroxide (Pb(HCOO)(OH))
Pure air	Plumbonacrite Litharge (α-PbO)

It is suggested that the corrosivity of gaseous acetic acid towards lead is explained by its high solubility in water, its acidity, and by the solubility of lead acetate and lead acetate oxide hydrate. The acidification of the surface electrolyte by acetic acid results in the dissolution of the passive film, enhancing the anodic dissolution of lead. Lead acetate oxide hydrate is somewhat soluble because of the complexing of lead ions with acetate and hydroxide. Because the surface electrolyte is stable also at neutral and slightly alkaline pH, a corrosion cell is formed where the anodic and cathodic areas on the surface are connected by an electrolyte.

As noted above, formic acid is somewhat less corrosive towards lead in comparison to acetic acid even if formic acid deposits more rapidly on the surface. This implies that the surface electrolyte formed in the presence of formic acid is less corrosive in comparison to that formed in the presence of acetic acid. A comparison of the properties of formic and acetic acid shows, that while formic acid is a stronger acid than acetic acid, formiate is a less efficient complexing agent for divalent lead.

Table 3. Wet and dry mass gain, amount of carbonates and the amount of water soluble anions found on lead exposed to 170 ppb acetic acid or 195 ppb formic acid vapour at 22.00 °C, RH 95 % and 350 ppm CO_2 for 4 weeks.

ABN 70 592 297 967

Exposure environment	Wet mass gain (mg/cm^2)	Dry mass gain (mg/cm^2)	Calculated contribution to mass gain by water soluble lead acetate oxide hydrate # (mg/cm^2)	Calculated contribution to mass gain by water soluble lead formate hydroxide ## (mg/cm^2)	Calculated contribution to mass gain by plumbonacrite * (mg/cm^2)
Acetic acid vapour (170 ppb)	0.124	0.112	0.058		0.041
Formic acid vapour (195 ppb)	0.113	0.097		0.089	0.012
Pure air	0.024	0.012			

#) Assuming that all acetate found forms lead acetate oxide hydrate.

##) Assuming that all formiate found forms lead formate hydroxide.

*) Assuming that all carbonate found forms plumbonacrite.

3.2.2 Influence of water leaching

In order to investigate different possible measures to decrease the corrosion rate in organs, the effect of water leaching on corrosion was investigated. The results from several exposures with and without leaching are presented in Fig 5. Curve (1) shows mass gain in the presence of HAc with no water leaching. As was already mentioned, mass gain is linear in time in the presence of acetic acid. Curve (2) shows the mass gain of samples that were first exposed to HAc for two weeks. Then the supply of HAc was interrupted, resulting in a sudden decrease in the corrosion rate. The effect of water leaching after 2 weeks exposure to HAc is illustrated by curves (3) and (4), note that the mass gain after water leaching is put to zero (**). When the water leached samples are again exposed to HAc (curve (3)), the mass gain curve has the same slope as without leaching, indicating that water leaching does not affect the corrosion rate (compare the slope of the mass gain curves nos. (1) and (3)). Curve (4) shows the mass gain of samples that were exposed to pure air after water leaching. The flat mass gain curve indicates that the corrosion rate is very low in this case, being comparable to curve (2) and to the clean air run in Figure 4. To summarize, while the corrosion of lead is strongly dependent on the presence of acetic acid, water leaching has no apparent effect on corrosion rate.

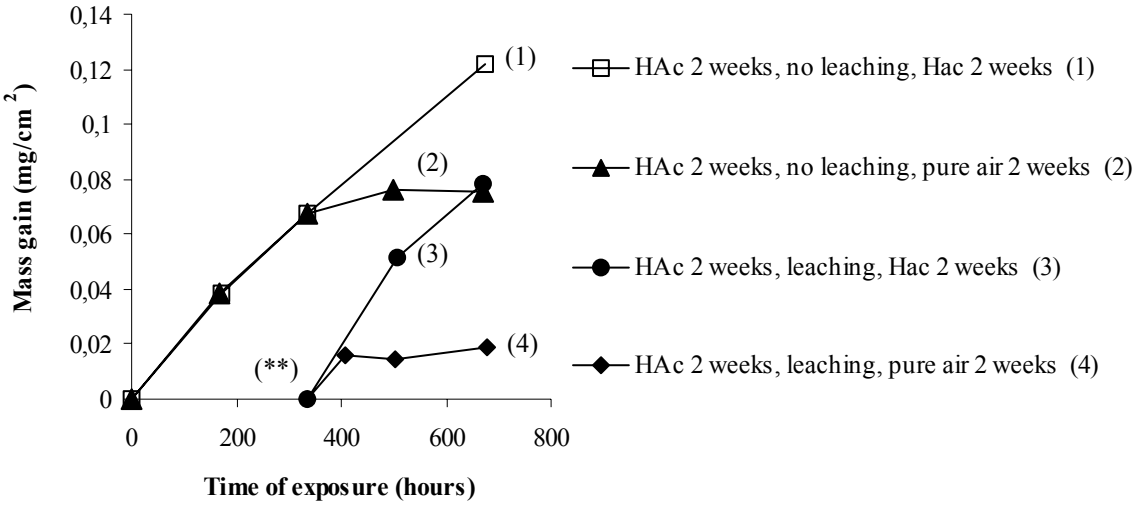

Figure 5. Mass gain as a function of exposure time for pure lead exposed in 95 % RH. Water leaching was performed on some samples after two weeks exposure.

ABN 70 592 297 967

The results of the quantitative analysis of the corrosion products are presented in Table 4. As expected, the amount of acetate on the samples is proportional to the time of exposure in the presence of HAc(g). It may be noted that the amount of acetate on the samples does not diminish upon exposure to pure humid air. This indicates that the conversion of lead acetate oxide hydrate to plumbonacrite must be slow. The results show that samples exposed to pure air during the last two weeks of exposure corrode very slowly even in the presence of ample amounts of acetate on the surface (see Figure 5 curve (2)). This implies that a continuous deposition of acetic acid is necessary to sustain a rapid corrosion process.

Table 4. Amount of acetate and carbonate found on lead exposed to 170 ppb acetic acid vapour at 22.00 °C, RH 95 % and 350 ppm CO_2.

No.	First Exposure (2 weeks)	Water leaching	Calculated contribution to mass gain by lead acetate oxide hydrate # (mg/cm^2).	Second Exposure (2 weeks)	Calculated contribution to mass gain by lead acetate oxide hydrate # (mg/cm^2)	Calculated contribution to mass gain by plumbonacrite * (mg/cm^2)
1.	HAc	No		HAc	0.06	0.04
2.	HAc	No		Pure air	0.04	0.04
3.	HAc	Yes	0.03	HAc	0.03	0.02
4.	HAc	Yes	0.04	Pure air	0.003	0.03

#) Assuming that all acetate found forms lead acetate oxide hydrate.

*) Assuming that all carbonate found forms plumbonacrite.

The samples that were leached in water and subsequently exposed to HAc-containing air produced qualitatively the same corrosion products as samples not leached in water. The only major change in corrosion product composition occurred for the samples exposed to pure humid air after water leaching. These samples formed the thermodynamically stable hydrocerussite rather than the metastable plumbonacrite.

This work deals with one important factor for the corrosion of lead pipes in historical organs namely the occurrence of organic acids in the organ wind system. However it must be emphasized that atmospheric corrosion of lead is influenced by a number of parameters including temperature, humidity, condensation in the pipe, emissions of other corrosive substances from materials inside and outside the organ etc. Combinations of the different corrosive factors should also be taken into account. Even so, the laboratory investigations have shown that the acetic and formic acid found can cause corrosion problems in the pipes all by themselves. It is assumed that the organic acids mainly originate in the wooden parts in the organ. This knowledge is important not only for the understanding of the existing corrosion problems but also to avoid creating a corrosive environment when restoring or repairing an historical organ.

4. Conclusions

Comparably high concentrations of acetic and formic acid vapour are present in the wind system of heavily corroded baroque organs in Europe. Laboratory studies show that the atmospheric corrosion of lead is strongly accelerated by traces of acetic acid, the deposition of acid and the mass gain being linear in time. The results imply that acetic acid vapour is a very important corrosive agent in the deterioration of lead pipes in historical organs. While formic acid also accelerates lead corrosion, it appears to be slightly less corrosive than acetic acid. The results show that a continuous deposition of acetic acid is necessary to sustain a rapid corrosion process. Water leaching has no apparent effect on the corrosion rate of lead in the presence of acetic acid vapour. The results imply that the rate of corrosion of lead pipes in historical organs can be effectively decreased by removing gaseous acetic acid from the wind system.

ABN 70 592 297 967

Acknowledgement

This work was supported within the EC Fifth Framework Programme: Energy, Environment and Sustainable Development. EVK4-CT-2002-00088, COLLAPSE.

References

Arni, P.C., Cochrane, G.C., and Gray, J.D., (1965) *Emission of corrosive vapors by wood. I. Survey of the acid release properties of certain freshly felled hardwoods and softwoods,* J. Appl. Chem., **15**, 305-313

Black, L. and Allen, G.C., (1999) *Nature of lead patination*, British Corrosion Journal, **34**, 3, 192-197

Black, L. and Allen, G.C., (2000) *Role of organic acid in lead patination*, British Corrosion Journal, **35**, 1, 39-42

Chiavari, C., Martini, C., Poli, G., Prandstraller, D., (2004) *Conservation of organ pipes: protective treatments of lead exposed to acetic acid vapours,* Metal 2004, in press, Canberra.

Graedel, T. E., (1994) *Chemical mechanism for the atmospheric corrosion of lead*, J. Electrochem. Soc., **141**, 4, 922-927

Niklasson, A., Johansson, L.-G. and Svensson, J.-E., (2004:1) *The Influence of Acetic Acid Vapour on the Atmospheric Corrosion of Lead*. Submitted to J. Electrochem. Soc.

Niklasson, A., Langer S., Pointet, K., Rosell, L., Johansson, L.-G. and Svensson, J.-E., (2004:2) To be published

Tétreault, J., Sirois, J., Stamatopoulou, E., (1998) *Studies of lead corrosion in acetic acid environments*, Studies in Conservation, **43**, 17-32

Tétreault, J., Cano, E., van Bommel, M., Scott, D., Dennis, M., Barthés-Labrousse, M.-G., Minel, L., Robbiola, L., (2003) *Corrosion of copper and lead by formaldehyde, formic and acetic acid vapours*, Studies in Conservation, **48**, 4, 237-250

Vernon, W.H.J., (1927) Trans. Faraday Soc. **23**, 113, 156-159

Conservation of organ pipes: protective treatments of lead exposed to acetic acid vapours

C. Chiavari[a], C. Martini[a], G. Poli[a], D. Prandstraller [b]

[a]Istituto di Metallurgia, Università di Bologna, Italia
[b]Dipartimento di Ingegneria dei Materiali e dell'Ambiente, Università di Modena, Italia

Abstract

Indoor atmospheric corrosion of lead pipes is a severe problem for European historical organs. The action of the organic acid vapours emitted by the wood structures is known to be one of the main causes accountable for lead corrosion.

In order to develop a conservation strategy, the protective efficiency of different surface treatments for lead exposed to organic acids has been evaluated. In the present paper, the results of electrochemical measurements and artificial weathering experiments are reported. Lead specimens were treated by different inhibiting solutions: (i) sodium decanoate, (ii) sodium undecanoate, (iii) thiourea, (iv) sulphuric acid and (v) phosphoric acid. Polarisation curves (PC) offered a preliminary screening of the protectiveness of the treatments in acetic acid solutions. The treated surfaces were then exposed to acetic acid atmospheres. The protectiveness of the surface treatments was checked by Optical Microscopy (OM), Stereo Microscopy (SM), X Ray Diffractometry (XRD), Scanning Electronic Microscopy (SEM) with EDS (Energy Dispersive Spectroscopy) analyses. Gravimetric measurements (mass variation and weight loss) were performed. On the basis of the results, a comparative evaluation of the protective properties of the treatments was performed.

Keywords: lead, organ pipe, corrosion, protective treatments, weathering tests, corrosion inhibitors.

1. Introduction

Historical pipe organs are an essential part of the European musical and cultural heritage. One major danger for this heritage is the indoor atmospheric corrosion of lead and lead-tin alloys of organ pipes. It is well known that wood emits organic vapours, including acetic acid, that are corrosive towards lead (Graedel 1994, Shreir et al.1994, Hallebeek 1994, Tetreault et al.1998). Many of the European historical organs suffer from an increasing corrosion attack on pipe metal (lead rich alloys) and the number of historical organs affected by corrosion seems to grow rapidly. The aggressiveness of this kind of corrosion is a major environmental threat against pipe organs.
When the organ pipes corrode through, there is no other way to solve the problem than replacing the historic pipes with modern ones and a part of the sounding cultural heritage is forever lost.
In order to identify all factors responsible for the decay of the instruments and so to develop a conservation strategy, a research project (COLLAPSE, Corrosion of Lead and Lead alloys of Organ Pipes in Europe; www.goart.gu.se/collapse) composed of both field studies and laboratory experiments has been set up. During field studies, samples from corroded pipes in reference historical instruments have been taken and analysed (Chiavari et al. 2004) and the concentration of organic compounds in the atmosphere of the organs has been measured by the Department of Environmental Inorganic Chemistry, Chalmers University of Technology, Göteborg (Sweden).

Corresponding author: TEL: +39(0)51 2093464, FAX: +39(0)51 2093467, email:dara@bomet.fci.unibo.it

Meanwhile, in the same laboratory, experiments for the evaluation of the influence of environmental factors on corrosion behaviour are in progress (Niklasson et al. 2004). Laboratory experiments within COLLAPSE also aim at identifying and testing a set of surface treatments for the protection of lead-rich pipes from corrosion. The first results obtained are reported in this paper.

Candidate surface treatments for the protection of pipes have been selected on the basis of a survey of the literature. Treatments for both corroded and uncorroded lead were surveyed, however, the first step of the work, reported in this paper, is dedicated to uncorroded lead.

Many organic compounds are reported to provide a high degree of corrosion inhibition for uncorroded lead and lead alloys: thiourea protects lead alloys in acetic acid media (Fawzy et al.1981), tosylhydrazine protects lead from acetic acid vapours by blocking anodic reaction sites (Sankarapapavinasam et al. 1989, Sankarapapavinasam et al. 1990), pyrazole derivatives (-CH_3, -OCH_3 and -Cl derivatives of 3(5) amino, 5(3) phenyl pyrazole) are effective as corrosion inhibitors for lead in HCl solutions (Badawy et al.1990). The most interesting data on the protection of lead are reported by Rocca *et al*. (Rocca and Steinmetz 2001, Rocca et al. 2004): the ability of sodium monocarboxylates to react with lead and to form lead monocarboxylates and so to inhibit the aqueous corrosion of lead has been demonstrated and, in particular, sodium decanoate has been proposed as a promising inhibitor treatment for lead object exposed to acetic acid atmospheres. Also inorganic compounds such as phosphates (Boffardi 1990) are known to be effective as corrosion inhibitors for lead in aqueous solution. The formation of a protective layer of lead phosphate is proposed as an explanation of the protective efficiency of phosphate-based inhibitors: this suggests conversion treatments with phosphoric acid as an interesting option for the protection of lead. Similarly, the well-known resistance of lead to sulphuric acid is due to the formation of a layer of lead sulphate and also conversion treatments based on sulphuric acid have been proposed for the protection of lead. The protectiveness of layers formed as a consequence of the reaction between lead and sulphuric acid is evaluated and discussed in many papers on lead acid battery grids (Ruetschi and Angstadt 1964, Winand 1978, Ijomah 1988) as well as in conservation literature (Lane 1979, Degrigny and Le Gall 1999).

Different options are described in the literature for the treatment of corroded lead objects, the choice of the treatment method being related to the state of conservation as well as to the need of preserving surface details such as inscriptions or engravings that give important historical and artistic information. In the latter case, consolidative reduction is a well established method (Organ 1963, Carradice and Campbell 1994, Degrigny and Le Gall 1999). A more simple option, i.e. the application of an overlay coating, is likely to be the best one for organ pipes, since in this case it is not necessary to retrieve surface details but only to consolidate and protect from further corrosion. Most of the protection treatments developed for lead antiquities consist of an overlay coating of wax or lacquer applied on the object after stabilisation/consolidation of the corrosion products (Organ 1953, Organ 1963, Lane 1979, Nosek 1985, Watson 1985, Green 1989).

The selection of candidate surface protection treatments for lead was made on the basis of the (i) environmental impact, user-friendliness and dimensional requirements of the process for treating the surface; (ii) reversibility/irreversibility and aesthetical impact of the treatment.

In the present paper, the results of a comparative evaluation of the protectiveness of candidate surface applied on uncorroded lead are reported.

2. Experimental

Among the protective methods for lead, a set of candidate surface treatments to be applied on sample pipes has been identified and tested on lead coupons produced so as to mimic the recrystallised microstructure with equiaxed grains, which is typical of lead-based pipes.

In particular, the selected treatments were based on the following compounds: (i) linear sodium monocarboxylates ($CH_3(CH_2)_{n-2}COONa$), (ii) thiourea ($SC(NH_2)_2$), (iii) sulphuric acid (H_2SO_4) and (iv) phosphoric acid (H_3PO_4). All these treatments could be performed simply by immersion of the material to be treated into an aqueous solution at room temperature.

The protectiveness of sodium monocarboxylates was reported to increase with the number of carbon atoms (n) in the range between 7 to 11 (Rocca 2001), therefore sodium decanoate (n=10, henceforward C10) and undecanoate (n=11, henceforward C11) were selected for the comparative testing campaign. On the contrary, other organic corrosion inhibitors such as tosylhydrazine and pyrazole derivatives were not considered for this study because of their toxicity and because they were not conveniently available on the market.

In the first step of the experimental evaluation of the protectiveness of candidate treatments, commercially available 99.95 pure lead coupons (3x3cm) were polished by SiC abrasive paper up to 1000 grit, degreased and inhibited by immersion in the different aqueous solutions (with a total volume of 100 mL per coupon and a concentration in the range 0.5-0.05 M). The pH of the solutions has been measured at the end of the treatment.

In order to define the treatment conditions (concentration of the treatment solution and time of immersion of the sample), different measurements, such as mass variation of the samples, concentration of dissolved Pb in the treatment solution (measured by Atomic Absorption Spectroscopy) and characterisation of the conversion products on treated samples (XRD, SEM), were performed at increasing immersion time. The immersion time has been selected in the range of constant mass gain and constant Pb concentration in the treatment solution, considering these conditions as indicative of the formation of a stable layer on the surface.

Once the optimised treatment conditions were defined, a preliminary screening of the protective efficiency of the treatments in acetic acid solutions was performed by polarization current (PC) measurements, at short times. Cathodic and anodic polarization curves (1mV/s) were recorded by using a Solartron Potentiostat/Galvanostat model 1280B, after 1h immersion of the lead electrodes in 0.01M acetic acid solution neutralised with NaOH.

2.1 Accelerated corrosion tests

In order to investigate the corrosion behaviour of the treated samples exposed to a very aggressive acetic acid atmosphere, an accelerated corrosion test was set up, according to the procedure suggested by the Department of Environmental Inorganic Chemistry of Chalmers University of Technology (Niklasson, Johansson, and Svensson 2003). The corrosion tests were performed by exposing the coupons, hanging from a coupon rack in a desiccator, to acetic acid in gas phase (about 7 ppm), as illustrated in Figure 1. During the exposure, the temperature (T=22°C) was controlled by a thermostatic chamber. The maximum exposure time was 168h. Lead coupons were weighed before and after exposure.

Figure 1 Accelerated corrosion test equipment.

Before and after exposure, the surfaces of metal samples were also observed by Stereo Microscopy (SM), Scanning Electronic Microscopy (SEM) with Energy Dispersive (EDS) microprobe. Corrosion products on square samples were analysed by X Ray Diffractometry (XRD).

At the end of each test, after the characterisation of the oxidation products on the metal surface, the corrosion rates were determined by gravimetric measurements. The samples were pickled by an aqueous solution of ammonium acetate (250g/L), according to the ASTM standard procedure for weight loss measurements of lead and lead alloy (G1-03).

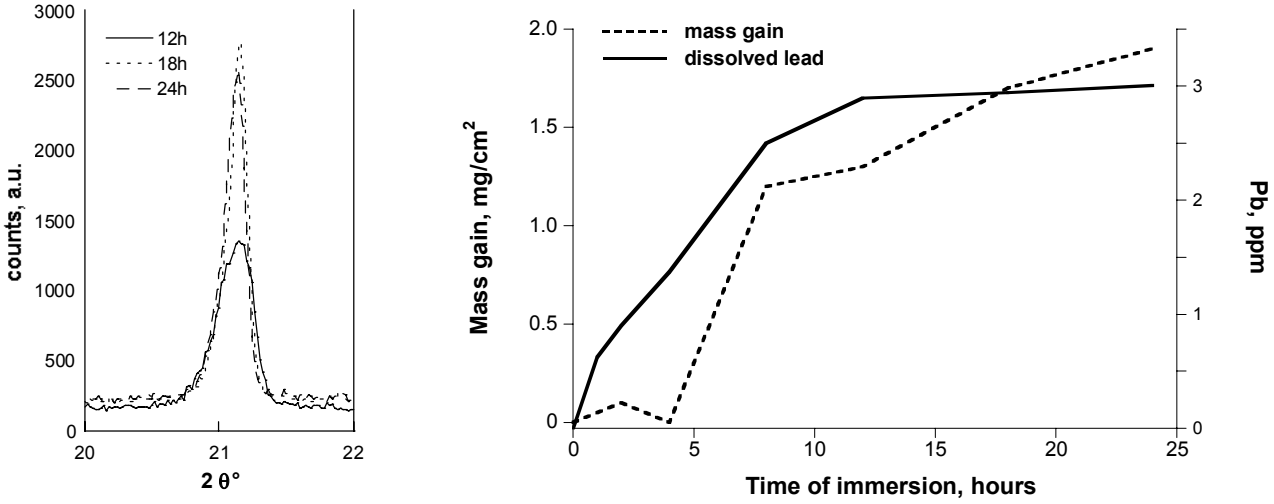

Figure 2

(a) (b)

Figure 2. Set-up of treatment conditions for lead sulphatising (immersion in H_2SO_4 0.05 M): (a) XRD pattern of the surface of suphatised lead: intensity of peak (101) of lead sulphate $PbSO_4$ at different immersion times; (b) mass gain of the lead coupon and concentration of lead dissolved in the treatment solution as a function of immersion time.

3. Results and Discussion

The lowest concentration in the testing range (0.05 M) produced a detectable layer of conversion products at different immersion times for each treatment; Figure 2 shows an example of the procedure for the definition of immersion time in the case of sulphatising. The intensity of peaks of lead sulphate ($PbSO_4$) increased with increasing immersion time from 12 to 18 h and then remained almost constant. Also mass variation and concentration of lead dissolved in the treatment solution remain constant from 18 to 24 h of immersion, probably indicating a complete coverage of the surface by a stable layer of conversion products.

Table 1 lists all the optimised treatment conditions. At the end of the treatment a very low amount of lead was measured in the sulphatising solution, whereas the highest amount of dissolved lead was determined in the phosphatising solution as indicated in table 1. It is worth noting that the treatments based on C10 and C11, applied in the conditions suggested by Rocca et al. (Rocca and Steinmetz 2001), were not aggressive towards lead, as demonstrated by the measurements of lead dissolved in the inhibiting solution (Table 1). Lead coupons have been immersed in the thiourea

inhibiting solution for a short time (1 h) according to the indications reported in the literature (Fawzy et al.1981).

The morphology of the treated surfaces before exposure is shown in the SEM images of Figure 3 and the phase composition of conversion products is summarised in Table 2. Samples treated with C11 and C10 were covered by a continuous layer of flake-shaped crystals (Figures 3 a-b). XRD analyses showed that lead was converted into lead monocarboxylate, in agreement with data reported by Rocca et al. (Rocca and Steinmetz 2001).

Figure 3 Morphology of the treated surfaces before the exposures: (a) C10; (b) C11; (c) sulphatised (d) phosphatised; (e) thiourea.

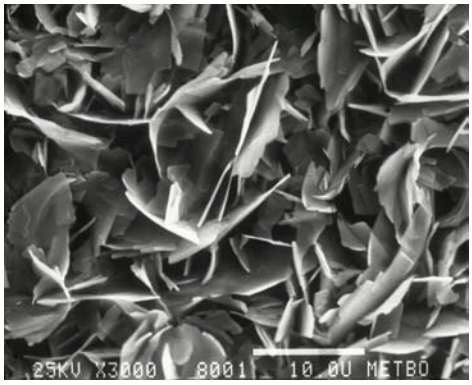

(a)

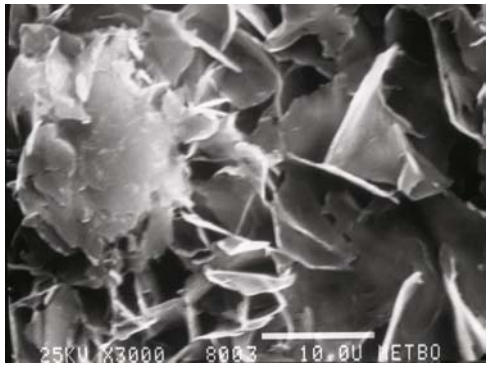

(b)

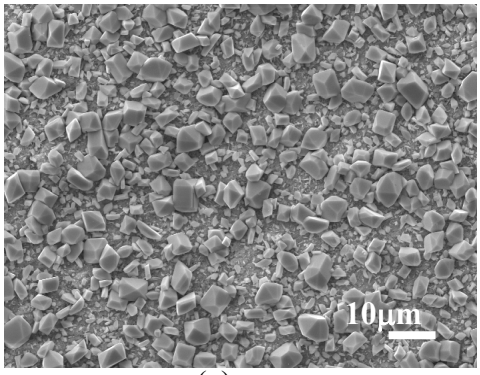

(c)

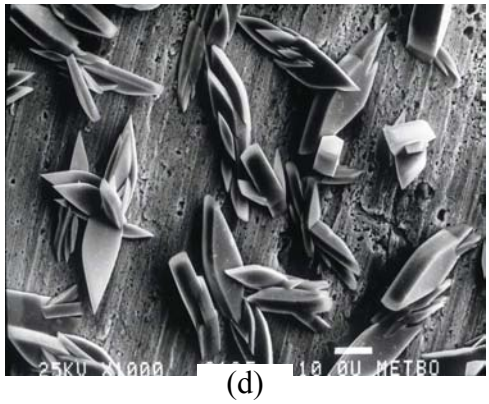

(d)

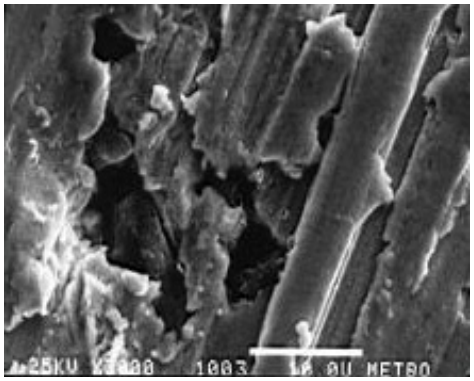

(e)

Sulphatising formed a continuous layer of fine-sized crystals (Figure 3c) of lead sulphate ($PbSO_4$), whereas phosphatising produced a discontinuous layer of lead hydrogen phosphate ($PbHPO_4$), consisting of isolated clusters and uncovered areas (Figure 3d) even after 30 h of immersion. After the immersion in the thiourea inhibiting solution, polishing marks were still visible on the surface (Figure 3e) and XRD spectra revealed the presence of an amorphous phase.

C10 and C11 treated surfaces showed a very high hydrophobicity, as reported in (Rocca and Steinmetz 2001, Rocca et al.2004), while the other treated surfaces were not hydrophobic, as demonstrated by the shape of a water drop in contact with the inhibited surfaces. It is also worth pointing out that C11 is less water soluble than C10, and therefore it tends to produce a less homogeneous layer of conversion products.

3.1 Electrochemical measurements

The anodic and cathodic polarisation curves are presented in Figure 4, where unprotected lead electrodes are compared with the treated ones. The PC plots show that, in the case of C10, the anodic current density decreased by two orders of magnitude compared to the blank electrode.

Figure 4 Anodic and catodhic polarisation curves of samples treated with organic inhibitors: thiourea (Th) or sodium monocarboxylates (C10, C11) compared with untreated lead (Pb) in neutralised acetic acid solution.

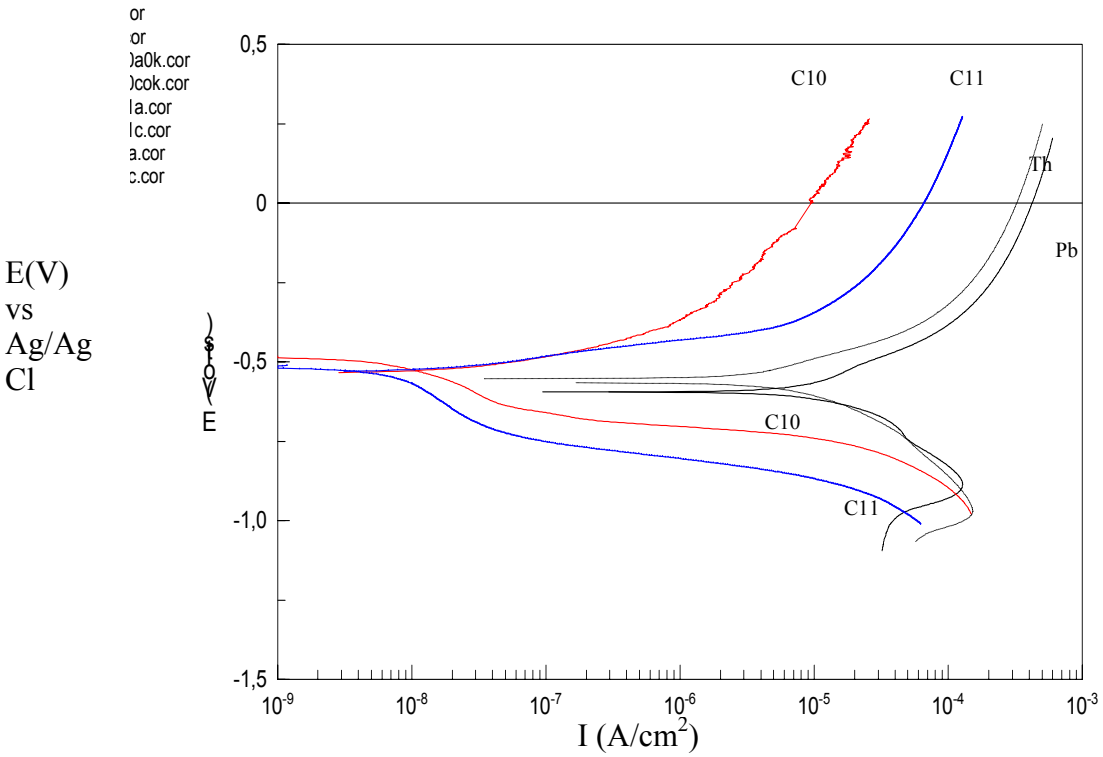

Treatments with C10 and C11 effectively reduced both the anodic and the cathodic polarization current values, whereas thiourea revealed a much weaker inhibiting action, showing a trend very similar to that of unprotected lead. As concerns sulphatised and phosphatised samples, the polarisation curves showed current values comparable to those of unprotected lead and, in the case of phosphates even lightly enhanced current densities were recorded.

The preliminary screening of the protective performance through electrochemical data showed that the most promising inhibitors for lead are C10 and C11.

3.2 Accelerated corrosion tests

Figure 5 **Treated (a: thiourea; b: sulphatised; d: phosphatised; e: C10) and untreated (c) lead coupons after exposure; untreated and unexposed lead (f) is also shown for comparison.**

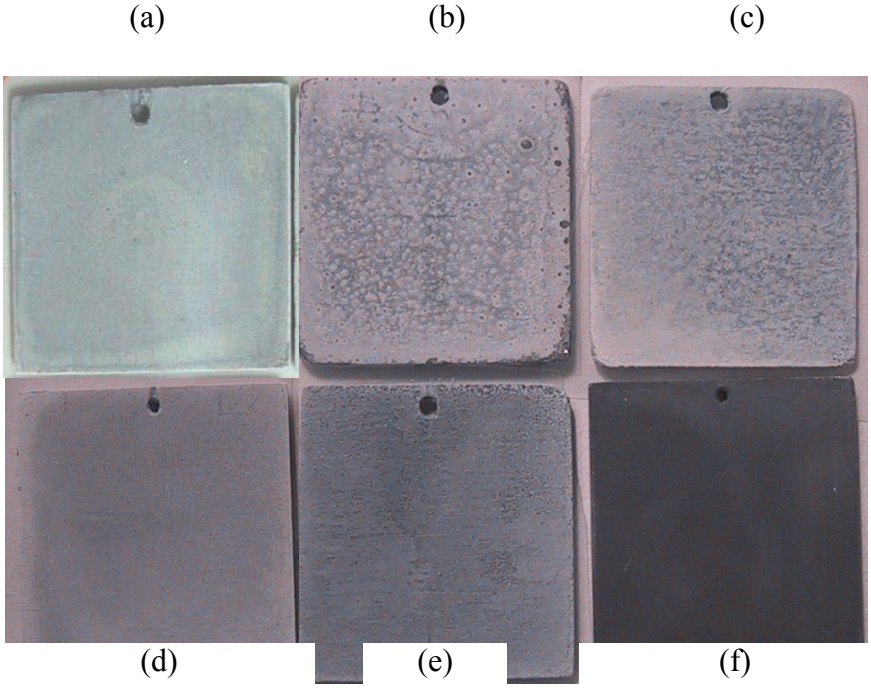

After exposure all treated surfaces showed the presence of corrosion products (Figure 5). In all cases the amount of corrosion products increased with increasing exposure time. Nevertheless, the morphology and the nature of the corrosion products change from treatment to treatment (Figure 6, Table 2). Actually, only scattered crystals of corrosion products grew on the unchanged surface of C11 and C10 treated samples: the layer of flake-shaped crystals of lead monocarboxylates was still clearly visible after exposure (Figures 6 a,b).

Figure 6 **Morphology of the treated surfaces after the exposures: (a) C10; (b) C11; (c) phosphates; (d) sulphates; (e) thiourea; (f) unprotected lead.**

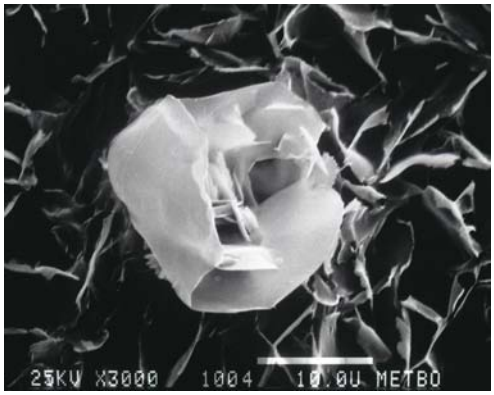

(a)

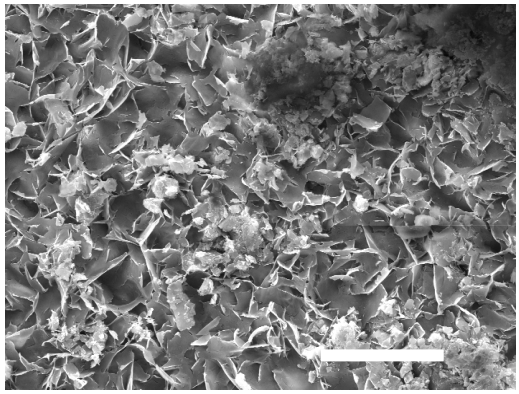

(b)

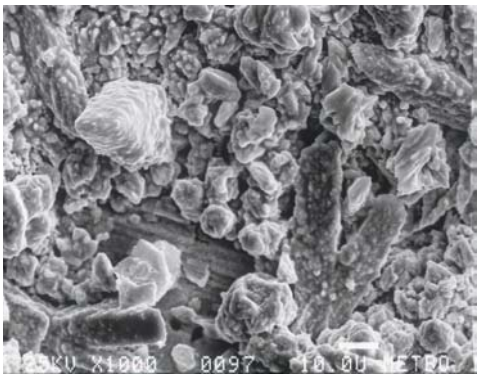

(c)

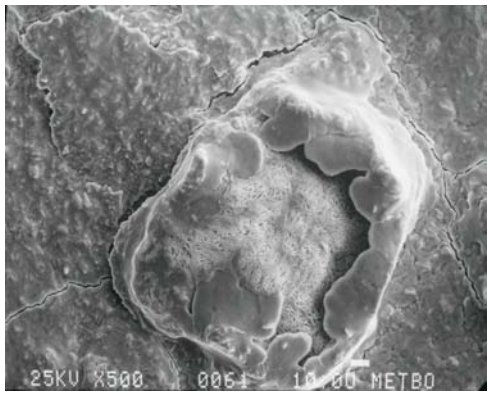

(d)

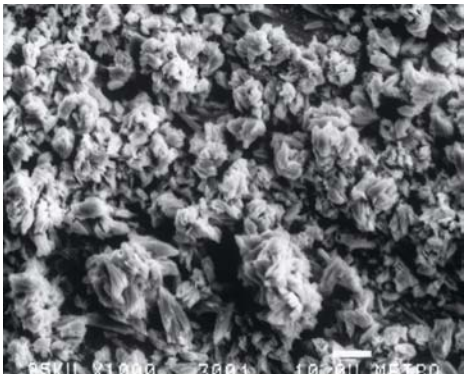

(e)

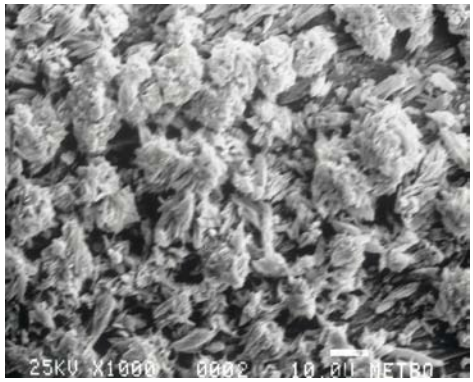

(f)

Phosphatised samples developed a fine grained and adherent layer of corrosion products that fills in the gaps between the needles of lead phosphate (Figure 6c). On the contrary, the oxidation layer grown on samples treated with sulphates was brittle and non-adherent (Figure 6d). The exposed surface treated with thiourea revealed a morphology similar to that of unprotected lead.

The phase composition of the oxidation layers determined by XRD is summarised in Table 2. The results point out the protective behaviour of the C10 and C11 treatments: after 168h of exposure to a very aggressive atmosphere, only traces of lead oxides and carbonates were detected. In addition, the peaks of lead and lead carboxylates were still well detectable as before exposure, revealing few alterations of the original protected surface. On the contrary, both on unprotected lead and on the other treated samples a thick oxidation layer formed, mainly consisting of hydrocerussite ($Pb_3(CO_3)_2(OH)_2$) and in some cases plumbonacrite ($Pb_{10}(CO_3)_6(OH)_6O$), which are final products resulting from active corrosion processes involving acetic acid (Niklasson et al. 2004). In the case of sulphatised samples, the layer of $PbSO_4$ was still visible after the exposure, probably because the corrosion layer spalls off, whereas in the case of phosphatised samples the height of the peaks of $PbHPO_4$ strongly decreased. Besides crystalline compounds, the presence of an amorphous phase was revealed, in most cases, by a rising of the background line at low angle.

Gravimetric measurements were also performed in order to have further information on the inhibiting performance of the tested treatments. In the graph of Figure 7a dry mass gain values are reported as a function of exposure time for treated samples exposed to acetic acid. Treatments with C10 and C11 induced a lower mass gain compared to the case of pure lead, which indicates the formation of a lower amount of insoluble corrosion products on the protected surface. In the case of thiourea, the mass gain was slightly higher than in the case of unprotected lead. The lowest mass gain was found in the case of phosphatised samples, showing low and constant values during all the exposure period. The results on sulphatised samples are not included in Figure 7a because the brittleness of the corrosion layer induced a random mass decrease and the values were not reproducible.

Figure 7 Gravimetric measurements: (a) mass gain vs exposure time; (b) corrosion rate (v_{corr}) vs exposure time.

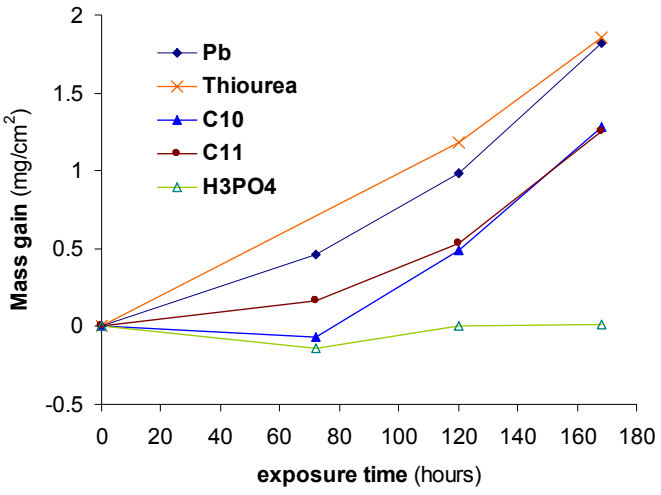

(a)

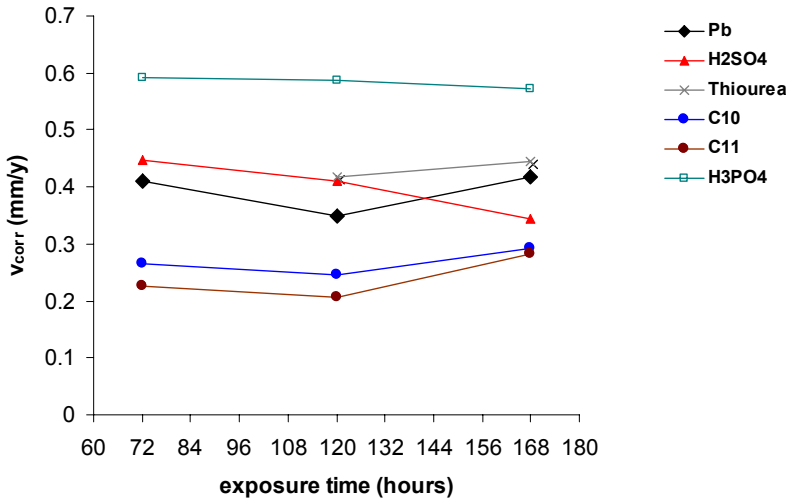

(b)

Table1 - Treatment conditions and data measured at the end of treatments.

	Concentration of treatment solution, mol/L	Immersion time, h	Mass gain, mg/cm^2	Concentration of dissolved lead, ppm	pH
C10	0.05	24	0.38	n.d.	8.7
C11	0.05	24	0.33	n.d.	7.3
Thiourea	0.05	1	0.03	1	6.6
H_2SO_4	0.05	24	0.40	3	1.3
H_3PO_4	0.05	30	0.07	30	1.9

n.d.: non detectable.

Table 2 - XRD analysis of products on the surface of lead coupons, before and after exposure.

Treatments	Pb	PbO	Hy	Pl	PbC10/C11	$PbSO_4$	$PbHPO_4$
Pb	++	--	--	--			
Pb, *168h ageing*	+/-	+	+	++			
C11	+	+/-	--	--	+		
C11, *168h ageing*	+	+/-	+/-	--	+		
C10	+	--	--	--	+		
C10, *168h ageing*	+	+/-	+/-	--	+		
Thiourea	+	--	+/-	--			
Thiourea,*168h ageing*	--	++	++	--			
Sulphate	+/-	--	--	--		+	
Sulphate, *168h ageing*	+/-	--	++	--		+	
Phosphate	+	--	--	--			++
Phosphate,*168h ageing*	+/-	--	++	++			+/-

-- (non detectable) ; +/- (traces) ; +(well detectable) ; ++ (abundant).
Hy (hydrocerussite, $Pb_3(CO_3)_2(OH)_2$); Pl (plumbonacrite, $Pb_{10}(CO_3)_6(OH)_6O$); PbC10/C11 (lead monocarboxylates)

The results of weight loss measurements, carried out by pickling the corroded samples in order to evaluate the corrosion rate, are shown in Figure 7b, where the values of the corrosion rate as a function of the exposure time are reported. The results of the weight loss measurements confirmed in most cases the trend of dry mass gain data. The corrosion rate of the C10 and C11 inhibited samples is lower by two orders of magnitude than that of all other samples. Thiourea and sulphatised samples corrode at the same rate of unprotected lead, confirming the low protectiveness of the two treatments. In the case of phosphates, the small mass gain and the very high corrosion rate suggest the formation of very soluble oxidation products and therefore a very unstable and unprotective patina that does not hinder the dissolution of lead. On the contrary, in the case of C10 and C11, the low mass gain and the low corrosion rates suggest a quite good insulation of the metal surface from the aggressive environment.

4. Conclusions

On the basis of the comparative evaluation of the candidate treatments, we can exclude treatments with sulphuric acid, phosphoric acid and thiourea as protective methods against corrosion of lead-rich organ pipes in acetic acid atmosphere.

The results of the comparison among the different tested treatments indicate that the protectiveness of the treatments with sodium undecanoate (C11) and sodium decanoate (C10) is (i) comparable and (ii) the highest among all the inhibitors tested on lead. Comparing the two monocarboxylate-based treatments, it can be said that, in the testing conditions, C11 is as protective as C10 but the lower solubility of C11 in water makes the production of an homogeneous layer more difficult. Consequently, the most promising candidate to be applied on uncorroded lead-rich pipes is C10.

It is also worth remembering that the reversibility of the treatment with C10 and C11, i.e. the possibility to remove lead carboxylates by a solvent like ethanol, is a feature of main importance in the case of organ pipes, where conservation measures have hitherto been mainly irreversible.

Acknowledgements

The COLLAPSE project is a research project supported by the European Commission under the Fifth Framework Programme and contributing to the implementation of the Key Action "The City of Tomorrow and Culture Heritage" within the Energy, Environment and Sustainable Development (contract n. EVK4-CT-2002-00088).

References

Badawy, W.A., Hefny, M.M, El-Egamy, S.S., (1990). *Corrosion behaviour of Pb-Sn binary alloys in acid solutions*, Corrosion, **46**(12) 978-982.

Boffardi, B.P, (1990). *Minimization of Lead Corrosion in Drinking Water,* Materials Performance, 29 (8) 45-49.

Carradice, L.A., Campbell, S.A., (1994). *The conservation of lead communion tokens by potentiostatic reduction,* Studies in Conservation, **39**, 100-106

Chiavari, C., Dinoi, C., Martini, C., Poli, G., Prandstraller, D. (2004). *Conservation of organ pipes: influence of microstructure and composition on corrosion of lead exposed to organic acid vapours*. EUROCORR 2004, Nice, September.

Degrigny, C., Le Gall, R., (1999). *Conservation of ancient lead artifacts corroded in organic acid environments: electrolytic stabilization/consolidation,* Studies in Conservation, **44**, 157-169.

Fawzy, M.A., Sedahmed, G.H., Mohamed A.A., (1981). *Corrosion behaviour of Pb-Sn binary alloys in acid solutions,* Surface Technology ,**14**, 257-264.

Graedel, T.E., (1994). *Chemical mechanism for the atmospheric corrosion of lead,* J.Electrochem. Soc., **141**, 4 922-927.

Green, L., (1989). *A re-evaluation of lead conservation techniques at the British Museum*, Conservation of Metals. In Jaro, M., Veszprem, (eds), p.121. (Hungary)

Hallebeek, P.B., (1994).*Comparison of the corrosive properties of seven types of plywood*. In: Verschoor, H. and Mosk, J. (eds) Contributions of the Central Research Laboratory to the Field of Conservation and Restoration, 95-108 (Amsterdam)

Ijomah, M.N.C., (1988). *Polarization of lead-tin alloys in sulphuric acid*, Journal of Applied Electrochemistry, **18**, 142-148

Lane, H., (1979). *Some comparisons of lead conservation methods, including consolidative reduction.* In SSCR (eds), The Conservation and Restoration of Metals, 50-60. (Edinburg)

Nosek, E.M., (1985). *The investigation and conservation of a lead paten from the eleventh century*, Studies in Conservation, 30, 19-22.

Niklasson, A., Johansson, L-G. and Svensson, J-E. (2004) *Atmospheric Corrosion of Historical Organs; Influence of Acetic and Formic Acid Vapour and Water Leaching on Lead-rich Pipes*. Metal 2004, Canberra, October .

Niklasson, A., Johansson, L-G. and Svensson, J-E., (2003) Chalmers University of Technology, Sweden, Personal communication,.

Organ, R.M., (1953). *Use of ion-exchange resin in the tratment of lead objects,* Museums Journal, 53, 49-52.

Organ, R.M., (1963). *The consolidation of fragile metallic objects*, Recent advances in conservation (Contributions to the IIC Rome conference, 1961). In Thomson, G., (eds), 128-134. (London Butterworths).

Rocca, E., Steinmetz, J., (2001). *Inhibition of lead corrosion with saturated linear aliphatic chain monocarboxylates of sodium,* Corrosion Science, **43**, 891-902.

Rocca, E., Rapin, C., Mirambet, F., (2004). *Inhibition treatment of the corrosion lead artefacts in atmospheric conditions and by acetic acid vapour: use of sodium decanoate,* Corrosion Science, **46**, 653-665.

Ruetschi, P., Angstadt, R.T., (1964). *Anodic Oxidation of Lead at Constant Potential*, Journal of Electrochemical Society, **111**, 1323-1330

Sankarapapavinasam, S., Pushpanaden, F., Ahmed, M.F., (1989). *Hydrazine and substituted hydrazines as corrosion inhibitors for lead in acetic acid*, British Corrosion Journal, **24** (1) 39-42.

Sankarapapavinasam, S., Ahmed, M.F., (1990). *Tosylhydrazine as Protector for Lead in Acetic acid Vapours*, J.Electrochemical Society of India, **39** (4) 255-256.

Shreir, L.L., Jarman, R. A., Burstein, G. T., (1994). In Butterworth-Heinemann (eds), *Corrosion*. (Oxford)

Tetreault, J., Sirois, J., Stamatopoulou, E., (1998). *Studies of lead corrosion in acetic acid environments,* Studies in Conservation, **43,** 17-32

Watson, J., (1985). *Lead and Tin: Studies in Conservation and Technology*. In Miles, C.E. and Pollard, S.C. (eds), UKIC Occasional Paper No. 3, p.44-45. (London)

Winand, R., (1978). *Comportement anodique du plomb en milieu sulfurique*, Metallurgie, **XVIII** (2), 43-59

Overview of archaeological iron: the corrosion problem, key factors affecting treatment, and gaps in current knowledge

L. Selwyn

Canadian Conservation Institute, 1030 Innes Road, Ottawa, Ontario K1A 0M5 Canada

Abstract

This paper contains a brief overview of iron corrosion, including a summary of what happens to iron during burial and after excavation. Also included is a discussion of the iron oxyhydroxide, akaganéite. Following this, there is a critical review of the key factors that play a role in the effectiveness of various iron treatments used to treat archaeological iron. Key areas are identified where there is a need for further research. The information is based on research carried out at the Canadian Conservation Institute and by others worldwide.

Keywords: Iron corrosion, archaeological iron, conservation treatments, akaganéite, chlorides, sodium hydroxide, alkaline sulphite, electrolysis.

1. Introduction

An ongoing problem with archaeological iron is continued corrosion after excavation caused by the accumulation of salts during burial. The treatment of archaeological iron is often based on immersing the object in an aqueous solution and waiting for the chloride ions to diffuse out. This paper addresses the current understanding of archaeological iron corrosion and treatment. Reviewed first are the corrosion processes that iron undergoes during burial and after excavation, including a discussion of the critical role of chloride ions and the formation of chloride-containing akaganéite. Two diffusion models currently used to interpret the time-dependence of the chloride ion concentration in treatment solutions are briefly described. Next, two key factors, which influence chloride ion diffusion, are discussed. These are whether the iron continues to corrode during immersion, and the porosity of the corrosion layer. Included in this discussion are how pH, Fe(II) ions, electrolysis, temperature, and the removal of dissolved oxygen contribute to continued iron corrosion, the corrosion layer porosity, and ultimately to the success or failure of an aqueous iron treatment.

2. Corrosion

2.1 During Burial

When iron is exposed to moisture during burial, it corrodes by an electrochemical process. The anodic reaction of iron dissolution takes place at the surface of the metal; the anodic half-reaction is $Fe(s) \rightarrow Fe^{2+}(aq) + 2e^-$; designations are solid(s), aqueous(aq), and gas(g). In aqueous solutions with pH greater than 4, this half-reaction is counterbalanced by the reduction of dissolved oxygen; the cathodic half-reaction is $O_2(g) + 2H_2O + 4e^- \rightarrow 4OH^-(aq)$. At the iron surface, iron(II) ions dissolve and accumulate. Each Fe^{2+} ion is hydrated with six coordinated water molecules $[Fe(H_2O)_6]^{2+}$ (or, for simplicity, written as Fe^{2+}). The +2 oxidation state is favoured at low levels of dissolved oxygen

The water associated with hydrated Fe^{2+} ions can react (e.g. undergo hydrolysis) and cause local acidification (e.g. $Fe^{2+}(aq) + H_2O \rightarrow Fe(OH)^+(aq) + H^+(aq)$). The rate of hydrolysis increases with increasing temperature. Different iron(II) species can form, depending on the pH. Hydrolysis of Fe^{2+} ions starts above pH 6 and involves the release of one or more protons from the coordinated water. In solutions containing only iron in the +2 oxidation state, the predominant species are: hydrated Fe^{2+} below pH 9; $Fe(OH)^+$ at pH 9-10; and

$Fe(OH)_3^-$ (also written $HFeO_2^- \cdot H_2O$) and $Fe(OH)_4^{2-}$ (also written $FeO_2^{2-} \cdot 2H_2O$) above pH 10 (Blesa et al. 1994). In the presence of dissolved oxygen, the Fe^{2+} ions can be oxidized to Fe^{3+} ions. These hydrated Fe^{3+} ions, $[Fe(H_2O)_6]^{3+}$, can also undergo hydrolysis, starting above about pH 1. In solutions containing only iron in the +3 oxidation state, the predominant species are: hydrated Fe^{3+} below pH 2; $Fe(OH)^{2+}$ at pH 2-3.5; $Fe(OH)_2^+$ at pH 3.5-8.5; and $Fe(OH)_4^-$ above pH 8.5 (Blesa et al. 1994).

The solids that precipitate from solutions containing any of the above-mentioned iron(II) and iron(III) ions depend on the pH (e.g. some cathodic half-reactions produce OH^- ions), the level of dissolved O_2, and the presence and concentration of environmental anions. Solid iron(II) hydroxide, $Fe(OH)_2$, starts to precipitate above pH 6 and has low solubility over the pH range 9-14, with its minimum solubility at pH 11. Under reducing conditions in the presence of carbonate or phosphate ions, siderite (iron(II) carbonate, $FeCO_3$) or vivianite (iron(II) phosphate, $Fe_3(PO_4)_2 \cdot 8H_2O$) can also form.

Once $Fe(OH)_2$ has precipitated, it is easily oxidized by dissolved oxygen and forms intermediate Fe(II)-Fe(III) compounds (e.g. magnetite Fe_3O_4, green rusts). Magnetite, an electronically conducting mixed Fe(II)-Fe(III) iron oxide, is a common corrosion product identified on archaeological iron. Green rusts can form in the presence of chloride ions, carbonate ions, or sulphate ions; these compounds have well defined layered structures of positively charged iron hydroxide sheets and negatively charged anions (Refait et al. 1997). Because green rusts are oxidized to iron oxyhydroxides when exposed to air, they are rarely identified as corrosion products.

Iron(II) hydroxide can also be oxidized to iron(III) compounds such as iron hydroxide $Fe(OH)_3$ or iron oxyhydroxides, FeO(OH). Freshly formed $Fe(OH)_3$ is amorphous but, over time, transforms into crystalline material, typically one of the iron oxyhydroxides. Lepidocrocite γ-FeO(OH) usually forms first, but it can transform into goethite, α-FeO(OH), which is thermodynamically more stable (Stratmann 1990). Iron(III) oxyhydroxides are orders of magnitude less soluble than iron(II) hydroxide. Goethite, for example, has a solubility product 10^{-41} whereas $Fe(OH)_2$ has a solubility product of 10^{-15} (Cornell and Schwertmann 1996). The iron oxyhydroxide, akaganéite β-FeO(OH), can form in the presence of chloride ions (Cl^-), but it does not appear to have been reported as a corrosion product that has formed on archaeological iron during burial. Iron(III) oxychloride, FeOCl, was once thought to be a major chloride-containing corrosion product on archaeological iron (North and Pearson 1975), but its identification was probably a mistake (Gilberg and Seeley 1981).

Archaeological iron is usually covered by a layered structure of corrosion products. The outer layer is a mixture of iron corrosion products (e.g. iron(III) oxyhydroxides, typically goethite) and extraneous material such as small rocks, sand, clay and soil minerals. Below this is another layer of iron corrosion products in a lower oxidation state, usually magnetite, lying on top of any remaining metal. When iron corrodes in a marine environment, it usually becomes covered with concretions, primarily calcium carbonate $CaCO_3$. The Fe^{2+} ions tend to react and precipitate in the concretion rather than on the surface of the object. Because of the acidity that develops beneath the concretion of marine iron, there may not be many corrosion products retained on the surface of wrought iron or cast iron. Wrought iron will have its characteristic fibrous structure while cast iron will usually have its original shape maintained by the remaining porous matrix of soft graphite filled with some iron corrosion products.

As long as iron is corroding, it is forming Fe^{2+} ions at the interface between the remaining metal and the corrosion products. These Fe^{2+} ions dissolve, accumulate, and depending on the local pH, undergo hydrolysis. Electrical neutrality must be maintained. This is achieved by anions diffusing in from the surrounding environment to balance the charge of the Fe^{2+} and H^+ cations. Chloride ions, in particular, tend to concentrate at the interface. The Cl^- ions remain in solution or are adsorbed onto the corrosion products. The degree to which Cl^- ions are adsorbed depends on the pH. The maximum adsorption of Cl^- ions occurs at low pH (acidic conditions) because of a net positive charge produced on the surface of iron oxyhydroxides by excess H^+ ions. The net result of on-going iron corrosion during burial is that the cracks, pores, and open spaces within the corrosion layer or beneath concretion become filled with an acidic iron(II) chloride solution, with the Cl^- ions concentrated at the metal surface (Turgoose 1993).

2.2 After Excavation

On-going corrosion problems occur on iron objects after excavation if they still contain an iron core and are contaminated with salts, especially an acidic iron(II) chloride solution (Selwyn et al. 1999). When a freshly excavated iron object is exposed to a new environment above ground, it generally experiences a lower relative humidity (RH) and a higher O_2 concentration relative to the burial environment. As the iron dries, the contaminating solution of acidic $FeCl_2$ plus other salts concentrate and the corrosion layers crack, allowing

greater access of oxygen to remaining metal. Rapid drying of freshly excavated iron can also result in the formation of yellow crystals of $FeCl_2$ (Costain 1984; Turgoose 1993).

Solids or dissolved ions that were stable in the burial environment may no longer be stable in air and may oxidize to new corrosion products or to new ions in solution. When an acidic solution of iron(II) chloride is exposed to air, the Fe^{2+} ions can undergo hydrolysis and be oxidized to Fe^{3+} ions and new compounds can form:

$$4Fe^{2+}(aq) + O_2(g) + 6H_2O \rightarrow 4FeO(OH)(s) + 8H^+(aq) \quad (1)$$

This corrosion process causes physical damage to the shape of the object and chemical damage to any remaining iron metal. Chemical damage is caused by the formation of hydrochloric acid (HCl). The following acid regeneration cycle has been proposed for the cause of ongoing corrosion of iron contaminated with HCl (Askey et al. 1993):

$$2Fe(s) + 4H^+(aq) + 4Cl^-(aq) + O_2(g) \rightarrow 2Fe^{2+}(aq) + 4Cl^-(aq) + 2H_2O \quad (2)$$
$$2Fe^{2+}(aq) + 4Cl^-(aq) + 3H_2O + \tfrac{1}{2}O_2(g) \rightarrow 2FeO(OH)(s) + 4H^+(aq) + 4Cl^-(aq) \quad (3)$$

The crucial factor in this cycle is that the Cl^- ions form a soluble salt with iron(II) ions and it is this solubility that allows the cycle in Equations 2 and 3 to proceed.

Physical damage is caused by the formation of new solids (i.e. iron oxyhydroxides, FeO(OH)) within the surface layers which causes stresses and cracks. The molar volumes of FeO(OH)'s are about three times greater than the molar volume of iron. Laboratory studies of the oxidation and hydrolysis of $FeCl_2$ found that at low Cl^- ion concentrations, goethite α-FeO(OH) and/or lepidocrocite γ-FeO(OH) precipitate, and at high Cl^- ion concentrations, akaganéite β-FeO(OH) forms (Refait and Génin 1997). A representative chemical formula of $FeO_{0.833}(OH)_{1.167}Cl_{0.167}$ for akaganéite (reflecting the presence of chlorine within the crystal structure) has recently been suggested (Ståhl et al. 2003).

One visual symptom that there is a corrosion problem on excavated iron is the formation of either wet bubbles of acidic liquid (weeping or sweating iron), or dry, hollow red spherical shells on an artefact's surface. Weeping is attributed to the hygroscopic nature of iron chloride salts. Iron(II) chloride and iron(III) chloride are both hygroscopic and form a series of salts with different waters of hydration depending on the relative humidity. Iron(II) chloride, for example, exists as yellow crystals ($FeCl_2 \cdot 2H_2O$) below about 20% RH, as green crystals ($FeCl_2 \cdot 4H_2O$) between 20-55% RH, and deliquesces above 56% RH (Turgoose 1982). When the relative humidity is high, these salts absorb water, dissolve, and form wet droplets of orange coloured liquid. Iron oxyhydroxides precipitate around the outside of the droplets and generate a framework for the spherical shells.

2.3 Akaganéite, β-FeO(OH)

Akaganéite can form only in the presence of Cl^- ions. It can be prepared in the laboratory from either Fe(II) or Fe(III) chloride solutions; it cannot be prepared from solutions having a pH >5. Akaganéite is thought to form on archaeological iron only after it has been excavated and exposed to air (Gilberg and Seeley 1981). Exposure to air promotes the oxidation and hydrolysis of accumulated acidic Fe(II) chloride. Because akaganéite only forms under conditions of relatively high concentrations of Cl^- ions (e.g. 2*M* (Refait and Génin 1997)), the presence of akaganéite on archaeological iron is considered evidence that the object is heavily contaminated with Cl^- ions (Ståhl et al. 2003).

There is concern that the formation of akaganéite might be a threat because it might somehow release chloride ions at high humidity, thereby stimulating further corrosion (Ståhl et al. 1998). In a study of synthetic akaganéite, it was demonstrated that as long as it remains dry, it is stable and the chlorine remains locked inside the tunnels (Ståhl et al. 2003). It was also demonstrated that heating could cause the release of the chlorine (but only when heated above 200°C which transforms akaganéite to hematite (α-Fe_2O_3)), and that the chlorine could not be removed from inside the tunnels of akaganéite by washing with water (Ståhl et al. 1998; 2003). Furthermore, past observations that Cl^- ions could be washed from synthetic akaganéite with water was attributed to the removal of adsorbed Cl^- ions rather than chlorine from the tunnels.

Although the chlorine cannot be washed out of akaganéite, there are reactions that can occur which promote the transformation of akaganéite to goethite or magnetite and therefore the release of chlorine as Cl^- ions. At room temperature, these reactions involve water. When akaganéite, for example, is immersed in an aqueous solution (including alkaline ones), it slowly transforms to goethite by a process of dissolution and

precipitation (Cornell and Schwertmann 1996). Furthermore, any of the iron oxyhydroxides can react with Fe^{2+} ions (or with $Fe(OH)_2$) to form magnetite:

$$Fe(OH)_2(s) + 2FeO(OH)(s) \rightarrow Fe_3O_4(s) + 2H_2O \quad (4)$$

or

$$Fe^{2+}(aq) + 2FeO(OH)(s) \rightarrow Fe_3O_4(s) + 2H^+(aq) \quad (5)$$

Laboratory studies have shown that α-FeO(OH), β-FeO(OH), and γ-FeO(OH) react with $Fe(OH)_2$ to produce Fe_3O_4 in the order β-FeO(OH) > γ-FeO(OH) >> α-FeO(OH) (Ishikawa et al. 1998).

The chlorine trapped within newly-formed akaganéite will be released when it is transformed into goethite or magnetite, but more research is needed to document the conditions under which this transformation takes place. If akaganéite transforms to goethite or magnetite during an immersion treatment, then the chlorine will be released into the solution as Cl^- ions, which will be removed by successive changes of the treatment solution. If the rate of these transformations is slow, pre-existing akaganéite may still remain after treatment.

3. Conservation

3.1 Untreated Iron

It is difficult to prevent the on-going corrosion of excavated archaeological iron if it remains untreated. It is usually recommended that untreated archaeological iron be stored below 20% RH (Turgoose 1982). It has been shown, however, that untreated archaeological iron can continue to corrode even if stored under desiccated conditions (RH less than 15%) (Keene 1994). One factor is the rough surface of corroded iron; inhomogeneities promote water condensation in the pores. Another factor is contamination by hygroscopic salts which can pick up moisture and promote corrosion. Because continued corrosion requires both oxygen and water, attempts have been made to minimize iron corrosion during storage by creating a sealed microclimate that keeps the relative humidity low and removes oxygen gas. Consideration is now being made for storing untreated iron in a dry, oxygen-free environment created using a scavenger (e.g. RP-A) sealed inside a transparent barrier film (e.g. Escal) (Becker 1999; Carrió and Stevenson 2003; Mathias 2003). Both RP-A and Escal are made by Mitsubishi Gas Chemical Company; more information about these products is available at the Mitsubishi web site (www.mgc-a.com). The drawback of the latter approach is that it depends on a perfect seal and only lasts about 5 years.

3.2 Immersion Treatments

Conservation treatments for archaeological iron are designed to remove as much of the salt contamination (especially Cl^- ions) as possible. If enough Cl^- ions are removed, then these objects can resist corrosion when stored or displayed in a controlled museum environment without special storage conditions. Archaeological iron has a significantly higher survival rate if it is treated by some form of desalination treatment (typically by immersion) compared to being left untreated (Keene 1994). In general, immersion treatments involve placing iron in an aqueous solution, usually a near-neutral or alkaline one, and waiting for the Cl^- ions to diffuse out. Studies have now shown that immersion of archaeological iron in water (at room temperature, warm, or boiling) is generally not effective in removing Cl^- ions (Watkinson 1996). One contributing factor may be that in neutral solutions, some fraction of the Cl^- ions remain adsorbed on the surface of the iron corrosion products. One advantage of using alkaline treatment solutions is that they promote the desorption of Cl^- ions because of the net negative charge induced on the surface of iron oxyhydroxides by excess OH^- ions. Another advantage is iron passivation; this is discussed below in more detail in the section "Iron passivation".

One approach to deciding if an immersion treatment has been successful is to expose the treated iron to high RH to find out if there are enough Cl^- ions remaining to cause new weeping. Another approach is to dissolve the artefact in acid after treatment to determine the quantity of residual chlorine. This approach can also be used to determine the relative effectiveness of a treatment: the total amount of Cl^- ions that have diffused into a treatment solution is measured; then the total amount of chlorine remaining in the artifact after treatment is determined (usually based on a destructive method, such as by completely dissolving the artefact in an acid). A few such studies have been carried out to determine the relative effectiveness of various immersion treatments (Watkinson 1996; Al-Zahrani 1999; González et al. 2003). Further studies are needed to better understand the effectiveness of different immersion treatments when used on cast and wrought iron from both terrestrial and marine sites.

The length of time an object is immersed in a treatment solution is usually based on monitoring the Cl^- ion concentration in the treatment solution (North and Pearson 1978b). The treatment solution is changed either on a regular basis or after the Cl^- ion concentration has stopped increasing, and treatment is stopped when the Cl^- ion concentration in the solution stays low, usually below 20 parts per million (Watkinson 1983). One drawback with monitoring the Cl^- ion concentration in treatment solutions is that this doesn't provide any information about whether there are still Cl^- ions remaining in the object. An advantage of this approach is that if the Cl^- ion concentration is measured as a function of time, then it may be possible to interpret the results using existing diffusion models developed for Cl^- ions diffusing out of archaeological iron.

North and Pearson, for example, developed a diffusion model for Cl^- ions diffusing from the corrosion layer of cast iron where the Cl^- ions are assumed to be evenly distributed (North and Pearson 1978b). Their model, which can be described as a 'uniform' model, provides a general expression for the diffusion of Cl^- ions from any shaped object for short times. The expression predicts that when the amount of Cl^- ions in solution is plotted against the square root of time ($t^{1/2}$), the resulting graph contains a straight line passing through the origin, and the slope of this line is proportional to the Cl^- ion diffusion constant. Their model predicts that Cl^- ions diffuse into a treatment solution immediately after an object is immersed because the Cl^- ions are assumed to be uniformly distributed in the solid.

Another diffusion model has been developed for Cl^- ions diffusing from iron that is corroding (at least when it is first placed in a treatment solution) (Selwyn et al. 2001). This model is based on Cl^- ions initially concentrated at the interface between the iron and the corrosion layer. This abrupt starting distribution ('abrupt model') can be viewed as the opposite limit of the uniform distribution of North and Pearson ('uniform model'). The abrupt model predicts a delay before any Cl^- ions appear in the treatment solution and an S-shaped (a sigmoidal shaped) variation of the Cl^- ions removed versus square root of time. The delay corresponds to the time needed for the Cl^- ions to diffuse from their initial position at the interface between the iron metal and the overlying corrosion layer, over the distance of the corrosion layer, and finally reach the outer surface where it can then diffuse into the solution.

Diffusion models contain a diffusion constant. If the model accurately reflects experimental data, then it is often possible to extract the diffusion constant, the magnitude of which reflects the rate at which diffusing species (e.g. Cl^- ions) move. The ability of Cl^- ions to diffuse through a solution permeating a corrosion layer depends on the pore size, channel size, and their connectivity within the solid. Diffusion constants are smaller for ions diffusing through a solution within the pores of a solid (e.g. a corrosion layer) than for ions diffusing through an open solution. Further research, based on systematic monitoring the Cl^- ion concentration as a function of time for various treatment solutions (with each solution used to treat an individual artefact), is needed to help identify the most effective treatments. It may or may not be possible to interpret the results using a diffusion model; such models apply only if the conditions under which they were derived remain valid (i.e. the solid remains physically unchanged and the diffusion distance remains constant).

3.3 Key Factors Affecting Chloride Ion Removal

Two of the key factors that influence the ability of dissolved Cl^- ions to diffuse out of archaeological iron are whether the iron metal is corroding, and whether the corrosion layer is porous. The Cl^- ions will be released to diffuse into a treatment solution if the corrosion of the iron can be stopped, and will diffuse more easily if the porosity of the corrosion layer can be increased.

3.4 Stopping Corrosion

As long as archaeological iron is corroding during immersion, the Cl^- ions are prevented from diffusing out because they are attracted to the Fe^{2+} ions being generated by the corrosion process. If the corrosion can be stopped, then the potential gradient (generated by Fe^{2+} ions) is removed. When Cl^- ions no longer act as counter ions, they are able to diffuse out of the corrosion layer into the treatment solution. Iron corrosion can be slowed or stopped by: passivating the iron surface using an alkaline treatment solution; removing dissolved oxygen from the treatment solution; using electrochemical methods; or using corrosion inhibitors.

3.4.1 Iron Passivation: The corrosion rate of iron is dramatically reduced if the surface is passivated by an adherent layer of insoluble corrosion products. When iron corrodes in an alkaline solution, Fe^{2+} ions precipitate as $Fe(OH)_2$. Iron(II) hydroxide, once formed, is easily oxidized and hydrolyzed to an essentially insoluble film of $Fe(OH)_3$. The corrosion film, if formed in direct contact with the iron surface, can prevent the transfer of Fe^{2+} ions from the iron metal to the solution. On clean (bare) iron, precipitation of $Fe(OH)_2$ starts to occur at about pH 8 in the presence of oxygen. In general, the iron corrosion rate slows as the pH is increased above 9 and

drops to a negligible rate above 12. In the presence of aggressive Cl^- ions (which form soluble complexes with Fe(II) and Fe(III) ions), film formation is more difficult and passivation may not be possible at high Cl^- ion concentrations (Hjelm-Hansen et al. 1992).

In alkaline solutions, the formation of an adherent and passivating oxide film generally requires both dissolved O_2 gas and OH^- ions. The dissolved O_2 is necessary to support the corrosion process and generate Fe^{2+} ions at the metal surface. The OH^- ions are necessary to react with the Fe^{2+} ions to form $Fe(OH)_2$ as well as maintain the pH in a region where this hydroxide is insoluble. Precipitation of $Fe(OH)_2$ depletes the local concentration of OH^- ions and so there must always be sufficient OH^- ions at the metal surface to ensure direct precipitation of $Fe(OH)_2$. Laboratory studies have shown that bare iron can be passivated in alkaline solutions such as sodium borate ($Na_2B_4O_7$, pH 9.2), sodium sesquicarbonate (equimolar Na_2CO_3 and $NaHCO_3$, pH 10), sodium carbonate (Na_2CO_3, pH 11.2), and sodium hydroxide (NaOH, pH 12.6–13.5) (Mayne and Turgoose 1975; Hjelm-Hansen et al. 1993).

Conservators favour aqueous NaOH solutions (0.1*M* to 0.5*M*, pH 13–14) for treating archaeological iron because they are relatively cheap, readily available, and have a high pH (Mathias 1994; North and Pearson 1978b; North 1987). Furthermore, many studies have demonstrated the effectiveness of NaOH solutions in removing Cl^- ions from archaeological iron (Al-Zahrani 1999; González et al. 2003; Selwyn and Argyropoulos 2004). A contributing factor to its success as a treatment solution is its high pH, giving it the ability to stop corrosion by passivating iron, even archaeological iron. Hjelm-Hansen *et al.* monitored the corrosion potential of archaeological wrought iron nails in a 0.5*M* solution of NaOH or in 0.5*M* solution of sodium sesquicarbonate (Hjelm-Hansen et al. 1992; 1993). After several months, they observed that the iron nails had not passivated in sodium sesquicarbonate, but those in NaOH had. This observation supports the assumption that it takes time for the OH^- ions to diffuse to the metal surface and increase the pH from acidic to alkaline, and that the time to passivate gets longer when a less alkaline treatment solution (one with a lower pH) is used compared to a more alkaline (higher pH) one (Selwyn et al. 2001).

3.4.2 Dissolved Oxygen Removal: At pH > 4, the corrosion of iron is usually caused by the presence of dissolved O_2 gas. The corrosion rate can be significantly reduced if dissolved O_2 is removed from the treatment solution. Laboratory studies on archaeological iron carried out by Al-Zahrani demonstrated that solutions without oxygen were more effective at removing Cl^- ions than similar solutions with oxygen present (Al-Zahrani 1999). Several conservation treatments are designed to remove dissolved O_2. Boiling the treatment solution removes dissolved oxygen because the solubility of oxygen gas decreases with increasing temperature. Bubbling an inert gas (e.g. nitrogen) through a solution also displaces dissolved oxygen (Scott and Seeley 1987; Al-Zahrani 1999). An oxygen scavenger (e.g. sodium sulphite) can be used to remove dissolved oxygen (i.e. $2Na_2SO_3(aq) + O_2(g) \rightarrow 2Na_2SO_4(aq)$). A near-neutral solution of sodium sulphite has been used to treat marine cast iron (Gilberg 1987). Although dissolved O_2 was successfully removed, the iron corroded because of sulphate-reducing bacteria contamination. Sodium sulphite has also been used in alkaline solutions, in a treatment commonly known as alkaline sulphite (0.5*M* NaOH and 0.5*M* Na_2SO_3, pH 13.5) (North and Pearson 1975). Many conservators use this treatment (or have studied it), and find it to be reasonably effective, especially on archaeological iron that has not been allowed to dry (Keene 1994; Al-Zahrani 1999; Costain 2000).

3.4.3 Electrochemical Methods: Another approach to stopping (or slowing) iron corrosion is to use an electrochemical approach (e.g. making the artefact the cathode in an electrochemical cell). (For electrochemical methods to work, the artefact must have a substantial core of metal left). If the corrosion rate of the iron can be slowed by using this approach, then any Cl^- ions that were being held as counter ions will be released. This effect is probably contributing to the release of Cl^- ions when iron is treated by electrolysis (North 1987), cathodic reduction at constant (or limiting) potentials (Beaudoin et al. 1997; Dalard et al. 2002), cathodic protection using sacrificial anodes (MacLeod 1996), and cathodic protection using an impressed current (Mardikian 2004). However, there is some question as to whether the presence of the electric field has any significant effect on the rate at which the Cl^- ions diffuse out. North and Pearson, for example, have suggested that the presence of the electric field has an insignificant effect on the rate of Cl^- ion removal in alkaline solutions because the negative component of the current is carried mainly by the OH^- ions rather than Cl^- ions (North and Pearson 1978a; North 1978).

3.4.4 Corrosion Inhibitors: It may be possible to use corrosion inhibitors to slow the corrosion rate of archaeological iron. Anodic inhibitors slow the anodic reaction (e.g. iron corrosion), and cathodic inhibitors slow the cathodic reaction (e.g. oxygen reduction). For an inhibitor to be effective, it must reach the region where either the anodic or cathodic reactions occur. As such, anodic inhibitors need to reach the metal surface

and cathodic inhibitors need to reach the electronic conductors making contact with the corroding iron (e.g. graphite on cast iron or conducting corrosion products such as magnetite). Corrosion inhibitors have been developed for use on clean metal surfaces (typically covered by only a thin air-formed oxide film) and, because of the thickness of corrosion products on excavated material, it is difficult to determine how effective such corrosion inhibitors might be when used on archaeological iron (Turgoose 1985).

One corrosion inhibitor that has been studied for use in treating archaeological iron is ethylenediamine ($H_2N\text{-}CH_2\text{-}CH_2\text{-}NH_2$, abbreviated *EN*) (Argyropoulos et al. 1997). This organic compound readily dissolves in water to form an alkaline solution. Laboratory studies have shown that *EN* solutions are effective as a corrosion inhibitor on non-archaeological iron because the *EN* molecule can be adsorbed onto oxide-free (Incorvia 1985) or oxide-covered (Incorvia and Contarini 1989) iron surfaces. Duprat *et al.*, for example, have compared the effectiveness of *EN* with NaOH (each solution at pH 11 and containing 3% NaCl) for inhibiting non-archaeological iron corrosion (Duprat et al. 1986). They observed that (at the same pH) an *EN* solution was more effective than an NaOH solution in slowing iron corrosion. They attributed the overall effectiveness of these two solutions to their alkalinity (a source of OH^- ions) and their ability to form a passivating film on iron. They ascribed the increased effectiveness of *EN* over NaOH at the same pH to the *EN* molecule contributing an additional inhibiting effect by being adsorbed onto the metal surface (Duprat and Dabosi 1981).

Unfortunately, in a quantitative study involving *EN* solutions (5% v/v, 0.75*M*, pH 11.5) to treat archaeological iron, the Cl^- ions were not removed effectively (Selwyn and Argyropoulos 2004). Furthermore, relatively high levels of iron were detected in the treatment solution. This observation was attributed to the formation of soluble complexes between the *EN* molecule and Fe^{2+} ions and suggested the possibility that iron corrosion was being stimulated. There have, in fact, been several reports in the conservation literature about rapid corrosion of archaeological iron immersed in *EN* solutions (Brown 1985; Busse 1997; Costain 2000). Ethylenediamine is well known for its ability to form complexes with transition metal ions in the +2 oxidation state (Paoletti 1984). Both nitrogen atoms on an *EN* molecule are capable of simultaneously interacting with the same metal ion and forming a five-membered ring. Iron(II) ions can form three different $[Fe(EN)_x^{2+}]$ complexes with ethylenediamine, with metal: *EN* ratios of 1:1, 1:2, or 1:3 (Paoletti 1984). As a consequence of the toxicity of *EN*, and its ability to stimulate corrosion, there has only been limited use of *EN* solutions to treat archaeological iron.

3.5 Increasing Porosity

The main driving force for the removal of Cl^- ions from archaeological iron is their diffusion from a region of higher concentration (in the corrosion layer) to a region of lower concentration (in the treatment solution). The ability of Cl^- ions to diffuse away from the metal surface into the treatment solution depends on the porosity of the solid material (e.g. corrosion layer, concretion) through which they must move. Because the Cl^- ions are dissolved in solution, they must diffuse through the solution filling the cracks, fissures, interconnecting pores, and tiny channels inside the solid material before they can reach the treatment solution. The rate at which Cl^- ions diffuse out depends on the size of the open spaces within the solid, how well they are linked together, and if continuous pathways exist from the metal to the outer surface of the object. It is the porosity within the solid material that allows the treatment solution to diffuse in and the Cl^- ions to diffuse out. If the Cl^- ions are trapped in discrete areas under relatively impermeable material, then the treatment solution will be unable to diffuse in and the Cl^- ions will be unable to diffuse out. If Cl^- ions are still trapped after treatment, then in the future, they may cause problems, especially if a channel opens up, water and oxygen enter, and corrosion is stimulated.

The porosity of the corrosion products may be increased by dissolving extraneous material in alkaline solutions. Many inorganic and organic materials are more soluble in alkaline solutions than neutral ones. The solubility of quartz, for example, increases above pH 9. Greasy dirt, fatty compounds, oils, and other organic material (e.g. cellulose, protein) are broken down in alkaline solutions into water-soluble compounds.

The porosity of the corrosion products may also be increased by heating the treatment solutions. It is recommended, for example, that alkaline sulphite treatment solutions be heated (50–70°C). Higher temperatures significantly increase the solubility of surface materials. In alkaline solutions, the solubility of iron oxyhydroxides increases with increasing temperature (Blesa et al. 1994). For iron in alkaline solutions (pH greater than ~ 12), there is a region of active corrosion that becomes larger at higher temperatures (and lower pH) because of the increased solubility (Townsend 1972).

On the other hand, the porosity of the corrosion products may be decreased when freshly excavated iron is exposed to air. Turgoose predicted that placing archaeological iron into an alkaline solution would cause any dissolved Fe^{2+} ions to precipitate within the corrosion layer, decreasing the porosity, restricting the Cl^- ion diffusion, and possibly trapping them (Turgoose 1993). More recently, González *et al*. demonstrated that if

excavated iron is exposed to air and allowed to dry before treatment, then not all the Cl^- ions can be removed by immersion treatments (González et al. 2003). They also demonstrated that all the Cl^- ions could be removed (in 1-2% NaOH solutions) from excavated iron samples that had been stored under dry argon until treatment.

Certain treatments (electrochemical reduction, alkaline sulphite) increase the porosity of the corrosion products because some of the iron oxyhydroxides are reduced to magnetite (or some other lower oxidation state iron oxide or iron hydroxide). The molar volume (per mole of iron) of magnetite (14.9 cm^3) is smaller than the molar volumes occupied by the iron oxyhydroxides [goethite (20.9 cm^3), akaganéite (26.7 cm^3), and lepidocrocite (21.7 cm^3)]. The smaller volume occupied by the solid magnetite corresponds to greater pore space and this increase in porosity increases the rate at which Cl^- ions diffuse through the solution within the pore space. Although such treatments may increase the porosity, they may also decrease the mechanical integrity of the corrosion layers and make the artifact more fragile.

3.6 Specific treatments discussion – increased porosity of the corrosion layer.

3.6.1 Sodium Hydroxide: Turgoose *et al.* demonstrated that when archaeological iron is placed in alkaline NaOH solutions, there is an increase in the porosity of the corrosion products (Turgoose et al. 1996). They attributed this beneficial effect to rapid electrochemical reactions occurring at the iron/corrosion interface, causing fissures and cracks to develop in the corrosion layer, and resulting in a more open, fragile structure. The rapid processes are thought to be oxidation-reduction reactions involving iron metal, magnetite, and iron(II) species (Hjelm-Hansen et al. 1993). They may also involve the precipitation of small amounts of solids within the corrosion layer. These reactions occur on electronically-conducting surfaces (e.g. magnetite) and cause irreversible changes and softening of the corrosion product layer (Hjelm-Hansen et al. 1993). Two other reactions that might also contribute to this process are the interactions between Fe^{2+} and FeO(OH) (see Equations 4 and 5). Recent laboratory studies of non-archaeological iron in NaOH solutions (pH 11–13) have detected the electrochemical activity of the passive film on iron and confirmed that oxidation-reduction reactions easily occur between the iron(II) and iron(III) oxidation states (Schmuki et al. 1998; 1999). These studies have also shown that there is little or no dissolution of the iron corrosion products making up the passive layer (e.g. FeO(OH), Fe_3O_4, $Fe(OH)_2$) in these alkaline NaOH solutions under oxidizing or reducing conditions. Under reducing conditions, the passive film does not dissolve but instead undergoes a solid-state conversion from Fe(III) compounds to lower oxidation-state compounds (e.g. probably with a structure related to $Fe(OH)_2$) having a porous structure (Schmuki et al. 1999). Based on electrochemical studies of archaeological nails in 0.5*M* NaOH or in 0.5*M* sodium sesquicarbonate, it was concluded that iron undergoes rapid electrochemical processes in NaOH, but not in sodium sesquicarbonate (Hjelm-Hansen et al.1992; 1993). It is not known if rapid electrochemical processes occur when archaeological iron is placed in any other alkaline solutions besides NaOH. Further research is needed to better understand the conditions under which these processes occur.

3.6.2 Alkaline Sulphite: When freshly excavated iron is placed in an alkaline sulphite solution, some of the iron oxyhydroxides may be converted to magnetite, thereby opening up the pore structure and allowing faster diffusion of the Cl^- ions into the treatment solution. The formation of magnetite takes place only if there are excess Fe^{2+} ions present, such as in freshly excavated iron that has not been allowed to dry (Gilberg and Seeley 1982). The formation of magnetite is probably the result of the reaction between Fe^{2+} ions (or precipitated $Fe(OH)_2$) and FeO(OH) (see Equations 4 and 5). An alkaline sulphite solution is reported to be more aggressive to the corrosion layers on archaeological iron than a NaOH solution (Keene 1994). Further research is needed to better understand and quantify exactly what the difference is between treating iron in an alkaline solution containing dissolved oxygen (e.g. NaOH) and without dissolved oxygen (e.g. alkaline sulphite), and to determine the role, if any, of the sulphite ion on the reduction or transformation of iron corrosion products.

3.6.3 Electrochemical Methods: Electrochemical methods, either electrolysis (North 1987), or more controlled cathodic reduction at constant or limiting potential (Beaudoin et al. 1997; Dalard et al. 2002), are thought to increase the diffusion rate of Cl^-, possibly by reducing the iron oxyhydroxides to magnetite, thus increasing the porosity of the corrosion layers. Electrolysis involves immersing an artefact (containing remaining metal) in an alkaline electrolyte and applying a voltage between it and another electrode. The artefact is made the cathode (i.e. polarized cathodically) and another electrode is made the anode (i.e. polarized anodically) (Dalard et al. 2002). If the potential of the artefact is not too negative, then the main species that are said to be reduced are dissolved oxygen or iron(III) oxyhydroxides. The iron(III) oxyhydroxides may be reduced to magnetite ($3FeO(OH)(s) + e^- \rightarrow Fe_3O_4(s) + H_2O + OH^-(aq)$) or to iron(II) hydroxide ($FeO(OH)(s) + H^+(aq) + e^- \rightarrow Fe(OH)_2(s)$). Electrochemical studies of iron corrosion have noted that lepidocrocite is more electrochemically active than goethite and so it is usually lepidocrocite that is reduced, either to magnetite or $Fe(OH)_2$ (Stratmann

and Hoffmann 1989). If the cathodic potential of the artefact is made even lower, then hydrogen gas may be produced by the electrolysis (i.e. reduction) of water ($2H_2O + 2e^- \rightarrow 2OH^-(aq) + H_2(g)$). The formation of bubbles of hydrogen gas at the metal surface (or some other conducting surface) can damage the overlying corrosion layers. For this reason, electrolysis is sometimes intentionally used to generate bubbles that knock off concretion and/or the corrosion crust. Hydrogen bubble formation may slow Cl^- ion diffusion (Carlin et al. 2001). Laboratory studies on non-archaeological iron have shown that once iron becomes covered with iron corrosion products, it is then not possible to electrochemically reduce the corrosion products back to metallic iron (Schmuki et al. 1999).

Although scientific studies of non-archaeological iron have shown that it is possible to reduce newly formed iron corrosion products (e.g. iron(III) oxyhydroxides) to magnetite or $Fe(OH)_2$, the conservation literature contains little scientific evidence that such reduction processes are possible on archaeological material covered with a relatively thick, well-aged corrosion crust. It has been noted, however, that archaeological iron artefacts change colour from rust red to black during electrolysis (Pearson 1972; North 1978). Furthermore, Pearson provides a graph of the Cl^- ion concentration plotted against the square root of time for an iron artefact undergoing electrolysis (Pearson 1981). The increase in the slope after a period of electrolysis suggests that the chloride ions are diffusing faster into solution, possibly by an increase in porosity. Further research is needed to better understand what happens to the corrosion layer on archaeological iron during electrolysis or when other electrochemical techniques are applied.

3.6.4 Plasma Treatment: A hydrogen plasma (a highly reactive gas containing partially ionized hydrogen molecules and atoms) can be used to treat archaeological iron (Schmidt-Ott and Boissonnas 2002). The reactive hydrogen plasma reacts with the iron corrosion products, reducing them to lower oxidation state compounds. If the plasma is used for a short period, some of the outer iron oxyhydroxides can be reduced to magnetite which increases the porosity of the corrosion crust. During exposure to the plasma, the temperature of the artifact is kept well below 400°C to avoid altering the metallurgical structure of any remaining metal. Use of the plasma at this low temperature has not proven to be effective in removing Cl^- ions (Schmidt-Ott 1997). The application of hydrogen plasma as a pretreatment, however, does create small cracks and fissures that improve the subsequent removal of the remaining Cl^- ions by immersion, such as in an alkaline sulphite solution (Schmidt-Ott and Boissonnas 2002).

4. Conclusions

The net result of iron corroding during burial is the filling of cracks, pores, and open spaces within the corrosion layer with an acidic iron(II) chloride solution, with the Cl^- ions concentrated at the metal surface. Exposure of this acidic iron(II) chloride solution to air after excavation leads to on-going corrosion of any remaining metal as well as mechanical damage to the corrosion layer by the formation of iron oxyhydroxides, including akaganéite. The presence of akaganéite on archaeological iron is considered evidence that the object is heavily contaminated with Cl^- ions.

- Further research is needed to characterize the stability of akaganéite to better determine when, under storage conditions, it can transform into goethite or magnetite, release its chlorine as chloride ions, and stimulate on-going corrosion.

Immersion treatments for archaeological iron remove salt contamination when the Cl^- ions diffuse through the corrosion layer into the treatment solution. As long as archaeological iron is corroding during immersion, the Cl^- ions are prevented from diffusing out because they are attracted to Fe^{2+} ions generated by the corrosion process. If the corrosion can be stopped, then the Cl^- ions no longer act as counter ions and they are able to diffuse through the corrosion layer into the treatment solution. Four approaches to slowing iron corrosion during immersion treatments are: (1) passivating the iron surface in an alkaline treatment solution, (2) removing dissolved oxygen, (3) using electrochemical methods, or (4) using corrosion inhibitors.

- Further research is needed to better understand treatments that help slow iron corrosion and to identify the most effective ones. It would be interesting to compare the effectiveness of an alkaline solution with and without oxygen (e.g. sodium hydroxide versus alkaline sulphite).

The Cl^- ions can diffuse out faster if immersion treatments contribute to an increased porosity (void space) in the corrosion layers.

- Further research is needed to study how treatments affect the porosity of the corrosion layer. Rapid electrochemical reactions contribute to an increased porosity of archaeological iron in sodium hydroxide solutions, but it is not known if similar processes occur in other alkaline solutions. Furthermore, it is claimed that several treatments (e.g. alkaline sulphite, electrochemical reduction) result in the reduction of solid corrosion products (e.g. reduce iron oxyhydroxides to magnetite) and an increase in porosity. These claims need to be studied in more detail.

Acknowledgements

The author gratefully acknowledges the contributions made to this paper by Vasilike Argyropoulos, Paul Begin, Judy Logan, Ross McKinnon, and Jane Sirois.

References

Al-Zahrani, A. A., (1999) *Chloride ion removal from archaeological iron and ∃-FeOOH* PhD Thesis, University of Wales, Cardiff

Argyropoulos, V., Selwyn, L. S. and Logan, J. A., (1997*) Developing a conservation treatment using ethylenediamine as a corrosion inhibitor for wrought iron objects found at terrestrial archaeological sites*. In MacLeod, I. D., Pennec, S. L. and Robbiola, L. (eds.) Metal 95, p. 153–158. (London: James & James)

Askey, A., Lyon, S. B., Thompson, G. E., Johnson, J. B., Wood, G. C., Cooke, M. and Sage, P., (1993) *The corrosion of iron and zinc by atmospheric hydrogen chloride.* Corrosion Science, **34**, 233–247

Beaudoin, A., Clerice, M-C., Francoise, J., Labbe, J-P., Loeper-Attia, M-A. and Robbiola, L., (1997) *Corrosion d'objets archéologiques en fer après déchloruration par la méthode au sulfite alcalin: caractérisation physico-chimique et rétraitement electrochimique*. In MacLeod, I. D., Pennec, S. L. and Robbiola, L., (eds.) Metal 95, p. 170–177. (London: James & James)

Becker, H., (1999) *RP System, ein neues Verpackungsmaterial für korrosionsempfindliche Materialien*. [Title translated to English: RP System: a new packing material for corrosion sensitive material]. Arbeitsblätter für Restauratoren*,* **32**, 72–76

Blesa, M. A., Morando, P. J. and Regazzoni, A. E., (1994) *Iron oxides*. In Chemical Dissolution of Metal Oxides, p. 269–308. (London: CRC Press)

Brown, C.E., (1985) *Ethylene-diamine treatment of iron.* Conservation News*,* **27**, p. 38

Busse, E., (1997*) The Manitoba North cannon stabilization project.* In MacLeod, I. D., Pennec, S. L. and Robbiola, L. (eds.) Metal 95, p. 263–268. (London: James & James)

Carlin, W., Keith, D. and Rodriguez, J., (2001) *Less is more: measure of chloride removal rate from wrought iron artifacts during electrolysis*. Studies in Conservation, **46**, 68–76

Carrió, V. and Stevenson, S., (2003) *Assessment of materials used for anoxic microenvironments*. In J.H. Townsend, J.H. *et al.* (eds.) Conservation Science 2002, p. 32–38. (London: Archetype Publications)

Cornell, R. M. and Schwertmann, U., (1996) *The Iron Oxides: Structure, Properties, Reactions, Occurrence and Uses*. (Weinheim: VCH)

Costain, C., (1984) *Cross sectional examination of nails: an evaluation following hot-wash or ethylenediamine treatment.* Analytical Research Services Report No. 2315. (Ottawa: Canadian Conservation Institute)

Costain, C. G., (2000) *Evaluation of storage solutions for archaeological iron.* Journal of the Canadian Association for Conservation, **25**, 11–20

Dalard, F., Gourbeyre, Y. and Degrigny, C., (2002) *Chloride removal from archaeological cast iron by pulsating current*.' Studies in Conservation, **47**, 117–121

Duprat, M., Shiri, A., Derbali, Y. and Pebere, N., (1986) *An electrochemical impedance approach to the corrosion inhibition of a carbon steel in neutral media*. Materials Science Forum, **8**, 267–279

Duprat, M. and Dabosi, F., (1981) *Corrosion inhibition of a carbon steel in 3% NaCl solutions by aliphatic amino-alcohol and diamine type compounds*. Corrosion, **37**, 89–92

Gilberg, M. R. and Seeley, N. J., (1981) *The identity of compounds containing chloride ions in marine iron corrosion products: a critical review*. Studies in Conservation, **26**, 50–56

Gilberg, M. R. and Seeley, N. M., (1982) *The alkaline sodium sulphite reduction process for archaeological iron: a closer look*.' Studies in Conservation, **27**, 180–184

Gilberg, M., (1987) *The storage of archaeological iron in deoxygenated aqueous solutions*. Journal of the International Institute for Conservation - Canadian Group, **12**, 20–27

González, N. G., de Viviés, P., Drews, M. J. and Mardikian, P., (2003) *Characterizing the chloride in the wrought iron rivets from the **Hunley***. In NACE Northern Area Eastern Conference, Ottawa, Sept 15-17. Proceedings on CD (Ottawa: NACE)

Hjelm-Hansen, N., van Lanschot, J., Szalkay, C. D. and Turgoose, S., (1992*) Electrochemical monitoring of archaeological iron artifacts during treatment*. In 3rd International Conference on Non-Destructive Testing*,* Microanalytical Methods and Environmental Evaluation for Study and Conservation of Works of Art, Viterbo, Italy*,* October 4–9, p. 361–373. (Brescia, Italy: Italian Society for Nondestructive Testing)

Hjelm-Hansen, N., van Lanschot, J., Szalkay, C. D. and Turgoose, S., (1993) *Electrochemical assessment and monitoring of stabilisation of heavily corroded archaeological iron artefacts*. Corrosion Science, **35**, 767–774

Incorvia, D. M. J., (1985) *Stereochemistry in corrosion inhibition*. In Proceedings of the 6th European Symposium on Corrosion Inhibitors*,* p. 81–93. (Ferrara: Universita Degli Studi di Ferrara)

Incorvia, M. J. and Contarini, S., (1989) *X-ray photoelectron spectroscopic studies of metal/inhibitor systems*: *structure and bonding at the iron/amine interface*. Journal of the Electrochemical Society, **136**, 2493–2498

Ishikawa, T., Kondo, Y., Yasukawa, A. and Kandori, K., (1998) *Formation of magnetite in the presence of ferric oxyhydroxides*. Corrosion Science, **40**, 1239–1251

Keene, S., (1994) *Real-time survival rates for treatments of archaeological iron*.' In Scott, D. A., Podany, J. and Considine, B. (eds.) Ancient & Historic Metals: Conservation and Scientific Research, p. 249–264. (Marina del Rey: Getty Conservation Institute)

MacLeod, I. D., (1996) *In situ conservation of cannon and anchors on shipwreck sites*. In Archaeological Conservation and Its Consequences, p. 111–115. (London: International Institute for Conservation)

Mardikian, P., (2004) *Conservation and management strategies applied to post-recovery analysis of the American civil war submarine **H.L. Hunley** (1864)*' International Journal of Nautical Archaeology, **33**, 137–148

Mathias, C., (1994) *A conservation strategy for a seventeenth century archaeological site at Ferryland, Newfoundland*. Journal of the International Institute for Conservation - Canadian Group, **19**, 14–23

Mathias, C., (2003) Archaeological Conservator, Memorial University of Newfoundland, private communication

Mayne, J. E. O. and Turgoose, S., (1975) *Significance of the redox potential in the inhibition of the corrosion of iron by non-oxidising inhibitors in the pH range 5–13*. British Corrosion Journal, **10**, 44–46

North, N. A. and Pearson, C., (1975) *Alkaline sulfite reduction treatment of marine iron*. In ICOM Committee for Conservation, 4th Triennial Meeting, Venice, 75/13/3, p. 1–14. (Paris: International Council of Museums)

North, A., (1978) *Electrolysis of marine cast iron*. In Papers from the First Southern Hemisphere Conference on Maritime Archaeology, 145–147

North, N. A. and Pearson, C., (1978a) *Methods for treating marine iron*. In ICOM Committee for Conservation, 5th Triennial Meeting, Zagreb, 78/23/3, p. 1–10. (Paris: International Council of Museums)

North, N. A. and Pearson, C., (1978b) *Washing methods for chloride removal from marine iron artifacts*. Studies in Conservation, **23**, 174–186

North, N. A., (1987) *Conservation of Metals*. In Pearson, C. (ed.) Conservation of Marine Archaeological Objects, p. 207–252. (London: Butterworths)

Paoletti, P., (1984) *Formation of metal complexes with ethylenediamine*: *A critical survey of equilibrium constants*, *enthalpy and entropy values*. Pure & Applied Chemistry, **56**, 491–522

Pearson, C., (1972) *The preservation of iron cannon after 200 years under the sea*. Studies in Conservation, **17**, 91–110

Pearson, C., (1981) *Conservation of the underwater heritage*. In Protection of the Underwater Heritage, p. 81–133. (Paris: UNESCO)

Refait, Ph. and Génin, J-M. R., (1997) *The mechanisms of oxidation of ferrous hydroxychloride β-$Fe_2(OH)_3Cl$ in aqueous solution: the formation of akaganeite vs goethite*. Corrosion Science, **39**, 539–553

Refait, Ph., Drissi, S. H., Pytkiewicz, J. and Génin, J.-M. R., (1997) *The anionic species competition in iron aqueous corrosion: role of various green rust compounds*. Corrosion Science, **39**, 1699–1710

Schmidt-Ott, K. and Boissonnas, V., (2002) *Low-pressure hydrogen plasma: an assessment of its application on archaeological iron*. Studies in Conservation, **47**, 81–87

Schmidt-Ott, K., (1997) *Applications of low pressure plasma treatment at the Swiss National Museum and assessment of the results*. Zeitschrift für Schweizerische Archäologie und Kunstgeschichte, **54**, 45–50

Schmuki, P., Virtanen, S., Isaacs, H. S., Ryan, M. P., Oblonsky, L. J. and Böhni, H., (1998) *In situ XANES study of the cathodic reduction behavior of the passive film on iron and artificial passive films*. Electrochemical Society Proceedings, **97-26**, 183–194

Schmuki, P., Büchler, M., Virtanen, S., Isaacs, H.S., Ryan, M. P. and Böhni, H., (1999) *Passivity of iron in alkaline solutions studied by in situ XANES and a laser reflection technique*. Journal of the Electrochemical Society, **146**, 2097–2102

Scott, D. A. and Seeley, N. J., (1987) *The washing of fragile iron artifacts*. Studies in Conservation, **32**, 73–76

Selwyn, L. S., Sirois, P. J. and Argyropoulos, V., (1999) *The corrosion of excavated archaeological iron with* details on weeping and akaganéite. Studies in Conservation, **44**, 217–232

Selwyn, L. S., McKinnon, W. R. and Argyropoulos, V., (2001) *Models for chloride ion diffusion in archaeological iron*. Studies in Conservation, **46**, 109–120

Selwyn, L. S. and Argyropoulos, V., (2004) *Removal of chloride and iron ions from archaeological iron with sodium hydroxide and ethylenediamine solutions*. Studies in Conservation, accepted for publication

Ståhl, K., Nielsen, K., Hanson, J. C., Norby, P., Jiang, J. Z. and van Lanschot, J., (1998) *The akaganeite-hematite reaction on the possibilities for chloride removal from iron artifacts*. In 25 Years School of Conservation, Preprints of Jubilee Symposium, May 18-20, p. 157–160. (Copenhagen: Det Kongelige Danske Kunstakademi)

Ståhl, K., Nielsen, K, Jiang, J., Lebech, B., Hanson, J. C., Norby, P. and van Lanschot, J., (2003) *On the akaganéite crystal structure, phase transformations and possible role in post-excavational corrosion of iron artifacts*. Corrosion Science, **45**, 2563–2575

Stratmann, M. and Hoffmann, K., (1989) *In situ Mößbauer spectroscopic study of reactions within rust layers*. Corrosion Science, **29**, 1329–1352

Stratmann, M., (1990) *The atmospheric corrosion of iron—a discussion of the physico-chemical fundamentals of this omnipresent corrosion process*; *invited review*. Berichte der Bunsengesellschaft für Physikalische Chemie, **94**, 626–639

Townsend, H. E., (1972) *Potential-pH diagrams at elevated temperature for the system Fe–H_2O*. In Hamner, N. E. (ed.) Proceedings of the Fourth International Congress on Metallic Corrosion, p. 477–487. (Houston: NACE)

Turgoose, S., (1982) *Post-excavation changes in iron antiquities*. Studies in Conservation, **27**, 97–101

Turgoose, S., (1985) *Corrosion inhibitors for conservation*. In Keene, S. (ed.) Corrosion Inhibitors in Conservation, p. 13–17. (London: UKIC)

Turgoose, S., (1993) *Structure, composition and deterioration of unearthed iron objects*. In Current Problems in the Conservation of Metal Antiquities, p. 35–52. (Tokyo: Tokyo National Research Institute of Cultural Properties)

Turgoose, S., Hawkins, C., Wrathall, N., Kalbeek, N., van Lanschot, J., Mathiesen, T. and Sjogren, A., (1996) *Development of Improved Conservation Procedures for Archaeological Iron*, Environment Program CT94-0561. (Manchester: Corrosion and Protection Centre, UMIST; Copenhagen: School of Conservation)

Watkinson, D., (1983) *Degree of mineralization: its significance for the stability and treatment of excavated ironwork*. Studies in Conservation, **28**, 85–90

Watkinson, D., (1996) *Chloride extraction from archaeological iron: comparative treatment efficiencies*. In Roy, A. and Smith, P. (eds.) Archaeological Conservation and Its Consequences, p. 208–212. (London: International Institute for Conservation)

Proceedings of Metal 2004 National Museum of Australia Canberra ACT 4–8 October 2004
ABN 70 592 297 967

Corrosion layers on historic iron artefacts

Cathodic protection of iron artefacts during cleaning in acid solutions

I. de Groot [a], H. A. Ankersmit [b], R. van Langh [c], W. Wei [d]

[a] Metal Conservation, Menadostraat 22, 3532 SM, Utrecht, the Netherlands.

[b,d] Netherlands Institute for Cultural heritage, Gabriël Metsustraat 8, 1071 EA, Amsterdam, The Netherlands.

[c] Rijksmuseum Amsterdam, postbus 74888, 1070 DN, Amsterdam, the Netherlands.

Abstract

Cathodic protection has been studied as a method for protecting iron objects during cleaning in acid solutions. The effect of the type of acid, potential and distance between the anode and cathode were investigated. Iron sheets, polished and corroded, were immersed in 0.5 M citric, sulphuric, or ortho-phosphoric acid baths while cathodic protection was used. Applying a potential of -650 mV and -850 mV Ag/AgCl to the immersed samples successfully protected them. Some of the samples were only slightly etched and this was related to surface size of the anode. Both the geometry and distance between anode and cathode have a large influence on the cleaning and etching of the original surface. Unprotected iron sheets were strongly etched by the acids after an immersion of three hours. Cathodic protection thus appears to be a good technique for protecting iron objects during acid cleaning. 0.5 M ortho-phosphoric acid baths was considered to be the best electrolyte for practical considerations. However, further research is needed before this treatment can be safely carried out on objects.

*Keywords:*Historic iron, iron corrosion, electrolytic cleaning, acid, cathodic protection.

1. Introduction

In the conservation field chemical and mechanical techniques are commonly used to remove iron corrosion products on historical iron objects (Tomozei and Balta 1998). If the corrosion products are located in a position which is difficult to reach, for example, for engraved surfaces, these methods are not always feasible. In industrial processes acid baths are commonly used to remove iron corrosion layers (Berry 1993). However, this can result in the dissolution of iron. Industrially this dissolution is not a problem, but in conservation this kind of attack is unacceptable.

A possible solution for the problem of the dissolution of iron in acid is the use of cathodic protection. Cathodic protection is a technique to prevent corrosion of a metal in aqueous environments by lowering the potential of the object. For iron in acid solutions, this means suppressing the iron dissolution (anodic) reaction and promoting the hydrogen reduction (cathodic) reaction, that is

(1) $Fe\,(s) \rightarrow Fe^{2+}\,(aq) + 2\,e^-$ (anodic reaction)

(2) $2\,H^+\,(aq) + 2\,e^- \rightarrow H_2\,(g)$ (cathodic reaction).

This technique is widely used in industry to protect iron and steel structures such as boats and buried pipelines (Jones 1996).

Corresponding author: TEL: +31 6.13057.316, ilonne@metal-conservation.com

The objective of this research project was thus to investigate the use of cathodic protection during the treatment of iron artefacts in an acidic environment so that corrosion products would be removed and the iron protected. Focus was placed on parameters which were considered to be important during treatment such as type of acid, potential needed for the cathodic protection, the required time for immersion, as well as the removal of the acid from the object (rinsing). Ethical and aesthetic issues concerning changes in appearance and the preservation of patina were also considered.

2. Experimental procedure

Three series of experiments were conducted in this research program. In series 1, the effect of the type of acid on the cathodic protection of polished steel sheet samples was investigated. In series 2, the use of cathodic protection during acid treatment of corroded material was tested. Finally, in series 3, a practical simulation was conducted to investigate the use of cathodic protection for objects with varying geometry.

Testing was conducted using samples cut from St. 37 [1], sheet having a thickness of 1 mm. Specimen dimensions were 50 x 20 mm for test series 1 and 2. In order to vary the shape of the cathode in test series 3, specimens were bent into the form as shown in Figure 5 of the results section. Specimens for test series 1 and 3 were polished on one side with 500, 800, 1200, and 2500 grit abrasive paper. A shiny surface with fine grinding marks was the result. The corroded steel sheets used in test series 2 were cut from a large sheet of St. 37 which had been placed outdoors for 33 days to form a corrosion layer [2]. The corrosion product was polished away on half of the surface of one side of the specimen, while the other half of the same side was left corroded. Photographs of all specimens were taken before and after the experiments with a standard camera and in the optical microscope. An identifying mark was made with a steel scribe to enable photographs to be taken at the same place before and after the experiment.

Citric acid, sulphuric acid and ortho-phosphoric acid were tested as electrolytes. A pH between 0 and 1 was used based on experience with industrial baths for the removal of corrosion on steel at Corus Group in IJmuiden, The Netherlands [3]. By using concentrations of 0.5 M these pH values were attained. All three acids were tested in series 1. The results, to be discussed later, showed that 0.5 M ortho-phosphoric acid was the best candidate for cathodic protection and was therefore used for testing in series 2 and 3. Testing was carried out in a fume-hood at room temperature. The solutions were not stirred. After immersion the samples were rinsed shortly with tap water and acetone and then dried with compressed air.

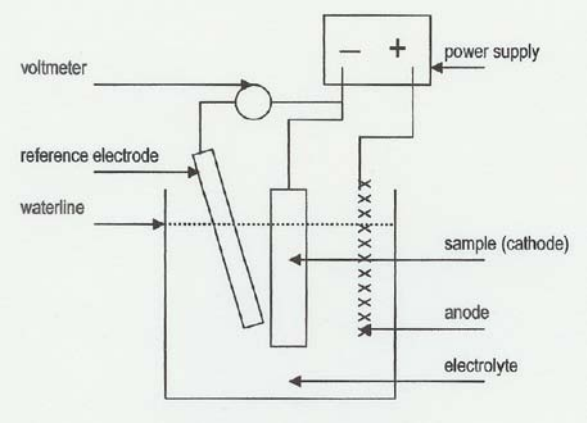

Figure 1, Schematic drawing of test system.

[1] St 37 is an alloy of steel which contains: C ≤ 0,12%, Mn ≤ 0,60 %, P ≤ 0,045 %, S ≤ 0,045 % and Fe ≤ 99 %, staalmarkt Den Bosch, the Netherlands.
[2] from 16-01-03 untill 18-02-03, in the garden of the Netherlands Institute for Cultural Heritage, Gabriël Metsustraat 8, Amsterdam, the Netherlands.
[3] Private communication, Dr. Ir. H. van der Weijde, Corus Group, IJmuiden, the Netherlands.

The testing system is shown in Figure 1. For cathodic protection, a stainless steel mesh [4] was used as the anode and a DC power supply [5] for the supply of electrons. The anode was connected to the positive terminal of the power supply and the sample (the cathode) was connected to the negative terminal. An Ag/AgCl (silver/silver chloride) reference electrode [6] and a digital multimeter [7] were used to measure the cathodic potential. The power supply with the required potential was switched on before the sample came in contact with the acid electrolyte. The samples were immersed in such a way that the electrical connections to the sample remained above the waterline.

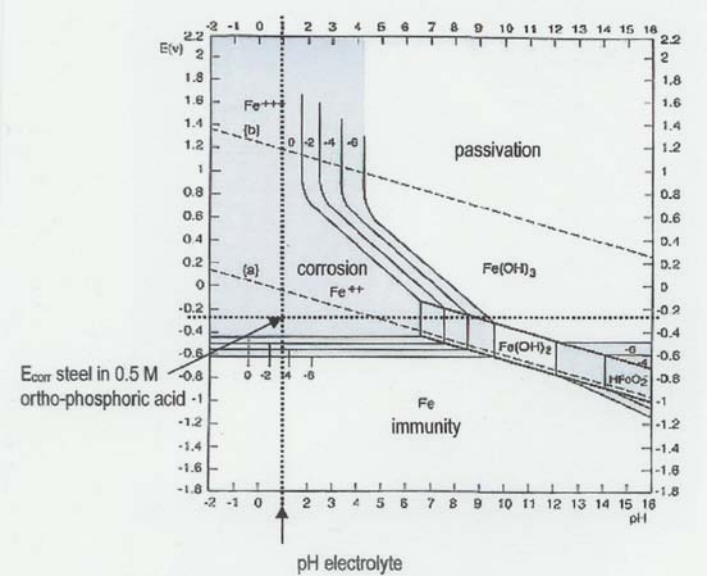

Figure 2, Pourbaix diagram for the iron/water system. E_{corr} for steel in 0.5 M ortho-phosphoric acid has been indicated (-295 mV SHE). When lowering the potential to a more negative value the immunity area is being reached and the steel will be cathodically protected (adapted from Jones 1996).

The anode used for test series 1 and 2 was flat while the anode used for test series 3 was placed around the cathode. The cathodic potentials used in the experiments were selected based on the Pourbaix diagram for the iron/water system, see Figure 2. The corrosion potential, E_{corr} , for steel in 0.5 M ortho-phosphoric acid was determined to be -295 mV SHE (Standard Hydrogen Electrode). If the potential is shifted to a more negative value which corresponds to the immunity area, the steel will be protected. This cathodic potential is dependent on the concentration of the Fe-species in solution. This is given by lines labelled 0, -2, -4 and –6 in Figure 2 , representing areas where the concentration of Fe-species are 10^0 M, 10^{-2} M, 10^{-4} M and 10^{-6} M respectively. It can be seen that this cathodic potential lies between -450 and -600 mV/SHE or -650 mV and -800 mV Ag/AgCl. This is close to the value given by Mattsson (1996) needed for the protection of steel and iron at low pH values, < -950 mV $Cu/CuSO_4$ (-850 mV Ag/AgCl). It should be noted that cathodic protection in an acidic environment is rarely used in industry for economic reasons. A high current is needed which is too expensive for providing permanent protection (Jones 1996).

In test series 1, a cathodic potential of -650 mV Ag/AgCl was used based on the Pourbaix diagram. For the other experiments a cathodic potential of -850 mV Ag/AgCl was used based on the literature. An immersion time of three hours was used for the polished steel sheets used in test series 1 and 3. For series 2, the immersion time was that required to remove all of the corrosion products.

3. Results

[4] XRF analyses for main elements: 15% Cr, 11% Ni, 3% Co, 2.6 % Mn and 67 % Fe
[5] type: EA-PS-3016-10, Schöne Edelmetaal, Amsterdam, the Netherlands.
[6] type; 6.0733.100, Metrohm, Eco chemie, Utrecht, the Netherlands.
[7] type: DVM 850 BL, Velleman, Muco Amsterdam bv., Amsterdam, the Netherlands

The results of the first series of tests indicate that all specimens were protected by cathodic protection regardless of the type of acid, compare micrographs in Figure 3. After an immersion time of three hours at a cathodic potential of –650 mV/Ag/AgCl no etching could be seen visually and in the stereo-microscope except for slight etching at the waterline. Total immersion of the sample would avoid this etching. The unprotected specimens on the other hand, were etched and had a dark grey colour after three hours. The unprotected specimen in sulphuric acid and ortho-phosphoric acid were more strongly etched.

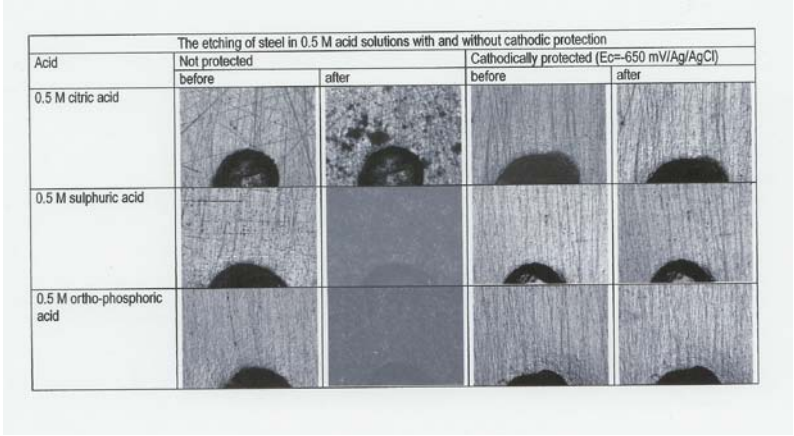

Figure 3, Surface of steel sheet specimens before and after testing in 0.5 M acid solutions with and without cathodic protection (test series 1). The dark half circles in the micrographs are the identifying marks (Ø~1 mm).

The results of the treatment of the half-corroded specimens, test series 2, are shown in Figure 4. During these experiments, the time for complete removal of the corrosion product was measured. The corrosion product was completely removed from the unprotected sheet in 110 minutes. The cleaned surface was dark grey in colour. On the protected sheet, the corrosion layer was removed after 70 minutes. The cleaned surface was a lighter grey except at one edge and the water line where it was dark grey. The polished side of the sheet remained shiny. No corrosive attack could be found by optical microscopy.

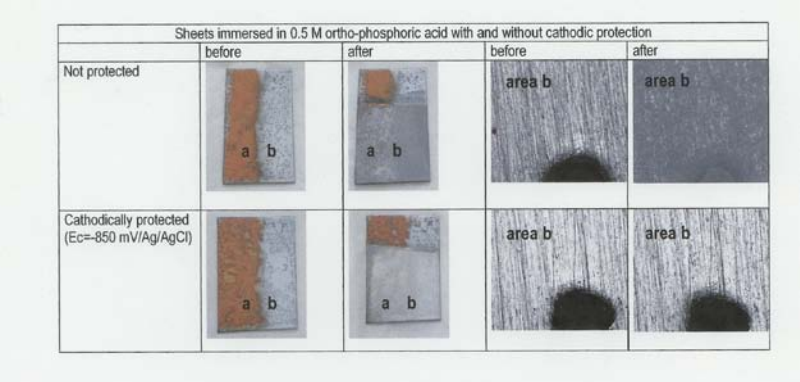

Figure 4, Surface of half-corroded steel sheet specimens before and after cleaning treatment in 0.5 M ortho-phosphoric acid with and without cathodic protection (test series 2).

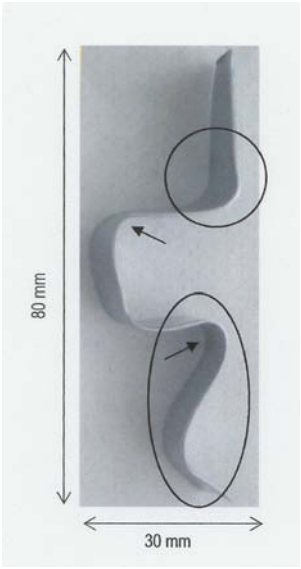

Figure 5, Bent steel sheet used in test series 3. The circles indicates the areas were etching has occurred with an anode-cathode distance of 2,5 cm. The sheet was less etched with an anode-cathode distance of 7 cm as indicated with the two arrows.

The third series of tests with the bent specimens showed uneven protection after immersion for three hours in 0.5 M ortho-phosphoric acid. The differences in protection can be seen in Figure 5. A specimen tested at a distance of approximately 2.5 cm from the round anode (as measured from the end of the specimen) was etched at both sides of the lower part of the sheet and at a higher position. These areas are indicated with circles. During another test where a specimen was hung 7 cm from the round anode, the electrolyte became yellow around the anode during immersion for 3 hours. However, after immersion, the sheet showed much less etching than the specimen which was closer to the anode. These areas are indicated with an arrow.

4. Discussion

The results of this program indicate that cathodic protection is effective in protecting iron objects from etching during cleaning in acid solutions. The immersion time is also shortened when an object is cathodically protected. The development of hydrogen helps the cleaning effect. This was demonstrated in test series 2, where the removal of the corrosion product on the unprotected corroded sheet took 110 minutes, while it only took 70 minutes for the cathodically protected materials. The treatment time also depends on the thickness of the corrosion layer on the object. When the corrosion layer is thick the immersion time is longer as a result. This was shown in supporting experiments performed on corroded iron pipes.

Cathodic protection appears to work regardless of the type of acid. All steel sheets were protected after 3 hours of immersion. However, further experiments indicate that ortho-phosphoric acid is a better choice for the acid bath based on practical considerations. Citric acid dissolves iron corrosion more slowly than sulphuric or ortho-phosphoric acid. This means that the treatment for an object immersed in citric acid would take longer. The time for the object to be immersed in an acid should be as short as possible to avoid problems that could occur with a power interruption or in the absence of the conservator. Rinsing is also very important when an acid is being used in the case where a residue can cause corrosion. Sulphuric acid cause serious corrosion when a residue is left behind (Wilthew 1985). The residue of ortho-phosphoric acid is, on the other hand, a stable iron phosphate which does not cause further corrosion (Galjaard and Van Leeuwen 1969).

The experiments also revealed a number of practical aspects which must be considered when working with cathodic protection. When a normal DC power supply is used as was the case for this project, the cathodic potential can fluctuate (~ +/- 50 mV) during the treatment due to the change in the surface condition of the corroded samples. During test series 2 with corroded samples, the cathodic

potential was not stable and had to be readjusted every 20 minutes. It should be noted that it is therefore important to use a reference electrode when setting and readjusting the cathodic potential. In any case, the conservator must be present to keep the cathodic potential at a constant value. To solve the problem of the fluctuation of the cathodic potential a potentiostat could be used. This computer controlled power supply automatically keeps the potential at pre-set values. It is much more expensive than a normal power supply and not available in most of the conservation laboratories. However, it is standard equipment in corrosion research laboratories.

The results of test series 3 show that protection varies over the surface of an irregularly shaped object. It appears that the distance to the anode is important, since there was more attack at a distance of approximately 2.5 cm that there was at 7 cm. However, the surface area of the anode used for the first specimen was three times smaller than the anode used for the second specimen. The difference in surface area of the cathode and the anode thus appears to be a more important parameter for the treatment to succeed. The geometry of the object will also be important. The etching on two areas on the second sheet with larger anode-cathode distance is located in the position were hydrogen bubbles can be trapped. It may be a reason that the protection has failed on these specific locations.

In test series 3, the electrolyte became yellow around the anode. This is due to the dissolution of the stainless steel anode. To avoid this dissolution an inert anode such as platinum should be used. However, these materials are more expensive than stainless steel.

Cathodic protection also produces hydrogen (reaction 2 in the introduction). The potential used for the cathodic protection in test series 1 was taken from the Pourbaix diagram for the iron-water system (-650 mV Ag/AgCl). For all other experiments, the more negative potential of –850 mV Ag/AgCl was used based on literature evidence that this value is better for low pH solutions (Mattsson 1996). However, at this more negative cathodic potential more hydrogen is developed. It is known that hydrogen embrittlement can be induced in steels during cathodic protection. However, this is generally only of concern for objects which are mechanically loaded after treatment, and is more a problem for high strength steels than iron and low carbon steels. Since the objects will not be mechanically loaded the effect of hydrogen embrittlement was not studied.

Ethical issues are also an important consideration in the cleaning of iron objects, with or without cathodic protection. The surface changes in an important way before and after the treatment. Acid treatment will remove any corrosion products. However, underneath the corrosion product, the surface is already damaged and after cleaning this can be seen. A light grey surface is the result. The corrosion pattern can still be recognised. This could be seen on iron pipes cleaned as part of this research project. The corrosion product was present as stripes. After treatment, this pattern could still be recognised on the cleaned surface. When a layer of microcrystalline wax was applied, the appearance of the surface became more homogeneous. Finally, it should be noted that the procedure described in this communication is not applicable for composite objects since some materials do not resist acids. The corrosion potential (E_{corr}) will also be very different for each metal.

5. Conclusion

A research project was conducted to determine the feasibility of using cathodic protection for protecting iron artefacts during treatment in acidic environments. The results of the experiments show that cathodic protection of iron in acid solutions can be used to protect objects during cleaning. Only a few of the samples showed slight attack. This is related to the area relationship and the distance between the anode and the cathode (object).

Further research is needed before this treatment can be routinely and safely carried out on objects. A better understanding of the relationship between the distance of anode and cathode, as well of the relation of the difference in surface size of the cathode and the anode, on the cathodic protection required. The use of a corrosion inhibitor in the acid solution may provide additional safety should cathodic protection fail. The use of a more conductive electrolyte may provide higher currents at the cathodic potential, resulting in better protection. Ethical aspects of the treatment must also be considered, since the treatment completely removes the corrosion layer which is not always desirable.

Acknowledgements

This project was funded by the Rijksmuseum Amsterdam, the Netherlands. The authors would like to thank Hans van der Weijde, Corus Group, IJmuiden, the Netherlands, for his advice and explanation about industrial processes concerning cathodic protection and corrosion removal, and Christian Degrigny, Malta Centre for Restoration, for his helpful comments. The authors also thank the scientific staff of the research department of the Netherlands Institute for Cultural Heritage, Amsterdam for their help and technical support during this research project.

References

Berry, F.J., (1993) *Industrial chemistry of iron and its compounds*, in Chemistry of iron, Silver, J. (ed.), Blackie Academic and professional, London, , 30-45.

Callister, W.D.Jr. (2000) *Material Science and Engineering, an introduction*, 5th ed., John Wiley and Sons, Inc.,New York, , 588.

Galjaard, D., Van Leeuwen, A. (1969) *Chemische oppervlaktebehandelingen van metalen*, Spruyt, van Mantgem & de Does N.V., Leiden, 39-40.

Jones, D.A., (1996) *Principles and prevention of corrosion*. 2th ed., Prentice hall, London, , 439-441.

Mattsson, E. (1996) *Basic corrosion technology for scientists and engineers*, 2nd ed., the institute of materials, , London, 101.

Tomozei, M and Balta. Z., (1998) *La restauration d'une plaque de corselet (Iran, dix-septième siècle),* in Metal 98, W. Mouray, L. Robbiola (eds), James and James Ltd, London, , 188-191.

Wilthew, P. T., (1985) *Corrosion inhibitors in acid stripping of iron*, in Corrosion inhibitors in conservation, Keene, S. (ed.), Occasional papers number 4, The United Kingdom for Conservation, London, , 24

ABN 70 592 297 967

INTENTIONALY BLANK
FOR NOTES

Electrochemical monitoring of marine iron artefacts during their storage / stabilisation in alkaline solutions

C. Degrigny[a] and L. Spiteri[b]

Abstract

Removing the protective crust that covers marine iron artefacts can lead to accelerated corrosion processes. To prevent this further damage the immediate storage of the artefacts in appropriate solutions is required. The additional analysis of chlorides extracted can even assure the monitoring of the stabilisation process.
After a thorough literature survey that presents these different aspects, this paper develops a new approach to monitor the storage / stabilisation of marine iron artefacts in alkaline solutions through the measurement of their corrosion potential, E_{corr} versus time. Preliminary investigations are performed on non-corroded and corroded steel plates in diluted KOH solutions and are followed by experiments in real conditions. Three steps are commonly observed when monitoring E_{corr}: first an abrupt decrease that is followed by a period where E_{corr} remains constant and a final phase where E_{corr} tends to increase again. Possible explanations for these behaviours are given according to the nature of the corrosion layer as well as suggestions to speed up the stabilisation process while monitoring both the amount of chlorides extracted and E_{corr}.

Keywords
Storage / stabilisation; marine iron artefacts; electrochemical monitoring; alkaline solutions

1. Introduction

Marine iron artefacts recovered from the sea are usually covered with a protective crust (concretion) that should be preserved until their transfer to conservation laboratories. When no budget for treatment is immediately available a simple immersion of the encrusted artefact in tap water is normally conducted. If left to dry the crust becomes so hard that during its mechanical removal some damage of the fragile altered artefacts might occur.
Unfortunately marine iron artefacts are often cleaned from their crust by their discovers and conservation professionals have no option than to immerse them in an appropriate storage / stabilisation solution that requires a thorough monitoring. With experience we have learnt that the short storage conditions expected initially (before a budget is allocated to the conservation treatment) become eventually long storage conditions. Because stabilisation treatments are time consuming processes, it seems logical to start the treatment straight away.

[a] C. Degrigny, Diagnostic Science Laboratories, Malta Centre for Restoration, Bighi, CSP 12, Kalkara, tel +356.21.80.76.75 ext 265, fax: +356.2167.44.57, cdegrigny@mcr.edu.mt
[b] L. Spiteri, Diagnostic Science Laboratories, Malta Centre for Restoration, Bighi, CSP 12, Kalkara, tel +356.21.80.76.75 ext 245, fax: +356.2167.44.57, lspiteri@mcr.edu.mt

The stabilisation process is monitored through the regular analysis of chlorides extracted in the storage / stabilisation solution. Other options have been suggested recently such as the monitoring of the corrosion potential of the artefact under treatment with time. It is the objective of this paper to investigate more thoroughly the information provided by this parameter and to see how its monitoring relates to the stabilisation process.

2. Scientific Background

2.1. Specificity of the corrosion of iron artefacts in seawater

The corrosion of iron artefacts in seawater is dominated by the formation of massive crusts which completely cover the metal surface. Marine crusts form a more or less protective barrier between the artefact and the surrounding environment. If it is compact corrosion processes slow down rapidly and the metal is well preserved underneath. If it is porous corrosion activity is maintained at the metal surface and thick corrosion layers are progressively formed (North 1976 and North & Pearson 1987).

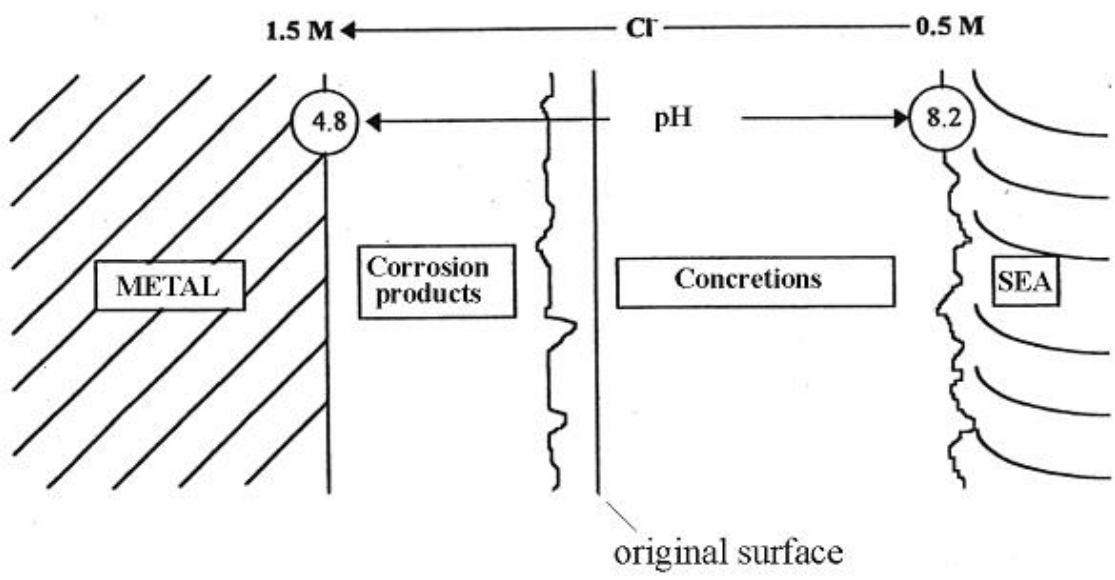

Figure 1 : Cross-section on a wrought iron exposed to seawater. The original surface is lost in the concretions (from (MacLeod 1989))

The composition of iron affects the way the corrosion proceeds. Wrought iron contains slag inclusions which provoke galvanic corrosion and allow the penetration of water deep into the metal (North & MacLeod 1987). Corrosion occurs then inside the metal resulting in a wood grain appearance with the details and form of the original surface being lost (Figure 1) (MacLeod 1989).
The corrosion of grey cast iron is much more complicated as it contains different solid phases rich in carbon. In addition to the principal phases, which are ferrite, pearlite, cementite and graphite, grey cast iron often contains varying amounts of phosphorus, silicon and sulphur. Of these different phases only the graphite lamellas remain

unaffected by the corrosion. They form a three-dimensional network, which tracks the iron corrosion products and so retains the original shape and the surface details (Figure 2) (North 1976). The resulting corrosion layer is called the "graphitic corrosion layer".

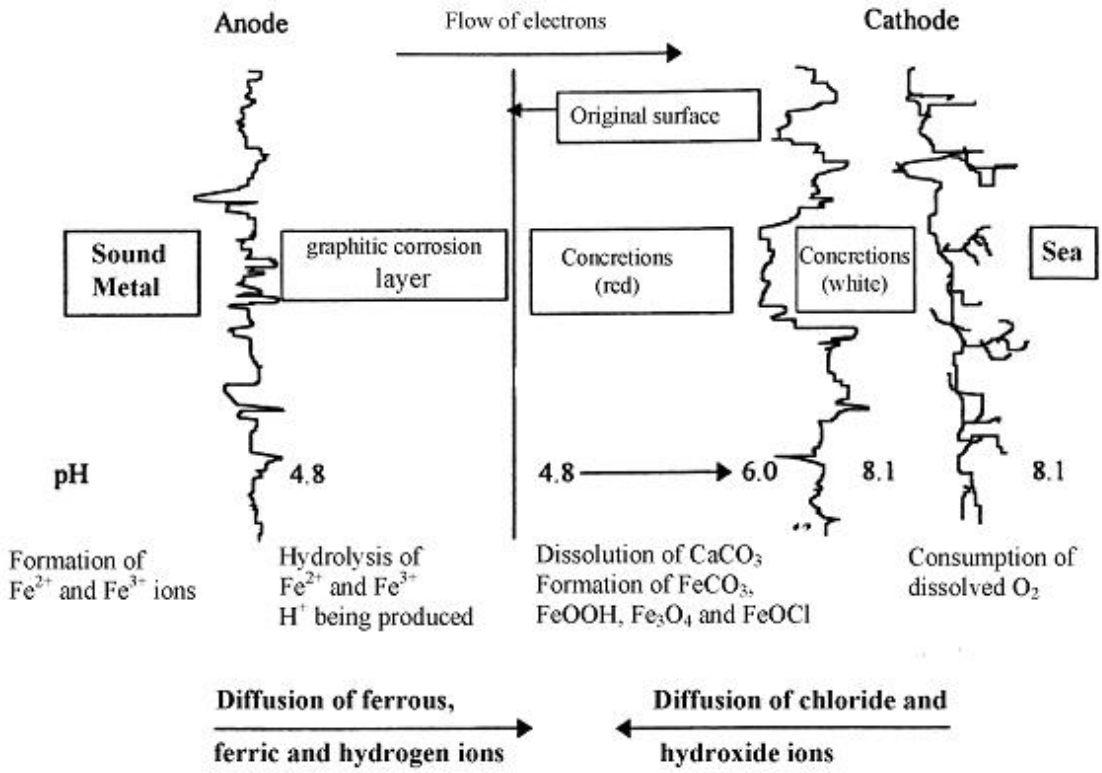

Figure 2 : Cross-section of a cast iron exposed to seawater. The original surface is preserved above the graphitic corrosion layer (from North 1976)

It is commonly agreed that the chloride ions in archaeological iron are situated at the metal / corrosion layer interface. However, the nature of the compounds containing them is still under research. Ferrous chloride ($FeCl_2$) has been suggested (North & Pearson 1977), although according to Turgoose its formation is not likely to occur thermodynamically (Turgoose 1982a and 1982b). Also iron oxychloride (FeOCl) has been detected, especially on marine archaeological iron artefacts (North & Pearson 1977). The corrosion layer itself is made both for grey cast iron and wrought iron of a mixture of magnetite, oxyhydroxides (lepidocrocite and goethite) and iron sulphides, although magnetite is the main iron oxide component due to the low oxygen content under the crust (North & MacLeod 1987).

2.2. Post-recovery corrosion

If cleaned from their marine crust and left to dry out the iron objects are exposed to a rapid oxidation. Corrosion layers crack allowing more oxygen to reach the metal surface. According to Turgoose (Turgoose 1982a) this oxidation causes the formation of solid iron oxyhydroxides and can be described by the reaction :

$$4Fe^{2+} + O_2 + 6H_2O \rightarrow 4FeOOH + 8H^+$$

There are several forms of iron oxyhydroxides. Their precipitation damages the corrosion layer as the formation of any of them results in an increase in its volume. At high chloride concentrations it is normally akaganeite (β-FeOOH) that is being formed. It appears underneath the upper corrosion layers introducing stresses to the object. Akaganeite is known to contain variable amounts of chloride ions in its tunnel structure (Schwertmann 1991).
Akaganeite is often accompanied by droplets of yellow solution which contains mainly ferrous (Fe^{2+}) and chloride ions but also some ferric ions (Fe^{3+}). The appearance of the solution on the surface of an iron object is called "weeping" and it is caused by the dissolution of iron oxyhydroxides in acidic environment (Selwyn 1999).

2.3. Storage / stabilisation of marine iron artefacts

As chloride ions are known to accelerate the corrosion of iron, marine iron artefacts cleared from their marine crust have to be conserved in solution before a proper conservation treatment is started. The Pourbaix diagram (Pourbaix 1963) for iron indicates that in strong alkaline solutions (pH≥10) the metal surface is passivated (figure 3). For that reason marine iron artefacts are often stored in NaOH, Na_2CO_3, or sodium

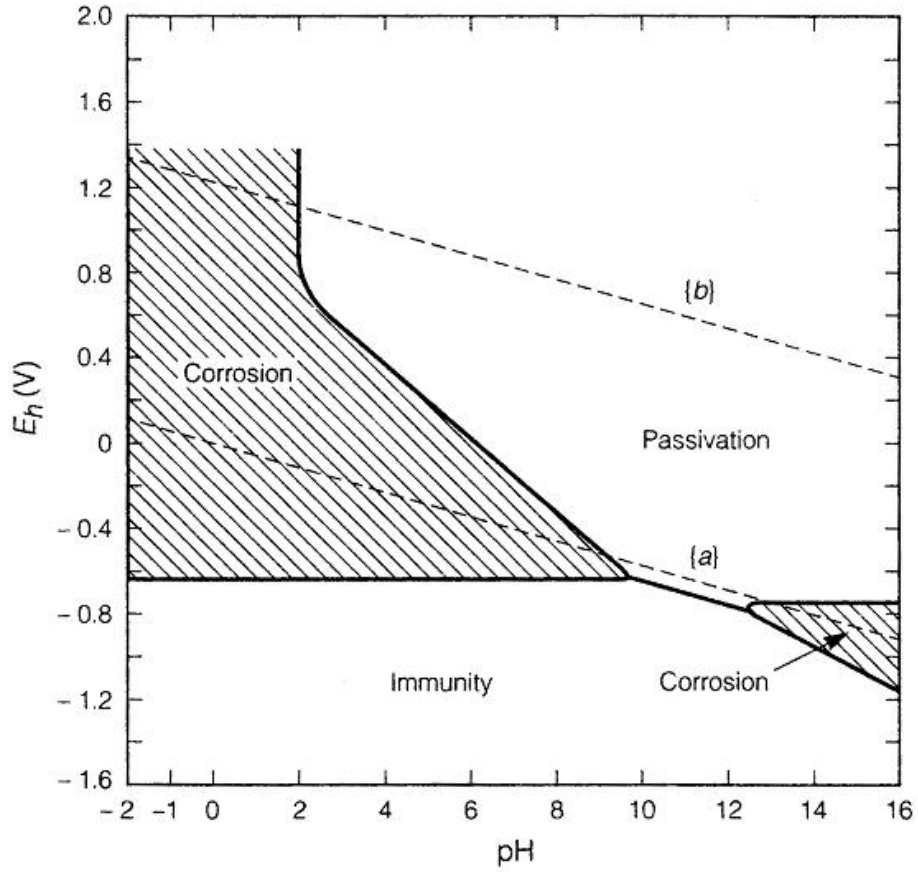

sesquic arbon ate solutions (Pearson 1987).

Figure 3 : Simplified Pourbaix diagram for iron.(concentration of Fe species (<10^{-6} M)) (from Pourbaix 1963).

Due to lack of budget, this storage step can sometimes lasts longer than initially planned. It is worth then starting the stabilisation process at once since the chemicals commonly used for the stabilisation of archaeological iron are the same as the ones mentioned above (North & Pearson 1978). The main difference between the storage and the stabilisation steps is that the stabilisation requires a thorough monitoring of the extraction of chlorides in the solution. The mechanisms by which chlorides are extracted from marine iron artefacts in basic solutions have been studied by North and Pearson (1976) and the extraction rate was found to be controlled by a diffusion law.

The quantity of chlorides released during the early stage of washing is after some time proportional to the square root of the total washing time (Figure 4). Plots of the chloride concentration versus the square root of time are then useful tools to monitor the stabilisation process. Deviations from linearity occurs only when the amount of chlorides extracted is equal to the chloride concentration of the iron corrosion products and the remaining metal.

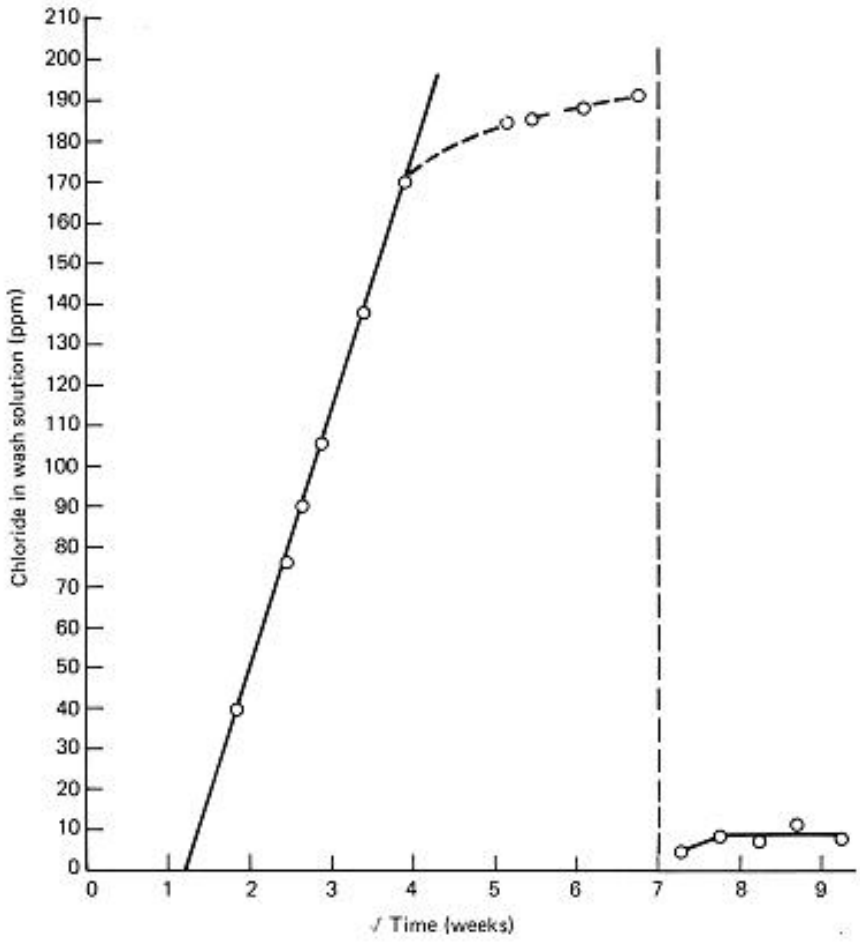

Figure 4 : A typical plot of $C_{Cl^-} = (\sqrt{t}, t \text{ in weeks})$ for a cast iron artefact pretreated by hydrogen reduction (North 1987)

ABN 70 592 297 967

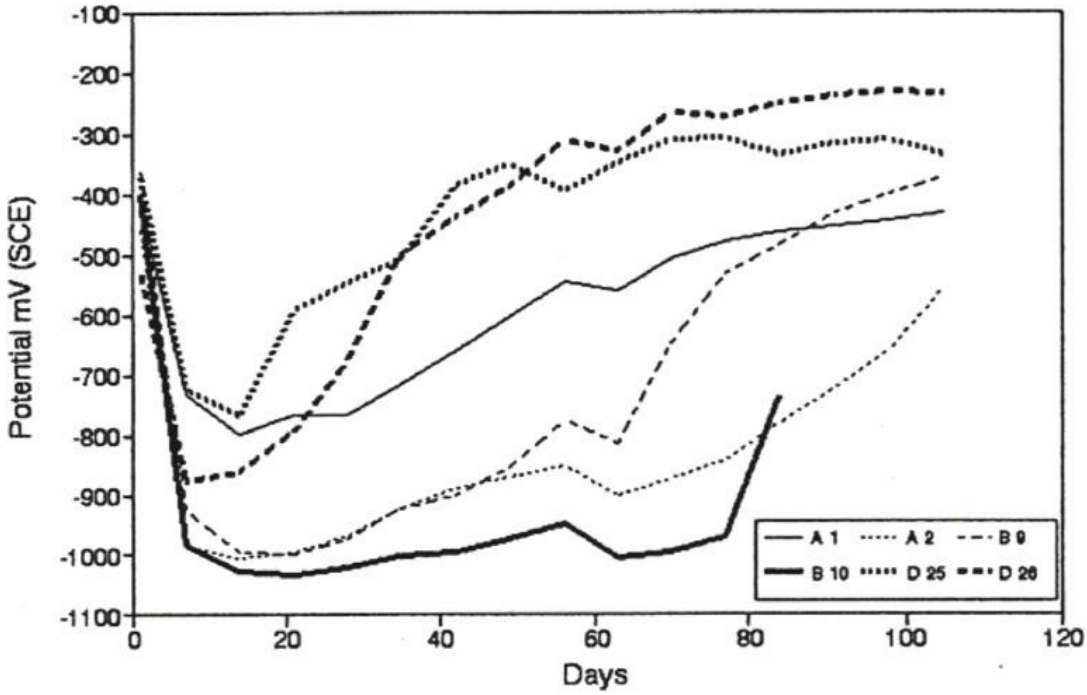

Figure 5 : E_{corr} (SCE) vs. time for iron archaeological artefacts immersed in 0.5 M sodium hydroxide (Hjelm-Hansen 1992)

The electrochemical monitoring of artefacts during storage (or stabilisation) is rarely mentioned in the literature. Only Hjelm-Hansen et al. reported results on several archaeological iron objects treated by immersion in sodium hydroxide and sodium sesquicarbonate (Hjelm-Hansen 1992). The objects came from four different Danish terrestrial sites with different post-excavation history and condition. A common behaviour of the objects immersed in sodium hydroxide was observed (Figure 5). The corrosion potential (E_{corr}) decreased to a very low value (-0.8 to –1.0 V/SCE, Saturated Calomel Electrode (SCE)=0.242V/SHE, Standard Hydrogen Electrode (SHE)=0V) soon after immersion, remained at this potential for a time depending on the object (a few days to 80 days), and then rose towards –0.2-0.3V/SCE (-0.058 to 0.042V/SHE). The same trends were observed for artificially precorroded mild steel plates. The extent of corrosion was noticed to affect the time scale in which the metal artefacts reached –0.2-0.3V/SCE corresponding to the passivation process. A much longer time was required for the archaeological artefacts with thick corrosion products (A2, A1 and B10) than for those with thin ones (D25 and D26) and the precorroded mild steel plates.

Therefore these experiments suggested that rapid electrochemical processes are taking place during immersion in alkaline solution. These processes are likely to cause irreversible changes in the corrosion product layers, which should be realised when considering the use of these solutions. On the other hand the effectiveness of the stabilisation may be associated with these changes.

3. Experiments and results

3.1. On artificial coupons

Several experiments were performed on artificial coupons simulating the behaviour of real artefacts to study the reactions taking place when they are immersed in alkaline solutions such as potassium hydroxide (KOH). A preliminary exercise consisted in immersing un-corroded steel plates E24-2 in 1% (w/v) KOH solutions and to monitor the corrosion potential (E_{corr}) with time. The curve obtained for one of these plates clearly shows an increase of E_{corr} which corresponds to a passivation phenomenon (figure 6). The potential gets stable after one hour and the value obtained is –0.660 V/HSE (or roughly 0V/SHE, Mercury Sulphate Reference Electrode (HSE)=0.658V/SHE). Note that this value is very close to the final value of the monitoring experiments performed by Hjelm-Hansen (see figure 5).

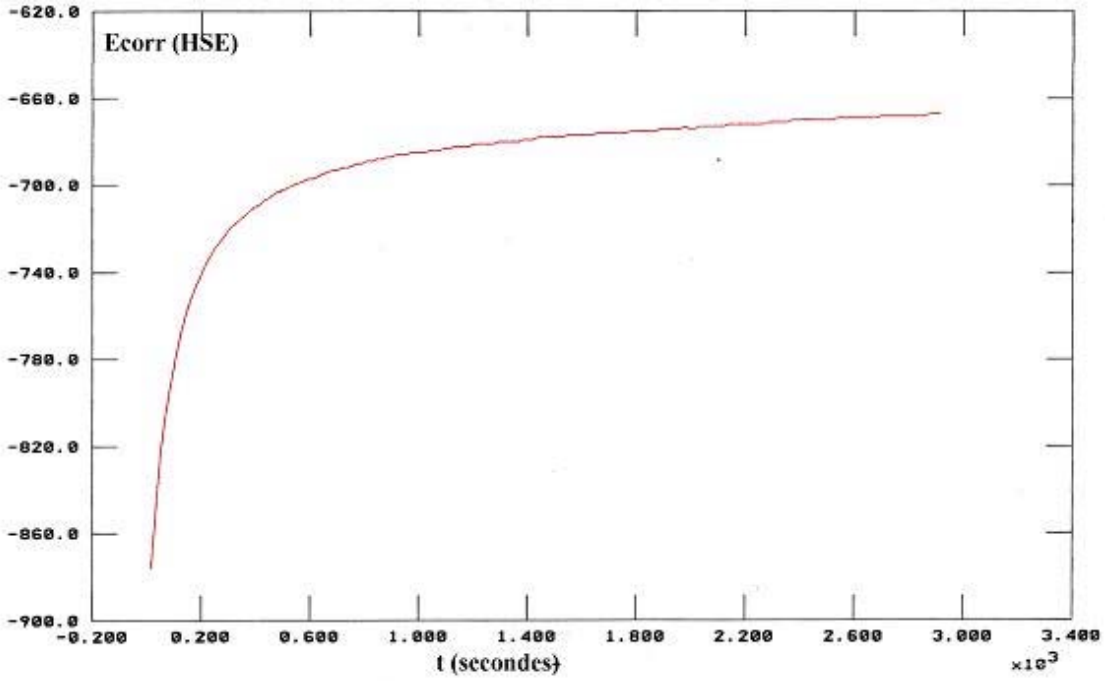

Figure 6 : Monitoring of E_{corr} versus time for an un-corroded steel plates E24-2 in 1% KOH solution. The potential is given versus the mercury sulphate electrode (HSE : 0.658V/SHE)

These steel plates were corroded artificially to simulate the behaviour of real artefacts. Four different preparation surfaces were considered (blasted with grey cast iron particles, just degreased, abraded and polished with 240 SiC paper) and the steel plates were then immersed 22 days in a $FeCl_2$ solution to form akaganeite and exposed 45 days vertically in a climatic chamber to the following conditions:
- 24 hours (30°C – 100% RH)
- 24 hours (20°C – 50% RH)
to form a double layer of corrosion products (magnetite and oxyhydroxides).

ABN 70 592 297 967

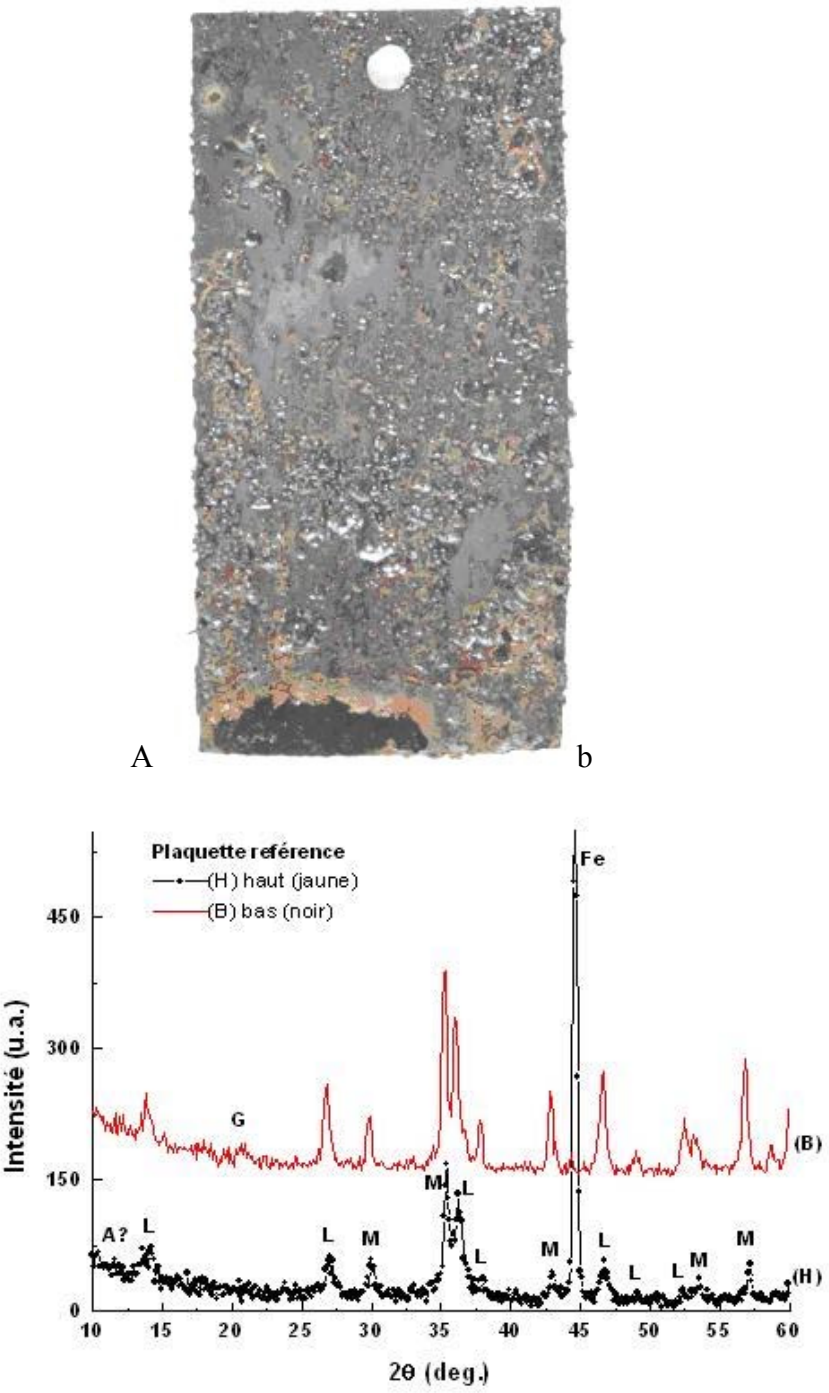

Figure 7: Degreased E24-2 steel plate after 22 days immersion in $FeCl_2$ and 45 days exposure in a climatic chamber (a/) and XRD analysis of the corrosion products, at the top (H) and the bottom (B) of the plate (b/). M (magnetite), L (Lepidocrocite) and G (goethite), A (akaganeite)

Figure 7a shows the visual appearance of one of the plates (degreased) after the ageing process. Corrosion layers do not depend on the surface preparation and observation on cross-sections indicate that they form a thin and multilayered film that is adherent to the metal surface. XRD analysis reveals the presence of lepidocrocite (γFeOOH) and magnetite (Chevalier 2001 – Figure 7b). Both observation and analysis of the corrosion layers show that the artificial coupons can be used to simulate the behaviour of real artefacts.

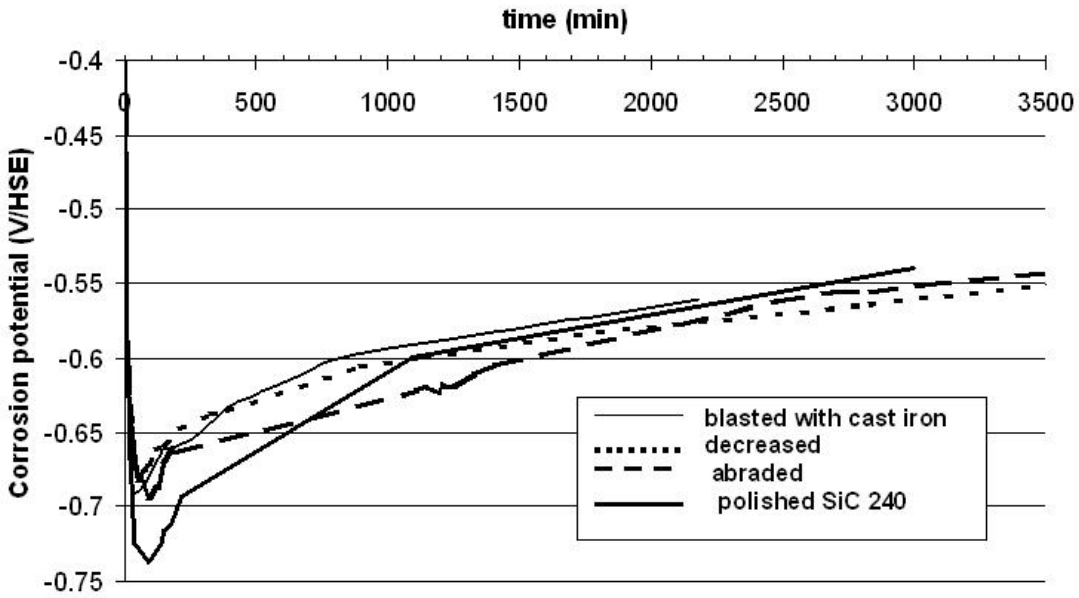

Figure 8 : Influence of the surface treatment of steel plates on the E_{corr} measurements with time in 1% KOH solution

These corroded steel plates were immersed then in 1% (w/v) KOH solutions and figure 8 shows that whatever the surface preparation of the steel plates is the corrosion potential E_{corr} decreases immediately to reach a stable value after less than 2 hours. The values obtained at that stage depend on the thickness of the corrosion layer but are comprised between –0.7 and –0.75 V/HSE (or –0.05 to –0.1V/SHE). These are much higher than the ones obtained by Hjelm-Hansen (figure 5) because of the thin corrosion layers present on the artificial coupons. E_{corr} increases progressively afterwards to reach a value close to –0.5V/HSE (or roughly 0.16V/SHE) which is quite a similar value than the ones obtained on figure 5. When comparing the monitoring of both E_{corr} and the concentration of chlorides in solution versus time we observe that a large amount of chlorides is extracted during the decrease of E_{corr} step (Figure 9). Electrochemical reactions conduct then to the transformation of the corrosion layers that permit the dissolution of chloride species. When the alkaline solution reaches the metal surface on the whole plate E_{corr} starts increasing (passivation effect).

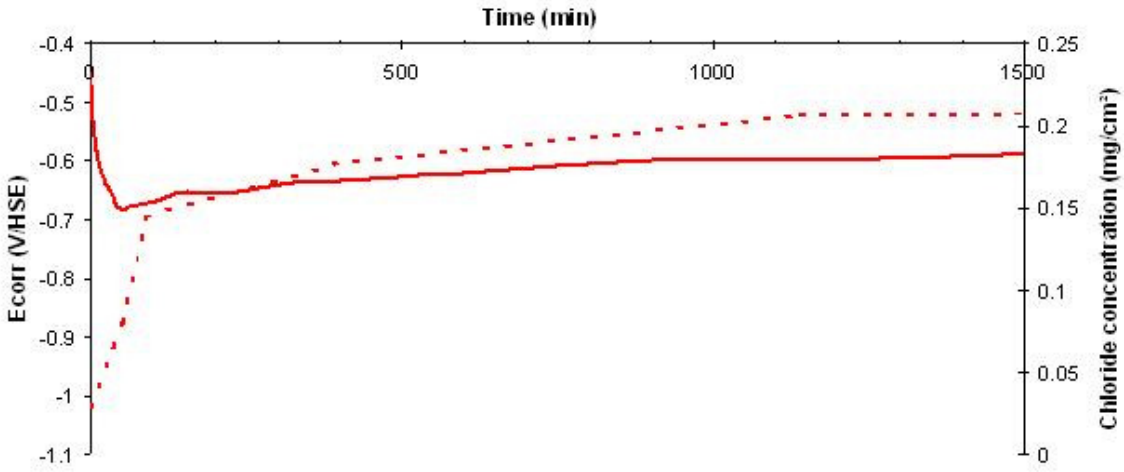

Figure 9 : Comparison between the E_{corr} (—) and concentration of chlorides (---) monitoring versus time for a steel plate corroded artificially and immersed in 1% KOH solution

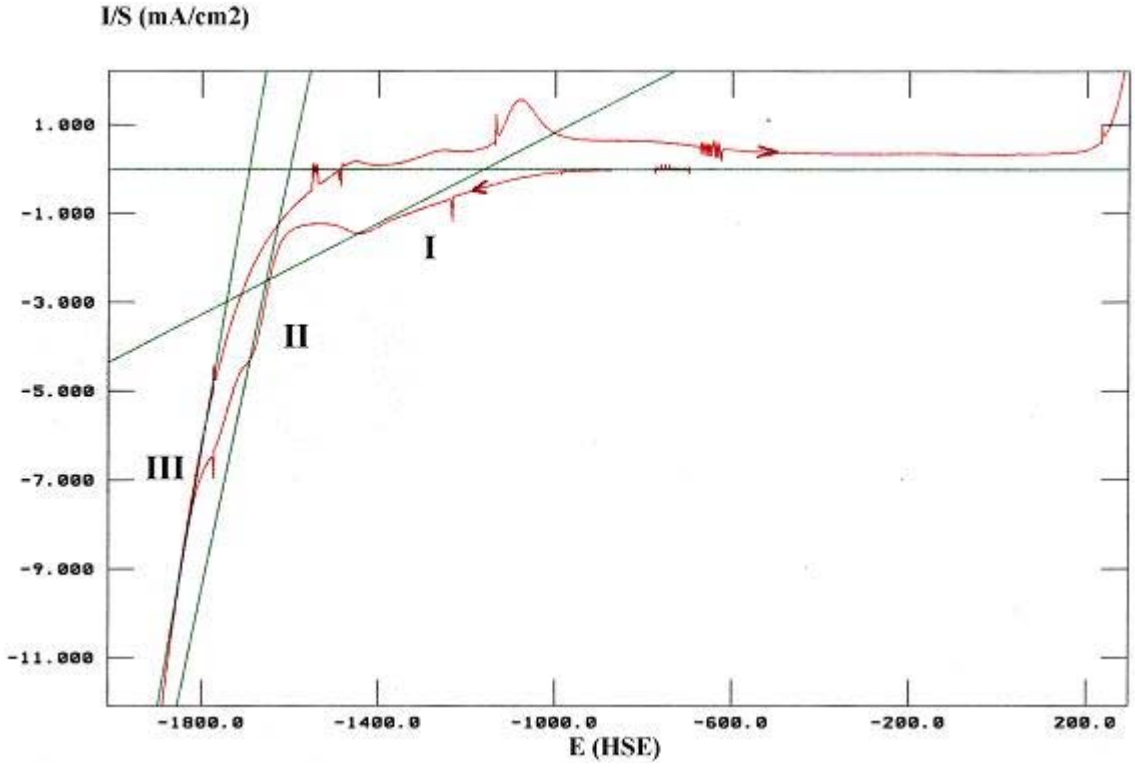

Figure 10: Voltammetric curve showing the behaviour of mild steel in 1% KOH solution when polarised cathodically from E_{corr} and then anodically (scanning rate=30mV/s), the counter electrode being a platinum grid. Reaction I corresponds to: Fe^{3+} ➔Fe^{2+} and reaction II to: Fe^{2+} ➔ Fe

Figure 10 shows the voltammetric I=f(E) curve obtained for a corroded steel plate in 1% (w/v) KOH solution from E_{corr} to –2V/HSE (cathodic part) and then back to 0.2V/HSE (anodic part). Two reduction peaks are obtained in the cathodic part. The first one corresponds to the reduction of Fe^{3+} in Fe^{2+} at the approximate potential of –1.15V/HSE

(-0.49V/SHE) and the second one to the reduction of Fe^{2+} in iron occurring at –1.6V/HSE (or –0.94V/SHE). This curve clearly indicates that none of these reactions occur during the immersion of the corroded plate in 1% KOH solution since the lower potential we could get is –0.75V/HSE (or –0.1V/SHE). The extraction of chlorides is not provoked then by the reduction of the oxyhydroxides.

Looking back at Hjelm-Hansen results (Figure 5) it seems though that E_{corr} measured on some artefacts can go as low as –1V/SCE (-0.758V/SHE), a potential for which the reduction of Fe^{3+} in Fe^{2+} is possible. In these cases the transformation of corrosion layers through reduction processes might occur.

3.2. On artefacts

Monitoring of the corrosion potential was performed on some marine artefacts that had been cleaned from their crust and were stored / stabilised afterwards in 1% (w/v) KOH or NaOH solutions.

3.3. Storage of *Saintes-Maries-de-la-Mer* iron ingots

These iron ingots were recovered in the Mediterranean Sea in 1996 from two different ancient Roman wrecks discovered and surveyed by the DRASSM (Département des Recherches Archéologiques Subaquatiques et Sous-Marines) (Baudat 1997).

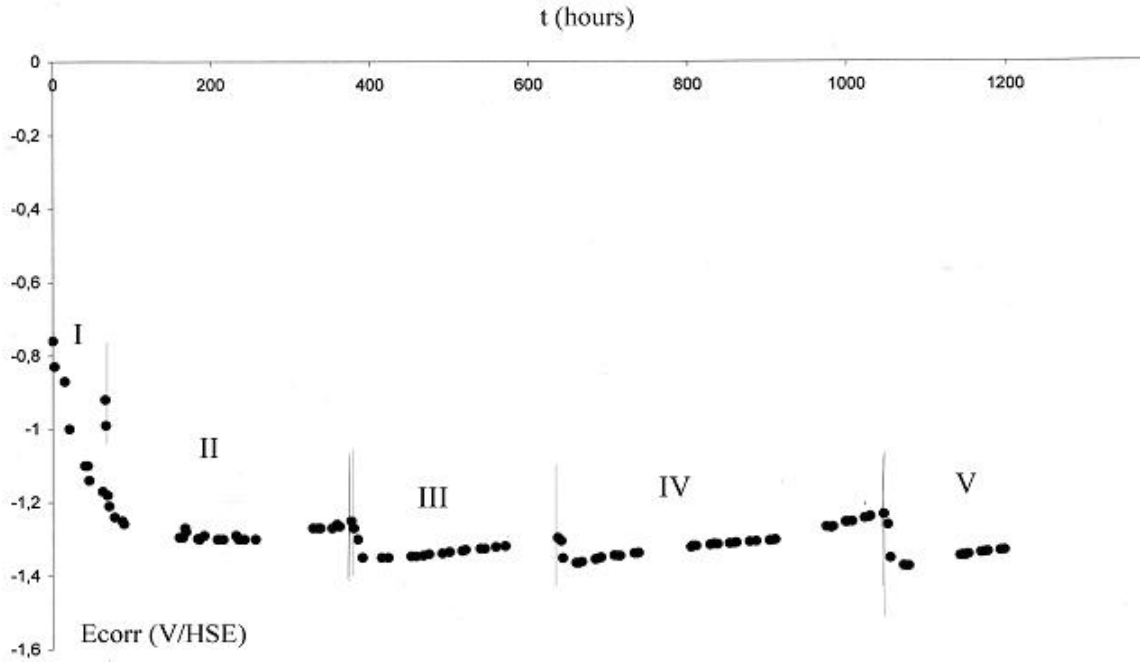

Figure 11 : Monitoring of E_{corr} versus time for one of the *Ste-Marie-de-la-Mer* iron ingot immersed in 1% KOH solution. Phases I to V correspond to the change of solution

Some of them were transferred for investigation and conservation to the conservation Laboratory Arc'Antique, France and were immediately immersed in KOH 1% (w/v) solution. The investigation of one ingot on cross-sections revealed that it was made of ferrite (αFe) and perlite (αFe + Fe_3C) and that the superficial corrosion layer was quite thin. Seawater had penetrated though in the metal structure through cracks and large amount of chlorides were expected. The monitoring of E_{corr} with time indicated three steps (figure 11). First an abrupt decrease of E_{corr} to values as low as –1.3V/HSE (-0.642V/SHE) followed by a step where E_{corr} remained stable. Later on the corrosion potential increased again but very slowly. The difference phases I to V correspond to regular changes of the solution when the amount of chlorides extracted started to reach a constant value. Large amount of chlorides were actually extracted. Note that the final potential (phase V) was still quite low although the stabilisation process was apparently finalised (only low amount of chlorides were obtained at that stage).

3.4. Stabilisation of a two arms iron anchor

This wrought iron anchor of the Admiralty type (shank with a movable iron stock) was found in the Baltic Sea in a depth of 17 m East West from Helsinki and brought dry to the conservation laboratory at the EVTEK, Institute of Art and Design clean of marine crust. The metal was directly apparent and most of the original surface was lost.

No active corrosion could be noticed on the metal surface (even after the humid chamber test). It was decided though to immerse the artefact in a 1% (w/v) KOH solution to check whether chlorides could be extracted from the internal structure.

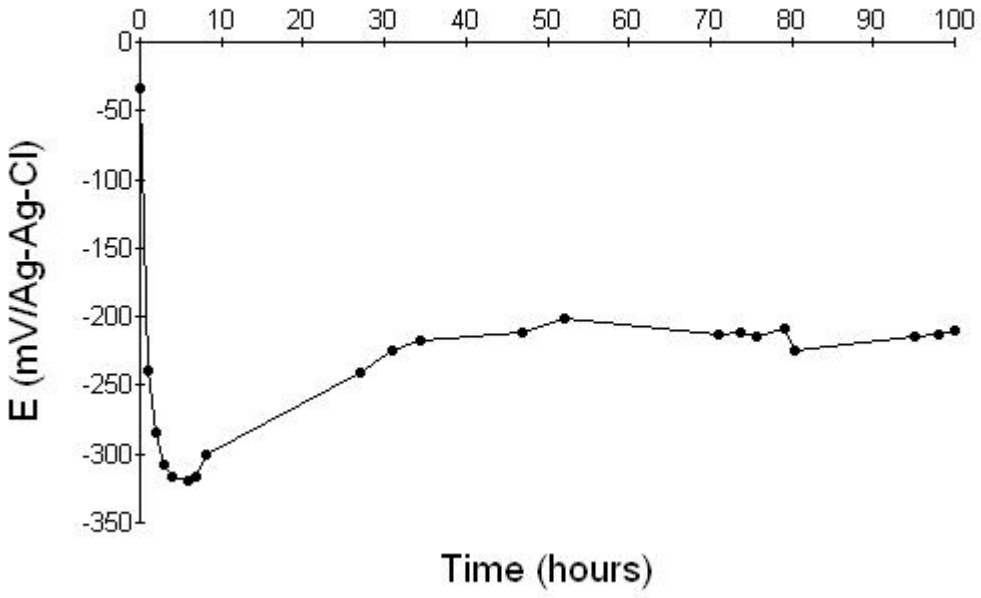

Figure 12: E_{corr} versus time for a wrought iron anchor immersed in 1% KOH solution

The monitoring of E_{corr} with time is given on figure 12. Although the common behaviour is obtained (preliminary decrease of E_{corr} followed by a short time where it remains stable followed itself by a re-increase of E_{corr}) the lower values obtained (-0.325V/Ag-AgCl or –0.125V/SHE) did not permit any reduction of Fe^{3+} in Fe^{2+}. The potentials measured here are quite similar to the ones obtained on artificial coupons, indicating then the presence of a thin corrosion layer which is confirmed by the metallic appearance of the artefact.

Noteworthy no chloride extraction was observed during this experiment.

3.5. Storage / Stabilisation of an iron based swivel gun

This breach loading swivel gun was recovered from the sea around Malta some years ago (June 2000) and will be exhibited at the Malta Maritime Museum. It seems to be made of a grey cast iron body with the swivel and the tiller made of wrought iron. The grey cast iron is heavily graphitised but the wrought iron elements are very well preserved. After been mechanically cleaned from its crust the swivel gun was conserved in a sodium carbonate solution that was changed every 2 months. The artefact was brought to the Malta Centre for Restoration for stabilisation and was immediately immersed in a 1% (w/v) NaOH solution (NaOH was used instead of KOH because of the presence of large quantities of chlorides in the KOH brand available in Malta). Figure 13 shows how the reading of E_{corr} were performed during the stabilisation process and figure 14 gives both the follow up of E_{corr} and the extraction of chlorides with time.

Figure 13: Principle of the measurement of E_{corr} with a reference electrode. The artefact is an iron based swivel gun immersed in 1% NaOH solution (credit: D. Vella)

Like in the examples above the common behaviour was once again obtained but the lower potentials measured were this time quite similar to the ones given by the iron ingots: -0.92V/Ag-AgCl (around –0.72V/SHE) indicating then that reduction reactions might have occurred. Like for the ingots the potentials did not re-increase straight away but only after more than 30 days. Large amount of chlorides were measured too in that case. These chlorides were obviously extracted from the body made in grey cast iron.

ABN 70 592 297 967

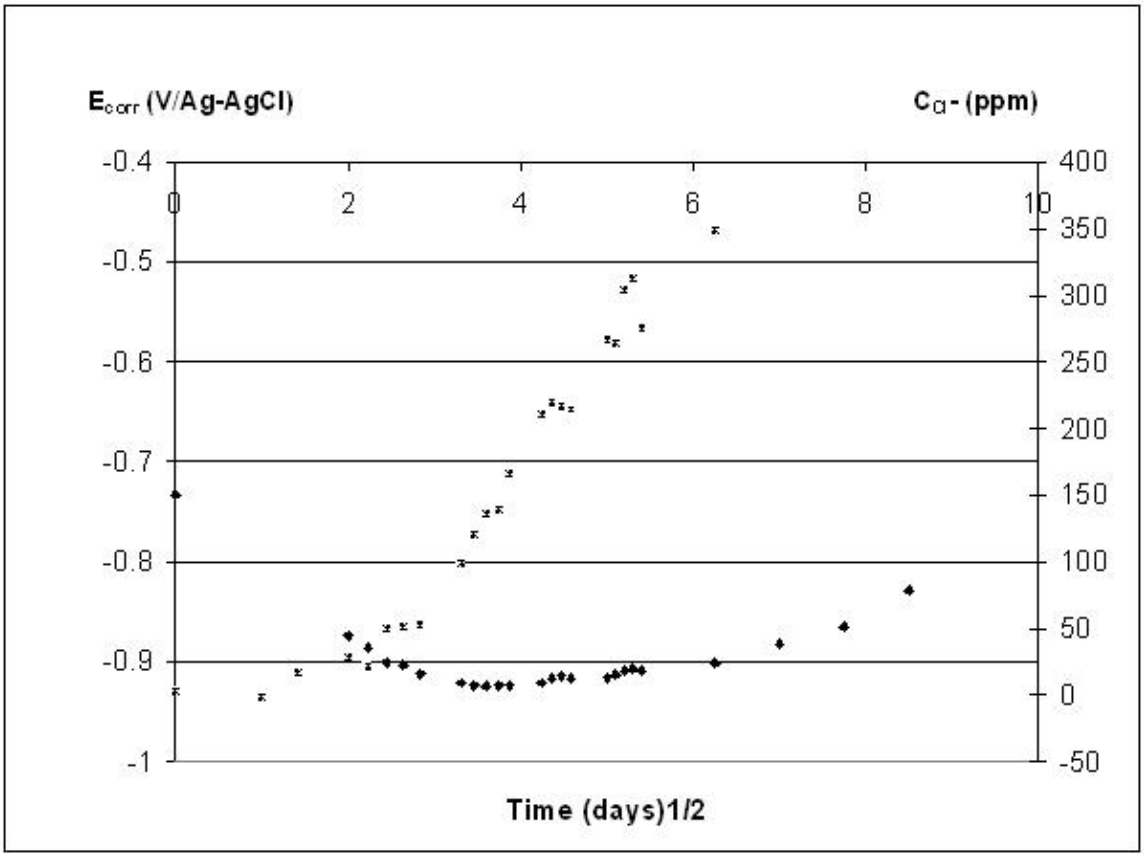

Figure 14: E_{corr} (♦) and concentration of chlorides extracted (✸) versus time for an iron based swivel gun immersed in 1% NaOH solution

4. Discussion

All our results show that the electrochemical behaviour of iron artefacts covered with corrosion layers and immersed in strong alkaline solutions given by Hjelm-Hansen (1992) is correct. Their corrosion potential first decreases abruptly to reach a value which depends on the nature of the corrosion layers. For archaeological artefacts covered with thick and compact corrosion layers this potential is comprised between –0.75 and -0.65V/SHE. For thin and/or porous corrosion layers this potential is closer to –0.1V/SHE. Voltammetric curves for iron in KOH solutions show that the reduction of Fe^{3+} in Fe^{2+} is possible below –0.49V/SHE. We can suspect then that some reduction reactions are taking place in the corrosion layers covering archaeological artefacts immersed in KOH but not on artefacts covered with thin corrosion layers.
Chlorides are either present at the interface remaining metal / corrosion layer as $FeCl_2$, FeOCl or at the surface of the artefact as βFeOOH. For thin and porous corrosion products most of the chlorides are released almost immediately. For archaeological artefacts covered with thick corrosion layers this extraction takes more time due to the slow penetration of alkaline solutions through the corrosion layers (through existing cracks or by decomposition/reduction of some of the corrosion products (oxyhydroxides mainly)).
The re-increase of E_{corr} corresponds to the normal behaviour of iron in alkaline solutions (either KOH or NaOH). It indicates that the solution has penetrated the corrosion layers and that the hydroxide anions are now passivating the metal

underneath. Figures 5, 8 and 12 show that this phenomenon occurs quite rapidly when the corrosion layer is thin and/or the concentration of chlorides to extract is quite small. This process takes much more time when corrosion layers are very thick and the quantity of chlorides to extract is quite important. In the former case the hydroxide anions will take more time to reach the metal surface. In the latter chloride and hydroxide anions might compete and prevent any passivation phenomenon to occur. It is necessary then to change the solution for a new one to protect the material and to increase the efficiency of the stabilisation process.

5. Conclusion

E_{corr} measurements during the storage / stabilisation of marine iron artefacts in diluted NaOH and KOH solutions are an important addition to the monitoring of the treatment via the regular analysis of chloride extracted. The latter approach will tell us when the extraction becomes less effective and the solution has to be changed or when the stabilisation is over. E_{corr} measurements are related to the behaviour of the surface of the metal artefacts. Corrosion potentials give us information on the thickness of the corrosion layer and the accessibility of chlorides species. They tell us whether the passivation of the remaining metal finally occurs not preventing though the extraction of chlorides. E_{corr} measurements alone cannot replace though the follow up of the storage / stabilisation process via the analysis of the chlorides extracted.
The monitoring of E_{corr} versus time offers a simple and safe way to store and stabilise iron metal artefacts in NaOH and KOH solutions but further research has to be performed to explain the way the corrosion products are really affected by the hydroxide anions and chlorides are then released. This knowledge could contribute to the optimisation of the stabilisation process.

Acknowledgements

The authors would like to thank Ms Saila Sorsa, objects conservator, for the information on the conservation of the ingots from Saintes-Maries-de-la-Mer, Ms Ilonne de Groot, private objects conservator, for providing similar information on the Admiralty anchor treated in the Marine conservation laboratory at EVTEK, Institute of Art and Design, Vantaa (Finland) and Mr Emmanuel Magro Conti, Curator of the Malta Maritime Museum, for the technical information on the breached loading swivel gun. Thanks should also go to Heritage Malta for its kind collaboration.

References

Baudat, M., Crau (1997), Alpilles, Camargue – Histoire et archéologie eds. Groupe Archéologique Arlésien, Actes du colloque des 18 et 19 Nov 1995 (France)

Chevalier, B. (2001), Expertise par diffraction X de plaquettes de fer corrodées artificiellement et ayant subies un traitement de déchloruration, rapport ICMCB, Université de Bordeaux (France)

Hjelm-Hansen, N., van Lanschot, J., Szalkay, C. D and Turgoose, S. (1992), Electrochemical monitoring of archaeological iron artefact during treatment, I.C.R., AIPnD, Non-destructive testing, microanalytical methods and environment evaluation for study and conservation of works of art, 3rd International Conference (Viterbo, Italy), 361-373

MacLeod, I.D. (1989), Electrochemistry and conservation of iron in seawater, Chemistry in Australia, 56, 7, 227-229
North, N.A. (1976), Formation of coral concretions on marine iron, The international journal of nautical archaeology and underwater exploration, 5.3, 253-258

North, N.A. (1987), Conservation of metals, in Conservation of marine archaeological objects, ed. by C. Pearson, Butterworths (London), p215

North,, N.A. and MacLeod, I.D. (1987), Corrosion of metals, in Conservation of marine archaeological objects, ed. C. Pearson, Butterworths (London), 68-104

North, N.A. and Pearson, C. (1977), Thermal decomposition of $FeCl_2$ and marine iron corrosion products, Studies in Conservation, 22, 146-147

North, N.A. and Pearson, C. (1978), Washing methods for chloride removal from marine iron artefacts, Studies in Conservation, 23, 174-186

Pearson, C. (1987), On-site storage and conservation, in Conservation of marine archaeological objects, ed. C. Pearson, Butterworths (London), p111

Pourbaix, M. (1963), Atlas d'équilibres électrochimiques à 25°C, Ed. Gauthiers-Villars, (Paris)

Schwertmann, U. and Cornell, R.M. (1991), Iron oxides in the laboratory, VCH Publishers (New York)

Selwyn, L.S., Sirois, P.J. and Argyropoulos, V. (2001), The corrosion of excavated iron with details on weeping and akaganeite, Studies in conservation, 44, 217-232

Turgoose, S. (1982a), The Nature of Surviving Iron Objects, in Conservation of iron, Eds. Clarke R.W. and Blackshaw S.M., Maritime monographs and reports, n°53, 1-7

Turgoose, S. (1982b), Post-excavation changes in iron antiquities, Studies in Conservation, 27, 97-101

Study of corrosion potential measurements as a means to monitor the storage and stabilisation processes of archaeological copper artefacts

K. Leyssens[a], A. Adriaens[a], E. Pantos[b] and C. Degrigny[c]

[a] Ghent University, Department of Analytical Chemistry, Krijgslaan 281 – S12, B-9000 Ghent, Belgium
[b] CCLRC, Synchrotron Radiation Department, Daresbury Laboratory, Warrington, UK WA4 4AD
[c] Malta Centre for Restoration, East Wing, Royal Naval Hospital, Bighi, Kalkara, Malta

Abstract

Archaeological copper artefacts recovered from wet saline environments are often stored in tap water and stabilized in sodium sesquicarbonate solutions. Modification of the natural patina and development of active corrosion can occur during these processes. This implies that monitoring of storage/stabilisation processes is necessary. The focus of the study consists of examining how corrosion potential (Ecorr) measurements can contribute in providing information on the effectiveness of storage and stabilisation treatments. This paper reports on the Ecorr versus time plots of artificially prepared copper coupons (covered or not with corrosion layers) immersed in tap water and a sodium sesquicarbonate solution. Synchrotron radiation XRD was performed in parallel to understand the reactions that take place during the immersion processes.
.

Keywords: corrosion potential measurements, XRD, copper, saline environments, storage, stabilisation, sodium sesquicarbonate, tap water

1. Introduction

Archaeological copper artefacts recovered from wet saline environments should not be exposed directly to the atmosphere, especially when they contain aggressive chloride species, as the metal will then corrode at an accelerated rate in the oxygen-rich air (Scott 2002, p125). Therefore it is best to store these objects in a solution until a treatment can be applied. The objects are usually stored in tap water or a sodium sesquicarbonate solution (Oddy et al. 1970 and MacLeod 1987a,b). The latter solution has the advantage that stabilization of the artifacts already starts as the chloride ions leach out of the corrosion layer. Nevertheless results often show a certain instability of the artefacts, such as the chemical transformation of the natural patina (for example the formation of tenorite (CuO) (Pollard et al. 1990) or chalconatronite ($Na_2Cu(CuO_3)_2.3H_2O$) (Horie et al. 1982)) and the development of active corrosion. The occurrence of these side effects means that monitoring of the treatments remains necessary.

2. Aims

The objective of this research project is to determine whether corrosion potential (Ecorr) measurements can be used to monitor the behaviour of copper based alloys during their storage and stabilisation processes and to provide early stage information about on-going corrosion processes.

This paper reports on Ecorr versus time plots performed on copper coupons (covered or not with corrosion layers) simulating the behaviour of real copper artefacts immersed in tap water and sodium sesquicarbonate solutions. Synchrotron radiation XRD was performed in parallel to understand the reactions that take place during the immersion processes.

Corresponding author: TEL: +32 9 264 48 26: FAX: +32 9 264 49 60: email: annemie.adriaens@UGent.be

3. Methods

3.1 Corrosion simulation

Pure corrosion products, commonly found on real artefacts, were artificially prepared on pure copper coupons (ADVENT, purity 99.9%). Five of these corrosion products were selected for the experiments.

Cuprite (Cu_2O) is a stable copper oxide that is regularly found on copper artefacts (Scott 2002; De Ryck 2003). To obtain a cuprite layer, the copper samples were polarized anodically at -360 mV/MSE for 16 hours in a 0.1 M Na_2SO_4 (Fluka) solution (Beldjoudi 1999).

Within the copper chlorides nantokite (CuCl), atacamite and paratacamite (both isomers of $Cu_2(OH)_3Cl$) were selected. Nantokite is considered as the main catalytic agent for active corrosion. The presence of this cuprous chloride as a corrosion product adjacent to the metallic surface can create long-term problems for the stability of an object. Bronze disease or pitting corrosion is usually attributed to this corrosion product (Scott 2002). Copper covered with nantokite is obtained by immersing pure copper samples for one hour in a saturated $CuCl_2.2H_2O$ solution (VWR International). After rinsing with deionised water they were exposed to the atmosphere for a night (Lamy 1997).

Atacamite and paratacamite are two other important chlorides in bronze corrosion. They are often considered as end products and are formed on top of the active corrosion areas. Atacamite is the most common of the $Cu_2(OH)_3Cl$ isomers, but often alters into paratacamite (Scott 2002; De Ryck 2003). In this respect atacamite as well as a mixture of atacamite and paratacamite were prepared in this study. For the atacamite corrosion a solution of 15.07 g $(NH_4)_2CO_3.NH_3$ (Fluka) and 10.02 g NH_4Cl (Aldrich) in 100 ml deionised water was prepared. The copper samples were wetted twice a day with this solution. This procedure was repeated for five days. Between each application the samples were left to dry to the air. After the period of five days the samples were left in the air for another five days without any treatment (Lamy 1997).

The protocol used to obtain a mixture of atacamite and paratacamite was almost the same; only the solution was different: 10.02 g $Cu(NO_3)_2.3H_2O$ (VWR International) and 10.01 g NaCl (Fluka) in 100 ml deionised water was prepared (Lamy 1997).

Chalcocite (Cu_2S) is typical for marine artefacts found in anaerobic environments (Scott 2002). The protocol to form this corrosion product included placing the samples in a closed box for 30 minutes together with a mixture of 4 ml 20 % NH_4S (VWR International) and 20 ml deionised water (Lamy 1997).

Prior to the corrosion simulation, the copper samples were ground first on 1200 grit SiC-emergy paper (Buehler) to obtain a fresh surface. To smoothen the surface they were further polished on a polishing cloth covered with alumina powder of 1 μm particle size. To remove any adherent Al_2O_3 particles the surfaces were rinsed thoroughly with deionised water and cleaned in an ultrasonic bath (Branson 3210).

3.2 Storage / stabilisation treatments

Tap water is often used for the storage of archaeological artefacts recovered from wet saline environments. For this study tap water was artificially prepared according to the composition of tap water of Wageningen (van Meeteren et al. 2000). The artificial tap water was prepared by dissolving 10.76 mg/l $CaSO_4.2H_2O$, 40.66 mg/l $MgCl_2.6H_2O$, 126.01 mg/l $NaHCO_3$ and 1.50 mg/l $CaCO_3$ in deionised water (pH = 7).

Various concentrations of sodium sesquicarbonate solutions are used by conservators for the stabilisation of bronze artefacts. Five to 10 wt% solutions are very common, but due to side effects, such as the formation of chalconatronite ($Na_2Cu(CuO_3)_2.3H_2O$), lower concentrations are now used. For this study a 1 wt% sodium sesquicarbonate solution was prepared by dissolving 11.89 g/l of $Na_2CO_3.NaHCO_3.2H_2O$ (Sigma) in deionised water (pH = 10).

3.3 Electrochemical measurements

For the evaluation of the treatments corrosion potential measurements were recorded in artificial tap water and in a 1 wt% sodium sesquicarbonate solution. The instrumentation was a PC-controlled potentiostat and software package type GPES4.9 (Autolab PGSTAT10, ECO Chemie). A Mercury Sulphate Electrode (MSE, $Hg/Hg_2SO_4,K_2SO_4(sat)$) electrode was used as reference electrode (= 640mV vs. Normal Hydrogen Electrode,

NHE). Copper coupon disc electrodes of 6 mm diameter, covered or not with corrosion product, were measured in 150 ml of the electrolyte solution.

3.4 Surface characterization

Synchrotron radiation X-ray diffraction measurements were performed to evaluate the effect of the treatment solutions on the corrosion products. 2D diffraction patterns were acquired using a CCD detector at station 9.6 of the Synchrotron Radiation Source at Daresbury Laboratory (UK). Each of the experiments was performed three times. Powder samples were prepared by scraping the corrosion products off the sample. The powder samples were deposited on tape stretched over thin metal sample holders which were then mounted on the goniometer. Exposure times of 30 s were used in multibunch (250mA) mode. The data were polar transformed and azimuth integrated using the ESRF program FIT2D (Hammersley et al. 1996). The tape gives a background in the spectra, which is more pronounced when a smaller amount of powder is measured or when the corrosion product has a diffracting power (see also the spectrum labelled 'background' in Figure 2 and 4).

4. Results

4.1 Artificial tap water

A set of artificially corroded copper coupons was prepared according to the description in subsection 3.1 'Corrosion simulation'. The samples were immersed in artificial tap water while corrosion potential measurements were made. In Figure 1 the first 18 hours of the immersion are presented. During the first day the corrosion potentials show the largest variation. For the pure copper samples large potential variations are even seen during the first six hours. Afterwards the potential rises to a steady state value around -0.35 V/MSE where it stays at the same level during at least the next two weeks (not shown). The stabilisation time of copper covered with cuprite is much shorter: after only two hours a more or less stable corrosion potential was achieved. The corrosion potential of copper covered with nantokite shows a strong decrease during the first few hours. Afterwards it rises to a steady state around the same value of the steady state plateau of copper covered with cuprite. The corrosion potentials of the remaining chloride containing corrosion products rise in the first few hours. The corrosion potential of atacamite rises to a steady state, whereas the increase of the corrosion potential of the mixture of atacamite and paratacamite is first followed by a descent before it rises again to its steady state. Finally the corrosion potential curve for chalcocite rises strongly in the first hour to decrease slowly after two hours and stabilise after 10 hours.

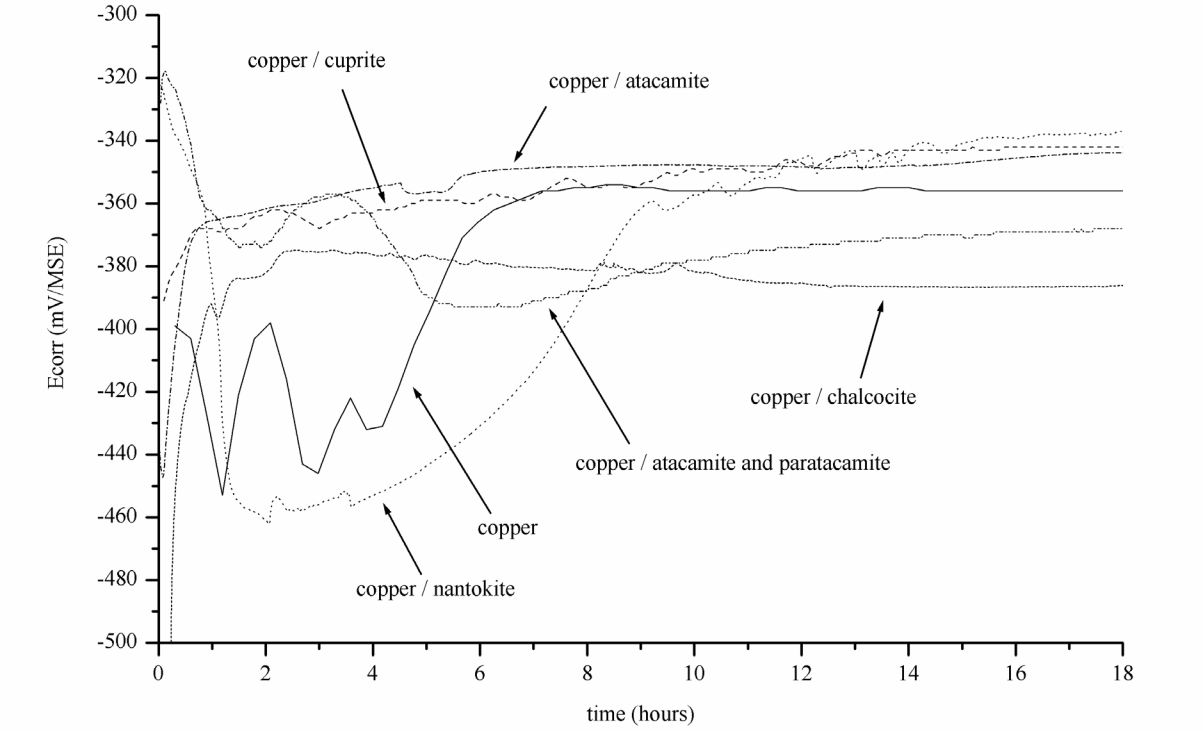

Figure 1. Corrosion potential versus time measurements for pure copper and copper covered with different corrosion products immersed in artificial tap water.

XRD measurements of the copper coupons covered with corrosion products were performed after one day and after 14 days of immersion in the solution. In Figs. 2a to 2e, a representative curve of each of the experiments is given. The XRD diffractograms of cuprite immersed in artificial tap water look the same before and after one day, seven days and 14 days immersion (Figure 2a). (The line basis of the last experiments is changed due to the use of a different tape in the sample holder). Each of the samples clearly shows peaks (Bragg reflections) corresponding to cuprite: 3.020 Å (9%), 2.465 Å (100%) and 2.135 Å (37%) (the relative intensities of the reference spectra are given between brackets). The copper peaks (2.088 Å (100%) and 1.808 Å (46%)) found in the first three diffractograms are most probably due to the sample preparation, as in some cases pure copper was scratched off as well. The XRD spectra show no indication that other corrosion products have formed during immersion.

The nantokite samples show more variation as a function of time (Figure 2b). The samples which have not been immersed yet show very clearly the nantokite peaks at 3.117 Å (100%), 2.710 Å (8%), 1.91 Å (55%) and 1.633 Å (30%). Cuprite peaks (2.465 Å and 2.135 Å) and copper peaks (2.088 Å and 1.808 Å) can be seen as well. After one day of immersion the peaks of nantokite have disappeared and only cuprite and some copper remain.

The atacamite samples (Figure 2c) clearly show the presence of atacamite with the largest peaks at 5.485 Å (100%), 5.03 Å (68%), 2.835 Å (51%), 2.78 Å (42%), 2.761 Å (28%), 2.280 Å (29%) and 2.265 Å (41%). These peaks are found in each of the samples, regardless of the time spent in the artificial tap water. The peaks around 4.2 and 6.4 are background and result from the tape used in the sample holder. In addition a few unidentified peaks show up at 3.91 Å, 2.67 Å and 1.96 Å on the samples which had not been immersed. They disappear once the samples have been immersed.

The XRD spectra of the mixture of atacamite and paratacamite are given in Figure 2d. Most of the diffraction lines of atacamite and paratacamite are closely related to each other (paratacamite has main peaks at 5.449 Å (100%), 4.68 Å (14%), 2.893 Å (19%), 2.758 Å (67.2%), 2.724 Å (13%), 2.261 Å (46%), 1.816 Å (17%) and 1.707 Å (19%)). Atacamite has a unique peak at 5.03 Å, where paratacamite has a unique peak at 6.48 Å. Both peaks are present in these spectra. The samples which have not been immersed also show a few unidentified peaks at 1.99 Å and between 3 Å and 3.3 Å. These peaks have not appeared on the immersed sample.

The chalcocite protocol gives a complex diffractogram (Figure 2e). Chalcocite is the principal corrosion product found in this diffractogram with the largest peaks at 3.71 Å (27%), 3.271 Å (36%), 3.162 Å (27%), 2.719 Å (36%), 2.403 Å (55%), 2.398 Å (73%), 2.393 Å (36%), 2.331 Å (27%), 2.192 Å (36%), 1.961 Å (73%), 1.87 Å (73%) and 1.867 Å (100%). After immersion, copper (2.088 Å and 1.808 Å) and cuprite (2.465 Å and 2.135 Å) are the main peaks. Small peaks of chalcocite can also be observed.

From the diffractograms we can conclude that only nantokite and chalcocite seem to be effected by this short time immersion. The other corrosion products remain stable.

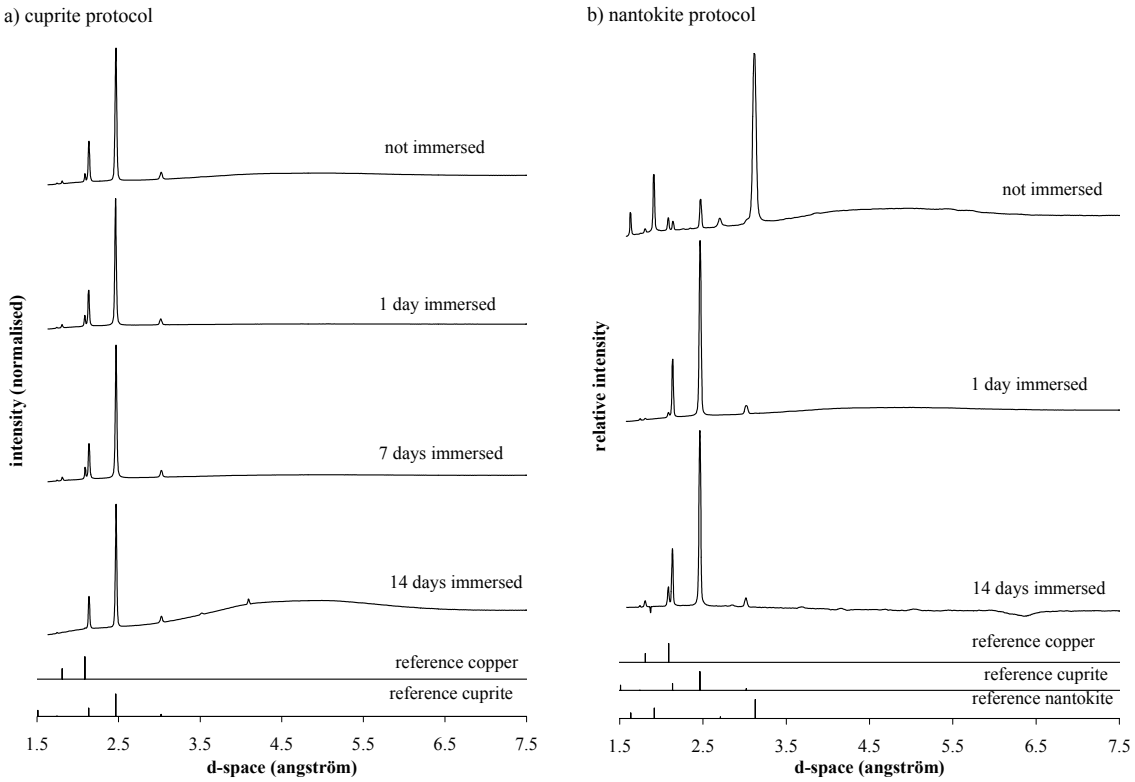

c) atacamite protocol

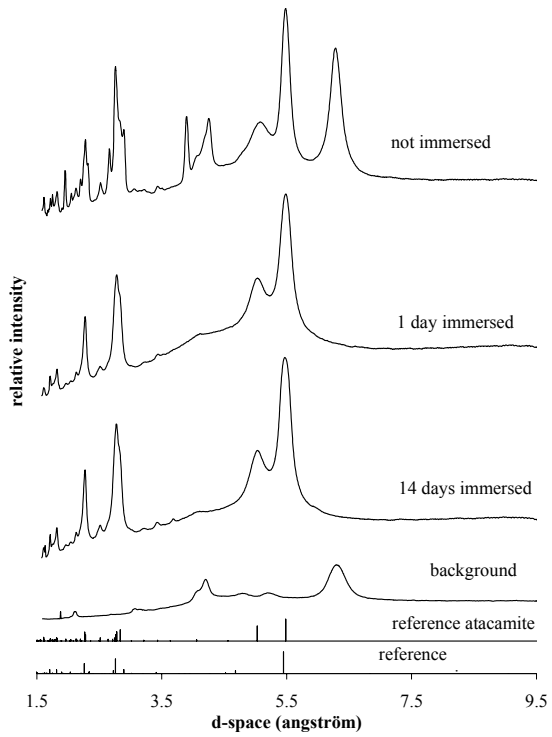

d) atacamite/paratacamite protocol

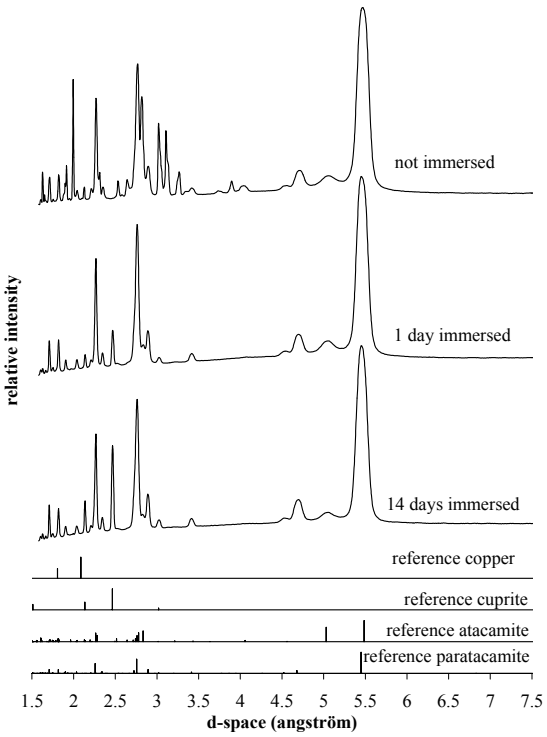

e) chalcocite protocol

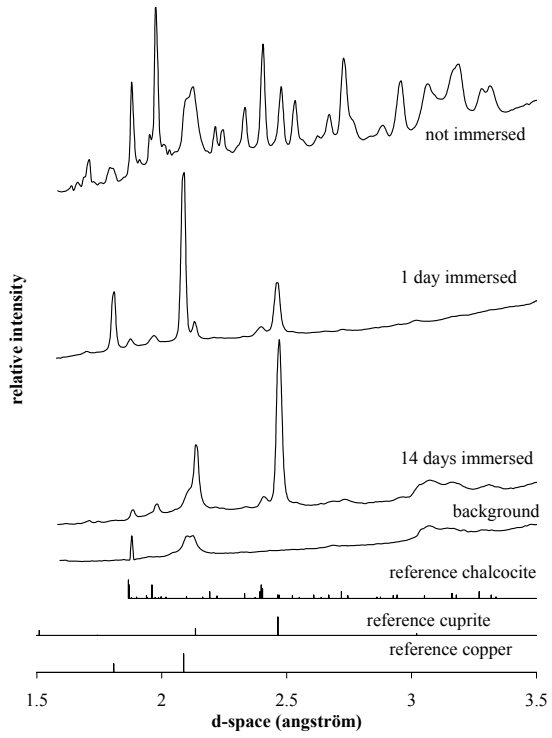

Figure 2. SR-XRD measurements of copper coupons covered with corrosion products after different immersion times in artificial tap water. a) cuprite b) nantokite c) atacamite d) atacamite and paratacamite e) chalcocite

4.2 Sodium sesquicarbonate solution

A similar set of coupons were prepared and immersed in a 1 wt% sodium sesquicarbonate solution. Figure 3 shows the corrosion potential measurements during the first 12 days for each of the coupons immersed in the sodium sesquicarbonate solution. It is obvious that the corrosion products in this solution exhibit a different behaviour to tap water. The corrosion potentials of copper and cuprite quickly reach equilibrium. The corrosion potential of nantokite on the other hand shows a quick descent at the beginning, followed by an increase which goes over a maximum to a more or less steady state. After seven days it starts a long rise again. The mixture of paratacamite and atacamite also seems to be unstable; the corrosion potential descending over more than 14 days. The corrosion potential behaviour of pure atacamite on the other hand gives a very slow but steady rise. This indicates the formation of a stable and protective corrosion layer. Finally chalcocite shows a long steady rise to reach a plateau after eight days.

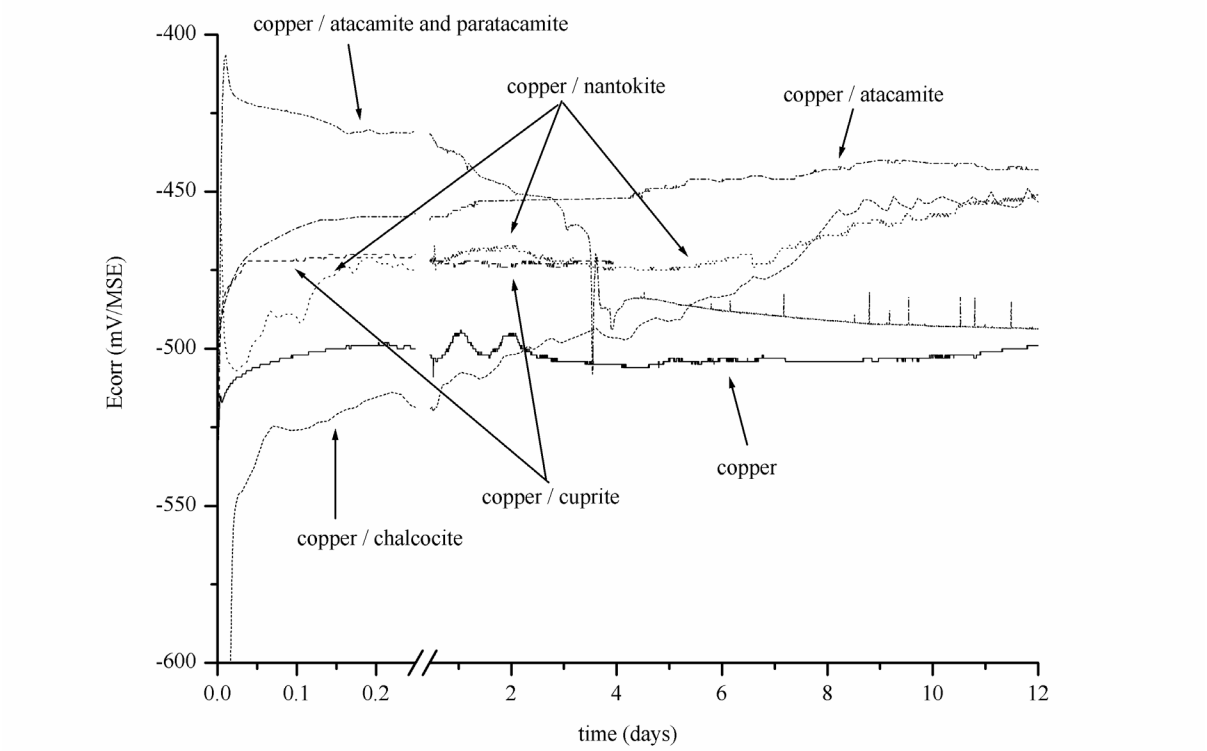

Figure 3. Corrosion potential versus time measurements for pure copper and copper covered with different corrosion products immersed in 1wt% sodium sesquicarbonate.

XRD measurements of the copper coupons covered with corrosion products were performed after one day and after 14 days immersion in the solution (Figs. 4a to 4e). The XRD measurements indicate that cuprite does not undergo chemical transformation in the sodium sesquicarbonate solution (Figure 4a.). The XRD spectra before immersion, after 1 day immersion and after seven days immersion in the sodium sesquicarbonate solution all show the presence of cuprite (2.465 Å and 2.135 Å) and copper (2.088 Å and 1.808 Å).

Nantokite on the other hand reacts relatively fast (Figure 4b) in the sodium sesquicarbonate solution. After only one day of immersion the presence of nantokite (3.13 Å, 1.91 Å) is less pronounced and is even missing in some of the samples. Cuprite (2.465 Å and 2.135 Å) and paratacamite (5.44 Å and 4.68 Å) have obviously been formed on the samples. After 14 days in the sodium sesquicarbonate solution nantokite is no longer observed. Cuprite and paratacamite are still present, but also malachite ($CuCO_3.Cu(OH)_2$) has shown up, with mean peaks

at 5.970 Å (84%), 5.040 Å (96%), 3.690 Å (100%), 2.985 (20%), 2.861 Å (73%), 2.781 (28%), 2.518 (55%), 2.128 (20%).

The other chloride species, atacamite and paratacamite (Figs. 4c,4d) show a similar behaviour: the chloride products disappear in the XRD spectra in favour of malachite.

Chalcocite on the other hand reveals a special behaviour. Chalcocite can be found as a hexagonal or as an orthorhombic system. The diffractogram in Figure 4e shows the samples which have not been immersed exhibit an orthorhombic structure. For the diffractogram recorded after one day, the pure copper peaks were the most pronounced. To reveal the corrosion layer the copper peaks were truncated in Figure 4e. The diffractogram now reveals the peaks for a hexagonal structure (indicated by arrows in Figure 4e). It is likely that there has been a rearrangement of the crystal structure in the sesquicarbonate solution. After 14 days the layer was too thin to remove and measure. The spectra only reveal pure copper.

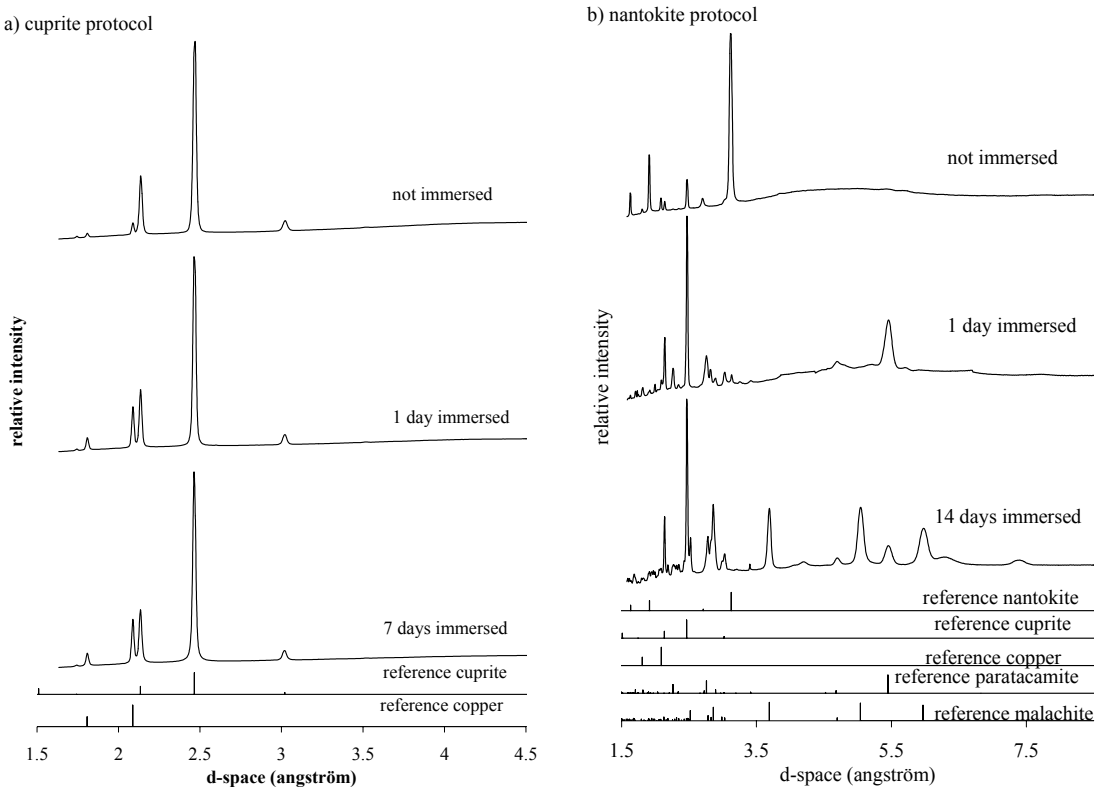

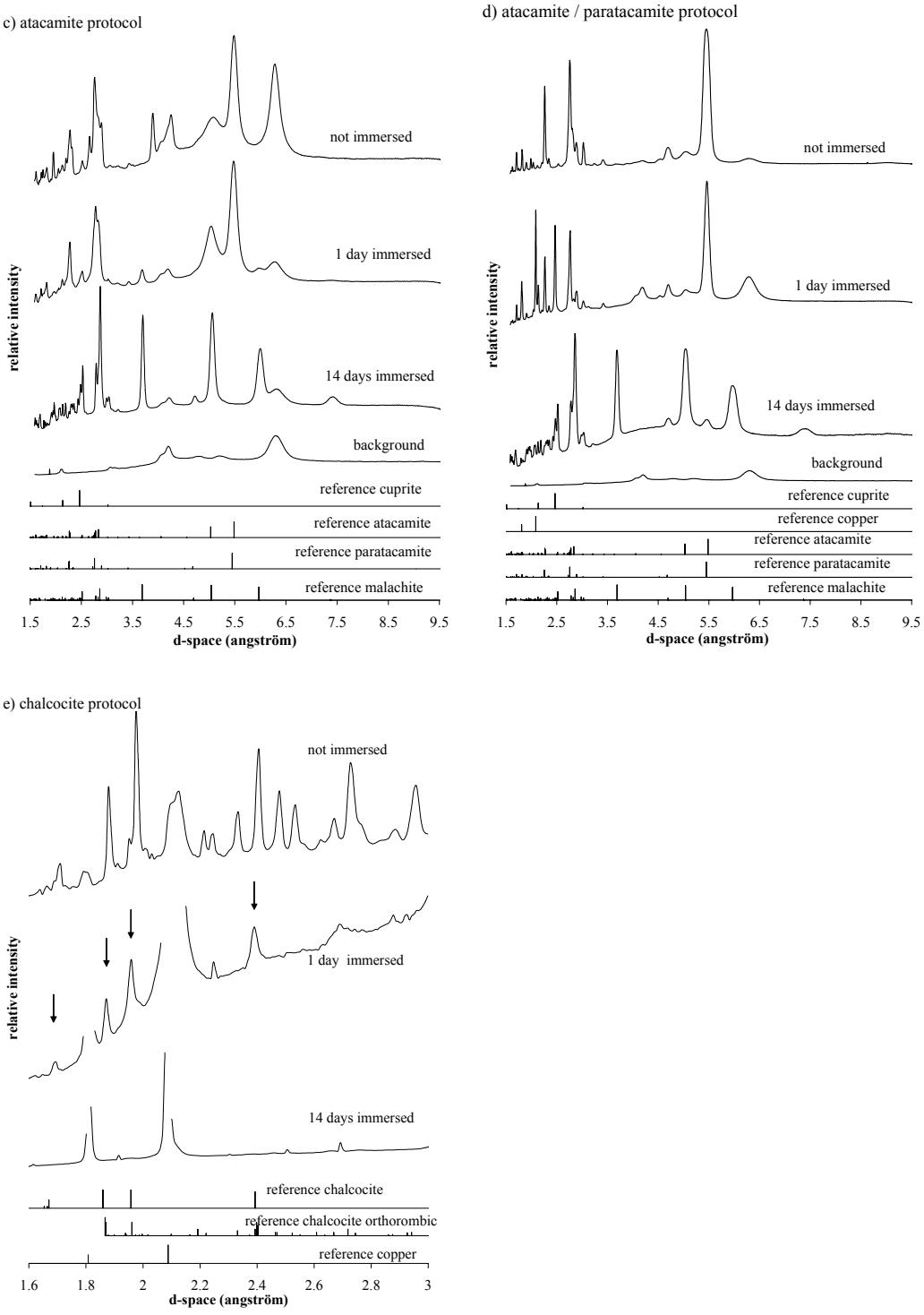

Figure 4. SR-XRD measurements of copper coupons covered with corrosion products after different immersion times in a sodium sesquicarbonate solution. a) cuprite b) nantokite c) atacamite d) atacamite and paratacamite e) chalcocite.

5. Discussion

Chemical and electrochemical transformation of the artificially prepared corrosion products occurring during immersion in tap water and the sodium sesquicarbonate solution were monitored for two weeks. A compilation of the XRD results is given in Tables 1 and 2. Corrosion potentials were recorded in parallel. The corrosion potential of cuprite quickly reached a steady state in both solutions. This is in agreement with the findings in the XRD measurements that cuprite is stable in these solutions. Nevertheless, a transformation at a microscopic level can occur and needs to be investigated.

The preliminary decrease of the corrosion potential for nantokite in the artificial tap water and in the sesquicarbonate solution is characteristic of a transformation process. According to Oddy nantokite can react with water in one of two ways, to give either cuprite or paratacamite by the following reactions (Oddy et al. 1970):

$$2\ CuCl\ (nantokite) + H_2O \rightarrow Cu_2O\ (cuprite) + 2\ Cl^- + 2\ H^+ \quad (1)$$

$$2\ CuCl\ (nantokite) + 2\ H_2O + O_2 \rightarrow Cu_2(OH)_3Cl\ (paratacamite) + HCl \quad (2)$$

In the artificial tap water the XRD spectra clearly indicate the disappearance of nantokite and the formation of cuprite. This can explain why the corrosion potential on copper coupons initially covered with nantokite reaches almost the same steady state value as on cuprite protocol coupons. On the nantokite protocol coupons in the sesquicarbonate solution cuprite as well as paratacamite is formed in the first instance. This is followed by the formation of malachite after a two weeks period. This can be due to the reactions suggested by MacLeod (MacLeod 1987a,b):

$$4\ CuCl + O_2 + 8\ HCO_3^- \rightarrow 4\ Cu(CO_3)_2^{2-} + 4\ H^+ + 4\ Cl^- + 2\ H_2O \quad (3)$$

$$Cu_2(OH)_3Cl\ (paratacamite) + 4\ CO_3^{2-} \rightarrow 2\ Cu(CO_3)_2^{2-} + 3\ OH^- + Cl^- \quad (4)$$

The ion $Cu(CO_3)_2^{2-}$ is supposed to be stable in the presence of bicarbonate ions but Oddy already indicated the precipitation of this compound. In this way a layer of malachite ($CuCO_3.Cu(OH)_2$) can be formed on the bronze (Oddy et al. 1970). It is probably the formation of the stable malachite that causes the corrosion potential to rise after six days. However, more experiments are needed to clarify how the formation of malachite is reflected in the change of the corrosion potential.

Similar results were obtained with the samples covered with a mixture of atacamite and paratacamite. The red-brown cuprite layer underneath the blue-green atacamite/paratacamite layer was grown in tap water. The relative quick descent of the corrosion potential in the beginning of the immersion can be caused by the decomposition of the copper chloride species. It is probably due to the cuprite layer that the corrosion potential reaches a sort of steady state after a day. In the sodium sesquicarbonate solution the decrease can be slowed down by the formation of a stable malachite (as mentioned in the discussion of nantokite) and cuprite layer. Further measurements are required to explain the behaviour of the corrosion potential in full detail.

The corrosion potential measurements of atacamite in tap water as well as in the sesquicarbonate solution show a quick rise in the beginning of the immersion. A steady state is reached very soon hereafter. Except for the disappearance of a few unknown peaks, the XRD spectra reveal no change of the corrosion products in the artificial tap water. In the sesquicarbonate solution the first malachite peaks can already be seen after one day immersion. The corrosion potential shows little variation after a few hours immersion, probably due to the quick appearance of the malachite.

The XRD spectra indicate that chalcocite is dominated by cuprite after immersion in the artificial tap water. In the sodium sesquicarbonate solution on the other hand no formation of cuprite is indicated and also malachite is not found in this case. As a result it is difficult to explain the large shift of the corrosion potential with time.

Table 1. Compilation of the XRD results before and after 14 days immersion in artificial tap water.

		corrosion products					
corrosion protocols		cuprite (Cu_2O)	nantokite (CuCl)	atacamite ($Cu_2(OH)_3Cl$)	paratacamite ($Cu_2(OH)_3Cl$)	chalcocite (Cu_2S)	malachite ($CuCO_3.Cu(OH)_2$)
pure copper	before						
	after	+					
cuprite	before	+					
	after	+					
nantokite	before		+				
	after	+					
atacamite	before			+			
	after	+		+			
atacamite and paratacamite	before			+	+		
	after	+		+	+		
chalcocite	before					+	
	after	+				+	

Table 2. Compilation of the XRD results before and after 14 days immersion in a 1wt% sodium sesquicarbonate solution.

		corrosion products					
corrosion protocols		cuprite (Cu_2O)	nantokite (CuCl)	atacamite ($Cu_2(OH)_3Cl$)	paratacamite ($Cu_2(OH)_3Cl$)	chalcocite (Cu_2S)	malachite ($CuCO_3.Cu(OH)_2$)
pure copper	before						
	after	+					
cuprite	before	+					
	after	+					
nantokite	before		+				
	after	+			+		+
atacamite	before			+			
	after	+		+			+
atacamite and paratacamite	before			+	+		
	after	+		+	+		+
chalcocite	before					+	
	after	+				+	

6. Conclusion

Artificially formed patina on copper does not seem to be affected during the immersion in tap water as is shown by both Ecorr and XRD measurements. In the sodium sesquicarbonate solution the decomposition of nantokite favours the stabilisation of artefacts but can change the surface appearance due to the formation of malachite. Monitoring of the corrosion potential with time appears as a very promising and simple technique to record these transformations, particularly when the corrosion layers are made of a single corrosion product. Further research is required as real artefacts are commonly covered with a stratigraphy of different corrosion products, which are all affected separately by the solutions used.

References

Beldjoudi, T. (1999) *Etablissement d'une procédure de formation électrochimique de patines sur alliages cuivreux*, unpublished Rapport Tech. STEP/EDF, Synthèse des Travaux, Valectra.

De Ryck, I. (2003) *Chemical characterization of ancient artifacts: Application of microbeam methods*, University of Antwerp, Antwerp.

Hammersley, A.P., Svensson, O., Hanfland, M., Fitch, A.N. and Hausermann, D. (1996) *Two-Dimensional Detector Software: From Real Detector to Idealised Image or Two-Theta Scan*, High Pressure Research, **14**, 235-248.

Horie, C.V. and Vint, J.A. (1982) *Chalconatronite: a by-product of conservation?*, Studies in Conservation, **27**, 185-186.

Lamy, C. (1997) *Stabilisation d'objects archéologiques chlorurés en alliage cuivreux – Définition des conditions d'une polarisation cathodique à potentiel constant en solution de sesquicarbonate de sodium 1%*, unpublished Rapport du Stage, Université de Nantes ISITEM.

MacLeod, I.D. (1987a) *Stabilisation of corroded copper alloys: a study of corrosion and desalination mechanisms*, in Proceedings of the 8th triennial ICOM-CC meeting, Sydney, 1079-1085.

MacLeod, I.D. (1987b) *Conservation of corroded copper alloys: a comparison of new and traditional methods for removing chloride ions*, Studies in Conservation, **32**, 25-40.

Oddy, W.A. and Hughes, M.J. (1970) *The stabilisation of "active" bronze and iron antiquities by the use of sodium sesquicarbonate*, Studies in Conservation, **15**, 183-189.

Pollard, A.M., Thomas, R.G. and Williams, P.A. (1990) *Mineralogical changes arising from the use of aqueous sodium carbonate solutions for the treatment of archaeological copper objects*, Studies in Conservation, **35**, 148-152.

Scott, D.A. (2002) *Copper and Bronze in Art: Corrosion, Colorants, Conservation*, The Getty Conservation Institute, Los Angeles.

Van Meeteren, U., van Gelder, H. and van Ieperen, W. (2000) *Reconsideration of the use of deionized water as vase water in postharvest experiments on cut flowers*, Postharvest Biology and Technology, **18**, 169-181.

ABN 70 592 297 967

Synergistic effects of corrosion inhibitors for copper and copper alloy archaeological artefacts

S. Golfomitsou and J. F. Merkel

Abstract

Benzotriazole (BTA) is one of the most widespread treatments used at present for the stabilisation of bronze disease. Unfortunately, BTA does not always work effectively when applied to heavily corroded copper and copper alloy archaeological artefacts. Combinations of corrosion inhibitors are extensively used in industry to retard copper corrosion. When two or more corrosion inhibitors are used, the inhibition efficiency of the mixture may be improved. This paper presents data that indicate the mixture of BTA with other inhibitors for chloride-containing corrosion products improve corrosion prevention under accelerated testing conditions. The six selected compounds. 5-Amino-2 Mercapto-1, 3, 4-Thiadiazole (AMT), Benzylamine (BZA), Ethanolamine (ETH), 1-Phenyl-5-Mercapto-Tetrazole (PMT), Potassium Ethyl Xanthate (KEX) and Potassium Iodide (KI) were tested individually and in combination with BTA. Factors such as concentration of the solution, time of immersion and solvent (de-ionised water, and ethanol) were examined. The inhibitors were applied initially on artificially corroded copper coupons and accelerated corrosion tests were assessed. The treated coupons were analysed using Scanning Electron Microscope (SEM-EDS) to examine the effects of such combinations. The results indicate that the combination of BTA with AMT improves the inhibitive efficiency at lower concentrations with ethanol or deionised water as a solvent. Finally, the combinations of BTA with AMT and BTA with PMT were applied on archaeological objects from the excavations of Kaman Kalehöyuk in Turkey and Mochlos in Crete, Greece. Treated objects have been monitored on an annual basis to investigate their long-term performance.

Keywords: Benzotriazole, 5-Amino-2 Mercapto-1, 3, 4-Thiadiazole, copper corrosion inhibitors, synergistic effect, accelerated corrosion testing.

1: Introduction

Although a number of chemical compounds can be used as corrosion inhibitors for copper, only a few have been tested for conservation and even fewer are currently in use. Research related to inhibitors for copper is largely dependent on industrial research. Unfortunately, inhibitors used in industry where copper is relatively free of corrosion have different aims and restrictions than those in conservation. For example, corrosion products can be viewed as part of the object's history and also often constitute a part of or even the whole of an object. The use of inhibitors for

ABN 70 592 297 967
conservation is also restricted by factors such as composition alterations, colour changes, toxicity and inhibitor film stability.
The main corrosion inhibitor used for the stabilisation of copper and copper alloy archaeological artefacts is benzotriazole ($C_6H_5N_3$); a nitrogen-containing organic heterocyclic compound. Benzotriazole (BTA) was first used by Madsen in 1967 and has been used widely in the field since then (Madsen, 1967: 163-166). For years the use of BTA was based on empirical assessment and the application methodology varied accordingly.
Although the inhibition of copper corrosion using BTA is one of the most thoroughly investigated processes, there is no comprehensive theory on its exact mode of action. Different analytical methods such as XPS, FT-IR, SERS, SIMS and electrochemical methods have been employed to examine the formation and protective action of the copper-BTA complex. BTA acts as a cathodic inhibitor retarding the cathodic reactions and as it has been also reported it acts predominantly as an anodic inhibitor (Dugdale and Cotton, 1963, Fox et al, 1979, Fiaud 1995).
Another controversy concerning BTA regards the properties of film formation. The film formed can be the result of either physisoption or chemisorption. BTA is thought to be physically adsorbed on the surface reacting with copper to form a polymeric film that acts as a physical barrier (Poling, 1970). Another theory is that BTA is chemisorbed on the metal surface and the film that is formed mainly prevents the adsorption of oxygen and slows down, or stops the initial corrosion reaction of copper: $2Cu + O_2 \leftrightarrows CuO_2$ (Mansfeld *et al.*, 1971: 293).
BTA efficiency as well as film formation depends on a number of factors including the pH of the solution. In low pH values the adsorption of BTA on copper is weakened (Musiani and Mengoli, 1987: 201). This might explain why BTA fails to inhibit corrosion of heavily corroded copper artefacts where the pH level is very low, such as in the case of pitting and active bronze disease.
Brusic *et al.* (1991) reported that BTA increases the corrosion potential, retarding the corrosion rate of copper. This implies that benzotriazole primarily blocks the exodus of copper ions and acts as a barrier to oxygen diffusion. The kinetics of the film formation, its thickness and the degree of polymerisation depend on the pH of the solution. In very acidic solutions (pH<2) a thick film (up to 25 nm) grows quickly following a dissolution-precipitation mechanism and, as such, the polymerisation is not complete. Therefore, although the film is thick, it is not that protective. At a pH of around 7, the film grows more slowly in a self-inhibiting manner. It is thinner (0.5-4 nm) and is completely polymerised providing the best protection. Therefore the degree of protection is found to be proportional to the degree of polymerisation. Finally different oxides give different films, and the structure of the film is dependent on the copper oxides formed (Brusic, 1991: 2253).
Archaeological artefacts are often covered with thick corrosion layers that hinder access to the remaining metal. The corrosion products often include anions such as chlorides or chloride containing corrosion products (i.e. nantokite) that impede inhibition. These anions contribute to a low pH (<3.5) resulting in a less effective partly polymerised film.
The aim of this paper is to examine whether the combination of different compounds could improve the effectiveness of BTA when treating archaeological copper and copper alloy artefacts. The properties of complex corrosion product compositions are beyond the range of BTA control alone.

ABN 70 592 297 967

In industry, it is very common to use more than one chemical compound to retard the corrosion process of a metal or alloy. When two or more corrosion inhibitors are added to a corrosive environment of a metal or an alloy, the inhibition efficiency of the mixture may be greater than the sum of each one of the additives. This is a synergistic effect (Rozenfeld, 1981: 110).

There are obvious benefits of the use of synergistic effects for the corrosion inhibition for archaeological copper and copper alloy artefacts. In most cases, the additives alone are not very effective inhibitors, but present good inhibitive properties when combined utilising different inhibitive features. For example, a combination of anodic and cathodic inhibitors could result in slowing down both the anodic and cathodic reactions of the electrochemical process.

The exact mechanisms of the synergism of inhibitors are not always clear. Some additives (e.g. halides) may modify the surface characteristics of a metal, assisting in the adsorption of the inhibitor. For example halide anions (Cl^-, Br^-, and I^-) act synergistically in the corrosion inhibition of iron, altering the properties of the surface, making possible the adsorption of organic cations on the metal surface (Kuznetsov, 1996: 40).

The combinations used have already been tested for industrial purposes. The selected combinations and their mode of action are shown in table 1.

Name	Formula	Mode of Action	*Main Advantages*	*Main Disadvantages*
Benzotriazole (BTA)	$C_6H_5N_3$	Cu-BTA complex	*Easy to apply, does not cause much colour change*	*Not effective on heavily corroded artefacts* *Not stable in acidic conditions* *Toxic*
2-Amino-5-Mercapto-1,3,4-Thiadiazole (AMT)	$C_2H_3N_3S_2$	Dissolve the Cl^-, forms a thin polymeric film	*Effective in very low concentrations*	*Causes colour alterations* *Moisture sensitive compound* *Toxic*
1-Phenyl-5 Mercapto-Tetrazole(PMT)	$C_7H_6N_4S$	Cu(I)-PMT complex	*Very good inhibitive properties in H_2SO_4*	*Possibly not effective in Cl^- containing environments*
Ethanolamine (ETH)	C_2H_7NO	Acts synergistically with BTA	*Not very effective when used alone*	*Toxic*
Benzylamine (BZA)	C_7H_9N	Acts synergistically with BTA forming mainly cupric compounds	*Not very effective when used alone*	*Toxic*
Potassium Ethyl Xanthate (KEX)	$KC_3H_5S_2O$	Acts synergistically with BTA	*Effective inhibitor for copper*	*Toxic,* *Causes colour alterations*
Potassium Iodide (KI)	KI	Acts synergistically with BTA, different theories on its mode of action, formation of Cu(IBTA)	*It is not an inhibitor alone*	

Table 1. Inhibitors tested and their observed general effects.

ABN 70 592 297 967

2: Research methodology

In order to examine the synergism of BTA with other compounds for the inhibition of archaeological copper and copper alloys, experiments were undertaken in both laboratory and field conditions. The initial laboratory experiments were performed on clean and pre-corroded copper coupons for comparison. The effectiveness of the selected treatments was assessed using weight change measurement and accelerated corrosion tests in relation to the copper substrate (clean, corroded), the concentration of inhibitive solution and the time of immersion. The topography and distribution of the inhibitive compounds was investigated foremost Scanning Electron Microscopy-Energy Dispersive Spectrometer (SEM-EDS). Following this, the more effective combinations were tested on archaeological artefacts.

2.1: Coupon preparation

The preparation of standard coupons was imperative to obtain consistent and comparable results. Several researchers in archaeological conservation have tried to reproduce artificially pre-corroded specimens for laboratory experiments (Angelucci et al, 1978; Faltermeier, 1995; Brostoff, 1997; Brazil, 1999).
To keep margins of errors within the same scale for all experiments, the coupons used had the same composition, size, and shape. Electrolytic copper (99.9% Cu) coupons (20x50x1mm) were corroded and treated following the technique proposed by Faltermeier (1995) as an easily reproducible and reliable method for routine production of pre-corroded surfaces for testing inhibitors. The coupons were air-abraded with glass beads to remove surface oxides, degreased in acetone in ultrasonic bath, weighed (±0.0001g) and immersed in 25 ml of 1M aqueous cupric chloride solution (dihydrate $CuCl_2.2H_2O$ in deionised water) for 24 hours at an ambient temperature (20-25°C). The coupons were washed in deionised water for an hour (in three 20-minute baths of 100 ml for each coupon) and, after a quick immersion in ethanol, dried under an infrared lamp (approx. 50°C). Following this, the coupons were placed in an oven and exposed to 105 °C for an hour. Nantokite and cuprite corrosion products were formed on the surface as confirmed by X-ray Diffraction (XRD) analysis. XRD of the coupons was undertaken using a Siemens D5000 Theta/2 Theta X Ray Diffractometer at the Chemistry Department at University College London. For every experimental run, at least three coupons were chosen as the minimum number of replicates statistically required to assess possible errors (Carter, 1982: 27).
The clean copper coupons used for the testing were treated within a few hours of air abrasion and degreased in acetone ultrasonic bath.
Accelerated corrosion testing aimed to assess and compare the properties of the different compounds in a reproducible corrosive environment.
Humidity testing at 25°C and 95% RH (±5%) was undertaken in a Fisons climate chamber with a Eurotherm 910D dual loop thermostatic controller.
The evaluation of the treatments was based on weight-gain measurements. The assessment of the corrosion by means of weight changes is valid when applied to specimens with uniform corrosion, as was the case for the ones produced for the purpose of these experiments. The formation of corrosion products results in a net mass increase and the weight uptake is related to the thickness of the corrosion

ABN 70 592 297 967

(Heitz, 1992: 12). Consequently, the mass change over time is associated to the corrosion rate and can be measured using the following formula (Skerry, 1985: 5):

$$IE\% = [(CR-CR_i)/ CR] \times 100$$

Where

IE is the inhibitive efficiency,
CR is the weight changes of the untreated coupons, and
CR_i is the weight change of the treated coupons.

Because of the humidity fluctuation in the chamber that could result in different corrosion rates of the exposed coupons, untreated control coupons were placed alongside the treated coupons and were used to calculate the inhibitive efficiency. It is remarkable how even small changes affect corrosion rates. The comparison of results of accelerated corrosion treatment testing is valid only if selected independent variables are controlled within known parameters (e.g. in attempt to control RH variation, coupons exposed to climatic chamber concurrently).
The treated coupons placed in the humidity chamber were monitored by weighing (±0.0001g) after 24, 48, 168, and 504 hours of exposure, and some at 840 hours.
The pH of aqueous solutions of the inhibitors used was measured to examine any relationships between the effectiveness of an inhibitor and the pH. A Corning pH meter 240 at the Chemistry Department of UCL was used. The values measured in the aqueous solutions are shown in Table 4.

ABN 70 592 297 967

SOLUTION	pH	COLOUR OF SOLUTION
BTA 0.1M, pure	5.8-5.5	Clear
BTA 0.1M,, 1h time of immersion	4.1-4.2	Clear, some green sediment
BTA 0.1M, 24h	3.5-3.6	Clear, some green sediment
BTA 0.1M, 1h/1h	4.1-4.0	Clear, some green sediment
BTA 0.1M, 1h/24h	3.5	Clear, some green sediment
BTA 0.1M, 24h/1h	3.7	Clear, some green sediment
BTA 0.1M, 24h/24h	3.2	Clear, some green sediment
BTA 0.01M, pure solution	5-5.1	Clear
BTA 0.01M, 1h	3.6-3.7	Clear, some green sediment at the bottom of the beaker
BTA 0.01M, 24h	2.75-2.8	Opaque/ light green
BTA 0.1M + AMT 0.01M, pure solution	4.1-4.2	Clear
BTA 0.1M + AMT 0.01M, 1h	4.1-4.2	Clear
BTA 0.1M + AMT 0.01M, 24h	3.9-4	Clear
BTA 0.01M + AMT 0.01M, pure solution	3.9-4.0	Clear
AMT 0.01M, pure solution	4	Clear
AMT 0.01M, 1h	3.3	Clear yellow with yellow sediment
AMT 0.01M, 24h	2.7	Yellow opaque, sediment
BTA 0.1M + ETH 0.1M, pure solution	9.6	Clear
BTA 0.1M + ETH 0.1M, 1h	9.6	Clear
BTA 0.1M + ETH 0.1M, 24h	9.5-9.6	Clear
ETH 0.1M PURE SOLUTION	11	Clear
ETH, 1h	10.7	Clear purple
ETH, (LOWER CONC.)	9.5	Purple
BTA 0.1M + KI pure solution	5.3	Clear
BTA + KI, 1h	4.3	Clear
BTA + KI, 24h	4.2	Clear
KI, PURE	7.0	Clear
KI, 1h	9.7	Whitish opaque and white sediment
BTA + BZA, pure solution	8.1	Clear
BTA + BZA, 1h	8.1	Clear
BZA, PURE	10.8	Clear
BZA, 1h	10.2	Semi-opaque with light green sediment
BTA + KEX, pure solution	7.4	Yellow/semi-clear
BTA + KEX, 1h	7.4	Yellow/ semi-clear
BTA + KEX, 24h	7.4	Bright yellow, semi opaque

Table 4. pH values of aqueous solutions of the inhibitor treatments.

ABN 70 592 297 967

3: Experimental design

The inhibition process is complex and affected by many interrelated variables. To evaluate each variable individually as well as, the interactions between the different variables, statistically designed experiments were employed. This way the effect of the variables and their interactions could be assessed using balanced experiments. One of the advantages is that possible experimental errors could be easily detected (Box et al, 1978: 7). The experiment outcome or response used to evaluate the results was the weight change % which is inversely proportional to the effectiveness of a treatment. In general, the higher weight uptake represents the less effective treatment.
The variables chosen were: additive with BTA solutions, concentration (of both BTA and the other compounds), time of immersion and solvent. The inhibitor concentrations selected were the ones recommended in the literature. Higher concentrations were also tested, because theoretically the more corroded an object, the higher inhibitor concentration is needed in order the treatment to be effective for archaeological copper alloys.
Minitab 12.1 was used for the experimental design and analysis. Small factorial experiments are very useful as they can reduce the amount of experiments needed by showing which factors have a significant effect in the process and which do not. The effect and the evaluation of the examined factors as well as possible interactions between factors are expressed in graphs based on mathematical formulae (Montgomery, 1997: 228).

ABN 70 592 297 967

Table 2 shows the colour changes of the copper coupons after the treatments.

Treatment	Clean copper	Pre-corroded copper	Comments after 840-hour exposure of pre-corroded copper coupons to 95±5%RH, 25°C
BTA 0.1M/H_2O	No colour changes/Metallic appearance	No colour changes although some transparent spots due to the slow evaporation of water can be seen.	Coupons covered with 'bronze disease' corrosion.
BTA 0.1M/EtOH	Metallic appearance. Some transparent inhibitor sediment at 24 hours of immersion	Coupons turned dark green.	Coupons covered with 'bronze disease' corrosion (but film still adhered on the surface).
BTA 0.25M	Metallic appearance. Some transparent inhibitor sediment at 24 hours of immersion	Coupons turned dark green with a lighter olive green residue.	'Bronze disease' overall, film still adhered on the substrate.
BTA + AMT	Coupons keep metallic appearance.	No colour changes except some few green or yellowish spots.	Surface darkened and there are some areas of 'bronze disease'.
BTA + BZA	Metallic appearance after 1h of immersion, but covered with a semi-transparent green layer after 24 h of immersion.	Coupons became slightly darker.	Only few areas of 'bronze disease' on coupons.
BTA + ET	Coupons immersed for 1h keep metallic appearance. After 24h immersion, they are almost wholly covered with a green layer.	Coupons became darker. At 24 hours of immersion there is a semi-transparent residue.	'Bronze disease' overall, film not adhered on substrate.
BTA + KEX	Coupons lose metallic appearance. Covered with a dark green/black/iridescent layer. After 24 h of immersion the film is flaking.	Coupons did not change colour after 1 h of immersion, but became slightly darker brown and yellowish after 24 hours.	Bronze disease overall, film not adhered on substrate.
BTA + KI	The coupons keep metallic appearance when immersed for 1h in all combinations. After 24h of immersion there is deposition of a light green semi-transparent residue.	The coupons become darker especially the BTA 0.25M and KI 0.1M were brown with some light yellowish brown residue.	The inhibitor film turned green and it is flaking and not well adhered on the substrate.
BTA + PMT	The coupons keep their metallic appearance.	Slight darkening of the surface which is more prominent after 24 h of immersion.	Coupons covered with a flaking layer of the film and there is BD overall the surface.

Table 2. Observations on colour changes induced by the selected treatments.

ABN 70 592 297 967

4: Results of Accelerated Corrosion Testing

4.1: BTA and AMT

AMT was tested as a corrosion inhibitor for archaeological copper and copper alloy artefacts by Ganorkar *et al.* (1988), Faltermeier (1995) and Uminsky and Guidetti (1995).
Ganorkar *et al.* proposed that AMT first reacts with copper chloride found on the metal surface and dissolves all the chlorides from the corrosion products. Following this, a thin polymeric layer is formed where copper ions are bonded to the sulphur (Ganorkar *et al.*, 1988: 97-100).
Uminsky and Guidetti (1995) tested AMT as a reagent to dissolve chloride ions from artificially corroded bronze plates and found that it cannot effectively remove copper chloride. They also stated that treated coupons appeared discoloured; grey-green with brown spots (Uminsky and Guidetti, 1995: 274-278). This is in direct contrast to earlier results (Ganorkar *et al.*, 1988: 97-100).
Faltermeier (1995) also tested AMT on artificially corroded copper coupons as well as on archaeological copper alloy artefacts and found that its inhibitive efficiency varied in different values of relative humidity. AMT was more protective than BTA, when tested for 24 and 48 hours at 95% relative humidity but it was less effective than BTA at long-term tests at similar RH values. He also mentioned colour changes on the copper surface, after the treatment. Copper coupons appeared to be brown-yellow. The discoloration was greater in higher concentrations and for immersion longer than 24 hours.
Ganorkar et al suggested that heavily corroded objects should be treated with both AMT and BTA. Faltermeier (1995) also used both AMT and BTA for the stabilisation of objects but not concurrently with satisfactory results (Ganorkar: 1988, Faltermeier: 1995).
Three factors were initially taken into account: the BTA concentration, the presence of AMT and the solvent. The factors and their levels (values) are shown in table 3. The results indicate that for the first 504 hours of exposure the most important factor is AMT whilst both BTA concentration and solvent are insignificant. After that both the concentration and the solvent become significant. Still the combination of BTA and AMT resulted in higher inhibitive efficiency throughout the exposure.

.

Factors / Level	-1	1
BTA	0.01M	0.1M
AMT	No	0.01M
Solvent	Water	Ethanol

Table 3. Factors and the values of their levels for the BTA-AMT experiment

Another set of experiments examined the combination of the inhibitors in relation to the concentration of BTA (0.25M and 0.1M) and the time of immersion (1 and 24 hours). All combinations of BTA with AMT were found to be highly effective. In all cases the BTA efficiency improves. From those the best was found to be the treatment of 0.25M BTA with 0.01M AMT immersed for one hour.

ABN 70 592 297 967

Graph 1 shows the average inhibitive efficiency of the different BTA-AMT treatments

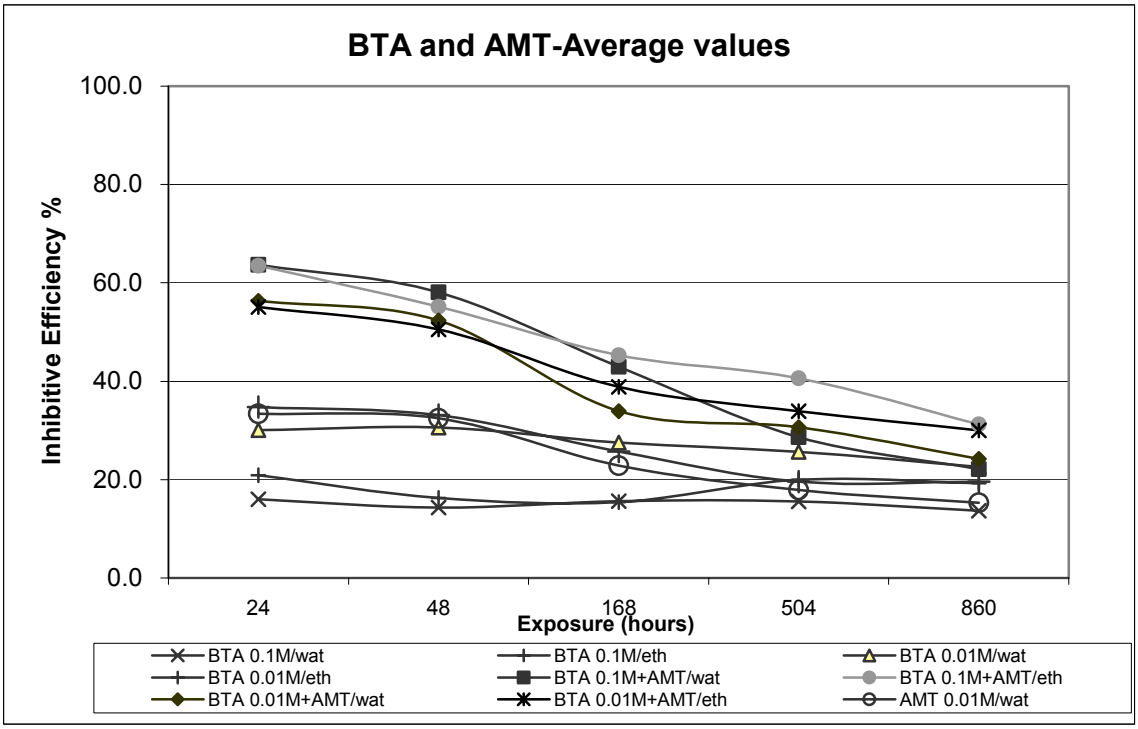

Graph 1. Average values of inhibitive efficiency for the BTA-AMT combinations.

4.2: BTA and BZA

In contrast, from the accelerated corrosion testing one can conclude that the combination of BTA with BZA had a negative effect on the inhibitive process. Instead of slowing down the corrosion of copper, it actually caused acceleration of the corrosion rate. Another disadvantage of this mixture was the colour changes caused on copper, especially in higher concentrations. After 24 hours of immersion, clean copper lost its metallic appearance due to the precipitation of a green residue, whilst the corroded coupons turned darker.

Although the pH of the solution was slightly alkaline after the addition of BZA (pH ≈ 8), the inhibitor film formed was not protective. Fleischmann et al (1985) suggest that BZA added to BTA solutions influences the kinetics of the film formation, one which is formed faster is less porous and highly protective. Since they did not find any adsorption of BZA on copper, it therefore affects the formation of the film itself (Fleischmann et al: 1985).

The analysis of the experimental designs confirms that whilst both BTA and BZA are significant in the inhibition process, BTA increases copper corrosion resistance but the presence of BZA causes an increase in the corrosion rate. The results were similar even when higher concentrations of both BTA (0.25M and 0.1M) and BZA (0.1M) in ethanol were used. The adjustment of pH to near neutral or slightly alkaline values did not result in the formation of a protective inhibitor film in this case.

4.3: BTA and ETH

Similarly to BZA, ethanolamine results in faster film formation when added into BTA solutions. BTA-ETH films were found to be more stable than those of BTA alone retarding both the anodic and cathodic corrosion reaction of copper (Wang and Zhang, 1987).
The presence of ETH in the BTA solutions adjusted the pH to alkaline values (9.5-10) affecting the process by decreasing the weight uptake. Still, the presence of inhibitive efficiency of the BTA-ET mixture was not much different than that of the BTA alone. The analysis of the results showed that there is no significant interaction between the inhibitors. In higher concentrations this mixture was less effective than BTA alone.

4.4: BTA and KEX

The presence of KEX into BTA solutions in a chloride containing environment was found to form a more compact film causing shifting of corrosion potential towards more positive values. Also, the presence of KEX results into a hydrophobic surface impeding the reacting of copper with moisture from the environment. The Cu-KEX film is porous with small holes that can result in local corrosion. The presence of BTA seals these holes creating a more protective layer (Gonzalez et al, 1993).
The experimental results of the 0.01M BTA and 0.01M KEX in deionised water, showed a slight improvement in the BTA effectiveness, however this dropped dramatically after 168 hours of exposure into 95±5 %RH. Similarly, in higher concentrations the overall efficiency was similar or less than that of BTA alone. Graph 2 illustrates the inhibitive efficiency of BTA, KEX and their combination.

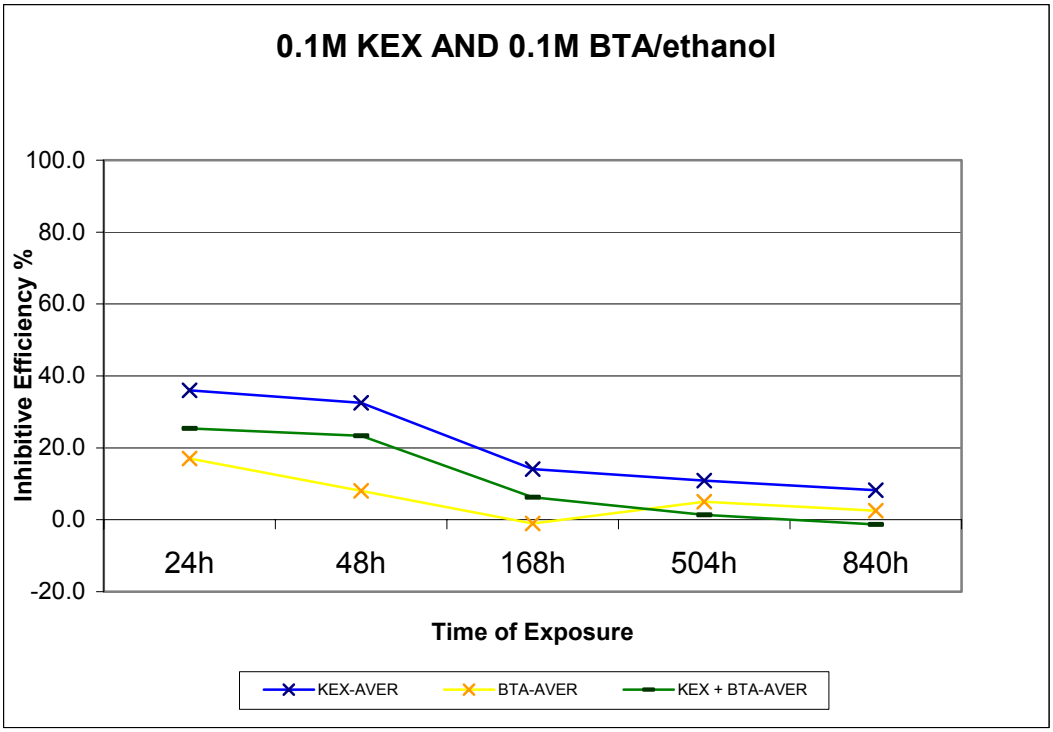

Graph 2. Inhibitive efficiency % for 0.1M BTA and 0.1M KEX and their combination in ethanol.

ABN 70 592 297 967

Moreover, the presence of KEX caused considerable colour alterations of the metal coupons.

4.5: BTA and KI

Wu et al (1993) suggested that the presence of iodide ions in the BTA solution improves the adsorption of the inhibitor on copper. The presence of KI in the BTA solution results in the formation of a thicker polymeric Cu(IBTA) film affecting the anodic reaction (Wu et al, 1997).
The combination of BTA with KI was tested taking three factors into account: BTA concentration, KI concentration and solvent (deionised water and ethanol). The experiments showed that the results and the possible synergistic effect between BTA and KI depend on their concentration and the solvent used. Consequently, the treatment of copper with this combination can lead to improved inhibition or increase of the corrosion rate. The mixture of 0.1M BTA with 0.01M KI in deionised water increased the efficiency of BTA, whilst in other cases the mixture accelerated corrosion. When a higher concentration of BTA was used, the presence of KI did not cause any significant effect in the process.

4.6: BTA and PMT

PMT reacts with cuprous ions to form a complex insoluble and compact film (Ye et al, 1998). PMT is a compound with low solubility in water. It was decided to test PMT alone and within BTA solutions to test possible synergism. PMT alone presented a good inhibitive efficiency, close to that of BTA (although a little bit higher). The combination of the compounds did not result in increased efficiency (0.005M was used for both inhibitors). When higher concentrations of BTA (0.1 and 0.25M) and PMT (0.1M) in ethanol were used, the results indicated that BTA alone is more effective than the mixture. There is no observed synergism between the compounds.

4.7: Colour changes

Table 2 shows the colour changes observed on the coupons after the treatments with the respective solutions. Some of the treatments are not acceptable for conservation purposes as they alter dramatically the colour of the copper/copper oxide. Still it is obvious that factors such as the time of immersion affect both the film formation and the colouration of the surface. In general, it was found the higher the time of immersion, the more the colour alteration. Some treatments caused total loss of the metallic appearance of the clean coupons especially in higher concentrations (e.g. KEX)
All the experiments performed on both clean and pre-corroded copper coupons. No results were obtained from the clean coupons, as the testing time (35 days) and the type of accelerated corrosion test used (humidity test) were not sufficient for this purpose. Still the application was valid for analytical purposes.

ABN 70 592 297 967

4.8: SEM-EDS analysis of copper-inhibitor complexes

The analysis took place on both clean and pre-corroded coupons and examined the same factors examined in the accelerated corrosion tests. The analysis carried out at the Wolfson Scientific laboratories of the Institute of Archaeology, UCL using a JEOL JSM-35CF with Link ISIS microanalysis system. The aim of the analysis was to obtain information regarding the topography and the structure of the copper-inhibitor films. The samples were not carbon-coated as the coupons were treated with organic compounds (inhibitors). Linescans were taken (elemental analysis across a line) which provided information about the distribution of the elements in comparison to copper.
From the images it is evident that some inhibitors follow the crystal formation of the corroded copper surface, forming a thin film (e.g. AMT, BTA, ETH), whilst in others (BZA, KEX, KI, PMT) the copper crystals are not distinctive anymore, as the surface is covered with a thick porous non-uniform layer. Figures 1-3 illustrate SEM images of corroded copper coupons treated with BTA, BTA and AMT and BTA and KEX respectively (Figs. 1-3).

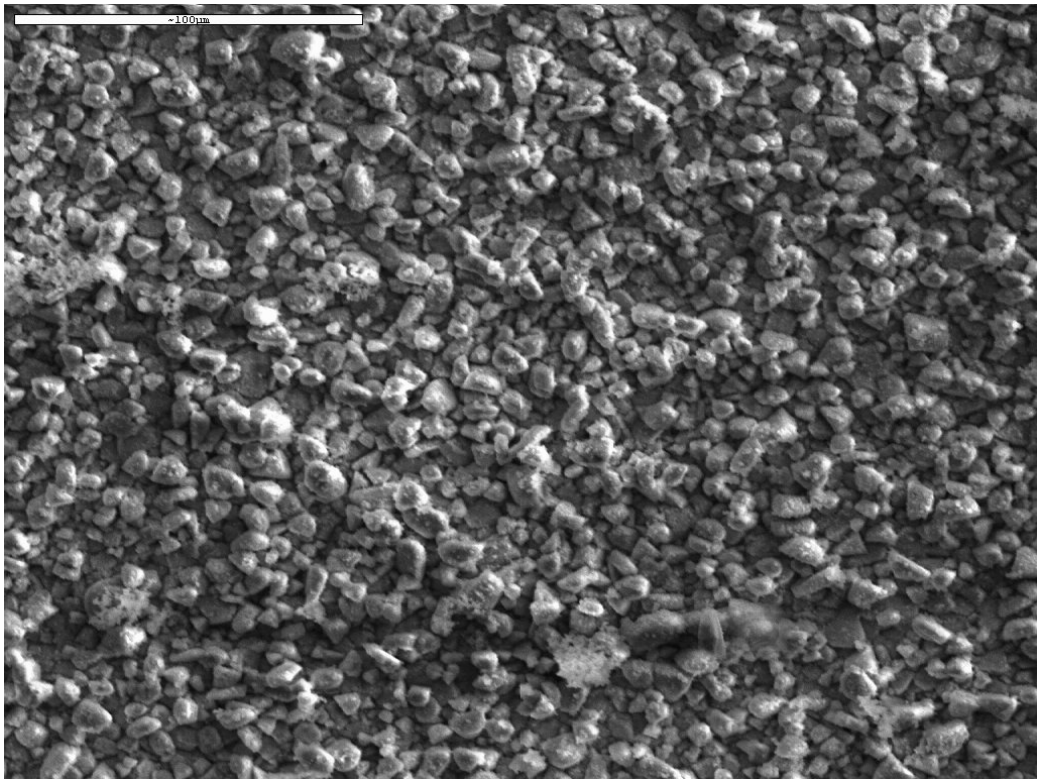

Figure 1: Corroded copper treated with 0.1M BTA in ethanol.

ABN 70 592 297 967

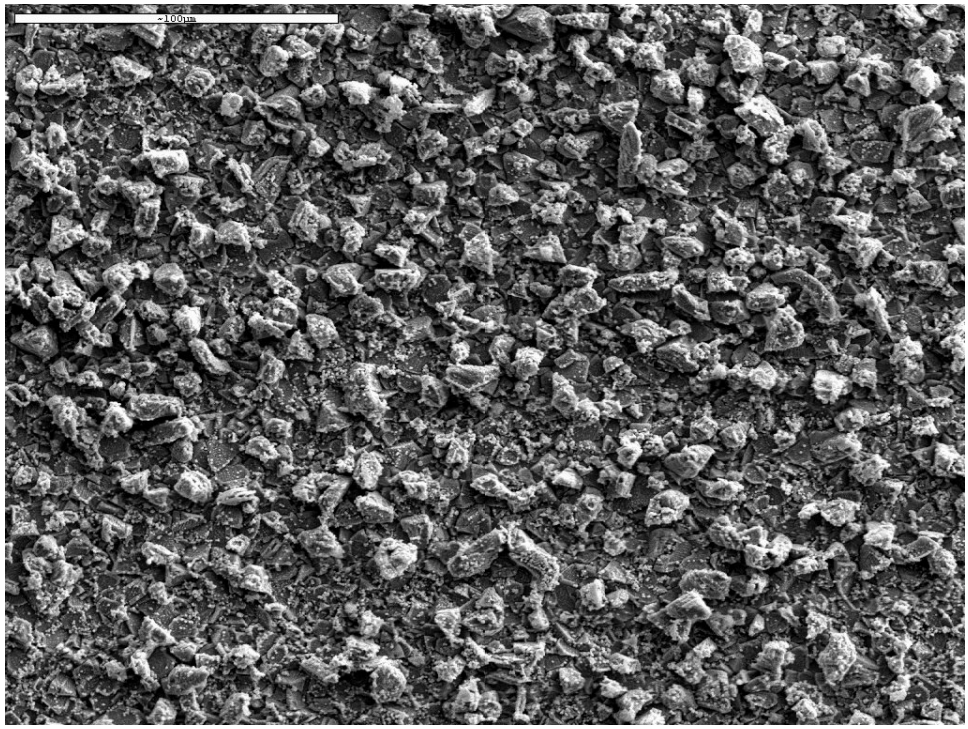

Figure 2: Corroded copper treated with 0. 1M BTA and 0.1M AMT in ethanol

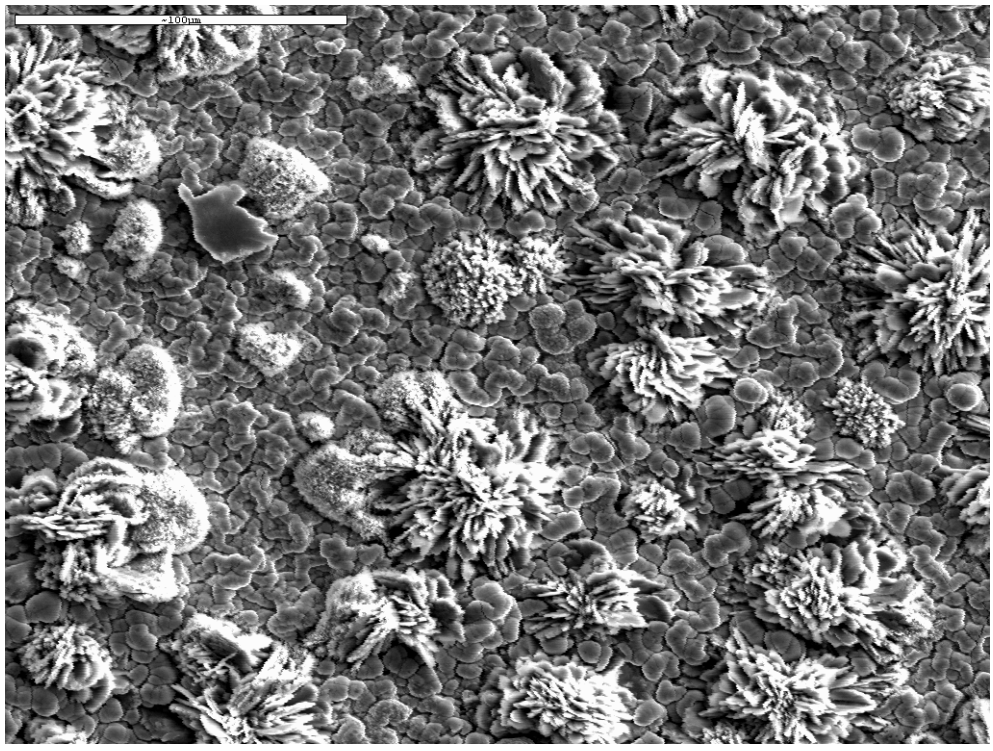

.

Figure 3: Corroded copper treated with 0.1M BTA and 0.1M KEX in ethanol

ABN 70 592 297 967

In the linescans the inhibitor film is represented by the elements it contains (e.g. C, N, S, K, I). Their distribution in comparison to copper shows that in general they follow the topography of the surface. In case of KI applied on copper, the distribution of I follows copper in reverse, when copper is low, I is high. The same was found on the linescans of the combination of BTA and KI. In case of BZA, carbon is distributed in a thicker layer, without following the copper, whilst the its combination of BTA shows both C and N following the copper distribution, which could be an indication about the complex formed. Similar results were found in the ETH and BTA and ETH combination, whilst KEX shows a better distribution of C, N and S in relation to copper both when applied on each own and in combination with BTA (Graph 3).

.

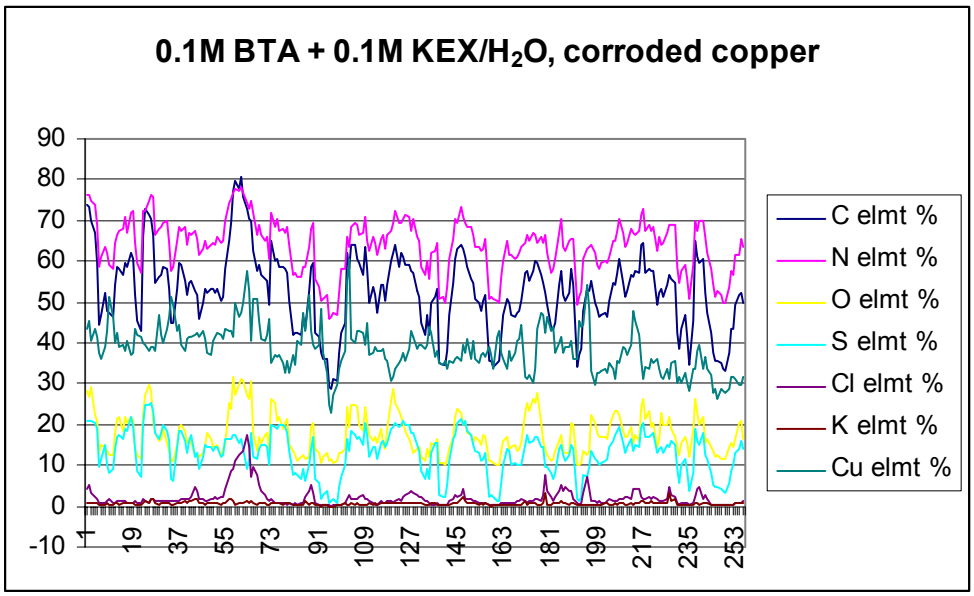

Graph 3. Linescan of 0.1M BTA and 0.1M KEX in deionised water, time of immersion 1h, superimposed elements

AMT linescans show a very low content of sulphur, whilst the BTA and AMT combination presents a better distribution of C, N as well as higher concentration of sulphur.

5: Testing of selected inhibitors on archaeological artefacts

The archaeological sites of Mochlos, Crete in Greece (Minoan period) and Kaman Kalehöyük, Turkey (dating from early Bronze Age to the Ottoman period) were chosen for the testing of inhibitors. Both sites have brought to light a significant number of copper alloy objects most of which are found heavily corroded. The site of Mochlos is located close to the sea and the soil has very high chloride content, whilst Kaman Kalehöyük is inland with alkaline environmental conditions which also result in poor preservation of metal artefacts (Merkel: 2002, Omura, S: 2000, Soles, : 2004).

Following the experimental results from the laboratory experiments, the inhibitors and inhibitor combinations which performed best (BTA and AMT, AMT, BTA and PMT, PMT) were applied on archaeological copper/copper alloy objects. The objects were mechanically cleaned and treated with the solutions then subjected to high relative

ABN 70 592 297 967

humidity (approx. 100%) for 24 hours. All the objects were heavily corroded and suffered from bronze disease.
Because of the complexity of the corrosion forms and diversity of the corrosion products present, weight changes were not valid in this case.
A method that is used is by choosing one form of corrosion in a fail/pass test (e.g. if an object presents bronze disease signs, the treatment fails). The method chosen for the evaluation was based on the visual observation of the objects under stereomicroscope recording bronze disease signs. The simple nominal scale (or fail/pass test) was of little use in this case as it does not give an objective picture about the treatment. The degree of the new corrosion is of greater importance. Consequently, a scale was created taking into account not only the presence of bronze disease but also the extent of bronze disease outbreaks on an object.

Clearly, the scale cannot take into account all the factors affecting the result. However, the number of the objects used (e.g. 10 for each treatment at Kaman Kalehöyük tests) can give a close approximation about the efficiency of the treatments.
The scale has 4 levels depending on the extent of bronze disease outbreaks found on the objects. The evaluation of a treatment takes into account both the number of objects with bronze disease and the severity and extent of the active corrosion (number of pits).
Each level (table 5) has a different number of significance. The evaluation takes place by multiplying the number of objects at each level by the number of significance and finally the numbers from each level are summed. The final number is a subjective way to assess how effective a treatment is and it is valid only when compared to experiments carried out under the same conditions and evaluated using the same scale and method.
The results were analysed using one-way ANOVA (Analysis of Variance).

Level	Degree of corrosion	Degree of significance
I	Minimum BD outbreaks (up to 4 small spots)	1
II	Few BD spots (>4)	2
III	BD in a larger extent	3
IV	BD overall	4

Table 5. Scale used for the evaluation of the testing on archaeological copper and copper alloys from Kaman Kalehöyük.

5.1: Kaman Kalehöyük

The testing took place during two summer field seasons (July-August 2000 and 2001). The objects selected came from different strata and periods. Some of them were freshly excavated and not treated before, whilst others had been excavated in past years and previously treated with BTA (3% in 1:1 ethanol:water) under vacuum. Most of the objects selected were bronzes. XRD analysis on six bronze fibulae performed by Twilley showed tenorite (CuO), cuprite (Cu_2O) and cassiterite (SnO_2) (Twilley, 1996: 239). XRF analysis on some of the objects showed leaded bronzes.

ABN 70 592 297 967

The procedure followed was the same as the treatment protocol of the lab, established by G.Wharton.

The objects, after mechanical cleaning, were classified into three groups, depending on the degree of corrosion. The first class included objects in good condition with metal core present, the second class included more corroded objects that had some metal core left, and the third class included heavily corroded objects most of which were totally mineralised, but still showing active corrosion.

The objects were cleaned mechanically, degreased in acetone for one hour and immersed in the inhibitor solutions. The application methodology followed in the lab is to immerse the objects for 3 hours under 40mmHg vacuum (Wharton, 2000). Some groups were treated using the same procedure, whilst others were only immersed in the solutions for one hour to examine if the application methodology affects the result.

To eliminate experimental errors because of the diversity in factors such as composition, corrosion forms and products, the treatments were applied in batches of 10 objects (3, 3 and 4 from each class). The objects were photographed and all the observations from the treatments were input into a database designed purposely.

After the treatment, the objects were subjected to high RH (approx. 100%) for 24 hours to evaluate the treatment efficiency. After the testing, the objects were allowed to dry, they were then photographed and examined under a stereomicroscope for outbreaks of bronze disease.

The treatments tested, observations after the immersion into the inhibitive solutions (i.e. colour changes), the number of objects in each group with bronze disease and the evaluation of the treatments (ranking) can be seen in table 6.

ABN 70 592 297 967

Group	Treatment	Factors examined	Colour changes after treatment	Number of objects with BD	Ranking
VI	BTA 0.1M + AMT 0.01M/EtOH	Synergism BTA-AMT, BTA concentration, solvent, application	No colour changes	0/10	**0**
VII	BTA 0.1M + AMT 0.01M/H_2O	Synergism BTA-AMT, BTA concentration, solvent	No colour changes	4/10	**6** (2xI and 2xII)
XXI	BTA 0.25M/EtOH	BTA concentration, solvent used, application	Darkening of the surface, few BTA crystals on surface	7/10	**8** (6x1 and 1xII)
VIII	BTA 0.25M + AMT 0.01M/EtOH	Synergism BTA-AMT, BTA concentration, application		7/10	**9** (5xI and 2xII)
XVIII	BTA 0.1M + AMT 0.01M/H_2O	Synergism BTA-AMT, BTA concentration, solvent	No colour changes	6/10	**12** (2xI, 2xII and 2xIII)
XIX	BTA 0.01M + AMT 0.01M/EtOH	Synergism BTA-AMT, BTA concentration, solvent	No colour changes	9/10	**13** (5xI and 4xII)
IX	BTA 0.1M + PMT 0.1M/EtOH	Synergism BTA-PMT, BTA concentration	White inhibitor residues that was easily brushed off	8/10	**14** (3xI, 2xII, 1xIII and 1xIV)
XVII	BTA 0.1M + AMT 0.01M/EtOH	Synergism BTA-AMT, BTA concentration, solvent, application	No colour changes	7/10	**15** (2xI, 3xII, 1xIII and 1xIV)
XIV	BTA 0.1M/ EtOH	BTA concentration, solvent used, application	No colour changes	7/10	**17** (2xI and 5xIII)
III	BTA 0.25M/ EtOH	BTA concentration, solvent used, application	Darkening of the surface, some BTA crystals formed on the surface	9/10	**19** (1xI, 6xII and 2xIII)
II	BTA 0.1M/H_2O	BTA concentration, solvent used, application	No colour changes	9/10	**20** (1xI, 3xII, 3xIII and 2xIV)
XVI	BTA 0.25M + AMT 0.01M/EtOH	Synergism BTA-AMT, BTA concentration, application		10/10	**20** (3x1, 4xII and 3xIII)
I	BTA 0.1M/ EtOH	BTA concentration, solvent used, application	Slight darkening	9/10	**23** (1xI, 3xII, 4xIII and 1xIV)
XX	BTA 0.01M + AMT 0.001M/ H_2O	Synergism BTA-AMT, BTA concentration, solvent	No colour changes	9/10	**23** (2xI, 2xII, 3xIII and 2xIV)
XIII	BTA 0.1M/H_2O	BTA concentration, solvent used, application	No colour changes	9/10	**24** (3xI, 3xIII and 3xIV)
IV	AMT 0.01M/EtOH	AMT, application		9/9	**26** (1xI, 2xII, 3xIII and 3xIV)
V	PMT 0.1M/EtOH	PMT	Surface covered with a thin white layer (which was brushed off)	10/10	**26** (1xI, 4xII, 3xIII, 2xIV)
XII	Controls (XII)	-	-	10/10	**27** (Ix2, 3xII, 1xIII and 4xIV)
XI	Controls (XI)	-	-	8/9	**29** (3xIII and 5xIV)

Table 6. Ranking of the treatments tested at Kaman Kalehöyük using the scale indicated in Table 5. The factors examined, colour changes and the number of objects with bronze disease are also shown.

As aforementioned the number given in the ranking column is not an absolute number. This number represents the extent of corrosion after the exposure and the lower the value, the more effective the treatment. The treatments on table 6 are placed according to their efficiency, starting from the most effective treatment and finishing with the least effective (which in this case are the two control groups).
There was only one group of objects that did not have any signs of active corrosion. This is group VI in which the objects were treated with the combination of BTA 0.1M and AMT 0.01M in ethanol (applied by immersion for 3 hours, under vacuum). Group VII treated with the same combination in the same concentrations but using de-ionised water as a solvent presented very good inhibition with only four out of ten objects having bronze disease. From the results one can see that all the factors tested (time of immersion, the application methodology, concentration of the solution, solvent and combination of inhibitors) affect the process.
These results are in agreement with the results obtained from the laboratory experiments where again the combination of BTA 0.1M with AMT 0.01M in both ethanol and water as solvents performed the best (see graph 1). During summer fieldwork season of 2001,a survey was conducted for the objects treated during summer 2000, this confirmed a continued the level of success regarding these treatments.
For the purposes of this research the objects were not covered with a protective coating. They are currently stored in silica gel containing polyethylene boxes.

5.2: Observations/colour changes

BTA is known to cause darkening of the surface. Because of the time of immersion used (1 and 3 hours) no colour changes were observed, with the exception of 0.25M where the objects darkened slightly. Also some of the objects treated with BTA 0.25M had BTA crystals formed during drying. These were removed by swabbing with ethanol. These crystals were not observed on objects treated with lower BTA concentrations.
The treatments of BTA and AMT did not induce colour changes, except where nantokite was exposed where there was a yellowish precipitant which was brushed off easily.
The objects treated with PMT were covered with a thin whitish precipitant which was swabbed off with ethanol. The objects treated with the combination of BTA and PMT showed the same white precipitant.

5.3: Mochlos

This project took place in two phases, the first of which was completed in 1999 and included the documentation and cleaning of the selected objects and the second was the application of the treatments and was carried out during August 2000. Only the combination of BTA with AMT in two different concentrations was tested on this site. The objects (CA-108 and CA-109) were mechanically cleaned and were stored for one year without any treatment to observe if any signs of new corrosion would appear. Although the objects were stored in a specially designed room for the storage of metals with a controlled environment (dehumidifier set at 35-45 % RH and 18-20°C) they presented extensive bronze disease after one year.

ABN 70 592 297 967

Figure 4: The CA-108 and CA-109 bronze bowls were found one inside the other. The objects were seperated during mechanical cleaning and were treated with the BTA and AMT

The powdery corrosion products were removed mechanically and the objects were immersed for 24 hours in the inhibitive solutions. No great colour changes were noticed except for the yellowish precipitation where nantokite had been exposed. Following this, the objects were exposed to higher RH (approx 100%) for a further 24 hours. None of the objects presented any signs of new corrosion. The objects were not covered with a protective coating and were stored as in the previous year. Unfortunately, during the winter of 2002-2003 the dehumidifier broke down for an unknown period of time causing damage to most of the metal artefacts stored in there. The objects were examined during July 2003 and it was found that CA-109, treated with BTA 0.1M and AMT 0.01M in ethanol, had only a few signs of active corrosion. CA-108 presented extensive active corrosion (figure 5). However, CA-108 had more nantokite and than CA109. Nonetheless, these objects were found in a better state than the untreated objects.
The objects were cleaned and degreased in acetone and were re-treated by a one-hour immersion in a BTA 0.1M and AMT 0.01M solution in ethanol. No signs of active corrosion were observed during the 2004 survey.

Figure 5: CA-108 after the treatment with BTA and AMT.

6: Conclusion

This paper is an assessment of experiments undertaken to investigate the synergism between selected inhibitive compounds. Based upon industrial publications, all the combinations tested had the potential to increase the inhibitive efficiency of BTA. However, the use of some of them was found to be ineffective, and in some extreme cases, the corrosion rate was increased after the treatment. There are various reasons that suggest the use of concentration and combinations are outside the effective range for the particular case. Depending on their mode of action, inhibitors can sometimes cause acceleration of the corrosion process if used in unsuitable concentrations (either higher or lower than required).

However, from the aforementioned results it is apparent that the combination of BTA with AMT increases the inhibitive efficiency of BTA. The concentration required is less than that commonly used in conservation (3% w/v). The use of water as a solvent can also be of great advantage in conservation, as it is less volatile, therefore safer for the user. Another advantage is that the cost is minimised with the use of both smaller concentrations of the inhibitors and the use of de-ionised water as a solvent.

These experiments investigated the use of different characteristics of chemical compounds to improve the BTA efficiency for archaeological copper and copper alloy objects. The results showed that there is a lot of potential when using the synergism between different inhibitors. Even the less effective combinations could be effective when used in different concentrations.

One of the main drawbacks of the use and combination of corrosion inhibitors for archaeological copper alloys is their toxicity. In these experiments, use of BTA and other additives has followed health and safety protocols for toxic substances.

More research is necessary to examine more combinations and to utilise more characteristics that might lead to more successful treatments. The research should focus more on new, less toxic, inhibitors that could retard corrosion. There are compounds that could be tested and could be effective inhibitors either on their own or in combination with other additives.

Scientific analysis carried out using FT-IR, XPS and Cyclic Voltammetry examined further how several factors affect the Cu-BTA complex formation as well as Cu-BTA-additives reactions and film formation. The results of the analysis will be presented in a future publication.

The archaeological objects treated with the BTA and AMT will be monitored in future years at Kaman Kalehoyuk and Mochlos to examine their performance in the long term. Field trials under real conditions and in real time will show if the initial results were accurate, and where research should focus next.

Materials

BTA, copper chloride and PMT were supplied by Sigma-Aldrich, AMT by Fluka, KEX by Lancaster, BZA and ETH by BDH.

Minitab 12.1 was used for the statistical design and analysis of the experiments. Link-ISIS was used for the SEM-EDS analysis.

Acknowledgments

Parts of this project were selected from the PhD research by S.Golfomitsou at the Institute of Archaeology, UCL, London.
We would like to thank Kevin Reeves for the help with the SEM-EDS, FT-IR and SEM-EDS analysis as well as the maintenance of the climatic chamber. Mrs Bernie Keohane for all the assistance with the XPS. Thilo Rehren for his interest and support. Clive Orton for his assistance on the statistical analysis of the results.
Dr.Omura director of the Kaman Kalehoyuk excavation for his support. Glenn Wharton for his trust, support and enthusiasm about this research project and the conservators of the site Noel Siver, Sara Moy, Katie Webbs, Georgina S. Garrett, Martin Ledergerber and Serap Çelik Professor Jeffrey Soles, director of Mochlos excavation for his faith and encouragement. Ms Stephania Clouveraki and all of INSTAP-EC team. Special thanks to George Garrett for the proof reading and the interesting discussions. This research was financed by State Scholarship's Foundation (Greece) and Kress Foundation.

References

Madsen, H B, 1967. A Preliminary Note on the Use of Benzotriazole for Stabilizing Bronze Objects, *Studies in Conservation,* **12**(4), 163-166.

Dugdale, I and Cotton J B, 1963. An Electrochemical Investigation on the Prevention of Staining of Copper by Benzotriazole, *Corrosion Science*, **3**, 69-74.

Fox, P G, Lewis G and Beden P J, 1979. Some Chemical Aspects of the Corrosion Inhibition of Copper by Benzotriazole, *Corrosion Science*, **19**, 457-467.

Fiaud, C, 1995. Inhibition of Copper Corrosion. The Complementary Role of Oxides and Corrosion Inhibitors. *Proceedings of the 8th European Symposium on Corrosion Inhibitors (8SEIC)* , 929-49, Ferrara, Italy.

Poling, G W, 1970. Reflection Infrared Studies of Films Formed by Benzotriazole on Copper (or Cu), *Corrosion Science*, **10**, 359-70.

Mansefeld, F, Smith T, and Parry E P, 1971. Benzotriazole as Corrosion Inhibitor for Copper, *Corrosion*, **27**, 289-294.

Musiani, M M, Mengoli G, Fleischmann M, and Lowry R B, 1987. An Electrochemical and SERS Investigation of the Influence of pH on the Effectiveness of Some Corrosion Inhibitors of Copper, *Journal of Electroanalytical Chemistry,* **217**, 182-202.

Brusic, V, Angelopoulos M, and Graham T, 1997. Use of Polyaniline and Its Derivatives in Corrosion Protection of Copper and Silver, *Journal Of the Electrochemical Society*, **144**, 436-442.

Rozenfeld, I L, 1981. *Corrosion Inhibitors*. USA: McGraw-Hill Inc.

Kuznetsov, Y I, 1996. *Organic Corrosion Inhibitors of Metals*. New York: Plenum Press.

Angelucci, S, Fiorentino P, Kosinkova J, and Marabelli M, 1978. Pitting Corrosion in Copper and Copper Alloys: Comparative Treatment Tests, *Studies in Conservation*, **23**, 147-156.

Faltermeier, R B, 1995. *The Evaluation of Corrosion Inhibitors for Application to Copper and Copper Alloy Archaeological Artefacts*. PhD Thesis, University College London, London.

Brostoff, L.B. 1997. Investigation into the interaction of Benzotriazole with copper corrosion minerals and surfaces. In Metal 1995. MacLeod, I.D., Pennec, S.L., Robbiola, L. (ed). James and James.

Brazil, R. 1999. Corrosion inhibitors of archaeological iron. PhD thesis, Institute of Archaeology, UCL, London.

Carter, V.E. 1982. Corrosion Testing for Metal Finishing. Butterworths (Published in Association with The Institute of Metal Finishing).

Heitz, E. , Henkhaus, R. , and Rahmel, A. 1992. Corrosion Science, an Experimental Approach. (translators: Dr. Waterhouse, R.B, transl.editor Dr. Holnes, D.R.). England: Ellis Horwood Limited.

Skerry, B S, 1985. How Corrosion Inhibitors Work, in S Keene (ed), Corrosion Inhibitors in Conservation, *Occasional Paper*, **4,** 5-12.

Box, G.E.P. Hunter, W.G and Hunter, J.S. 1978. Statistics for experiments: an introductionto design, data analysis, and model building. John Wiley & Sons: New York.

Montgomery, D.C. 1997. Design and analysis of experiments. 4th ed. John Wiley & Sons: New York.

Ganorkar, M C, Panditrao V, Gayathri P and Sceenivasa Rao T A, 1987. A Novel Method for Conservation of Copper-Based Artifacts, *Studies in Conservation* **33**, 97-101.

1988,

Uminski, M, and Guidetti V, 1995. The Removal of Chloride Ions from Artificially Corroded Bronze Plates, *Studies in Conservation*, **40**, 274-278.

Fleishmann, M, Hill I R, Mengoli G and Musiani M M, 1983. The synergistic Effect of Benzylamine on the Corrosion Inhibition of Copper by Benzotriazole, *Electrochimica Acta* **28**, 1325-1333.

Wang, X. and Zhang, Y. 1987. The synergetic effect of Ethanolamine and Benzotriazole on the corrosion inhibition of copper. *In10th International Congress on Metallic Corrosion*, Vol. III, 2799-2806.

Gonzalez, S, Laz, M M, Souto, R M, Salvarezza, R C and Arvia, A J. 1993. Synergistic Effects in the Inhibition of Copper Corrosion. In *Corrosion*, **49**(6), 450-456.

Wu, Y C Zhang P Pickering H W and Allara D L. 1993. Effect of KI on Improving Copper Corrosion Inhibition Efficiency of Benzotriazole in Sulfuric Acid Electrolytes. *Journal of the Electrochemical Society*, **140**(10), 2791-2800.

Ye, X R, Xin, X Q, Zhu, J J and Xue, Z L. 1998. Coordination Compound Films of 1-Phenyl-5-Mercaptotetrazole on Copper Surface. In *Applied Surface Science*, **135,** 307-317

Merkel, J.F. 2002. Soil and corrosion research at Kaman Kalehöyük, progress report. In Kaman Kalehöyük 11. Anatolian Archaeological Studies, Vol. XI, Japan, 167-171.

Omura, S. 2000. A preliminary report on the 14th excavation at Kaman Kalehöyük. In Kaman Kalehöyük 9. Anatolian Archaeological Studies, Vol. IX, Japan, 1-35

Twilley, J. 1996. Scientific analysis of six bronze fibulae from Kaman-Kalehöyük. In Kaman Kalehöyük 5. Anatolian Archaeological Studies, Vol.V, Japan, 237-250.

Wharton, G.E. 2000, Kaman Kalehöyük, conservation lab protocol for the treatment of copper and copper alloys.

Soles, J.S. 2004. Mochlos IC: Period III. Neopalatial Settlement on the Coast: The artisan's quarter and the farmhouse at Chalinomouri. The small finds. The Institute for Aegean Prehistory Press, Prehistory Monographs 9.

ABN 70 592 297 967

Performance of copper corrosion inhibitors in a museum environment - a comparative study using FTIR spectroscopy

W.A. Mohamed [a], N.M. Rateb [b], A.A. Shakour [c]

[a] Conservation Department, Faculty of Archaeology, Cairo University, Giza, Egypt.
[b] Chemistry department, Faculty of Science, Cairo University, Giza, Egypt.
[c] Air Pollution Department, National Research Center, Dokki, Giza, Egypt.

Abstract

The study aims to evaluate the ability of corrosion inhibitors to protect archaeological copper from corrosion in a museum environment. This test required a five years test period. For this test coupons were prepared and treated with the inhibitors and placed in the display cabinet together with the exhibited metal objects in the Old Egyptian Department of the museum of the Faculty of Archaeology in Cairo University.

Indoor air quality was evaluated; the concentrations of pollutants such as sulfur dioxide, nitrogen dioxide, ammonium, hydrogen sulfide, formaldehyde and suspended particulates and their water soluble constituents were measured. During the test period temperature and relative humidity were recorded. Corrosion inhibition of each inhibitor after five years exposure to museum environment was estimated by weight gain measurements. Inhibitors complexes formed on the surfaces of the test coupons were studied with Fourier transform infrared spectroscopy (FTIR). The spectra of such complexes were taken before and after five years exposure to the museum environment and then they were compared.

Keywords: copper, corrosion inhibitors, museum, environment, FTIR.

Corresponding author: TEL:+02 3841297 e-mail: wafaaanw@hotmail.com

1. Introduction:

It is well known that after the treatment of corroded metal objects in the laboratory it is important to apply a protective material on the metal surface. Corrosion can readily start unless the metal surface is properly protected with a suitable material such as a corrosion inhibitor. Some inhibitors, referred to in published literature, were tested in the laboratory by accelerated corrosion tests. Their performance has been evaluated against artificial corrosive conditions of high relative humidity and high temperature (Brusic, et al., 1991, Bastidas and Otero, 1996, Zucchi et al., 1995, Zucchi et al., 1996, Faltermeier, 1999 and Mohamed, 2000), but only a few of them gave satisfactory results (Borea, et al., 1971, Stambolov, 1978, Turgoose, 1985 and Skerry, 1985,). However, the performance of such inhibitors in long term exposure to the museum environment has not been evaluated. The tested inhibitors are 1H-benzotriazole (BTA) ($1,2,3C_6H_5N_3$), 2-amino-5-mercapto-1,3,4-thiadiazole (AMT) ($C_2H_3N_3S_2$) and 2-mercaptobenzothiazole (MBT) ($C_7H_5NS_2$). The concentrations of sulphur dioxide, nitrogen dioxide, ammonia, hydrogen sulphide, formaldehyde and suspended particulates were measured in this research. These air pollutants are expected to affect metal objects in display cases and consequently are supposed to affect the inhibition efficiency of the tested inhibitors.

Sulphur dioxide (SO_2) catalyzes the formation of cuprous oxide in damp atmosphere (Wiederholt, 1964), while hydrogen sulphide (H_2S) is extremely corrosive to copper, and more than one volume of the gas in 600 million volumes of air can tarnish copper. H_2S is able to promote lattice imperfections, High concentrations of the gas produces black copper (I) sulphide on the copper surface (Stambolov, 1985).

Nitrogen dioxide NO_2 produces three reaction processes in an indoor atmosphere; production of nitric acid, rapid equilibration with ozone and nitric oxide (NO), and generation of nitrous acid (HONO) (Brimblecombe, et al., 2001). Nitric acid is known to be a strong oxidizing agent, but, it is volatile, so the free acid formed from NO_2 polluted air cannot be entrained on dry surfaces. This makes it of lesser harm if compared with SO_2.

Chlorides are the most dangerous contaminants for metals; (Thomson, 1986). High concentrations of HCl gas in any kind of environment catalyzes the formation of copper (I) oxide (Feitknecht, 1952) In the presence of even a small amount of chloride cuprous oxide film is broken up causing further anodic dissolution of the metal (Stambolov, 1985). Formic acid vapor is usually released in display cabinets made of wood hence; it surrounds the museum objects in the case's atmosphere. High emission of the vapor while the case is airtight makes the carboxylic acid concentration extremely high (Ryhl-Svendsen, 2001). Wood-related materials, adhesives, varnishes and paints, all off-gas carbonyl pollutants (primarily aldehydes and organic acid vapors) (Gibson, 1998). Formaldehyde converts to formic acid in the presence of water. Formic acid formed from formaldehyde is much more dangerous than formaldehyde itself (Moller, 1984). Copper, bronze and brass can be attacked after 100 days in the presence of only 1,200 ppb of formaldehyde at (50% RH and 20°C ± 3°C) (Stulik and Grzywacz, 1992).

2. Experimental Procedure

2.1 Weight gain measurements

Copper coupons 50 x 25 x 1mm were cut from 99.997% copper sheets. Five coupons were used for each treatment. The coupons were polished by 600-800 grit SC papers, washed with running tap water, distilled water then degreased. The coupons were weighed then immersed in inhibitor solutions. The inhibitors were dissolved in 96% pure methanol. The inhibitors concentrations were 25 x 10^{-2} mol, 1 x 10^{-2} mol and 1 x 10^{-2} mol for BTA, AMT and MBT respectively. The immersion durations in the inhibitor solutions were six hours, six hours and 24 hours respectively. After the coupons were removed from the inhibitor solutions they were dried and weighed. The coupons were placed in the museum inside a display cabinet together with a collection of metal objects in the exhibition hall. The percentage of inhibition (P.I.) was calculated according to the formula: $$P.\,I. = \frac{UCR - ICR}{UCR} X\ 100.$$

(Trabanelli and Carassiti, 1970). Where UCR (unhibited corrosion rate) is the mean weight of the corrosion products after exposure to test conditions; and ICR (inhibited corrosion rate) is the corresponding mean value of the inhibited coupons.

2.2 Air Quality Measurements

Atmospheric contaminants in both forms (particulates and gases) were measured inside the main show hall of the Old Egyptian Department of the museum. The museum is a concrete construction, located in the fourth floor of the main building of the faculty of archaeology. It is naturally ventilated and illuminated. Artificial light is rarely used. Windows are the sources of light during museum open hours and ventilation is supplied by the door and some side windows. Curtains are used to prevent direct sunlight from falling on the museum objects and they are always closed when the museum is closed. A (HVAC) facility is added but it usually works from 9am. to 2 pm. on very hot days in summer. It rarely works in winter for reasons of economy.

The measuring apparatus was placed in the exhibition hall as close as possible to the display case which contains the test coupons. It was not permitted to put the measurement apparatus which contains a vibrating vacuum pump inside the display cases. Sulphur dioxide (SO_2), nitrogen dioxide (NO_2), ammonium (NH_3), hydrogen sulphide (H_2S), formaldahyde (HCHO) and suspended particulates were measured through four consecutive months (from September 2002 to January 2003).

SO_2 was determined colorimetrically by the West and Geak method. Nessler's reagent was used for ammonia determination. NO_2 was determined by a modified Harrison and Jacobs method (Stern, 1976). The filtration technique was used in order to collect the total suspended particulate. The apparatus consisted of a vacuum pump, a calibrated dry gas meter to determine the sample volume and a filter holder. The used membrane filter was weighed before and after measurements. The weight gain is attributed to the weight of the particulate matter. Sulphate, chlorine and ammonium ions were determined in the water-soluble portion of suspended particulate matter.

2.3 FTIR spectroscopy:

Reference spectra of solid powders of the inhibitors were produced with FTIR spectroscopy .FTIR spectra of copper /inhibitors complexes formed on the surface of pure copper coupons treated with the tested inhibitors were also produced. The resulting spectra were compared with the spectra of the same copper /inhibitors complexes after exposure to the museum environment for five years. Samples were scratched off the surfaces of the coupons using a sharp hand engraver and they were compressed as pellets with KBr,

3. Results

3.1 Results of air quality measurements

It was found that the concentration of gaseous pollutants changed significantly during the test period. The results of air pollution measurements are given in Figures 1 & 2.

In Figure 1 the measured concentrations of gaseous pollutants are shown. The value of the mean concentration of SO_2 measured in the museum atmosphere (19.25 $\mu g/m^3$) greatly exceeded the limit given by the National Bureau of Standards (NBS) which is 1 $\mu g/m^3$ (Stern, 1986). The concentrations of (NO_2) ranged from 6 to 36 $\mu g/m^3$, the mean of which was 18.75. This value exceeded the acceptable concentration for archaeological objects (10 $\mu g/m^3$) given by Thomson, 1986.

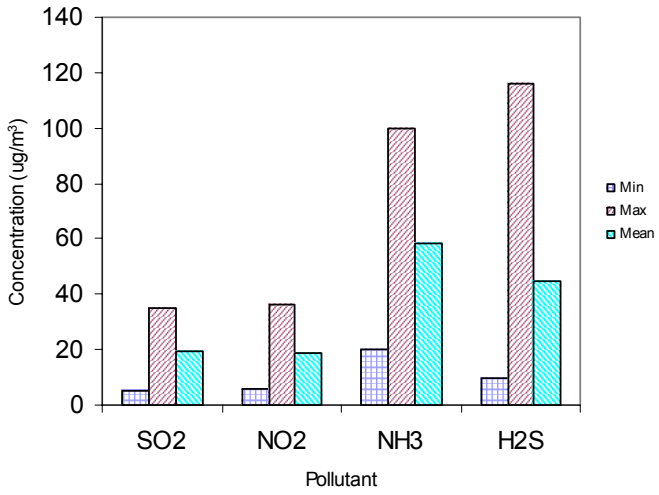

Figure 1. Concentrations of measured pollutants ($\mu g/m^3$) in the museum environment.

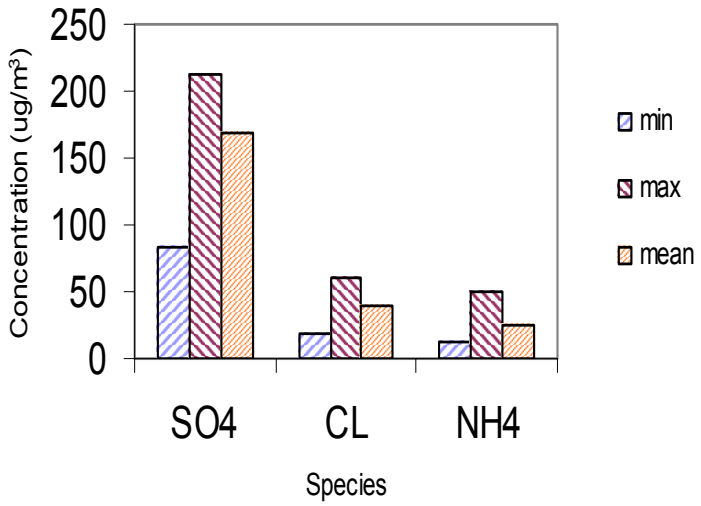

Figure 2. Concentrations of water-soluble constituents (μg/m^3) of suspended particulates.

The mean concentration of ammonium was 58.25μg/m^3 while the mean concentration of hydrogen sulphide was 45 μg/m^3. The concentration of formaldehyde was 32 μg/m^3. The mean concentration of suspended particulates was 123.50 mg/m^3, while the maximum and minimum values were 201.70 and 90.0 mg/m^3 respectively .The size of particulate was found to be less than 10 μm. The concentration of suspended particulates ranged from 90 to 201.7 mg/m^3, the mean concentration of which is 123.5 mg/m^3.

Water-soluble constituents of the suspended particulates NH_4, Cl and SO_4 were measured, results are given in Figure 2. The mean concentration of chlorine was as high as 39.54 μg/m^3, the mean concentration of ammonia was 24.71 μg/m^3, the mean concentration of sulphate was 167.85 μg/m^3. It was found that temperature values fluctuated inside the show-case from 16^{0}C to 35 ^{0}C and humidity fluctuated from 60% to 75%. These are very high values if compared with the acceptable temperature values for museum display. The acceptable value is 19 ±1 ^{0}C in winter and 24 ± 1 ^{0}C in summer; however it should be reasonably constant to stabilize RH value, which must be limited to 50 or 55 ± 5% (Thomson, 1986).

3.2 Results of weight gain measurements

The assessment of inhibition efficiency is based on weight gain measurements; results are represented in Figure 3. It has been found that after six months of exposing the inhibitor treated copper coupons to the museum environment the weight of the coupons treated with AMT and MBT increased, while the copper coupons treated with BTA showed no increase in weight after six months. The inhibition efficiency of BTA treatment was 100%, while for AMT treatment it was 28%. MBT treatment gave 5% inhibition efficiency.

After five years an increase in weight was measured in BTA, AMT and MBT treated coupons, but generally all the inhibited coupons gained less weight than the untreated coupons. The value of the inhibition efficiency of MBT treatment did not change after five years while the inhibition efficiency of BTA treatment decreased to 83%, but AMT inhibition efficiency increased to 30%. It can be concluded that after five years all the values of inhibition efficiency changed except the value of MBT inhibition efficiency.

Table (1): Gravimetric data of weight gain measurements.

Inhibitor	Wt. before Exp. (mean)	Wt. after 6 M. (mean)	Average change of Wt.	Wt. after 5 Y. (mean)	Average change of Wt.
Non	11.46800	11.46956	0.001560	11.47160	0.00360
BTA	11.29684	11.29684	0.000000	11.29744	0.00060
AMT	11.41464	11.41576	0.001122	11.41716	0.00252
MBT	11.12720	11.12868	0.001480	11.13062	0.00342

Wt. = weight in grams.
Exp. = exposure to museum environment.
M. = months.
Y. = years.

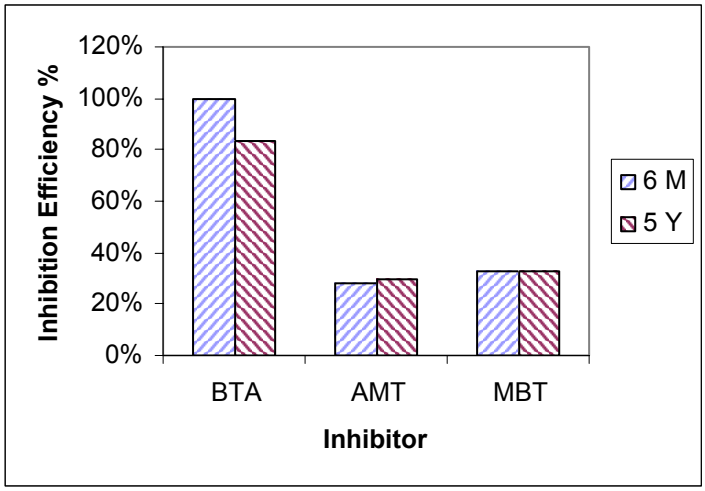

Figure 3. the inhibition efficiency of tested inhibitors after six months (6M) and five years (5Y).

3.3 Results of FTIR Spectroscopy

Figure 4a shows a reference transmission spectrum of solid BTA on KBr pellet. The spectrum shows a multi peak band at 2516-3247 cm^{-1} which indicates the presence of the NH group, also it shows a peak at 1209cm^{-1} due to the presence of the N=N group.
Figure 4b represents the transmission spectrum of Cu (I)BTA complex in which the band characteristic to the N-H group has disappeared. This indicates that Cu treated with BTA was bonded to the amino nitrogen in the BTA structure.

The noticeable shift in the intensity of the band N=N at 1209 cm^{-1} in Figure 4b illustrates that Cu was also coordinated to the unsaturated ring nitrogen. This coordination was first suggested by Poling 1970. Figure 4c represents the transmission spectrum of Cu (1) BTA complex after the exposure of the sample to the museum environment for five years. In this spectrum a band appeared at 3267 cm -1 indicating the presence of the N-H group and a band at 1210 cm^{-1} with higher intensity, the latter indicating the presence of the N=N group.
It can be concluded that after five years exposure to the museum environment the inhibitor complex lost the bonding with the copper surface. The band which appeared at 1622 cm^{-1} representing the C=N group was shifted to 1644 cm^{-1} as shown in Figure 4c.

Figure 5a represents the transmission spectrum of AMT on KBr pellet. In this spectrum there are bands at 3340 cm^{-1}, 3251 cm^{-1} and 3127 cm^{-1} indicating the presence of NH_2 and S-H groups. Figure 5b shows the spectrum of Cu (I) AMT complex .The sharp band in Figure 5a at 3127 cm^{-1} is assigned to the S-H group. This band disappeared in the spectrum in Figure 5b as the complex was formed through S-H and NH_2 groups. The disappearance of the band indicated the bonding of sulphur to the metal ions. This is in agreement with the IR results of studies undertaken by Gajendragad and Agrawala 1975 and Ganorkar et al., 1988. The

multiple band at 2925-3400 cm^{-1} of the AMT spectrum in Figure 5a is due to stretching of the NH bond. This was shifted to 2923-3434 cm^{-1} in the spectrum of the AMT complex Figure 5b. There is a significant band appearing at 443 cm^{-1} which is attributed to the M-N bond. This indicates the participation of the nitrogen of the NH_2 group in active coordination. The spectrum of the complex after five years exposure to a museum environment shown in Figure 5c shows a shift in the band representing the M-N bond from 443cm^{-1} (as shown in Figure 5b) to 449 $cm^{-1.}$ This shift was accompanied by an increase in the intensity, this indicated that the M-N bond became a little stronger with time.

Figure 6a shows the transmission spectrum of solid MBT on KBr pellet. In Figure 6a the spectrum shows a band at 3111 cm^{-1} which indicates the presence of the N-H group and the presence of a band at 1153 Cm^{-1} which indicates the presence of the C=S group. Figure 6b shows the spectrum of the Cu(I)MBT complex, in which the N-H group disappeared. Hence it is suggested that the complex was formed via a bonding between Cu(I) and nitrogen atom as explained by Chadwick and Hashmi, 1979 - as elimination of H(-N) atoms. The complex was reanalyzed with FTIR spectroscopy after five years in the environment specified above. If the spectra of the MBT complex before and after five years (Figures 6a and b) are compared , it will be found that there is no evidence of the presence of the N-H group but there is a new band that appeared in Figure 6c at 1115 cm^{-1} indicating the presence of the C=S group. Another band appeared at 443 cm^{-1} and it is attributed to the M-N group which indicates the participation of the nitrogen in the coordination. This band shifted to 440 cm^{-1} , as shown in Figure 6b, with a sharp decrease in the intensity. It can be concluded that in time the MBT complex lost bonding with the copper, although this loss of bonding is not as sharp as it is in case of the BTA complex.

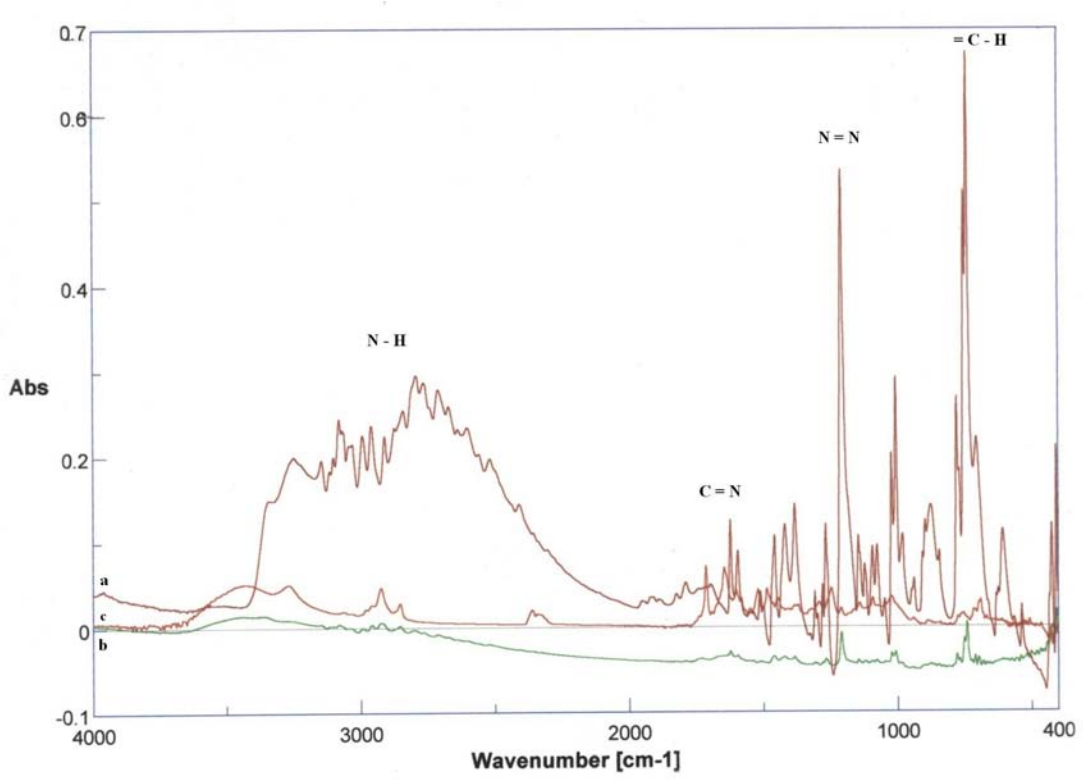

Figure4. FTIR spectra of BTA (a) BTA on KBr pellet, (b) BTA complex and (c) BTA complex after 5 years.

ABN 70 592 297 967

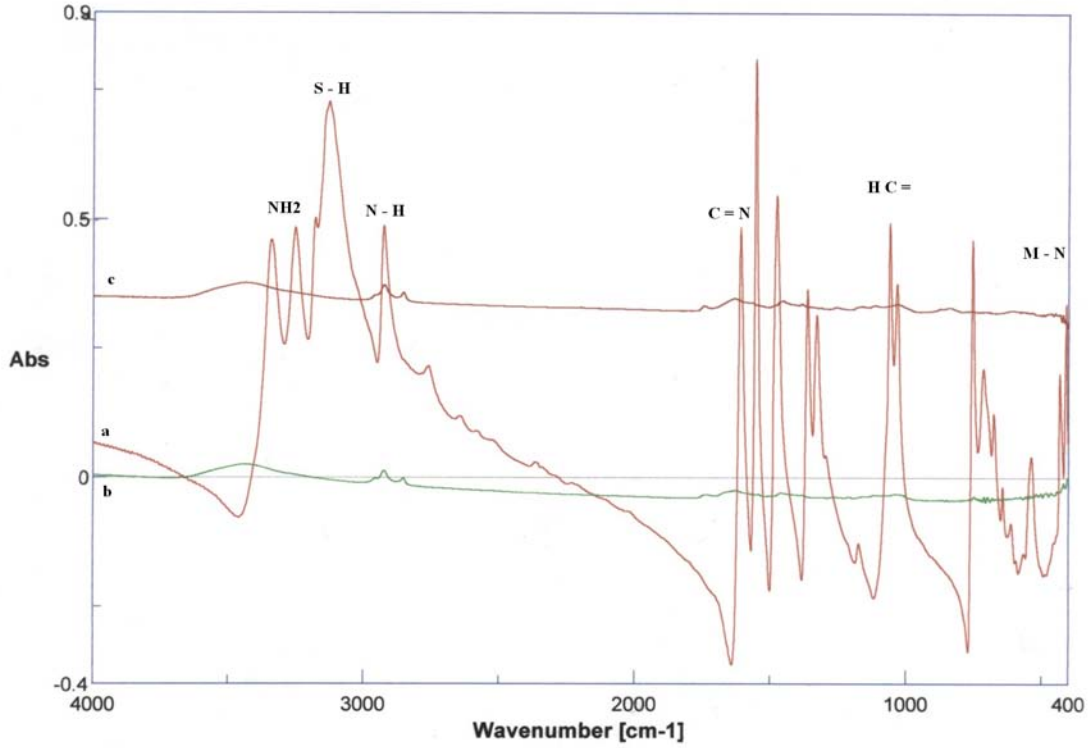

Figure 5. FTIR spectra of AMT (a) AMT on KBr pellet, (b) AMT complex and (c) AMT complex after five years.

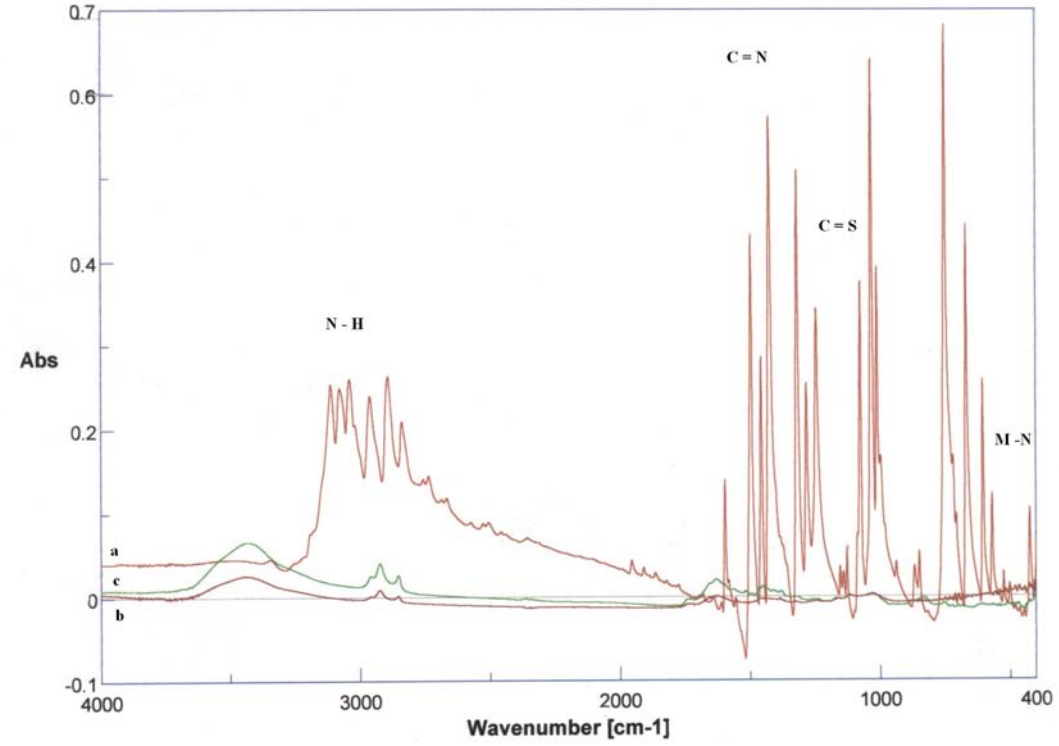

Figure 6. FTIR spectra of MBT (a) MBT on KBr pellet, (b) MBT complex and (c) MBT complex after five years.

4. Discussion

The evaluation of the durability of corrosion inhibitors in an actual museum environment is of great importance, as it gives a more realistic picture of the performance of the inhibitor after treatment of the metal object is completed and the object is returned to the display-case. The experiments proved that BTA was the best of the tested inhibitors to protect copper from corrosion in an uncontrolled museum environment. However its inhibition efficiency decreased to 83% after five years.

The results indicated that polluted atmosphere, high and uncontrolled RH and temperature negatively affected the inhibition efficiency of the tested inhibitors. Although it was found in the literature that these inhibitors gave good inhibition efficiencies when tested in the laboratory against accelerated corrosion tests, the current research proved that the long term service test undertaken in the actual environment (uncontrolled museum environment) gave comparatively low inhibition efficiencies.

The concentrations of the measured pollutants in the museum of Cairo University were very high compared with the acceptable limits given by Thomson and the National Bureau of standards (NBS). The natural ventilation through windows made the situation even worse.
Standards for the acceptable concentrations of NH_3 and H_2S in a museum environment have not been found in the literature. This may suggest further areas of study to establish the ideal limits for metals display and the effects of the combination of the different pollutants on the metal surfaces

Although the weight gain and weight loss measurements are of the most commonly used procedures in corrosion studies, they must be accompanied by another procedure to explain the results. FTIR spectroscopy was very helpful in giving an explanation about the alterations that have taken place in the complex film. The decrease in inhibition efficiency was due to dislocation of bonding with the metal surface.

5. Conclusion

From the study it can be concluded that after six months exposure to a museum environment BTA gave 100% inhibition. AMT and MBT after six months gave low inhibition efficiencies 28% and 5% respectively. The value of BTA inhibition decreased to 83% after five years because of the partially breaking up of bonding with the metal surface. MBT lost bonding with copper to a lesser extent, although this loss of bonding is not as sharp as it was in case of BTA inhibition and did not affect inhibition efficiency after long term exposure. Surprisingly AMT inhibition efficiency increased to 30% after five years as the M-N bond became stronger. This may suggest a further area for study.

Acknowledgements

Thanks are due to Prof. Dr. Abdou Othman, Cairo University, Faculty of Science; and to Mr. Mohamed Darwish the Director of the Egyptian Department of the Museum of the Faculty of Archaeology for sincere help when it was needed.

References

Bastidas, J. M. and Otero, E., (1996) *A Comparative Study of Benzotriazole and 2-amino-5-mercapto-1,3,4- thiadiazole as Copper Corrosion Inhibitors in Acid Media,* Materials and Corrosion 47, 333-337.

Borea, P.A., Gilli, G., Trabanelli, G. and Zucchi, F. (1971) *Characterization, Corrosion and Inhibition of Ancient Etruscan Bronzes*, Annali dell' Universita Di Ferrara, Italy, V, 893-917.

Brimblecombe, P., Raychaudhuri, M., and Bowden, D. (2001) *Surface reactions of Deposited NO2 in The Museum Environment* ,4th Meeting of The indoor Air pollution working group, IAP Copenhagen 4-6.

Brusic, V., Frisch M.A., Eldridge B.N., Novak F.P., Kaufman F.B., Rush B.M., and Frankel G.S. (1991) *Copper Corrosion with and without Inhibitors*, Journal of the Electrochemical society 138, 8, 2253-2259.

Chadwick, D. and Hashmi, T. (1979) *Electron Spectroscopy of Corrosion Inhibition: Surface Film Formed by 2-mercaptobenzothiazole and 2-mercaptobenzimidazole on Copper ,* Surface Science 89,1-3, 649-659.

Faltermeier, R.B. (1999) *A Corrosion Inhibitor for Copper-Based Artifacts*, Studies in conservation 44, 121-128.

Feitknecht, W. (1952) Chimia, (Zurich), 6, 1, 3-13.

Gajendragad, M.R. and Agrawala, U. (1975) *Complexing behavior of 5-amino-2-thiol-1,3,4-thiadiazole*; Part III. Indian Journal of Chemistry 13,12. New Delhi, The Council of the Scientific and Industrial Research, 1331-4.

Ganorkar, M. C., Pandit Rao, V., Gayathri P. and Sreenivasa Rao T.A. (1988) *A Novel method for Conservation of Copper and Copper-based Artifacts*, Studies in Conservation 33, 97-101.

Gibson, L. (1998) *Standardization: Is It Essential?* , 4th Meeting of The indoor Air pollution working group, IAP Copenhagen 1-3.

Mohamed, W.A., (2000) *The electrochemical evaluation of copper corrosion inhibitors*, synopsis of Ch.4, PhD research, Cairo University, Faculty of Archaeology, Conservation Department, unpublished.

Moller, D. (1984) *On the Global Natural Sulphur Emission*, Atm. Env. 18, 36.

Poling, G. W. (1970) *Reflection Infra-Red Studies of Films Formed by Benzotriazole on Cu*, Corrosion Science 10, 359-370.

Stern, A. C. (1986) *Air Pollution*, VI, 3rd ed, Academic Press, New York, 168,179.

Ryhl-Svendsen, M. (2001) *Luftschadestoffe in Museen. Eine Wirkungsweise, Monitoring und Kontrolle*, Restauro 8, 614.

Skerry, B. S. (1985) *How Corrosion Inhibitors Work,* Corrosion inhibitors in conservation, London: The United Kingdom institute for conservation, Occasional papers 4, 5-12.

Stambolov, T. (1978) *Corrosion Inhibitors*, Icom committee for conservation, 5th triennial meeting, Zagreb, 1-8 Oct., 782391-6.

Stambolov, T. (1985) *The Corrosion and Conservation of Metallic Antiquities and works of Arts*, CL Publication, Amsterdam 74-75.

Stern, A.C., (1976) *Air pollution, III*, 3rd Ed, Academic Press, New York, 14,15,54.

Stern, A.C., (1986) *Air pollution, VI*, 3rd Ed, Academic Press, New York, 168,179.

Stulik, C. and Grzywacz, C. (1992) *Carbonyl Pollutants in the Museum Environment: An integrated Approach to the Problem,* dans: La conservation préventive, Actes du 3e Colloque international, éd. par D. Guillemard, (Paris : Association des restaurateurs d'art et d'archéologie de formation universitaire, ARAAFU, 199-205.

Thomson, G. (1986) *The Museum Environment*, 2nd ed., Butterworths , London, 152,153, 158.

Trabanelli, G., Carassiti, V., (1970) *Mechanism and phenomenology of organic inhibitors*, In: Advances in corrosion science and technology, Fontana and Staehle Eds, 1, 149-190

Turgoose, S. (1985) *Corrosion Inhibitors in Conservation*, The United Kingdom Institute for Conservation, Occasional papers 4, 13-18.

Vernon, W.H.J. (1934) Journal of Chemical Society, Part 2, 1853-59.

Wiederholt,W. (1964) *Werkstoffe und Korrosion*, 15, 8 633-644.

Zucchi, F., Trabanelli, G. and Gonzales, N. A. (1995) *Pyrimidine and Thiadiazole derivatives as Inhibitors of Copper Corrosion in Sodium Chloride Solution*, Journal of ACH Modles in Chemistry 132, 4, 579-588.

Zucchi, F., Trabanelli, G. and Fonsati, M. (1996) *Tetrazole Derivatives as Corrosion Inhibitors for Copper in Chloride Solutions*, Corrosion Science 38, 11, 2019-2029.

Bibliography

Drakou, G., Zerefos, Ch., Ziomas, I. and Ganitis, V., (2000) *Numerical simulation of Indoor Air Pollution Levels in A Church and in A Museum*, Studies in Conservation 45, 85-94.

Hatchfield, P. and Carpenter, J. (1987) *Formaldehyde: How great is the danger to museum collections?* , Center for Conservation and Technical Studies, Harvard University Arts Museums, Cambridge Mass., 44.

Ling, Y., Guan, Y. and Han, K. N. (1995) *Corrosion Inhibition of Copper with Benzotriazole and Other Organic Surfactants*, Corrosion Science 51, 5, 367-375.
Mohamed, W.A. (2000) *The Electrochemical Evaluation of Copper Corrosion Inhibitors,* A synopsis of chapter 4 of the Ph.D. research undertaken at Cairo University, Faculty of Archaeology, Conservation Department, unpublished.

Miles, C.E., (1986) *Wood Coating for Display and Storage Cases*, Studies in conservation 31, 114-124.

ABN 70 592 297 967

Laboratory and field tests on patinas and protective coating systems for outdoor bronze monuments

P. Letardi

CNR – Istituto di Scienze Marine, I-16149 Genova, Italy

Abstract (English)

Six protective coating systems, commonly used in conservation practice, have been tested both on polished bronze coupons and on selected areas of a bronze statue in similar exposure conditions. Patinas have been characterised both on outdoor exposure on the monument and as developed on the polished bronze coupons. Electrochemical Impedance Spectroscopy measurements, using a specially designed contact probe, have been conducted on coupons and in situ on the bronze statue. Data for the first two years of weathering in a marine environment are reported. The coating performance on the polished coupons and on the corroded bronze monument is discussed.

Keywords: EIS, bronze, in situ characterisation, coatings, patinas, Atmospheric Corrosion

1. Introduction

The conservation of outdoor bronze monuments is widely studied. Several publications have examined the complex interplay between the properties of sculptures and environmental parameters (Drayman-Weisser 1992, Graedel 1987, Strandberg 1998). The number and the range of all the parameters involved produces a very wide range of possible situations, and holistic understanding therefore remains elusive. Several studies for new protective coatings have been undertaken (Brostoff and de la Rie 1997, Pilz and Römich 1997), but typical requirements for cultural heritage objects (aesthetic appearance, reversibility, etc.) seems not to be easily satisfied, and no common accepted solutions have been established for the protection and maintenance treatment

Table 1. Coating systems and application methods, from Letardi and Cozzolino 2002.

	Commercial name	Description	Application method
[A]	Soter 201 LC	commercial product consisting of 20-24 wt% crystalline wax, BTA and synthetic organic polymer, dispersed in turpentine and ether	Three layers were applied cold with a paint-brush by 24/48 hours intervals. After each application was dried the surface was polished with a soft brush.
[B]	R21	22 w% microcrystalline wax dispersed in white spirit	Three layers applied as above but on the surface warmed with a hairdryer
[C]	Tromm TeCe 3534F	33 wt% microcrystalline wax dispersed in white spirit	One layer was applied as above on a heated surface (100 C on the bronze plates, 50 C on the monument). This wax was used in a higher concentration to obtain a thicker layer since only one layer could be applied hot
[D]	Incralac	commercial product consisting of acrylic lacquer with BTA	Four layers were applied by brush in 24 hours intervals
[E]	Incralac + Soter LC	double-layer system	2 lacquer + 3 wax layers were applied as above
[F]	Incralac + R21	double-layer system	2 lacquer + 3 wax layers were applied as above

strategies have been adopted. Electrochemical methods have received growing interest as tools for metal conservation (Otieno-Alego et al 1998a, D'Ercoli et al. 1999, Letardi 2000, Cicileo et al. 2004).

A project has commenced in 2001 as a cooperation between a research laboratory (CNR), a conservation institution (ICR) and local authorities, (Soprintendenza PSAD Liguria, Museum branch of the local Municipality) (Letardi et al. 2003). The project was planned to compare the behavior of selected coating systems upon natural weathering, both on polished bronze samples and on selected areas of a bronze monument. Six protective coating systems, widely used in conservation practice, were chosen, as summarised in Table 1. Waxes [A] and [B] are widely applied by Italian restorers; wax [C] is largely adopted in Germany. The acrylic-based Incralac [D] has been used worldwide; also the use of coating [D] with a wax topcoat has been widely reported. In this project it was decided to test coating [D] with both [A] and [B] wax topcoat; the coating system [D]+[B] (labelled [F]) has been widely used by Italian restorers.

The bronze statue *Monumento ai Mille* (E. Baroni, 1910) chosen for this study is located in Genoa, right next to the sea. Patina samples from the statue were characterised by XRD (Letardi et al. 2002). The more abundant corrosion products identified are Cuprite, Atacamite, Paratacamite and Mushistonite, with Nantokite, Gypsum and Quartz in some places. Six areas with various patinas were selected on the monument for monitoring and comparison of the coating system behaviour. The patina was evaluated as relatively homogeneous in each area. Four areas (labelled I, II, III, IV) were on the front side facing towards the sea and two (labelled V, VI) were on the rear facing towards the street. On each area, a number of 6 x 4.5 cm zones were cleaned by a restorer and then coated with the above described systems [A] to [F]. One or two zones for each area were left without coating.

Samples both of un-coated bronze and coated with the coating systems [A] to [F], were placed on an exposure rack in the urban marine environment at a site inside the Genoa Harbour, not far from the *Monumento ai Mille*. Exposure commenced in late June 2001, as soon as the treatment on the areas on the monument was completed. Orientation and position according to ISO 9223 standard were selected: the samples were facing south exposed skyward in the position of 45 degrees from horizontal level.

The application of several laboratory and field measurement techniques is in progress, in order to provide a wide characterisation of alloys, patinas, and coatings both on the coupons and on the monument. This paper will report the characterisation on coating thickness and coupons patina composition, and will mainly focus on the Electrochemical Impedance Spectroscopy measurements both on the samples and on Area III on the monument (Figure 1).

2. Experimental Procedure

The bronze samples for the natural weathering program were obtained from cast ingots with the composition Cu 90%, Sn 8%, Pb 2%. Coupons (size 3x3 or 6x6 cm, 3 mm thickness) were polished using SiC metallographic grinding paper 1200 grit in water, washed in ethanol and dried in air.

The conservator-restorer (I.Reindell) treated test areas on the *Monumento ai Mille*. Each selected zone was outlined with scotch tape and was cleaned by rotating brush, washed with water and acetone and dried.
The coatings were brush-applied by the restorer, following the standard methodology used in conservation, both

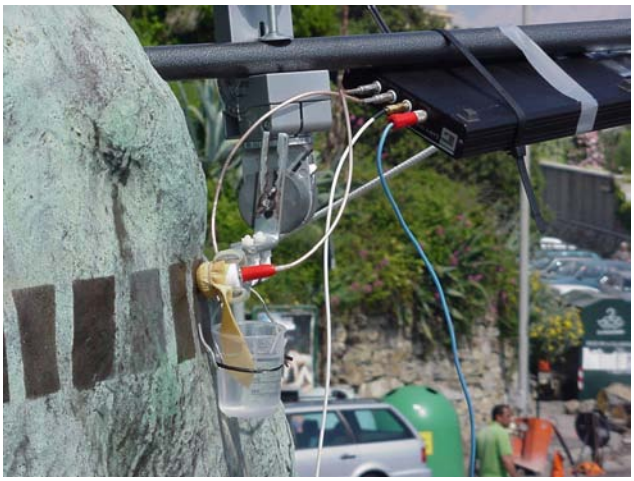

Figure 1 Electrochemical Impedance Spectroscopy measurement with the contact probe on *Monumento ai Mille* (test area III). From left to right, the visible 6x4.5 cm test zones are the ones for [B], [C], no coating, [E], and [F].

on coupons and on the monument zones. This was chosen in order to stay as close as possible to practical restoration world. Details on coatings and their application methods are reported in Table 1 (Letardi and Cozzolino 2002).
Coupons not exposed to weathering as well as after removal from the exposure rack have been stored in a sealed cabinet with silica gel.

2.1 Thickness measurements

Patina and coating thickness have been measured by Eddy Current technique [(Namicon DuoCheck with QE2 probe (0-1500μm)]. As the Eddy Current probe marks the waxy coatings, in order to check samples homogeneity, each coupon was weighted before and after coating application, and the weight gain per unit area has been computed for each sample. Coating thickness has been measured on two 3x3 and two 6x6 coupons for each coating system; for each series samples for measurement were chosen as the ones with the higher and the lower weight gain per unit area upon coating application. On each sample, 9 or 16 measurements on 3x3 and 6x6 coupons respectively were conducted, evenly distributed on the sample surface. Samples with waxy coatings have been cleaned and coated again after thickness measurement (Letardi et al. 2003). Unfortunately no characterisation of the coating thickness was possible on the Monument.

2.2 EIS measurements

EIS measurements were performed with a contact probe prototype and a method being developed in order to be applicable for field measurement on outdoor bronze statues (Letardi et al. 1998, Letardi 2002). The area probed in each measurement is 1.77 cm^2. A commercial cleaning-cloth soaked with a mineral water (electrical conductivity 318μS/cm^2, pH=7.9) is fixed to the contact cell, and the system obtained is then leant on the surface to be measured. The cloth has been immersed in the mineral water for 130min before being fixed to the contact cell; the system has been left to stabilise the open circuit potential for 30min before measurement start. EIS measurements have been made with a Gamry Femtostat, with Framework/EIS300 V3.11 software© 1999, Gamry Instruments. Spectra with 10 point per decade have been acquired in potentiostatic mode with 10mV AC signal level at open circuit potential.

Measurements were made in the frequency range 100KHz - 10mHz. For many exposures, 2 to 4 coupons for each coating system were measured; and 2 to 4 measurements were done in different parts of the 6x6 samples. On the monument it was not possible to record more than 2 to 3 spectra for each zone at each exposure time, especially since favorable weather conditions was necessary in order to take measurements. The average value of the Impedance Modulus |Z| at 10 mHz (low frequency limit) was computed for each coating system at each exposure, both for coupons and monument area III. The low frequency value of Impedance modulus is generally used to quickly assess coating protection ability: the higher is the value, the lower the corrosion rate of the system.

2.3 Patina composition characterisation

A Rigaku diffractometer was used to record X-Ray Diffraction spectra for corrosion product characterisation. The operating condition was: Cu K_α radiation with Ni filter, 40 kV, 30 mA. Spectra were directly measured using the 3x3 coupons.

3. Results

3.1 Patinas

Monitoring of patina thickness on the bare bronze coupons showed quick growth in the first 3 months, with an average value of 10 μm; afterwards the growth measured in the present conditions was slower with an average value of 11μm after 1year and 13μm after two years. Characterisation of patina components by XRD shows Cuprite is abundant from the very beginning of exposure; Atacamite and Paratacamite were present after the first month, then increasing with respect to Cuprite as weathering progresses. Ammonium Phosphate (JCPDF 22-0062) was also identified in the first month, with a slower increase with exposure. Small amounts of Quartz were also identified.

All the EIS measurements on the non-coated zone of Area III of the monument gave similar results during the time, with an average value of the Impedance modulus 0.15 ± 0.05 MΩcm^2. The bronze alloy used for the coupons, soon after polishing, was characterised by a value 0.09 ± 0.02 MΩcm^2, which grows rapidly in the first 3 months exposure, with a value 0.3 ± 0.2 MΩcm^2 after 1 year of exposure.

Table 2. Characterisation of the coatings applied on coupons with the application methods described in Table 1, as weight gain per unit area W and thickness Σ measured with Eddy Current method. The best fit value obtained for the parameters in the equation W = a Σ + b are reported for each coating, along with the coefficient of determination χ^2.

		W [mg/cm^2]	**Σ [μm]**	a	b	χ^2
[A]	6x6	1.2 ± 0.2	6 ± 3	0.13±0.02	0.63±0.09	0.95
	3x3					
[B]	6x6	1.0 ± 0.1	6 ± 2	0.08±0.02	0.6±0.1	0.81
	3x3					
[C]	6x6	0.8 ± 0.3	4 ± 2	0.19±0.02	0.0±0.1	0.97
	3x3					
[D]	6x6	1.6 ± 0.1	11 ± 3	0.09±0.01	0.52±0.09	0.98
	3x3	1.1 ± 0.1	6 ± 2			
[E]	6x6	2.0 ± 0.2	13 ± 2	0.12±0.03	0.4±0.03	0.95
	3x3	2.3 ± 0.3	6 ± 3	0.12±0.07	1.42±0.04	0.997
[F]	6x6	1.6 ± 0.1	10 ± 2	0.08±0.01	1.0±0.1	0.98
	3x3	1.6 ± 0.2	7 ± 2			

3.2 Coating systems

On the coupons, weight gain per unit area after coating application showed a good Gaussian distribution for all the coatings. A wider distribution characterised wax [C] and sharper one was obtained for wax [B]; for coating [D] the same application methods produced different results on samples 3x3 and 6x6, and the weight gain per unit area is clearly bimodal. The distribution is quite wide for coating [E] and it appears to be bimodal also, while for system [F] the distribution is narrow. The Eddy Current measurements provide an average value between 4 and 7 μm for all the coatings on the 3x3 samples. The same value is obtained on the 6x6 samples coated with the waxes (coatings [A], [B], and [C]), while the measured thickness is higher for 6x6 samples with Incralac containing coatings ([D], [E], and [F]). In particular it is almost double for coating [D] and [E]. Results are summarised in Table 2.

The linear correlation between the coating thickness Σ and the coupon weight gain per unit area W after coating application has been tested; fitting of data with the curve W = aΣ +b (see Table 2) gave very satisfactory results for coatings [A], [C], [D] and for coating [B] the regression results were satisfactory also. For the double layer systems [E], [F] very good fits were obtained, with two different curves for 3x3 and 6x6 samples in the case of coating [E]. It could be easily calculated that this was due to the quite different values obtained for the

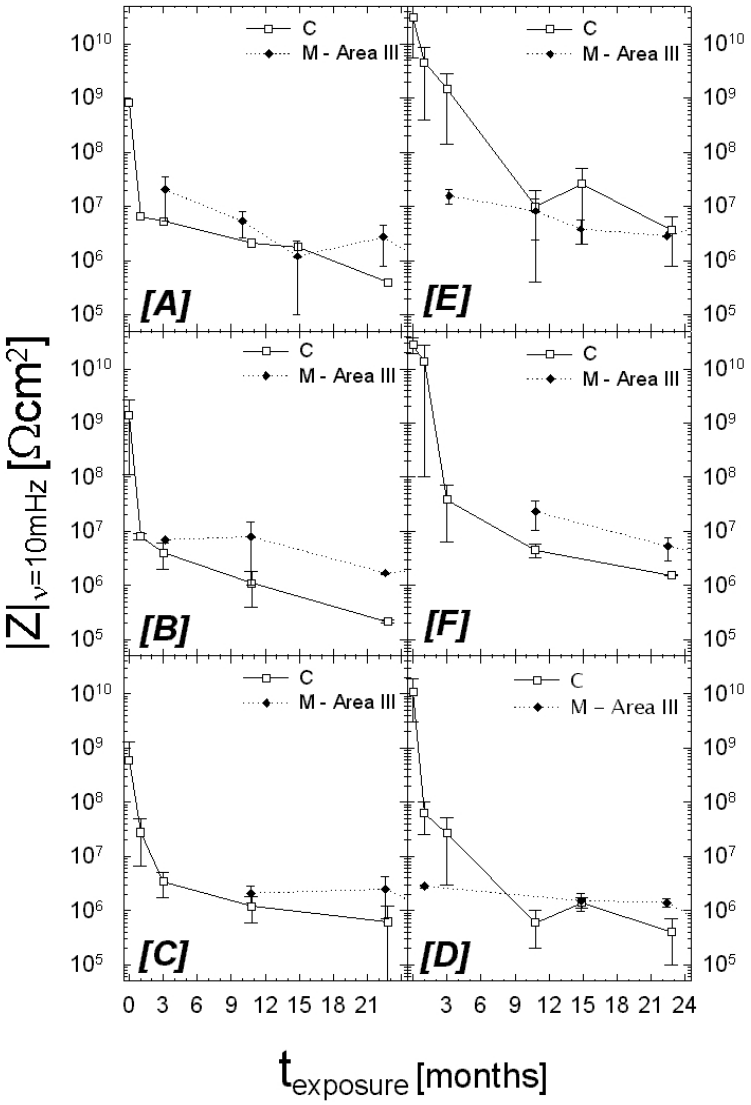

Figure 2 Low frequency value of Impedance modulus as a function of exposure time. Average data are plotted for the six coating systems [A] to [F] under test. Label C is for coupons and label M for monument.

parameter "a" of the coatings [D] and [A], which forms the double layer [E]. On the contrary, the value "a" for the wax [B] has almost the same value than for coating [D], so the corresponding double layer [F] is characterised by a single straight line for both 3x3 and 6x6 coupons. Except for wax [C], the parameter "b" is different from 0, as one could expect. Possible explanations for this behavior could be the way coatings are conforming to surface roughness and/or could be unevenly distributed on the sample border.

EIS measurements for 0, 1, 3, 11, 23 months exposure time were performed on coupons for all the coating systems under test (Figure 2, solid lines). At the beginning the average value of the Impedance modulus is about 1 GΩcm^2 for the three waxes, one order of magnitude higher for coating [D] and a bit higher for the double layer systems. Apart the double layer [E], all the other coatings showed a very quick decrease in the first three months, with values two order of magnitude or more lower than the initial ones; after 23 months only the double layer systems [E] and [F] had values over 1 MΩcm^2.

Measurements on coatings on the monument at the beginning of exposure was not advisable since solvents need to evaporate. Soon after the environmental conditions were not completely suitable, and only a few measurements were possible. A wider characterisation was then commenced after 10 months weathering (Figure 2, dotted lines). After three months both waxes [A], [B] and the double layer [E] gave average value in the range of 10 MΩcm^2; notwithstanding an high scatter of data, a similar trend is observed upon weathering, with values

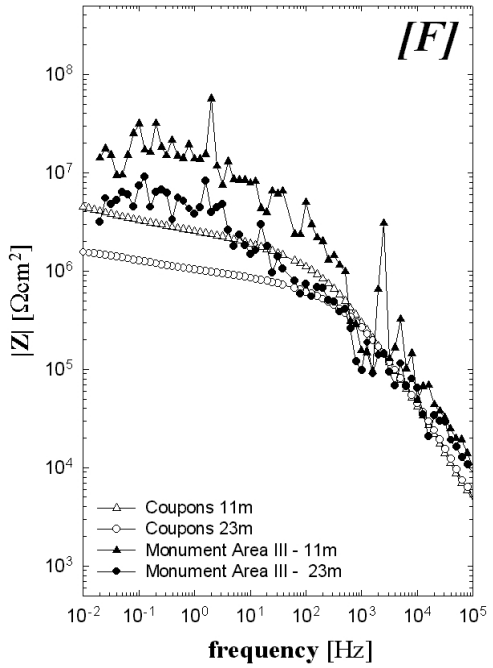

Figure 3 Impedance Modulus for coating [F] measured on coupons and on monument area III.

of a few MΩcm^2 after 23 months. The few data on wax [C] seem to suggest a slow variation, with values around 2 MΩcm^2 both at 11 and 23 months. Coating [D] also seem to present a slow variation, with a value around 3 MΩcm^2 after only one month, which became around 1 MΩcm^2 after 23 months. The double layer [F] presents the higher values, with about 20 MΩcm^2 after 11months and 5 MΩcm^2 after 23 months.

4. Discussion

The use of thickness measurement with the Eddy Current portable instrument on the monument was prone to very wide dispersion of data, due to the high roughness of surface with respect to the probe area; nonetheless the technique could give a rough determination of patinas thickness (Letardi et al. 2003). On the *Monumento ai Mille* average values between 80 and 130 μm were measured on the test areas before cleaning, which reduces to 50 to 110 μm afterwards; in particular 90±33 μm is measured in area III. On the contrary, coating thickness measurement on the monument was meaningless. In fact the coating thickness obtained with the application method adopted, whose measured values on coupons range from 4 to 13 μm, is lower than the dispersion of data obtained in the patina thickness measurements. As the treated zones have an area little less than coupons 6x6, one can guess similar thicknesses are obtained on the monument, even though a characterisation of coatings applied on patinated samples could help in verifying this hypothesis.

The comparison of the corrosion products identified on the monument and on the weathered coupons shows quite a similar composition, apart from the Mushistonite, which is identified on the monument only and Ammonium Phosphate that is identified on coupons only. The more abundant corrosion products identified both

on the monument and on the coupons are the typical one reported for marine exposure (Cuprite, Atacamite, and Paratacamite).

The Impedance measurements performed show a fairly wide scattering of data. Many factors, which are not strictly controlled in these natural/field conditions may influence data, and a more detailed analysis of the several measured parameters is under way. The field measurements on the monument are still quite noisy (Figure 3), and further improvement on the data acquisition method are in progress, even though the spectra quality is acceptable for the type of analysis performed.

Notwithstanding the scattering of data, a number of comments can be made. Average values of the low frequency Impedance Modulus are quite similar both on the patina on monument Area III and on the exposed bronze samples after one year. As already noted, these patinas do not have meaningful protective qualities, as the Impedance is only a little higher than for the bare bronze.

Comparison of coatings performance on the coupons and the monument area III is shown in Figure 2:

- Wax [A] performed better on the monument than on the coupons after three months exposure; as weathering continues the difference seems to decrease, even though data at 23m would require further comparison for longer exposure time.
- Wax [B] is characterised by average values systematically higher on the monument than on the coupons.
- Wax [C] has average values higher on the monument than on the coupons.
- Coating [D] is characterised by an average value one order of magnitude less on the monument than on the coupons after one month exposure. The trend observed indicates that values are quite similar on the monument and on coupons around one year exposure, and possibly are higher on the monument than on coupons after 23 months.
- Double layer [E] has an average value two orders of magnitude less on the monument than on the coupons after three months exposure; from 11 months differences are more or less negligible.
- Double layer [F] performs better on the monument than on coupons (Figure 3), with an average value almost one order of magnitude higher on the monument than on the coupon after 11 months.

The results obtained show that after only one year coating [D] offers no advantage with respect to the waxy coatings [A], [B] and [C], which have the advantage of a better accepted aesthetic appearance and are known to give fewer problems concerning reversibility and re-coating. The wax [B], both alone and in the double layer system [F], is the product whose performances on coupons showed the largest differences with respect to the ones on the monument area III. The different trends observed for the selected coatings on the polished bronze coupons and on the monument area III should be considered in more detail. The patina, which is present between the metal and the coatings applied on the monument, is supposed to be the main source for the differences observed on coating behavior with respect to the polished bronze coupons, as indicated by other studies (Otieno-Alego et al. 1998b, Letardi 2004). Further analyses are in progress to better enlighten relevant parameters for conservation purposes.

Acknowledgements

This work was in part financially supported by PROGETTO FINALIZZATO BENI CULTURALI. The parallel testing program has been developed in co-operation with the Istituto Centrale del Restauro (M.Marabelli, G.D'Ercoli). The Genoa Municipality is acknowledged for support and co-operation.

G. Gaggero (CNR-IBF, Genoa) constructed the EIS contact-probe. U.Montini (CNR-ISMAR, Genoa) took care of the CNR Marine Exposure Site.

Many thanks to M.Mach (Bayerisches Landesamt für Denkmalpfledge, München) for comments and suggestions on the use of coating [C].

H.Strandberg (Göteborg, Sweden) is gratefully acknowledged for co-operation on XRD and useful discussion.

References

Brostoff, L. B. and de la Rie, E. R. (1997) *Research into protective coating system for outdoor bronze sculpture and ornamentation*. In Proc. Metal 95, MacLeod, I. D., Pennec, S. L., and Robbiola, L. (eds.), (London: James & James (Science Publishers) Ltd), p. 242-244

Cicileo, G., Crespo, M., and Rosales, B., (2004) *Comparative study of patinas formed on statuary alloys by means of electrochemical and surface analysis techniques*. Corrosion Science, **46**, 929-953

D'Ercoli, G., Letardi, P., Marabelli, M., and Santin, V. (1999) *The resistance of polarization for the testing of corrosion: practice and problems*. In Proc. ART99 - 6th International Conference on Non-Destructive testing and Microanalysis for the diagnostics and Conservation of the Cultural and Environmental Heritage, Marabelli, M. and Parisi, C. (eds.), (Rome: Euroma)p. 1727-1738

Drayman-Weisser, T. (1992) *DIALOGUE/89 - The conservation of bronze Sculpture in the outdoor environment: a dialogue among conservators, curators, environmental scientists, and corrosion engineers*, (Houston: NACE)

Graedel, T. E., (1987) *Copper patinas formed in the atmosphere-II.A qualitative assessment of mechanism*. Corrosion Science, **27**, 721-740

Letardi, P. (2000) Electrochemical impedance measurements in the conservation of metals. In Creagh, D. C. and Bradley, D. A. (eds.), *Radiation in Art and Archeometry*, p. 15-39. (Amsterdam: Elsevier)

Letardi, P. (2002) Outdoor bronze protective coatings: characterisation by a new contact-probe Electrochemical Impedance measurements technique. In *The Science of Art*, (Padova: Libreria Progetto), p. 173-178

Letardi, P. (2004) *EIS measurements on Bronze/Copper samples with different Patina/Coatings*, CNR-ISMAR Report for Universität für angewandte Kunst Wien - Abteilung Archaeometrie

Letardi, P., Beccaria, A. M., Marabelli, M., and D'Ercoli, G. (1998). *Application of Electrochemical Impedence measurements as a tool for the characterization and protection state of bronze works of art*. In Proc. Metal 98, Mourey, W. and Robbiola, L. (eds.), (London: James & James (Science Publishers) Ltd), p. 303-308

Letardi, P. and Cozzolino, D. (2002) *Contact-Probe EIS Characterisation of Protective Coating Systems for OUTDOOR Bronze Sculpture: Atmospheric Weathering Behaviour in Marine Environment*. In Proc. 15th International Corrosion Congress, Frontiers in Corrosion Science and Technology, International Corrosion Council (eds.), paper 538

Letardi, P., Marabelli, M., D'Ercoli, G., and Guida, G. (2002) *Comparative study of Protective Coating Systems for OUTDOOR bronze sculpture*. In Proc. 3nd International Congress on Science and Technology for the Safeguard of Cultural Heritage in the Mediterranean Basin, Guarino, A. (eds.), (Rome: Litoflash), p. 272-275

Letardi, P., Marabelli, M., D'Ercoli, G., Guida, G., and Artioli, M., (2003) *Valutazione in campo di protettivi per bronzi esposti all'aperto in ambiente marino - Progetto Pilota sul Monumento ai Mille di Quarto: Relazione n.1 "Introduzione e caratterizzazione iniziale"*. CNR-ISMAR Report

Otieno-Alego, V., Heath, G., Hallam, D., and Creagh, D. (1998)a *Electrochemical evaluation of the anti-corrosion performance of waxy coatings for outdoor bronze conservation*. In Proc. Metal 98, Mourey, W. and Robbiola, L. (eds.), (London: James & James (Science Publishers) Ltd), p. 309-314

Otieno-Alego, V., Hallam, D., Viduka, A., Heath, G., and Creagh, D. (1998)b *Electrochemical impedance studies of the corrosion resistance of wax coatings on artificially patinated bronze*. In Proc. Metal 98, Mourey, W. and Robbiola, L. (eds.), (London: James & James (Science Publishers) Ltd), p. 315-319

Pilz, M. and Römich, H., (1997) *Sol-Gel Derived Coatings for Outdoor Bronze Conservation*. Journal of Sol-Gel Science and Technology, **8**, 1071-1075

Strandberg, H. (1998) *Perspectives on bronze sculpture conservation - Modelling corrosion*. In Proc. Metal 98, Mourey, W. and Robbiola, L. (eds.), (London: James & James (Science Publishers) Ltd), p. 297-302

Table of Registered Trade Items

Product	**Soter 201 LC**	**R21**	**TECE 3534 F**	**Incralac**
Producer/supplier	Baraldi Lubrificanti Via Decumana, 5 I-40133 Bologna ✆+39-051.381.744	Clariant *(producer)* Phase *(supplier)* Via T.Cremona, 7 I-40139 Bologna ✆+39-051.623.1295	TH.C.Tromm Feuerstrasse, 7-17 D-50735 Köln ✆+49-(0)221974552	Bresciani s.r.l. *(supplier)* Via Socrate 71.3 I-20128 Milano ✆ +39-0227002121

An EIS Method for assessing thin oil films used in museums

*D. Hallam,[a]*D. Thurrowgood, [a] V. Otieno-Alego, [b] D. Creagh [c]

[a] National Museum of Australia, Canberra ACT 2601 Australia
[b] Division of Science and Design, University of Canberra, CANBERRA ACT 2601 Australia
[c] Division of Management and Technology, University of Canberra, CANBERRA ACT 2601 Australia

Abstract

Electrochemical impedance spectroscopy (EIS) is a well established technique for evaluating the corrosion preventive properties of protective coatings. National Museum of Australia (NMA) staff have used this technique in the past to evaluate and rank the corrosion performance of a number of commercial waxy coatings in routine conservation use. This testing procedure is relatively simple and gives quantitative *snapshot* data about the performance of protective coatings, allowing them to be ranked objectively. The EIS test cell presently available is suitable for testing relatively hard, thick coatings. It cannot be used in the investigation of thin, delicate and easy-to-break films such as those formed by engine oil. The objective of this investigation was to fabricate an electrode suitable for testing thin oily films using conventional EIS test cells. We desired an EIS method that could be used for rapidly testing commercial engine oils and ranking their performance. Such a test protocol is particularly crucial to the NMA who aim to identify the best engine oils for use in their functional collection of technological objects and for developing a "just noticeable wear" criteria for use in museums.

Keywords: corrosion, corrosion protection, metals, petrochemical oils, functional objects, corrosion inhibitors, engine oils.

1. Introduction

Mechanical wear inside engines is substantially related to the effectiveness of the lubricant during use and the rate of corrosion when in storage. The problems associated with lubrication are understood by most people at an anecdotal level: that is, if a lubricant is poor or absent, then a working part will wear as a result of friction. In museum practice the lubrication properties of high quality oils produced by reputable manufactures can be considered adequate to meet our requirements providing the lubricant and application are appropriately matched. Corrosive wear (Ricardo, 1992) and internal corrosion are probably a greater issue for museums than for most users. This paper is part of a body of work designed to evaluate the importance of corrosion and wear to museum collections of mechanical objects. Where the effect is significant we aim to develop strategies for reducing its impact.

Operational engines in particular have high potential for corrosive wear. Combustion processes produce hot corrosive gasses, which, with the use of uninhibited lubricants, cause a flash rusting of exposed metal cylinder bores. During

the next engine stroke these corrosion products are scraped from the surface, and a proportion of these will enter the oil system and be flushed through the engine as a fine abrasive. Iron oxide (e.g. Fe_2O_3) has a Mohs hardness of six compared to a hardness of 4-5 for iron (Weast, 1986). It is commonly used as a polishing compound in the form of jeweler's rouge. Its abrasive hexagonal crystalline structure gives it potential to damage working surfaces under high load. It exists as a powder down to 0.003 microns, and is not necessarily removed by the filtration system. In addition, a proportion of the corrosive combustion gasses will be passed into the bottom of the engine where they form nitric and sulphuric acids in combination with (Hallam F.S.T (1987)) water. To some extent this type of corrosion has been almost eliminated by modern fuel and oil additives.

Figure 1 Corroded cylinder bore from an infrequently used Landrover in the NMA's collection. Note the horizontal banding, possibly due to contact with piston rings at rest. The vehicle was operated approximately three years prior to this image being taken.

Of concern to museums is the corrosion that develops during long periods of mechanical inactivity. Most lubrication products are designed for environments of frequent use. Operation has the effect of reforming the protective oil film and distributing inhibitors. In a museum like the NMA use at intervals of 3-6 months is common. An example of the consequence of using standard oils in a museum vehicle can be observed in Figure(1). Over a twenty year period this vehicle was run for a short periods on the basis of irregular display requests, often years apart. During this period condensation and remnant aggressive combustion products combined to result in a thin film of corrosion on the cylinder bore. In particular ring shaped markings are evident where more aggressive corrosion has taken place. These correspond to where the piston ring was in contact with the cylinder bore during a period of inactivity. The processes of differential aeration, which creates a more active localized anodic site at the point of contact, may be the cause of the defined ring markings. The effect can be observed with the unaided eye as pitting in the metal surface. When an engine in this condition is started the immediate effect is that corrosion product is burnished between the bore and the piston rings, having an abrasive effect. Fracture of the crystalline corrosion product from the surface may also tend to leave a more porous metal surface. To combat this, lubricants should

ideally be effective corrosion inhibitors when present as the thin residual films remnant after operation and cool down periods.
There is an increasing awareness in museums about the benefits of additives in chemically engineered oils. Contemporary oils differ dramatically from oils used in the 1920s. These were often only cleaned crude oils that had undergone minimal processing (Thomsen,1926) There does persist in the minds of some enthusiasts a perception that because non-additive oils were used when a machine was new then they should be used now. This is a reasonable approach for a museum if the objective is to replicate the short mechanical life span and high wear rates experienced when the machine was new. There is no advantage of this approach when the objective is to preserve significance. Museums seek longevity from their collections. To accomplish this they need to take advantage of approaches that will allow them to make educated decisions about the care of their collections. A more effective approach exists than that available in manufacturers' handbooks, and searching for bottles of long obsolete products from the back of storerooms. This approach involves the development of a rationally understanding of the problem and the development of a logical approach to resolving the issue based on the best chemical and physical understandings available.

We contend that a majority of the wear experienced by museum collection objects is due to corrosive effects rather than friction effects.

If the corrosive factors can be reduced or removed then it is probable that the safe operational life of the collection object can be increased. The NMA's objective is to develop a set of operational conditions in which we can eliminate most of the corrosive wear. In a method analogous to "just noticeable fade" standards used for (Derbyshire and Ashley-Smith, 1999), we are interested in developing operational standards where the rate of wear is given a similar weighting to the just noticeable fade deterioration level: that is, just as we display paintings under conditions where we predict that their deterioration will be at a particular acceptable level after a particular display exposure, we ought also be able to establish conditions where mechanical wear will be an acceptable consequence of a certain amount of display use. A "just noticeable wear" criteria would facilitate the making of more sophisticated decisions about the care and use of mechanical objects.

It is our hypothesis that if internal corrosion in storage can be substantially reduced, the wear of engines under museum use will be insignificant to the objects long term survival. Just as there is benefit from displaying a painting though it is known to be fading, there are advantages from operating machinery even though it is undergoing a level of wear. By attaching a significance to the level of deterioration, then balance it against any benefits of operation, a museum can make decisions about the justification of a particular level of use. It is possible that with a correct scientific approach to the use of machines in museums that wear will be negligible in long term survival, and it will be factors such as human error, recrystalization of metal alloys, polymer deterioration or loss of knowledge of operation that will be the limiting factor and the greater risk for their survival. We further speculate that the controlled operation of machines can be beneficial to their survival as it facilitates the distribution of inhibitors and lubricants through systems, promotes regular human contact with the object allowing early detection of deterioration, and prevents loss of knowledge surrounding the object. The level and type of appropriate use generally needs to be decided on an individual basis, however the NMA is endeavoring to develop a body of scientific work which will facilitate informed decision making around the preservation of mechanical objects.

A focus of current work is the development of methods to establish if there are differences in the corrosion protection afforded by different types of commercially available engine oils. If particular types of oils can be shown by experiment to provide

greater protection from corrosion than others then their performance in the museum environment can be investigated.

Electrochemical impedance spectroscopy (EIS) is a well established technique for evaluating the corrosion preventive properties of protective coatings (Kendig et al 1993, Scully et al 1994). Conservators have used this technique in the past to evaluate and rank the corrosion performance of a number of commercial waxy coatings currently in routine conservation use (Hallam et al 2001, Otieno-Alego et al 2001). This testing procedure is relatively simple and gives quantitative *snapshot* data about the performance of protective coatings, allowing them to be ranked objectively. The EIS test cell presently available in the NMA laboratories is suitable for testing relatively hard, thick coatings. It cannot be used in the investigation of thin, delicate and easy-to-break films such as those formed by engine oil. The objective of this investigation was to fabricate an electrode suitable for testing thin oily films using conventional EIS test cells. We desired an EIS method that could be used for rapidly testing commercial engine oils and ranking their performance. Such a test protocol is particularly crucial to the NMA who aim to identify the best engine oils for use in their functional collection of technological objects.

The fabricated electrode has successfully been used to test and rank six NMA nominated commercial engine oils. In addition, the corrosion performances have been compared to salt spray chamber exposure results.

2. Experimental Procedure

2.1 Test Oils

Six oils were selected to be representative of commercial oils used by old vehicles and numbered 1 to 6. The commercial identity of the products used for experimentation are not revealed here because 1) the objective of this research was to develop a testing method that allowed identification of differences between products and 2) the testing of six products is not considered sufficient for us to begin making product recommendations. If the testing method progressively demonstrates its usefulness, in correlation with other available evaluation techniques, the NMA may begin to identify which product types have been found to be best suited to specific museum applications.

Oil products were selected that were anticipated to display a range of corrosion inhibition effectiveness. Product (1) was a commercially available engine oil marketed for infrequently used older vehicles. Product (2) was an approximately 15 SAE grade mineral oil which contained no additives, i.e. it is the refined mineral oil used by oil manufactures to manufacture their additive package retail product. Product (3) was a commercially available oil designed for daily use in pre-1980 passenger vehicles. Product (4) was an approximately 40 SAE grade mineral oil which contained no additives, i.e. similar composition but higher viscosity than product (2). Product (5) was a low viscosity spray type oil to which tackifiers and corrosion inhibiting agents had been added. The product is designed to both cling to metal surfaces, displace surface moisture and inhibit corrosion reactions. Product (6) was a “new old stock” commercially available 50 weight engine oil from circa 1950. The product was selected for testing because oils of this vintage, with distinctive “inhibitor” odor, are on occasion found in service in museum collections. They are particularly common in differentials and gearbox applications. It is acknowledged that any active ingredients in this product may have deteriorated since manufacture.

2.2. Electrochemical Impedance Spectroscopy

After a comprehensive literature survey, the EIS test procedure published in *Corrosion Science* by Nowosz-Arkuszewka and Krawczyk (1992?) was adopted in this project. After further consultations with Prof. Nowosz-Arkuszewka, we chose to make the working electrode from a commercial mild steel rod of diameter 3.18 mm

and a length 200 mm, coated by dipping in the oil of interest. The simple rod-electrode design fits well with the EIS testing rigs and equipment already available. A special Teflon holder was designed for holding the coated mild steel electrode in the electrochemical cell (see Figure 2). Both ends of the steel rod were rounded (to form a semi circle) using a lathe machine tool. This edge rounding was important to ensure that the thin oily films was not broken by hard corners. Prior to use the electrode was polished using a 1200 grit SiC paper, degreased thoroughly with acetone, then half immersed in the appropriate oil sample contained in a test tube. Care was taken to ensure that no section of the immersed electrode was in direct contact with the sides of the test tube. The electrode was left to equilibrate in the oil for 24 h after which it was removed and clamped vertically to drain off the excess oil (approximately 30 min) before use.
No attempt was made to determine the final thickness of the oil films. The experiment was designed to give information about the efficacy of films formed at museum storage temperatures of approximately 21°C.

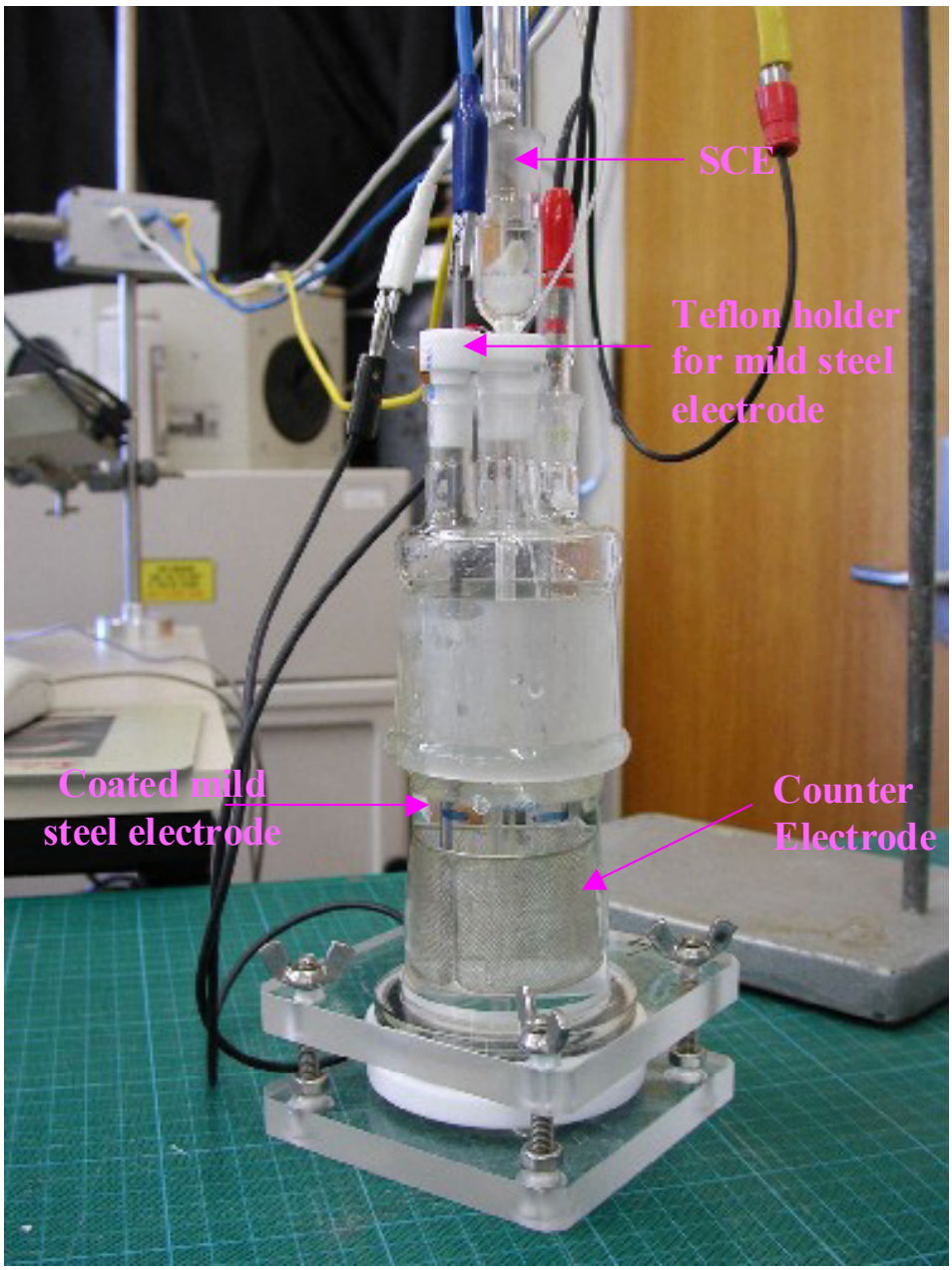

Figure 2.Close-up photograph of the EIS electrochemical cell showing the coated mild steel rod electrode in testing position.

EIS data was collected in quiescent 0.25 M K_2SO_4 with the coated mild steel rod as the working electrode (exposed area = 4.75 cm^2). A large cylindrical platinum mesh and a saturated calomel electrode (SCE) were used as the counter and reference electrodes, respectively. The 0.25 M sulphate solution was chosen based on the previously published work by Nowosz-Arkuszewka and Krawczyk (1992?). A pseudo-reference electrode made of a gold wire mounted in soda glass except for its tip was coupled to the SCE through a 0.1 μF capacitor. Impedance measurements were performed using a computer controlled EG&G PAR 273A potentiostat coupled to an EG&G M5210 lock-in amplifier. The alternating current amplitude was 10 mV and was applied about the open circuit potential over the frequency range 100 kHz to 10 mHz (5 points per decade). The coated electrode was left to equilibrate in the test solution for 20 min before recording the impedance data. The impedance data were analysed using the circuit analysis program ZSimpWin, Version 2.00 (EChem Software web: http://www.echemsw.com). The capacitors in the circuit were mathematically modelled using a constant phase element (CPE) that takes into account heterogeneity in surface morphology and diffusion related processes (Deflorian et al 1993). Four repeated experiments were conducted for each coating.

Visual observation of the electrode in solution did not suggest that immersion of the electrode caused the oil coating to be washed from the surface. An oil slick on the surface of the electrolyte did indicate some loss of surface protection, however the EIS data collected indicated that all samples had a coherent film present on the electrode when the experiment was commenced. In some instances this film broke down rapidly when current was applied. The immersion of an oily film in an aqueous solution is an extreme test of its corrosion resistance. By exposing the oily films to both this and the salt spray environment we hope to select oils which show some resistance to extreme environments and make trial application under the more benign museum environment.

2.2 Salt Spray Testing

The salt spray test was carried out in a Singleton SCCH Corrosion Test Cabinet. The corrosive nature of the chamber specified by ASTM D117 (ASTM, 1985) is a continuous spraying with a 3.5% (by weight) solution of sodium chloride. In this testing, however, the standard sodium chloride solution was substituted with 0.25 M K_2SO_4 solution (pH ≈ 6.8, temperature 35^{o} C). This modified test environment was adopted to match the EIS test conditions. Rectangular mild steel panels (60 x 45 x 2 mm) were initially sand blasted, polished using 1200 grit SiC paper, washed in deionised water, degreased in acetone and placed in an oven (60^{o}C) for 2 h to dry. The cleaned coupons were then coated by completely immersing them in the different test engine oils for 24 hr before being removed and allowing the excess oil to drain for 30 min. Samples were prepared in duplicates. The coated samples were placed in the salt spray chamber angled at 45 degrees and left to corrode until sufficient corrosion had formed on all the surfaces. Specimen surface was monitored and the degree of rusting was rated by visual examination of the surface corrosion behaviour after every 24 hr. The samples were given a rust grade rating from 0% (no rust on surface) to 100% (surface completely rusted). A total of 6 commercial oils (listed in *Section 2.1*) were tested.

3. Results and Discussions

3.1 Electrochemical Impedance

Representative Bode magnitude plots are shown in Figure 3. The low-frequency impedance (Z_{lf}) estimated at the plateau region of the Bode magnitude plot in the frequency range 0.1 to 0.05 Hz has been proposed as the optimal EIS parameter to evaluate the performance of corrosion inhibiting coatings (Grandle and Taylor 1994). The impedance at this frequency includes the response of the coating as well as part of the response of the oxide and/or corrosion product in the pores at the metal interface. Referral to Figure 3, this *snapshot* method of EIS data treatment shows that all the oily films offered some corrosion protection to the mild steel (i.e. Z_{lf} for all oil coated steel is greater than the impedance of the bare metal). The overall effectiveness of the films could be ranked best to worse for the tested oils as in the product order: 1 > 5 > 3> 2 > 4 ≈ 6. Except for products 1 and 5 which show some capacitive behaviour (ie. The Bode plots in the high frequency regime converge to the same straight line with a slope of approx. –1), all the tested oily films were readily penetrated by the electrolyte after 20 min of immersion.

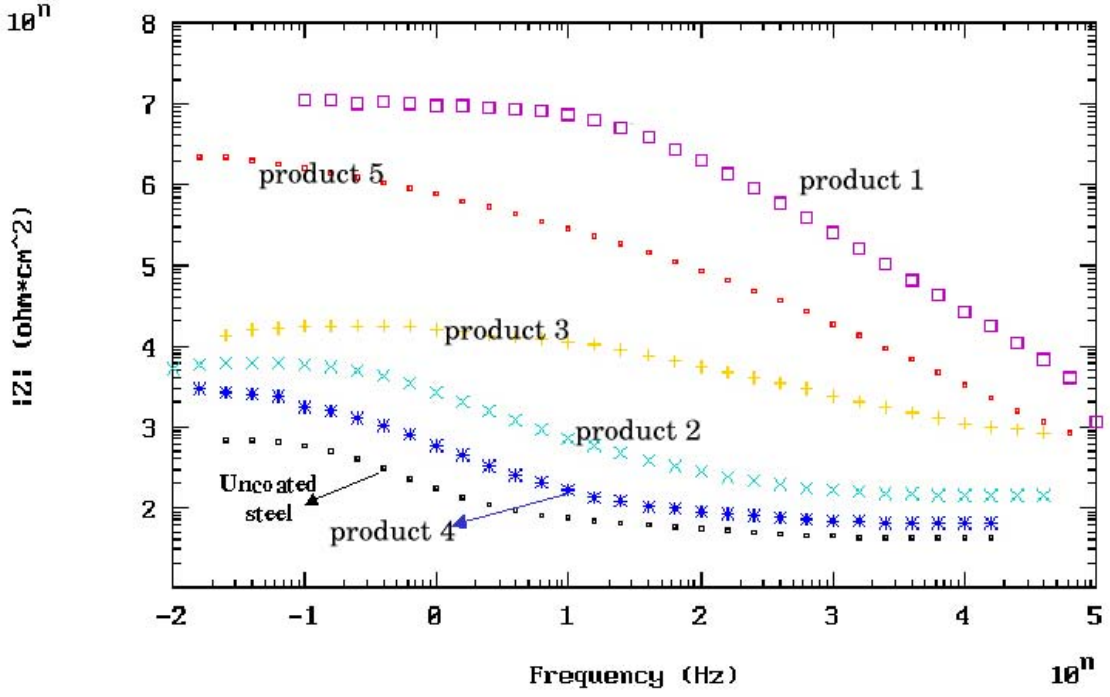

Figure 3. Representative Bode magnitude plots for the uncoated and engine oil-coated mild steel electrodes immersed in quiescent 0.25 M K_2SO_4 solution (equilibration time = 20 mins).

EIS data can also provide kinetic and mechanistic information on the coating's physical-chemical behaviour through the analysis of the equivalent resistance and capacitive elements that contribute to the observed electrical behaviour of the coating. The impedance spectra were analysed by fitting the data to the equivalent electrical circuit shown in Figure 4, where Rs is the resistance of the electrolyte; R1 is the coating or pore resistance; R2 is the charge-transfer resistance of the corrosion reaction; C1 is the capacitance of the coating; and C2 is the double layer capacitance at the metal-electrolyte interface. All the capacitors (C1 and C2 in Figure 4) were mathematically modelled using a constant phase element (CPE). Figure 5 shows examples of overlays of the measured Bode plot and that calculated from the simulated circuit. Good agreement was obtained between the measured and

calculated results. The values for coating resistance (R1) and the coating capacitance (C1) can be used as a quantitative measure of the effectiveness of the coating. Table I gives a summary of the calculated R1 and C1 values. Larger R1 values accompanied by smaller C1 values equates to good corrosion protecting coatings. As with the Z_{lf} ranking, the efficacy of the coatings based on the calculated R1 and C1 values (See Table 1) could be arranged in the product order: 1 > 5 > 3 > 2 > 4 > 6, starting from the most resistant.

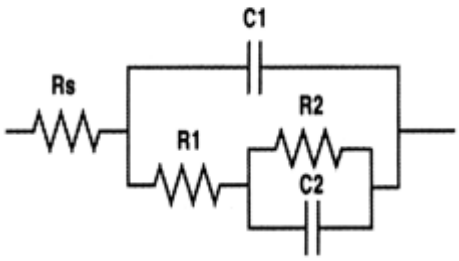

Figure 4: Equivalent circuit model of a coated metal. Rs represents the solution resistance, R1 and C1 correspond to the resistance and capacitance of the coating whilst R2 and C2 correspond to the resistance and capacitance of the metal interface

It is worthwhile noting that the overall impedance of a coating depends on, among other things, the thickness of the coating. In this investigation, the oil film was applied simply by immersion and the excess oil allowed to run off leaving a thin film on the metal surface. The above ranking is based upon this scenario. No attempt was made to determine the actual final thickness of the thin films.

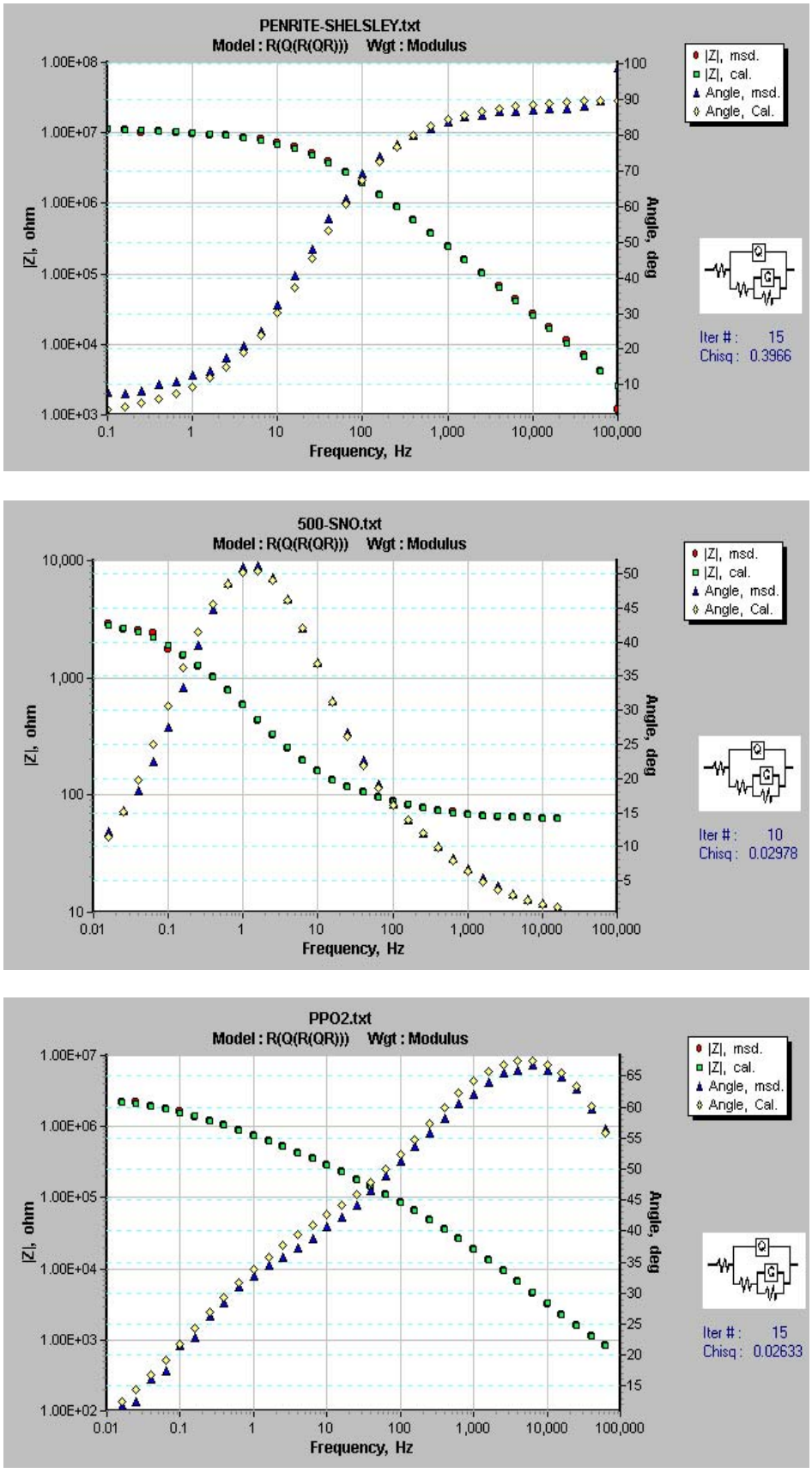

Figure 5. Examples of computer fit for impedance data obtained for oil coated mild steel exposed in quiescent 0.25 M K_2SO_4. Inset shows circuit used for computer simulations

Table I: Electrochemical impedance parameters R1 and C1 calculated for oil coated mild steel immersed in quiescent 0.25 M K_2SO_4 solution.

Product number	Immersion Time (min)	R1 (Ω cm^2)	C1 (μF cm^{-2})
1	20	3.19×10^5	0.0006
2	20	6.57×10^2	46.6
3	20	8.07×10^2	3.88
4	20	9.12×10^1	290.6
5	20	8.75×10^4	0.041
6	20	7.81×10^1	166.5

3.2 Salt Spray

The corrosion performances of the oil coated steel panels exposed to the salt spray chamber are presented in Table II. The samples were given a rust grade rating from 0% (no rust on surface) to 100% (surface completely rusted). It was not possible to effectively rank the performance of the thin oily films under this relatively aggressive salt environment and after a short exposure (24 hr), only the coupons coated with *product 1* experienced some corrosion protection (with ranking of 20%). All the other coatings failed (ranking 100%) and the mild steel coupon's surfaces were heavily corroded. After 48 hr the surface of the steel panels coated with *product 1* showed 60% rust. The observed rapid failure of most of the oily films can be attributed mainly to their poor physical barrier to electrolyte penetration. This observation corroborates well with the EIS data that indicated most of the oil films to be easily penetrated by the electrolyte within the first 20 min of immersion. Corrosion of the underlying mild steel is expected to occur rapidly in this salt laden environment once the electrolyte/metal contact is established. The superior performance of the *product 1* agrees well with the EIS ranking.

Table II. Salt-Spray Test rating of the wax coated steel panels (average of three panels)

Product number	**Ratings$^\theta$ (after 24 hr)**	**Ratings (after 48 hr)**	**Ratings (after 72 hr)**
1	20%	60%	100%
2	100%	F*	F
3	100%	F	F
4	100%	F	F
5	100%	F	F
6	100%	F	F

Ratings$^\theta$ 0% = No rust on surface; 100% = Surface completely rusted
F* Surface of steel panels coated with oil coating showed 100% rust
(ie total failure) from previous recording

4. Conclusions

The thin rod-electrode fabricated in this investigation can be used to establish the corrosion efficacy of thin, delicate and easy-to-break oily films using the technique of electrochemical impedance spectroscopy. The test procedure provided reproducible and quantitative results allowing the performance of the protective coatings to be ranked more objectively and within a short testing time. The system was successfully used to evaluate the efficacy of six commercial oils in a sulfate-containing environment. The thin films exhibited poor barrier properties and were readily penetrated by the electrolyte resulting in heavy corrosion of the base metal within 12 hr of exposure in a salt laden environment. The ease of film penetration may support an argument for regular film replenishment in museum collection vehicles.

Testing by EIS showed product 1 to be orders of magnitude more effective at preventing corrosion under the test conditions than the remaining 5 products. This product was also the only one to exhibit any significant resistance to the salt spray environment. The conventional engine oil, product 3, displayed no meaningful improvement in corrosion resistance over the unimproved base oil samples. The aged oil (product 6) achieved only comparable protection to product 4, an unimproved base oil. The presence of inhibitors in products 1 and 5 has made these oily films more effective at reducing corrosion. A method of accessing the corrosion protection afforded by thin oil films is one of the criteria required in the development of a *just noticeable wear* standard form operational museum objects. By better defining the risk factors to museum collections we have a higher probability of ensuring survival and of effectively applying resources to areas of greatest need.

It must be borne in mind that the engine oils are used in a much milder corrosive environment than the aggressive salt solution used in this investigation. It is envisaged that outstanding oils will be very efficient under natural engine operating conditions

If the lubricant is not effective as an inhibitor in this situation then more proactive measures have to be taken to reduce corrosion during storage, e.g. vapor phase inhibitors, dehumidification, flooding the system with a wax containing oil such as PX115. These “mothballing” techniques render the vehicle not available for display operation without lengthy start up and re-mothballing procedures and are not conducive to the conservation of both the form and function of the object.

The following further research programme is planned:

- ranking commonly available “classic car” oils by the technique described in this paper
- developing a method for the assessment of the relative wear and corrosion rated of engines in storage in museum maintenance and storage programs
- developing engineering conservation procedures and practices to assess the Just Noticeable Wear (JNW) criteria for museum and collector objects.

References

ASTM Standard B 117, *Standard Method of Salt Spray (Fog) Testing*, ASTM Annual Book of Standards, Vol.06.01 (1985)

Deflorian, F., Fedrizzi, L., Locaspi, A. and Bonora, P.L. (1993) *Electrochimica Acta* **38**, pp1945-1950

Derbyshire, A. and Ashley-Smith, J. (1999) *A proposed practical lighting policy for works of art on paper at the V&A* Triennial meeting (12th), Lyon, 29 August-3 September 1999: preprints. Vol. 1 James & James London

Grandle, J.A. and Taylor, S.R. (1994) *Electrochemical Impedance Spectroscopy of Coated Aluminum Beverage Containers: Part1 - Determination of an Optimal Parameter for Large Sample Evaluation* Corrosion **50**, 792-803.

Hallam F.S.T (1987) *Repco engine service manual* Repco Limited Melbourne Australia page 81

Hallam, D., Thurrowgood, D., Otieno-Alego, V., Creagh, D., Viduka, V. and Heath, G. (2002), *Studies of Commercial Protective Petrochemical Coatings on Ferrous Surfaces of Historical and Museum Objects*, In Metal 2001. Proceedings of the ICOM-CC Metals Conference, Santiago, Chile. (Ed. I. McLeod), James and James Scientific Publishers, London. In press.

Kendig MW, Jeanjaquet S and Lumsden, J, (1993), *Impedance: Analysis and Intepretation*, Philadelphia, PA:, ASTM, ASTM STP 1188, eds. J.R. Scully, D.C. Silverman, M.W. Kendig

Nowosz-Arkuszewska and Krawczyk, M. (1992?) Corrosion Science **33**, pp.861-871.

Otieno-Alego, V., Creagh, D., Hallam, D., Viduka, A. and Heath, G. (2001), *In-Situ and Laboratory Studies of the Ageing of Protective Wax Coatings on Metal Surfaces of Museum Objects and Outdoor Statues*, in Les Mallinson (ed.), Ageing Studies and Lifetime Extension of Materials, Kluwer Academic/Plenum Publishers, UK. pp.609-618.

Ricardo, H.R. (1992) *The Ricardo Story : autobiography of Sir Harry Ricardo, pioneer autoimotive engineer* SAE Historical Series SAE Warrendale PA. USA ISBN 1-56091-211-1

Scully, J.R. and Hensley, S.T. (1994) Corrosion **50**, pp705-716
Thomsen, T.C. (1926) *The practice of lubrication* 2nd edition, The McCraw-Hill Book Company, New York, Chapters 1-4.

Weast, R. C. (1986) *CRC Handbook of Chemistry and Physics* Chemical Rubber Publishing Company Boca Ration Florida

ABN 70 592 297 967

Development and Evaluation of Removable Protective Coatings on Bronze

T. J. Shedlosky, A. Huovinen, D. Webster, G. Bierwagen[a]

North Dakota State University, Department of Polymers and Coatings
1735 NDSU Research Park Drive, Fargo, ND 58105 USA

Abstract

Coatings are often used to help protect bronzes from destructive erosion caused by outdoor weathering. Experiments looking at improved coating systems for bronze have been a focus of research at North Dakota State University. Previous research has shown that the most protective coatings tend to be impervious to conventional solvent removal techniques and standard mechanical removal methods may damage bronzes and their patinas. This research has focused on viable coatings that afford protection to the underling bronze surface while remaining removable under specific conditions not typically found in the outdoor environment. The preparation and evaluation of various unconventional coatings for bronze has been accomplished through synthesis and combinatorial methods. The results of the initial testing of the new coating will be discussed.

Abstract

Amenudo se aplican recubrimientos para proteger los bronces de la erosion destructiva causada por los agentes atmosféricos. Ensayos a fín de desarrollar sistemas de revestimientos protectivos eficaces han sido un tema de investigación privilegiado en North Dakota State University. Experimentos llevados a cabo anteriormente probaron que los revestimientos que mejor protegen tienden a volverse impermeables a los medios convencionales de eliminación con disolventes y que los métodos de
mecánicos de extracción pueden ser perjudiciables para los bronces y sus patinas. Este trabajo de investigación se ha focalizado en desarrollar recubrimientos viables que protegen la superficie subyaciente del bronce y que se pueden quitar en condiciones específicas atípicas de un ambiente exterior. La elaboración y evaluación de varios revestimientos no convencionales para bronce se han estblecido por medio de síntesis y métodos combinatorios. Los resultados de la fase inicial de pruebas sobre el nuevo revestimiento seran discutidos.

Abstract

Des revêtements sont souvent utilisés afin de protéger les bronzes de l'érosion destructive causée par les agents atmosphériques. Des experiences visant à développer des systèmes de revêtements améliorés pour les bronzes ont été menées à North Dakota State University. Des recherches antérieures avaient démontré que les enduits protecteurs les

[a] Corresponding author: TEL: 01-701-231-8294: FAX: 01-701-231-8439: email: Gordon.Bierwagen@ndsu.nodak.edu

ABN 70 592 297 967

plus efficacies sont souvent imperméables aux solvants par les techniques conventionnelles d'enlèvement, et que les techniques classiques mécaniques d'enlèvement peuvent endommager les bronzes et leur patine. Notre recherche a été de développer des revêtements viables qui permettent de protéger la surface sous-jacente du bronze tout en demeurant faciles à enlever dans des conditions spécifiques atypiques d'un environnement extérieur. C'est par la synthèse et les méthodes combinatoires que la préparation et l'évaluation de plusieurs revêtements non conventionnels pour le bronze ont été accomplies. Les résultats des essais préliminaires sur le nouveau revêtement seront discutés.

Keywords: removable, coating, reversible, film, paint, bronze, polyurethane

1. Introduction

Removability is a property demanded of the materials used in the conservation of art. When a conservator works with a piece of artwork, there is a certain code of ethics that is maintained. It is the role of the conservators to help prevent future damage to the artwork they are treating. In this preventive process, the conservator must choose materials that will not further harm the object. It is often specified that the reversibility of a treatment is essential (Weil, 1981). The challenge presented by the conservation community is that everything applied to a piece of artwork must be *reversible*. In the case of a coating on bronze sculpture, the protective coating needs to be removable without damaging or changing the sculpture's surface. Although a protective *and* removable coating is a seemingly simple requirement of the conservator, from the perception of the coating scientist, they are opposing properties and it is difficult to achieve both.

Currently, the two common methods of removing a coating from a substrate are blasting abrasive materials (Djurovic et al., 1999) and solvent removal. Although blasting and stripping techniques have been used in the field of preservation, there are dangers of damaging the substrate, associated with these techniques (Grimmer, 1979). It has been proven that the reflection of sand particle off of a copper or brass substrate results is "considerable erosion" (Carter et al., 1991 and Fang et al., 1999). Water-blasting is also a method used to remove paint from a metal surface ("High-pressure water removes paint build-up", 1996; "Achieving surface preparation standards by waterjetting", 1998; Kierkegaard, 2000). When water-blasting is used on a bronze substrate, it is likely that water is forced into pores and will cause long term problems when trapped underneath a coating. When using solvents to remove a coating, they must be used in large quantities. This does not help the international drive to reduce the hazardous air pollutants (HAPs) and volatile organic compounds (VOCs). Laser removal of a coating on bronze holds much potential, but currently, the controlled irradiation of various coatings on bronze has not lead to universally positive results (Cooper, 2001). In conclusion, blasting, high-pressure water jet, and solvent removal methods not only can potentially damage the bronze surface, but these methods also present environmental hazards due to the resulting dust, dispersed liquid particles, and fumes. To avoid the necessity of solvent stripping or blasting methods, the synthesis of coatings that have inherent chemical decomposition mechanisms, which are different than their curing mechanisms are currently being studied (Van der Wielen et al., 2001; Olson et al., 2003; Shedlosky et al., 2004).

ABN 70 592 297 967

Protective coatings are needed for outdoor bronze sculptures because the monumental alloy is especially susceptible to deterioration caused by atmospheric corrosion. Coatings put on any outdoor metal substrate, if not solely for aesthetic purposes, are meant to protect the underling metal from corrosion. These coatings must endure a wide range of temperature conditions, ultraviolet radiation, pollutants, snow, acid rain, wind and particulate matter. Because of these considerable set of conditions, coatings, when used outside of conservation are typically developed to have the most robust properties possible. Such materials are usually made of crosslinked polymers. It has been found in previous studies, various coatings that are not removable with solvents outperform, in terms of coating protection and lifetime, those that are "removable" (Grimmer, 1979). It is also noted that crosslinked systems, offer a significantly higher protection and lifespan than that of their uncrosslinked counterparts. Because of the said restrictions, the sphere of material options in conservation has been diminished and crosslinked systems do not fit within the usable realm. The current procedure is to only apply coatings that are removable by solvents, as non-removable coatings have been interpreted as "adversely (effecting) cultural property or its future."(AIC) The primary coating used on bronze sculpture is wax (Kipper, 1996), but previous studies (Brostoff et al., 1997 and 1998; Bierwagen et al. 2001; Bierwagen et al. 2000 and 2001; Bierwagen et al., 2003) have shown less permeable coatings provide better protection and longer lifetimes between treatments.

The seemingly contradictory properties of removability and durability stand at odds with each other in coating design. When developing good protection of a metal from the coating, one needs adhesion and chemical stability to external stresses. When looking for removability, these properties must be decreased. Hence the ethics of conservation appears to run counter to normal coating design. The method in which this research project is attempting to get around this combination of incompatible requirements is to add a weak link within the coating that is activated within a manufactured set of conditions that is unlikely to occur in natural exposure.

1.2 Methods of Development

As stated previously, there are many robust coatings that cannot be considered when treating an outdoor bronze due to their irreversible nature. If this research is successful, it will free a set of high performance coatings from the removability restrictions. We aim to prepare clear protective coatings of controlled removability that have as little as possible impact on the bronze. Much of our development of removable coatings was based on the use of combinatorial synthesis and testing methodologies

The technique of combinatorial chemistry, new to the field of material science, is an incredibly useful tool for making minor formulation modifications of synthesized coatings, and for rapid and extensive screening of the coatings. The methodology is just being implemented in the field of coatings (Vratsanos et al., 2001; Schrof et al., 2001; Chisholm et al. 2002a and Chisholm et al. 2002b) and our studies have extended these methods into the specific area of formulating coatings with removability and high performance. The application of combinatorial chemistry, allowed this research to handle and screen many more materials than possible using standard practice. One is able to produce a large variety of products in a relatively short time frame. Coatings are multi-component systems that can have many complex interactions, (Pilcher, 2001) and, as such, are good candidates for the application of combinatorial

methods. This technique enables one to rapidly synthesize and characterize new coating polymers at a rate up to 100 times greater than standard practice

One of the challenges in using combinatorial chemistry is the design of the experiment. The method of analysis must be direct and have a clear pass or fail result. Our first analysis was to determine the removability of the coating. We used an increased pH to change the chemistry of the coating making it removable. We also tested the coatings in water to make sure the system was not so hydrophilic that the system would fail if exposed to water. This type of analytical measurement, when it can be miniaturized and automated, is ideally suited to use in combination with rapid synthetic methods for preparing new polymers of designed but unevaluated removability.

2. Experimental

2.1 Polyester synthesis

Typically polyurethane coatings are very durable and when applied to metals provide a high degree of protection (Koch et al., 1985; Wicks et al., 1999). The problem of using polyurethanes in an application on bronze sculptures is that they are permanent and only removable by mechanical methods. Through this research we are attempting to develop a polyurethane coating that is both protective and removable. Polyesters are synthesized by reacting a polyacid and a polyol as shown in Figure 1.

Figure 1. The reaction of a polyol and polyacid to form a polyester and water.

Commonly polyesters are formulated to have excess hydroxyl groups that are then used for crosslinking. The polyester urethane is made by crosslinking a multifunctional, hydroxyl-terminated polyester with an isocyanurate as seen in Figure 2.

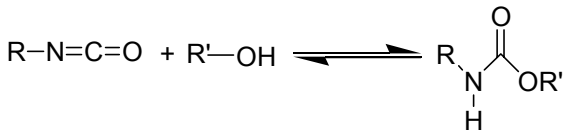

Figure 2. The crosslinking reaction of an isocyanate and a alcohol group.

Dimethylolpropionic acid (DMPA) was used as a monomer in the polyester synthesis. DMPA has two hydroxyl groups that are reactive and one protected acid group (see Figure 3).

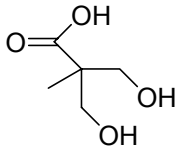

Figure 3. Structure of dimethylolpropionic acid.

Because of the hindered status of the acid group it is unlikely to react during the polymerization, and therefore does not need to be protected during the synthesis. This monomer is used in water-borne polyurethanes; once the polyester is synthesized the carboxylic acid can be neutralized with an amine, and it becomes water soluble

(Wicks et al., 1999). In the case of developing a removable coating, the polymer would not be neutralized until the coating is being removed. The means in which this occurs is the base catalyzed hydrolysis reaction, as seen in Figure 4. In this process the hydroxide attacks electrophilic carbon of the ester, the intermediate collapses reforming carbon-oxygen double bond, finally a fast acid/ base reaction, deprotonates the carboxylic acid.

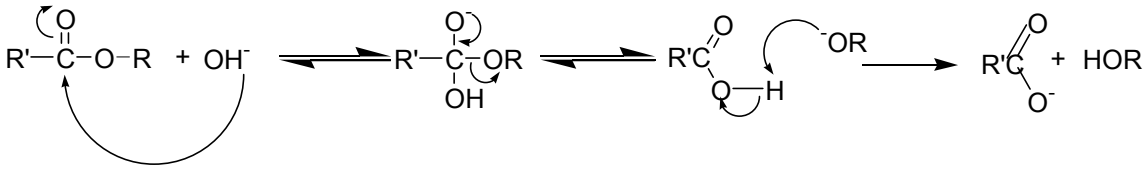

Figure 4. Based catalyzed hydrolysis reaction.

2.2 Crosslinking/ Formulations

The type of isocyanate and its crosslink density has a marked effect on the stability of the urethane system. Higher crosslink densities lead to more stable coatings and a smaller probability that the system will be removable. In addition a hydrophilic component within the coating could potentially help promote removability. All these variables were tested with each other in a series of factorial experiments with center points and star points to create a response surface for the different factors. The DMTA based polyester was then crosslinked and formulated varying the (1) crosslink density or the NCO:OH ratio, (2) the type of isocyanate, (3) the hydrophile content and (4) the type of hydrophile. Three separate isocyanates were used in the crosslinking reaction as well as 5 different hydrophilic additives. The three separate isocyanates were chosen for their specific properties.

Isocyanate A is a difunctional isocyanate with an aromatic component. This aromatic ring will increase the rigidity of the crosslinked system. *Isocyanate B* is trifunctional and is known to crosslink well with polyester polyols and result in a coating that has a high resistance to weathering. *Isocyanate C* is also a trifunctional molecule that has excellent adhesion and toughness.

A hydrophilic component was included in the study. Two hydrophilic molecules were chosen for their distinct properties and added in various amounts during the crosslinking reaction. By adding a hydrophilic molecule to the crosslinked structure, water uptake will be increased, increasing the degradation rate (Vogel et al. 2004). It was thought that this approach would also help the crosslinked polymers breakdown when exposed to the high pH material. *Hydrophile 1* had a molecular weight of 200 and is a very hydrophilic molecule. *Hydrophile 2* is composed of a hydrophilic chain sandwiched between two hydrophobic molecules. The molecular weight of this system is about 2000. A possible structure of the crosslinked system is found in Figure 5.

ABN 70 592 297 967

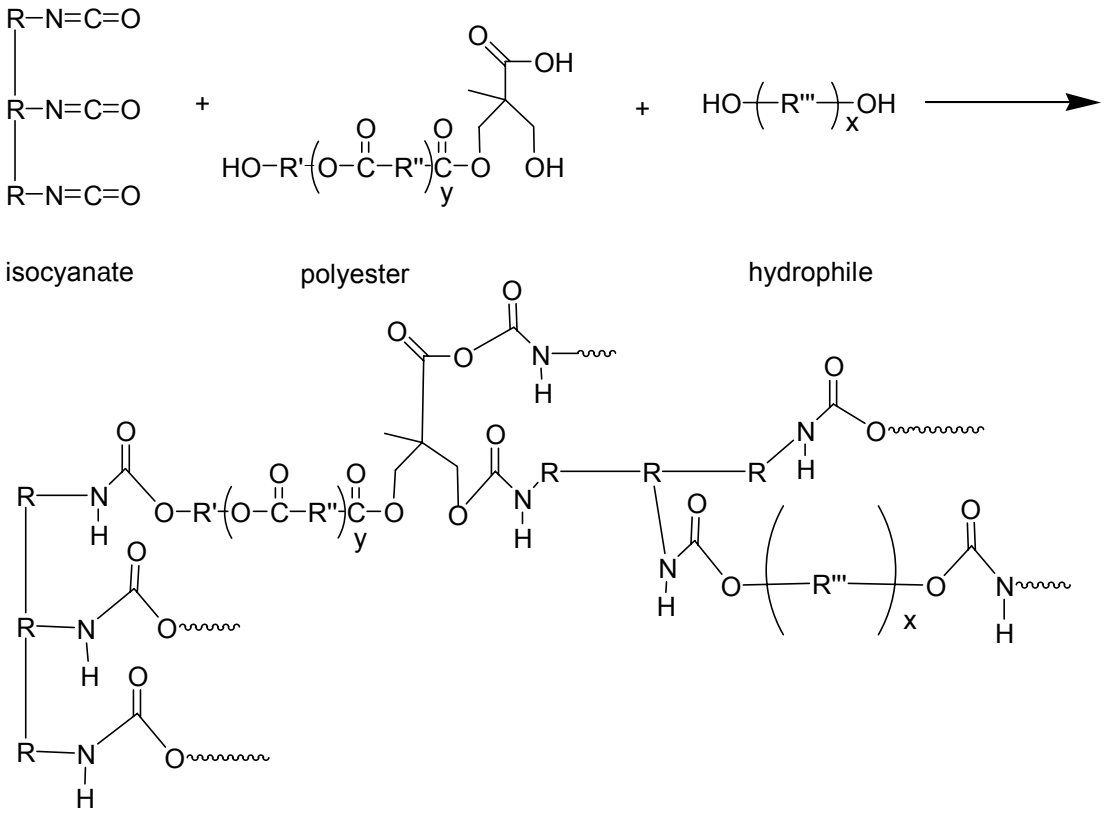

Figure 5. Possible structure of the crosslinked coating.

The isocyanates were crosslinked with a polyester in ratios of 0.295:1, 0.5:1, 0.589:1, 0.8:1, 0.995:1, 1.1:1, 1.304:1, 1.593:1 and 2.190:1. Additional samples were crosslinked in the same ratios with the hydrophilic additives 5, 10 and 13 wt.% of the polyester. Each of these samples were cast with a 37μm Sheen Cube film applicator onto polished, degreased spring loaded rolled bronze (Lubaloy Co.) with an alloy composition of 87.547% Cu, 0.005% Pb, 0.038% Fe, 10.6% Zn, and 1.76% Sn. These coatings were allowed to cure in ambient room temperature for 5 days and were evaluated for curing.

2.3 Removability evaluation

Each coating was exposed to the 3M varnish remover, Safest Stripper™ modified to a pH of 9 for 30 minutes. The system was lightly abraded with a plastic scraper and rinsed with deionized water. Each urethane was evaluated visually to see if the coating was removed after the exposure. Subsequently the urethanes were immersed in a water bath for 30 minutes, and the coatings were analyzed to determine if the coating was adversely affected by the water exposure.

ABN 70 592 297 967

3. Results

The response surfaces, Figures 6-11, display the durability and removability of each of the coating as a function of the variables. By analyzing the response surface, one can identify the areas of water resistance and removability. The following symbols have been used to represent the coating properties. The ○ represents that the coating was not affected by the water immersion, and was removed after the exposure to the high pH paste. The X through the point indicates that the system did not cure, and remained tacky five days after it was cast. The symbol  represents a system that was removable after the water immersion. The symbol  indicates that the system was not removable in the water bath or when the high pH paste was applied. The points represented by a lighter shade are the center points and were duplicated 6 times.

Figure 6. Isocyanate A + Hyrophlic Component 1

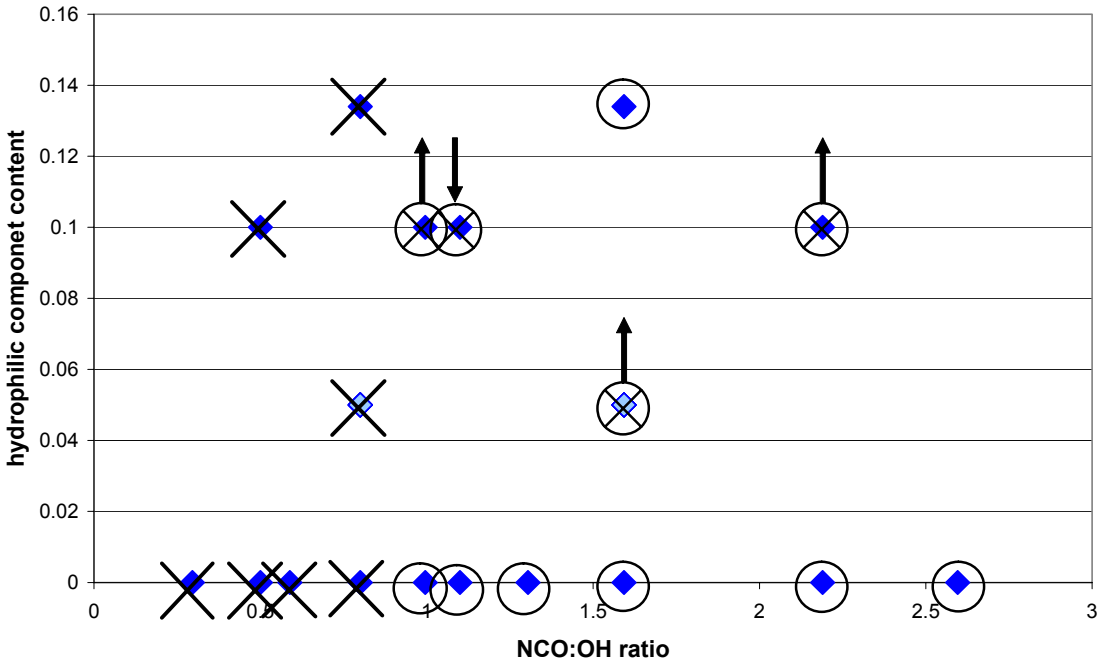

ABN 70 592 297 967

Figure 7. Isocyanate A + Hyrophlic Component 2

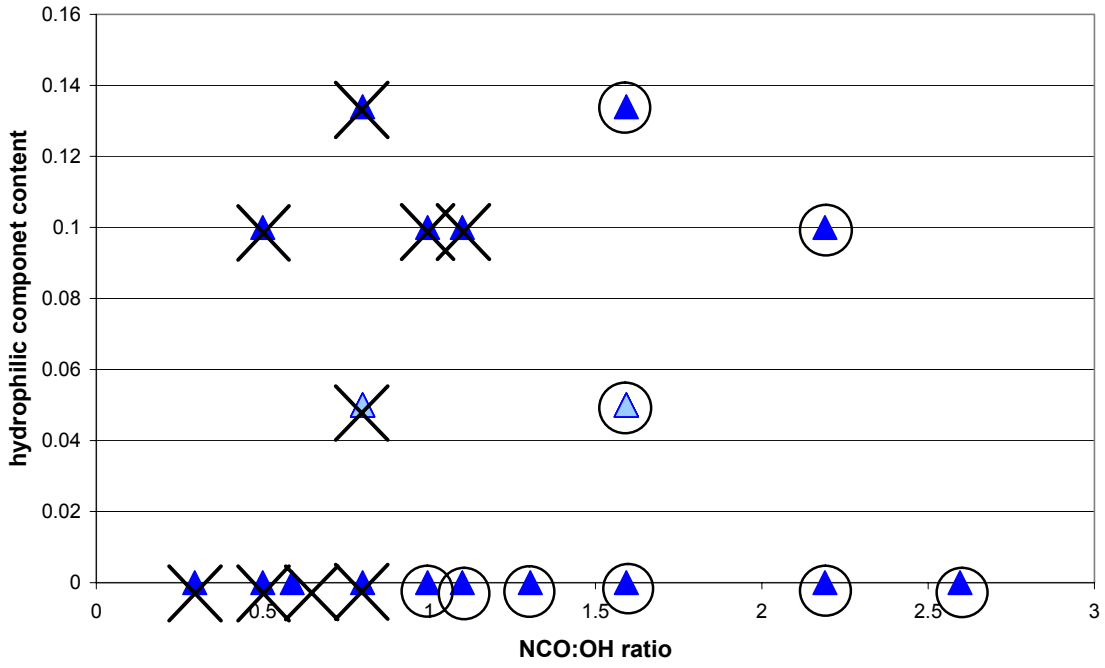

Figure 8. Isocyanate B + Hyrophlic Component 1

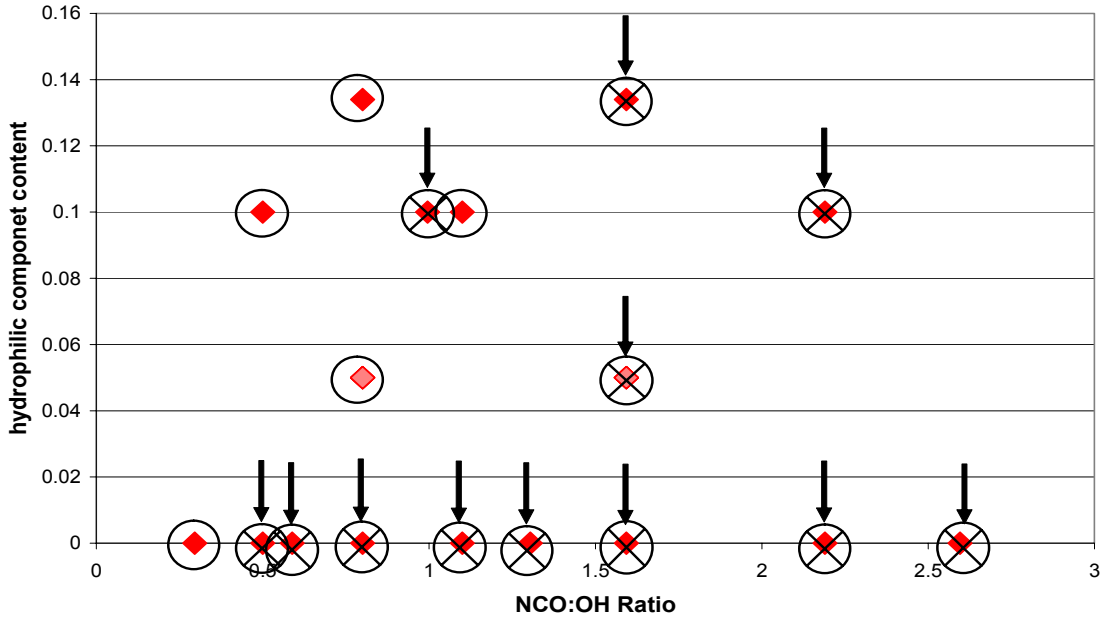

Figure 9. Isocyanate B + Hyrophlic Component 2

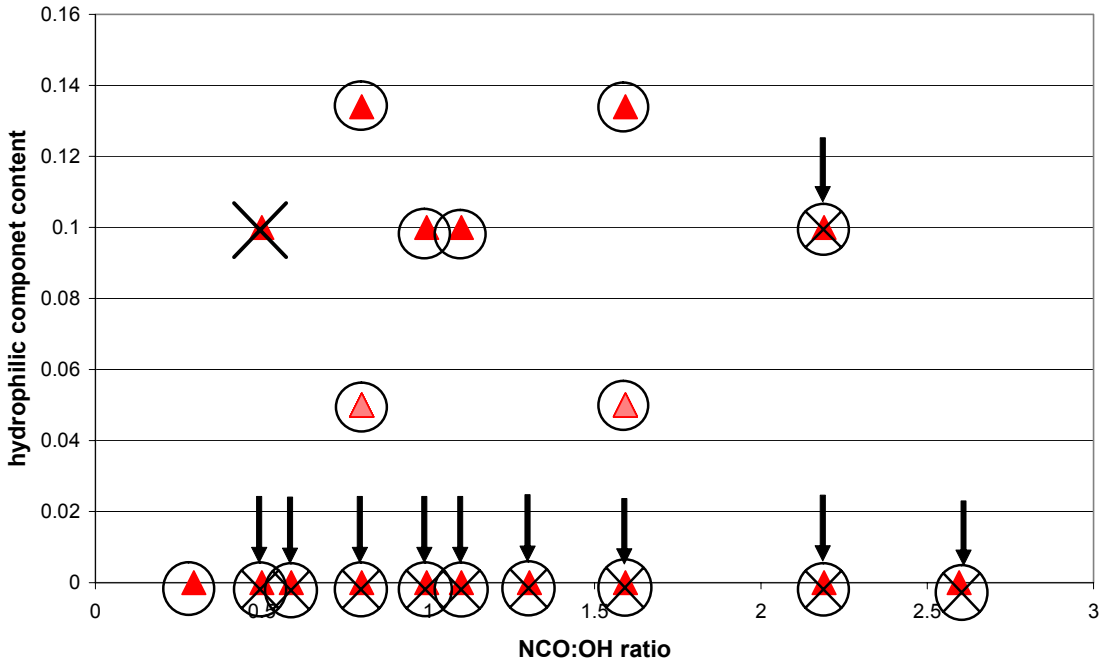

Figure 10. Isocyanate C + Hyrophlic Component 1

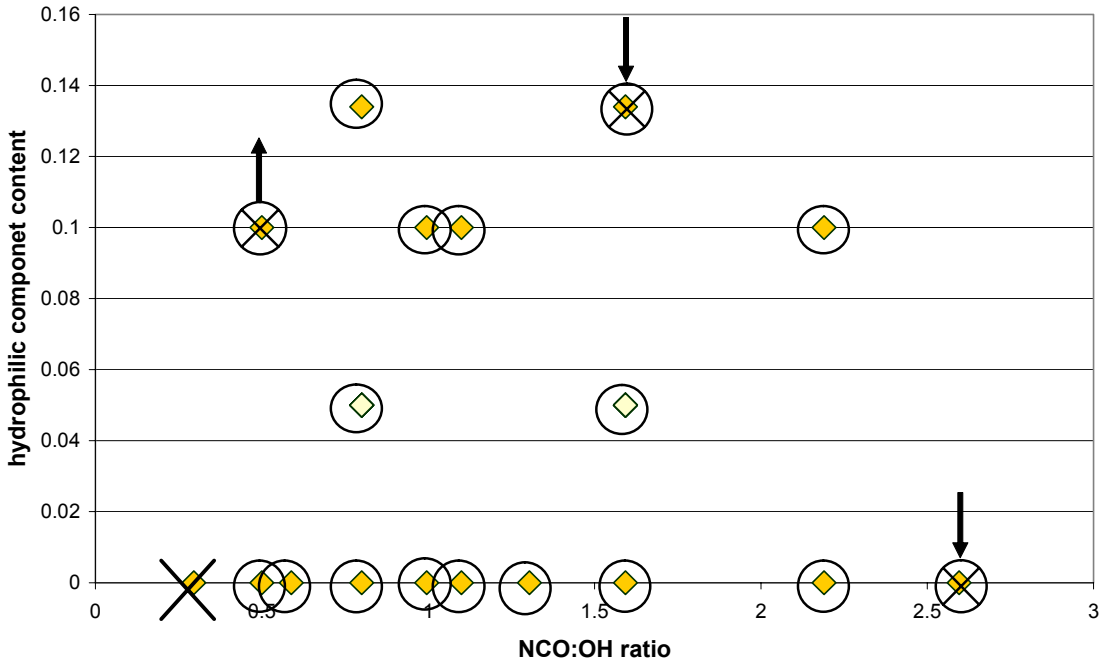

Figure 11. Isocyanate C + Hyrophlic Component 2

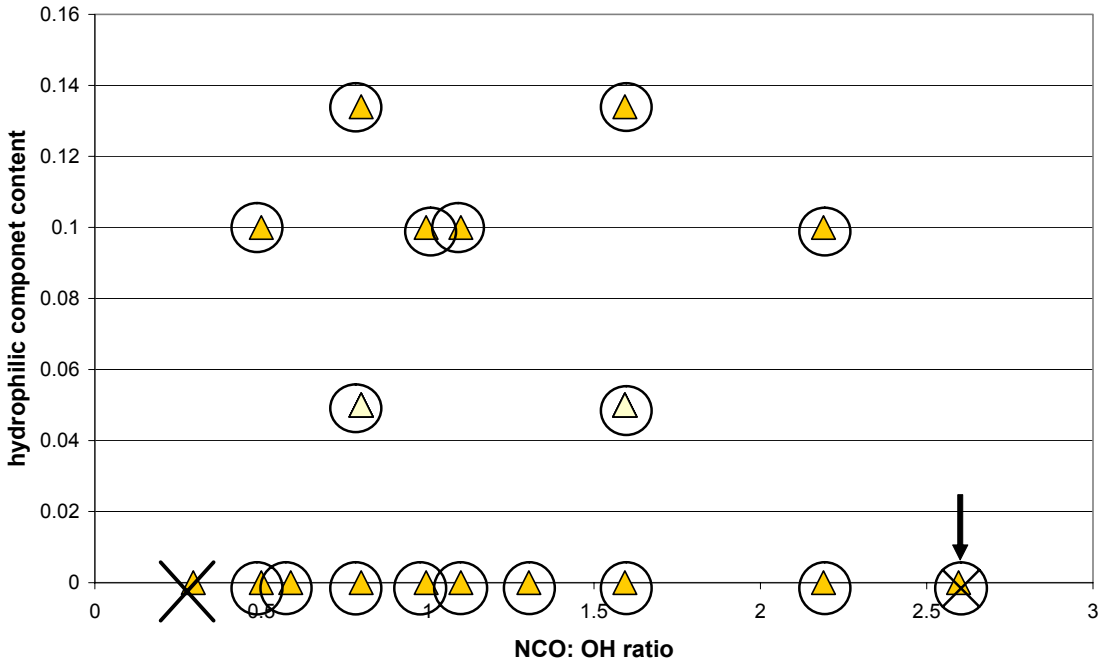

4. Discussion

Without the hydrophilic additives, the three isocyanates perform differently at the various crosslinking ratios. *Isocyanate A* did not cure at the lower crosslink densities, but above a crosslinking ratio, of 1:1 (NCO:OH), the system was cured and removable when the high pH paste was applied. *Isocyanate B* formed a very stable system above a ratio of 0.3:1 (NCO:OH), and was found not to be removable. *Isocyanate C* was not cured at the very low crosslink densities, and formed a non-removable coating at the highest crosslink density, but between the two extremes, formed a coating that was stable verse water exposure, but removable when exposed to the high pH paste.

The hydrophilic additives did have an effect on the removability of *Isocyanate A*. *Hydrophile 1* increased the hydrophilicity of the coating, so when it was added in higher quantities, the coatings were removed with water. *Hydrophile 2*, which is the system that contains the hydrophilic component within a sandwich of the hydrophobic entities, was not affected by the water immersion and proved to form a removable coating at the higher crosslink densities.

Isocyanate B with the addition of *Hydrophile 1*, was very stable, and was not removable, except at a very low crosslinking density. With the addition of the *Hydrophile 2* the system was removed with the high pH paste at crosslinked ratios between 0.8:1 and 1.593:1 (NCO:OH). In both cases the increase in the hydrophile component did not change the results.

Overall the removability of *Isocyanate C* with the high pH paste was very successful. The addition of the hydrophilic components did not have a marked effect on the performance, as the system was already removable.

ABN 70 592 297 967

5. Conclusions

Polyurethanes have been identified as a durable and potentially long life coating system. This research has developed a series of polyurethanes based on a DMPA polyester. This resultant crosslinked system was tested for its removability with a high pH material and water. *Isocyanate A* and *C,* when fully crosslinked, formed coatings that were removable with the high pH paste. The *Hydrophile 1* added too much hydrophilicity to *Isocyanate A* and caused the systems to be removable with water. *Isocyanate B* gained increased removability with the *Hydrophile 2* versus *Hydrophile 1*. The fully crosslinked systems that do not have any hydrophilic additives are expected to form the most durable coatings.

6. Future Work

The next stage of the research will consist of using the most durable formulas from this research and incorporating paint additives such ultraviolet light absorber, a hindered amine light stabilizer, leveling agent, and a fungicide. Other possible additives may be investigated if they seem beneficial to the coating. The successful candidates from this stage of the research will be applied to bronze substrates and will be tested to determine their resistance to weathering via electrochemical and accelerated methods.

Acknowledgements

The authors are grateful for the financial support from the US National Center for Preservation Technology and Training and the NSF North Dakota EPSCoR .

References

Achieving surface preparation standards by waterjetting. (1998) Achieving surface preparation standards by waterjetting. *J. Protective Coatings & Linings*, **15**, 37, 39-43.

AIC, Code of Ethics of the American Institute for Conservation of Historic & Artistic Works.

Bierwagen, G., Shedlosky, T., and Ellingson, L. (2001) Electrochemical Studies of the Protection of Bronzes from Corrosion by Organic Coatings. *In: Metals 2001, ICOM Metals Working Group: Proceeding of a conference, Santiago, Chile, April 2001.*

Bierwagen, G., Shedlosky, T., Stanek, K. "Final Report to the NCPTT 2000 and 2001 Grant Program: Development and Testing of Organic Coatings for the Protection of Outdoor Bronze Sculpture from Air-Pollutant Enhanced Corrosion."

Bierwagen, G., Shedlosky, T., Stanek, K. (2003) Developing and Testing a New Generation of Protective Coatings for Outdoor Bronze Sculpture. *Progress in Organic Coatings.* **48**, 289-296.

Brostoff, L., Shedlosky, T., de la Rie, E. R. "Final Report to the NCPTT 1997 and 1998 Grant Program: Research into Protective Coating Systems for Outdoor Bronze Sculpture and Ornamentation. Phase II."

Carter, G., Bevan, I.J., Katardjiev, I.V., Nobes, M.J. (1991) Erosion of copper by reflected sandblasting grains. *Materials Science & Engineering A: Structural Materials: Properties, Microstructure and Processing*, **A132**, 231-236.

Chisholm, B., Potyrailo, R., Cawse, J., Shaffer, R., Brennan, M., Molaison, C., Whisenhunt, D., Flanagan, B., Olson, D. and Akhave, J. (2002a) The development of combinatorial chemistry methods for coating development: I. Overview of the experimental factory. *Progress in Organic Coatings,* **45**, 313-321.

Chisholm, B.; Potyrailo, R. A.; Cawse, J. N.; Brennan, M.; Molaison, C.; Shaffer, R.; Whisenhunt, D.; Olson, D. (2002b) In: *29th International Waterborne, High-solids, and Powder Coatings Symposium*: New Orleans, 2002.

Cooper, M. I. (2001). Laser removal of paint layers from corroded copper; possible applications to bronze sculpture cleaning. Monuments and the Millenium, Proceedings of the conference organized by English Heritage and UKIC (20-22 May 1998, Victoria and Albert Museum), 109-119.

Djurovic, B., Jean, E., Papini, M., Tangestanian, P., Spelt, J. K. (1999) Coating removal from fiber-composites and aluminum using starch media blasting. *Wear*. **224**, 22-37.

Fang, C.K., Chuang, T. H. (1999) Surface morphologies and erosion rates of metallic building materials after sandblasting. *Wear*. **230**, 156-164.

Grimmer, A. E. (1979) Dangers of Abrasive Cleaning to Historic Buildings. *Preservation Briefs*: **6** 1-8.

High-pressure water removes paint build-up. (1996) High-pressure water removes paint build-up. *Products Finishing (Cincinnati).* **60**, 108-109.

Kierkegaard, H. (2000) Using UHP waterjetting for coating maintenance on ships at sea. *J. Protective Coatings and Linings*, **17**.

Kipper, P. V. (1996) *The Care of Bronze Sculpture*, Rodgers & Nelsen Publishing Co.

Koch, H., G. Mennicken, F. Muller, H. Toepsch, H. Traubel, W. Wieczorrek (1985) In *Polyurethane Handbook*; Oertel, D. G., Ed. New York: Oxford University Press.

Olson, K. E., Kackson, Victoria Jeanne (2003) *Strippable coating system.* Ecolab Inc. United States, 838873. April 20, 2001.

Pilcher, G. R. (2001) Meeting the Challenge of Radical Change: Coatings R&D as We Enter the 21st Century. *J. Coatings Tech.,* **73**, 921.

Schrof, W.; Lehmann, S.; Hadeler, J.; Oetter, G.; Dralle-Voss, G.; Beck, E.; Paulus, W.; S.Bentz (2001) *In*: *Athens Conference on Coatings Science and Technology*: Athens, Gr. pp 283.

Shedlosky, T. J., Andrew M. Huovinen, Gordon P. Bierwagen, Dean Webster (2004) Protective Removable Coatings for Outdoor Bronze. *In: AIC 2004 Conference, Portland, OR, 2004.*

Van der Wielen, M. W. J., Cohen Stuart, M.A., Fleer, G.J., Nieuwhof, R.P.,Marcelis, A.T.M., Sudholter, E.J.R. (2001) A paint removal concept with side-chain liquid crystalline polymers as primer material. *Prog. Organic Coatings*. **41**, 157-165.

Vogel, B. M., Mallapragada, Surya K.(2004) Synthesis of novel biodegradable polyanhydrides containing aromatic and glycol functionality for tailoring of hydrophilicity in controlled drug delivery devices. *Biomaterials*. In Press.

Vratsanos, L. A.; Rusak, M.; Rosar, K.; Everett, T.; Listemann, M. (2001) *In: Athens Conference on Coatings Science and Technology: Athens, Gr.,* pp 435.

ABN 70 592 297 967

Weil, P. D. (1981) *Maintenance Manual for outdoor Bronze Sculpture being particularly intended for sculpture that has previously been given conservation treatment including a protective coating of Incralac*. St. Louis: The Center for Archaeometry Washington University in St. Louis.

Wicks, Z. W., Frank Jones, S. Peter Pappas (1999) *Organic Coatings Science and Technology*; 2 ed. New York: Wiley-Interscience.

